ENCLOSURE 10

GEH Technical Report

WG3-U71-ERD-S-0001 Revision 4

Reactor/Fuel Building Complex Seismic Analysis Report

REVISION STATUS SHEET

Document Title: Reactor/Fuel Building Complex Seismic Analysis Report

Revision #: 4 **Type:** Engineering Report – Design

Safety Related Classification Code: N/A **MPL No.:** A25-5040, U71-5040, U97-5040

"|" Vertical Sidebar Denotes Change

Rev #	DOORS BL	Change Number	MM/DD/YYYY	Preparing Organization	Issue / Release Status	Verification Status
0	N/A	ECO-0015261	05/26/2015	GEH	Issued for Use-Design	Verified
1	N/A	ECO-0015970	05/29/2015	GEH	Issued for Use-Design	Verified

MADE BY	APPROVALS	AUTH. DATE
Luben Todorovski GEH	Tanya B. Kirby GEH	05/26/2015

REVISION CHART (CONT)

Rev #	DOORS BL	Change Number	MM/DD/YYYY	Preparing Organization	Issue / Release Status	Verification Status
2	N/A	ECO-0018888	09/25/2015	GEH	Issued for Use-Design	Verified
3	N/A	ECO-00020087	10/30/2015	GEH	Issued for Use-Design	Verified
4	N/A	ECO-0023186	03/08/2016	GEH	Issued for Use-Design	Verified

RECORD OF REVISION

Rev #	Description
0	Initial issue
1	Revised to correct editorial errors.
2	Incorporate comments on Rev.1
3	Incorporate comments on Rev.2
4	Correct errors in Section B.4 tables and figures, provide references for damping values in Table 4.1-1, and incorporate comments on Rev. 3. Changes made in this revision do not affect other technical reports.

TABLE OF CONTENTS

LIST OF TABLES

LIST OF FIGURES

LIST OF ACRONYM

ARS	Acceleration Response Spectra
BE	Best Estimate
CB	Control Building
CPSD	Cumulative Power Spectral Density
CSDRS	Certified Seismic Design Response Spectra
DCD	Design Control Document
D/F	Diaphragm Floor
DM	Direct Method
EW	East-West
FE	Fully Embedded
FFT	Fast Fourier Transformation
FIRS	Foundation Input Response Spectra
FSAR	Final Safety Analysis Report
GDCS	Gravity-Driven Cooling System
GMM	Ground Motion Model
ISG	Interim Staff Guidance
ISRS	In-Structure Response Spectra
LB	Lower Bound
LMSM	Lumped Mass-Stick Model
MSM	Modified Subtraction Method
NA3	North Anna Unit 3
NEI	Nuclear Energy Institute
NS	North-South
OBE	Operating Basis Earthquake
PCCS	Passive Containment Cooling System
PE	Partially Embedded
PSD	Power Spectral Density
RB/FB	Reactor/Fuel Building Complex
RCCV	Reinforced Concrete Containment Vessel
RPV	Reactor Pressure Vessel
RSW	Reactor Shield Wall
SDOF	Single Degree of Freedom
S/P	Suppression Pool
SRP	Standard Review Plan
SRSS	Square Root of the Sum of the Squares
SSE	Safe Shutdown Earthquake
SSI	Soil-Structure Interaction
UB	Upper Bound
VW	Vent Wall

1. INTRODUCTION AND PURPOSE

This report presents the North Anna Unit 3 (NA3) site-specific Soil-Structure Interaction (SSI) analyses performed for the ESBWR Reactor/Fuel Building Complex (RB/FB).

The NA3 site-specific SSI analysis follows the standard design methodology presented in the ESBWR Design Control Document (DCD) RB/FB seismic analysis report (Reference 2-k) using the SASSI2010 and ACS SASSI computer programs. The SASSI structural (HOUSE) models are developed from the standard design SASSI model described in Section 4.3 coupled with site-specific strain-compatible dynamic subsurface properties. The RB/FB structural models used for the SSI analysis represent stiffness properties of uncracked reinforced concrete structures and full (100%) stiffness contribution of in-fill concrete to the concrete-filled steel structures. The use of models with these upper bound stiffness properties in conjunction with lower OBE damping values provides conservative seismic responses for the NA3 rock site with high frequency design ground motion. The results of the site-specific structural stiffness variation sensitivity analyses presented in Appendix B ensure that the site-specific design basis that is based on the model with upper bound stiffness properties adequately addresses effects of structural stiffness variations due to concrete cracking.

The structural (HOUSE) model also includes near-field solid elements representing:

- The concrete fill that is backfilled around the building to replace the excavated Zone III rock up to the top elevation of the Zone III rock
- The structural fill backfilled in the excavation above the Zone III rock to the finished ground level grade elevation

The site-specific SSI analysis considers two different embedment configurations representing: (1) the RB/FB as being Partially Embedded (PE) up to the Zone III rock nominal top elevation, and (2) the RB/FB as being Fully Embedded (FE) up to the finished ground level grade elevation. A total of six subgrade profiles are considered in the SSI analyses to account for the effects of the potential variability in the properties of the subgrade materials at the NA3 site:

- Best Estimate (BE) partial and full column profiles
- Lower Bound (LB) partial and full column profiles
- Upper Bound (UB) partial and full column profiles

The envelope of responses obtained from the analyses of these six subgrade profiles provides the NA3 site-specific seismic demands used for site-specific design and evaluation of the RB/FB. These enveloping site-specific seismic demands are compared with the seismic design envelopes documented in the standard design RB/FB seismic analysis report (Reference 2-k) to determine any exceedances of the NA3 site-specific seismic demands relative to the corresponding seismic demands of the standard design. The results of the SSI

analyses presented in this report are also used as the basis for the site-specific seismic design of the RB/FB.

1.1 Limitations on Use

This report is issued without limitation.

2. REFERENCES

a TODI WG3-3-A25-TDI-0004, "North Anna 3 Maximum Ground Water Level", Revision 0
b TODI WG3-3-A25-TDI-0005, "North Anna 3 Power Block Excavation/Backfill Drawings, Concrete Backfill Properties & Plot Plan", Revision 5
c TODI WG3-3-A25-TDI-0006, "North Anna 3 Best Estimate Elevation of Top of Zone III Rock and Top of Zone III-IV Rock for RB/FB, CB and FWSC Structures", Revision 0
d TODI WG3-3-A25-TDI-5002, "North Anna 3 OBE Damping Values for RPV Components", Revision 0
e TODI WG3-A25-TDI-S-0004, "North Anna 3 RB/FB, CB & FWSC SSI Analyses EPRI 2013 GMPE Based Inputs", Revision 0
f TODI WG3-A25-TDI-S-0005, "North Anna 3 RB/FB, CB & FWSC Distances from Adjacent Structures & Sheet Piling", Revision 0
g TODI WG3-A25-TDI-S-0006, "North Anna 3 RB/FB, CB & FWSC Outcrop SSI Design Motion Time-Histories", Revision 0
h 105E3908, "ESBWR Nuclear Island General Arrangement Drawing", Revision 5
i 26A6642AL, "ESBWR Design Control Document Tier 2 Chapter 3 Appendices 3A – 3F", Revision 10
j 26A6642AN, "ESBWR Design Control Document Tier 2 Chapter 3 Appendices 3G – 3L", Revision 10
k 26A6647, "ESBWR Seismic Analysis of Reactor/Fuel Building Complex", Revision 7
l 26A6651, "ESBWR Reactor Building Structural Design Report", Revision 5
m 26A6652, "ESBWR Stability Analysis of Reactor/Fuel Building Complex", Revision 4
n SER-DMN-019, "North Anna 3 RB/FB Seismic Analyses Bounding Results and In-Structure Response Spectra", Revision 1
o USNRC, NUREG-0800, "Standard Review Plan for the Review of Safety Analysis Reports for Nuclear Power Plants – LWR Edition", Section 3.7.1, "Seismic Design Parameters", Revision 3, March 2007
p USNRC, NUREG-0800, "Standard Review Plan for the Review of Safety Analysis Reports for Nuclear Power Plants – LWR Edition", Section 3.7.2, "Seismic System Analysis", Revision 4, September 2013
q USNRC, "Interim Staff Guidance on Ensuring Hazard-Consistent Seismic Input for Site Response and Soil Structure Interaction Analyses", DC/COL-ISG-017 (NRC ADAMS Accession Number ML092230543)
r USNRC, Regulatory Guide 1.60: "Design Response Spectra for Seismic Design of Nuclear Power Plants", Revision 1, December 1973

s WG3-U71-ERD-S-0003, "North Anna 3 Reactor/Fuel Building Complex Stability Analysis Report", Revision 1
t SER-DMN-011, "Benchmarking of SASSI2010 MSM Results from NA3 Site-Specific SSI Analysis", Revision 1
u USNRC, "Interim Staff Guidance on Seismic Issues Associated with High Frequency Ground Motion in Design Certification and Combined License Applications", DC/COL-ISG-01 (NRC ADAMS Accession Number ML081400293)
v USNRC, Regulatory Guide 1.61: "Damping Values for Seismic Design of Nuclear Power Plants", Revision 1, March 2007
w ASCE 43-05: "Seismic Design Criteria for Structures, Systems, and Components in Nuclear Facilities"
x S/VTR-SAS, "Validation Test Report for SASSI2010 Version 1", Revision I
y Ostadan, F. and Deng, N., "SASSI2010 Version 1.0 User's Manual", May 2012
z DBR-0006613, "Site-Specific Seismic Soil-Structure Interaction Analysis of Reduced Stiffness RB/FB Models for Best Estimate and Upper Bound Full Columns and Full Stiffness (uncracked) Model for Upper Bound Full Column", Revision 1
aa SER-DMN-014, "Additional Oscillators for Fully Cracked Model for RAI 3.7.2-14(f) Response", Revision 1
bb DBR-0009791, "Soil-Structure Interaction Absolute Acceleration Transfer Functions With Respect to Outcrop Motion and Design Motion Power Spectral Densities For RB/FB SSI, CB SSI, FWSC SSI, CB-FWSC SSSI, and CB-RB/FB SSSI Analyses", Revision 5
cc SER-DMN-033, "Evaluation of the Adequacy of the Frequencies Used for Seismic Response Analyses", Revision 1
dd 26A6642AJ, "ESBWR Design Control Document Tier 2 Sections 3.1 to 3.8, Design of Structures, Components, Equipment, and Systems", Revision 10
ee ANSI/AISC N690-12 & ANSI/AISC N690s1-15: "Specification for Safety-Related Steel Structures for Nuclear Facilities, Including Supplement No. 1"

3. SITE-SPECIFIC INPUT

3.1 Site-Specific Subsurface Properties

The RB/FB site-specific SSI analyses are performed for two different embedment configurations representing two limiting SSI system stiffness conditions:

- Lower bound stiffness represented by partial column profiles that neglect stiffness of softer soil materials located above the rock top elevation
- Upper bound stiffness represented by full column profiles simulating full contact of embedment with below-grade exterior walls (no soil separation) and fully saturated stiffness properties of soil located below the NA3 nominal ground water level

In order to address the variability of the subgrade properties, the RB/FB SSI analyses are performed for partial and full column profiles representing BE, LB, and UB dynamic

properties of in-situ materials compatible to the strains generated by the 2013 GMM-based design ground motion. These strain-compatible properties of in-situ rock and saprolite subgrade materials are assigned to the far-field SASSI SITE models and excavated volume elements of the SASSI HOUSE models. Reference 2-e provides the strain-compatible dynamic properties of the far-field site-specific in-situ subgrade materials used as input for the RB/FB SSI analysis that are listed in Tables 3.1-1 through 3.1-3.

The RB/FB SSI analyses also consider BE, LB, and UB dynamic properties for the structural and concrete fill materials placed around the RB/FB exterior walls. These dynamic properties are assigned to the near-field solid elements in the SASSI HOUSE models. The structural fill dynamic properties are compatible to the strains generated by the 2013 GMM-based design ground motion. The dynamic properties used for the concrete fill are linear elastic stiffness properties independent of strain reflecting the small earthquake-induced strains in the concrete fill. Reference 2-e provides the BE, LB, and UB dynamic properties of the structural and concrete fill materials that are listed in Tables 3.1-4 through 3.1-6.

The P-wave velocity of the saprolite and structural fill materials located below the ground water level is set not less than that of the water to capture the effect of ground water on the P-wave velocity of saturated soil unless the Poisson's ratio value, that relates the S and P wave velocities, becomes too high. A maximum value of 0.48 is used for the Poisson's ratio of subgrade materials in order to ensure the numerical stability of the SASSI analysis results.

The partial and full embedment configurations considered in the RB/FB SSI analyses provide responses that bound the effects of subgrade stiffness variations related to the soil separation, backfill horizontal extent and ground water level variations, and minimize the effects of dissipation of energy in the SSI system due to damping of the embedment materials. The PE models provide a lower bound representation of the stiffness of the RB/FB embedment because they do not consider the stiffness of the subgrade materials (saprolite and the structural fill) above the Zone III rock surface. The PE models also neglect the dissipation of energy in the SSI system that is due to the material damping of the saprolite and the structural fill. The RB/FB FE model considers a minimum horizontal extent of the structural fill to provide an upper bound representation of the stiffness of the embedment because the structural fill has a lower shear wave velocity (and thus lower shear modulus and stiffness) than the surrounding in-situ saprolite. The consideration of the minimum horizontal extent of the structural fill reduces the dissipation of energy in the SSI system because the material damping of the structural fill is higher than that of the in-situ saprolite.

The comparisons between the shear wave velocity and damping ratio of the structural fill and in-situ saprolite, provided in Figure 3.1-1, show that the structural fill has lower stiffness and higher damping properties than the surrounding in-situ saprolite. The same can also be observed from the comparisons of the average strain-compatible shear wave velocities ($V_{s\text{-}ave}$) and shear column frequencies (f_{sc}) of the concrete fill, structural fill and in-situ materials presented in Table 3.1-7.

3.2 Site-Specific Input Motion

Reference 2-e provides the six sets of ground motion time histories used as input control motion in the three orthogonal directions for the SSI analyses of the RB/FB for the BE, LB, and UB partial and full column profiles. These ground motion time histories represent the in-column free-field motion at the RB/FB foundation bottom elevation. These time histories are developed from the outcrop motion time histories that are compatible with the envelope of the RB/FB FIRS and the broadband spectra specified in RG 1.60 (Reference 2-r) anchored at 0.1g. The in-column ground motion time histories are checked using the NEI method as recommended by ISG-017 (Reference 2-q). The duration of the outcrop motion time histories is 29.98 seconds and the time step is 0.005 seconds.

Figures 3.2-1 through 3.2-3 present the 5% damped Acceleration Response Spectra (ARS), the Power Spectral Density (PSD) and Cumulative Power Spectral Density (CPSD) of the RB/FB SSI analysis input control acceleration time histories illustrating the energy content of the input motion at different frequencies. The presented PSDs are computed based on the strong motion portion of the time record for which duration is defined by the time interval required for Arias intensities to increase from 5% to 75%. Plus/minus 20% frequency averaging intervals are applied in compliance with SRP 3.7.1 (Reference 2-o).

4. SOIL-STRUCTURE INTERACTION ANALYSIS

4.1 Analysis Method

The NA3 site-specific SSI analyses of the RB/FB follow the methodology presented in DCD Section 3A.5.2 (Reference 2-i) for the SSI analysis of the RB/FB with its foundation. All of the site-specific SSI analyses of the RB/FB are performed using the SASSI2010 computer program with the exception of the sensitivity analyses of the FE RB/FB models with reduced stiffness properties described in Appendix B, which also use the ACS SASSI computer program. The SASSI2010 and ACS SASSI computer programs use exactly the same SASSI methodology to provide the solution for the seismic response of the structure-subgrade interaction system based on the frequency domain complex response method. The verification study presented in Appendix I demonstrates that the two programs provide virtually identical numerical results for the SSI response of the RB/FB at the NA3 site.

The analyses of the PE RB/FB model use the flexible volume (Direct) Method (DM) where all nodes of the excavated volume are specified as interaction nodes to calculate the SSI system impedance matrix. The analyses of the large FE RB/FB model use the Modified Subtraction Method (MSM) simplification, where only a selected set of nodes of the excavated volume are specified as interaction nodes, as described in Section 4.3. Reference 2-t provides the benchmarking evaluations of the accuracy of MSM solutions.

Finite elements with complex moduli are used for modeling the dynamic properties of the structure, foundation, near-field backfill materials, and the excavated volume. The model details are described in Reference 2-k and Section 4.3. Structural responses in terms of

accelerations, In-Structure Response Spectra (ISRS), relative displacements, element forces and moments are computed directly from the SASSI2010 and ACS SASSI results.

The SSI analyses are performed separately for each one of the three directional components of input ground motion. The maximum co-directional seismic forces, moments, accelerations and displacements for each of the three ground motion time history components are combined with the corresponding cross-directional responses using the SRSS method as presented in sections 5.2 and 5.4 of this report. The co-directional soil/rock reactions are combined using the algebraic sum method in the time domain for sliding, soil bearing and base contact area evaluations as presented in section 5.6. The absolute sum method in time domain is used for the lateral soil pressure evaluation as presented in section 5.5 of this report. The absolute sum method is a conservative alternative to performing the algebraic sum method for all possible combinations of the input directions.

The co-directional ISRS are combined with cross-directional responses using the SRSS method. The ISRS are developed for responses at the edges of the building to take into account coupling effects between vertical and rocking and between lateral and torsion motions. Section 5.3 presents the procedure used for the development of the ISRS.

4.2 Soil-Structure Interaction Analysis Cases

Table 4.2-1 summarizes all SSI cases analyzed for the NA3 RB/FB as follows:

- Cases 1 through 6 are analyzed by the SASSI2010 computer program utilizing the structural models with upper bound stiffness properties to develop the NA3 site-specific seismic design basis.
- Cases S1 through S12 are analyzed by the SASSI2010 and ACS SASSI computer programs utilizing the structural models with reduced stiffness properties to provide responses for the structural stiffness effects sensitivity evaluations described in Appendix B. Cases S5, S6, S11, and S12 are analyzed by the ACS SASSI computer program as described in Reference 2-z.
- Cases P1 through P3 are analyzed by the SASSI2010 computer program utilizing different point radius input values and models with different meshing of excavated volume to verify the accuracy of the RB/FB FE model as described in Appendix C. These analyses are performed for the UB full column profile using models representing upper bound stiffness properties of the RB/FB structures.
- Case V1 is analyzed by the ACS SASSI computer program utilizing the UB full column profile and structural models with upper bound stiffness properties. In Appendix I, the results from this analysis case are compared with the SASSI2010 analysis Case 6 results to demonstrate the accuracy of the ACS SASSI SSI solution for the NA3 site.

The frequency step and Fast Fourier Transformation (FFT) number used for all of the analysis cases are 0.0244 Hz and 8192, respectively. Table 4.2-2 provides a list of

frequencies of analysis used for the SASSI2010 runs for the RB/FB models with upper bound stiffness properties. The frequencies used for the sensitivity analyses of the RB/FB models with reduced stiffness are presented in Appendix B. As described in Section 5.1, acceleration transfer function results obtained from each analysis case are inspected to ensure that selected frequencies of analyses provide sufficient numerically accurate results.

Values of cut-off frequencies of analyses are used that are equal to or lower than the passing frequency of the SSI model (the highest frequency of seismic waves that can be transmitted through the SSI model). The selected values of cut-off-frequencies of analysis ensure that the SSI analyses provide RB/FB site-specific design ISRS that, per guidelines of ISG-01 (Reference 2-u), are adequate for design and qualification of components and equipment for frequencies up to 50 Hz. As shown in Table 4.2-1, the cut-off frequencies of analyses are equal to or higher than 50 Hz for all analysis cases with the exception of the analysis of the LB full column profile for which cut-of frequency of 33 Hz is used.

Results presented in Section 5 show that the site-specific SSI analyses adequately capture the response of the RB/FB structures at high frequencies and provide site-specific design basis that meets the ISG-01 (Reference 2-u) requirements. Section 5 of this report presents the SSI analyses results in terms of maximum accelerations, maximum member forces, and the ISRS at key locations. As noted in Section 5.2, the comparisons of maximum accelerations and member force results in Figures 5.2-1 through 5.2-4 show that the analyses of UB subgrade profiles typically govern the maximum responses of the RB/FB structures. This conclusion is also confirmed by the comparisons of maximum accelerations of the SDOF oscillators presented in Table 5.2-1 that also shows that UB subgrade profiles typically yield bounding results for the out-of-plane response of flexible slabs and walls. ISRS results presented in Figures 5.3-1 through 5.3-3 show that the analyses of UB subgrade profiles typically govern the responses of the RB/FB at high frequencies. As noted in Section 5.3, the comparisons of the 5% damped ISRS results in Figures 5.3-1 through 5.3-3 show that the analyses of the LB full column profile only provide bounding results for the ISRS envelopes at frequencies below 9 Hz. This is at least 24 Hz lower than the lowest cut-off frequency value of 33 Hz used for the analyses of the LB full column profile. The cut-off frequencies used for the analyses of the UB partial and full column profiles that typically govern the design at high frequencies capture virtually all ($\approx$ 99%) of the input motion energy. The other analysis cases use cut-off frequencies that enable the capturing of at least 82% of the input motion energy.

4.3 Analysis Models

The model used for the site-specific SSI analysis of the RB/FB shown in Figure 4.3-2 is based on the three-dimensional Lumped Mass-Stick Model (LMSM) that was used for the standard design seismic response analysis in the DCD, which considers shear, bending, torsion and axial deformations. This model is designated in DCD Table 3A.6-1 (Reference 2-i) as the base model including wall oscillators considered for RU-7 and RL-6 without concrete cracking and updated properties considered for RU-4. The configuration of the

RCCV is shown in Figure 4.3-1. The site-specific SSI model differs from the standard design model in that:

- The lower 4% OBE damping value, as described in Table 4.1-1, is assigned to the reinforced concrete structure.
- The meshing of the below-grade portion of the model is modified to fit the layering and stiffness properties of the NA3 subgrade.
- The rigid outriggers are installed at each floor elevation to facilitate calculation of ISRS and displacements at floor edges.
- Near-field subgrade elements are included in the structural (HOUSE) models to represent the fill materials placed around the RB/FB.
- OBE damping values are assigned to the Reactor Pressure Vessel (RPV) in accordance with Reference 2-d.

Stand-alone RB/FB SSI models are developed for the site-specific RB/FB SSI analyses for the two embedment configurations as follows:

- PE RB/FB model presented in Figure 4.3-3 and used for analyses of BE, LB, and UB partial column subgrade profiles
- FE RB/FB model presented in Figure 4.3-4 and used for analyses of BE, LB, and UB full column profiles

A minimum value of 3.13 m is used for the lateral extent of the near-field concrete and structural fill elements at all four sides of the RB/FB model. This value is based on the dimensions provided in Reference 2-f and represents the smaller of one-half of the distance between RB/FB and adjacent buildings and the actual width of the gap between the building and the inside face of sheet piling at the sides without adjacent buildings, as shown in Table 4.3-1.

The RB/FB lumped mass seismic stick models in Figure 4.3-2 correspond to DCD Figure 3A.7-4 (Reference 2-i). The SASSI2010 models used for RB/FB site-specific SSI analyses are shown in Figures 4.3-5 through 4.3-8 for the PE model and in
Figures 4.3-9 through 4.3-12 for the FE model. The model axes in the X-direction and Y-direction represent the North-South (NS) direction and the East-West (EW) direction of the NA3 site, respectively. These directions are referenced to plant north. Plant north for NA3 is oriented 23.54 degrees east of true north (Reference 2-b). The Z-axis represents the vertical direction.

The exterior walls below-grade and the foundation basemat are modeled using plate (flat shell) elements similar to the SASSI model used for the standard design RB/FB SSI analyses. However, because the soil medium between the top of the finished ground level grade or Zone III rock elevation and the foundation basemat elevation are modeled in the NA3 site-specific SSI analysis, the vertical spacing of the wall nodes is adjusted to match the site-specific subsurface layers.

The mesh size of the below-grade portion of the model is adjusted to:

- Satisfy the SASSI2010 user's manual (Reference 2-y) requirement that limits the size of the elements to not more than 20% of the length of the shear wave passing through the modeled soil material
- Ensure the model can capture at least 80% of the input motion energy for the LB subgrade profiles and at least 95% of the input energy for the UB subgrade profiles

The basemat plate elements are shown in Figures 4.3-5 and 4.3-9. The thickness of the basemat is 4.0 m. The side wall plate elements are shown in Figures 4.3-6 and 4.3-10. The thickness of the shells modeling the exterior walls from EL -11.5 m to 4.5 m is set to 2.0 m. The thickness of the shells along the thickness of the RB/FB slab from EL -11.5 m to -15.5 m is set to a quarter of the basemat width with zero unit density to model the rigid connections between the exterior walls and the basemat.

The use of models with these upper bound stiffness properties in conjunction with lower OBE damping values provides conservative seismic responses for the NA3 rock site with high frequency design ground motion. The upper bound stiffness properties and OBE damping values provided in Table 4.1-1 are assigned to the structural members in the RB/FB structural models representative of:

- Full (uncracked) stiffness of the reinforced concrete structures
- Full (100%) stiffness contribution of the in-fill concrete to the concrete-filled steel structures

The OBE damping values reflect the lower dissipation of energy in the structures experiencing lower stress levels associated with the uncracked concrete condition.

The use of upper bound stiffness properties and OBE damping values ensure that the requirements of SRP 3.7.2 (Reference 2-p) and RG 1.61 (Reference 2-v) for calculations of site-specific ISRS are met. The use of upper bound stiffness properties and OBE damping values provides conservative results for the site-specific SSE load demands on the RB/FB structures for the NA3 rock site and high frequency design motion. Appendix B presents the site-specific evaluation of the effects of concrete cracking on the SSI response of the NA3 RB/FB that is based on the results of the site-specific SSI analyses performed on the RB/FB structural models with reduced stiffness properties and SSE damping values representative of dynamic properties of reinforced concrete structures under the fully cracked condition (i.e., the condition when all of the concrete structural members are cracked). Consistent with the approach used for the standard design to address the effects of in-fill concrete on the stiffness of the Vent Wall (VW) and Diaphragm Floor (D/F), the site-specific sensitivity analyses consider a 50% and 0% stiffness contribution of the in-fill concrete to the concrete-filled steel structures.

For the PE model, the excavated volume is modeled from the top of the Zone III rock at EL -0.68 m (EL 273.0 ft, NAVD 88 per Reference 2-c) to the bottom of the excavation at EL -15.5 m (EL 224.4 ft, NAVD 88 per Reference 2-c). For the FE model, the excavated volume

is extended upward to the finished ground level grade at EL 4.5 m (EL 290.0 ft, NAVD 88). The mesh size of the excavated volume elements is set to ensure that per SASSI2010 criteria, the maximum element size in all three directions does not exceed 20% of the shear wave length of the excavated soil at the highest (cut-off) frequency of analysis. The mesh of the near-field solid elements of the backfill surrounding the RB/FB is consistent with the mesh of the excavated volume and the mesh of the plate elements of the basemat and exterior walls.

In the PE model, the excavated volume is modeled using a uniform and regular mesh. However, the top layers of the soft soil medium and the structural fill added to the FE model between the Zone III rock and the finished ground level grade elevation require a more refined mesh in order to capture sufficient input motion energy. The FE model also requires a coarser mesh of the rock and concrete fill below the Zone III rock level to ensure the overall model size does not exceed the program limitations. Therefore, in the transitional layers below rock surface elevation, the FE models use non-uniform mesh with irregular triangular shell elements, prism, tetrahedral and pyramid solid elements. Appendix C presents the results of the benchmarking study for determination of an adequate value for the point-load radius used as input in the SASSI2010 computation of the site impedance matrix. The evaluation is based on the results from three sets of SSI analyses of the RB/FB models for the UB full column profile.

The passing and cut-off frequencies of analysis for the models used for the SSI analysis of the RB/FB are shown in Table 4.2-1. The passing frequencies are calculated based on both the maximum horizontal and vertical dimensions of the excavated volume mesh and the near-field mesh. The table shows that the model maximum passing frequencies for all subsurface profiles are no smaller than the cut-off frequency of analysis. The last three columns of Table 4.2-1 show the percentage of input motion energy captured by the RB/FB SSI analysis. The input motion energy values are obtained at the cut-off frequencies of analyses of the input motion CPSDs presented in Figures 3.2-1 through 3.2-3. The table shows that the SSI analyses of the UB subgrade profiles that govern the response of the building at high frequency capture 99% of the input motion energy. The analyses of LB and BE profiles capture at least 82% and 94% of the input motion energy, respectively.

The maximum aspect ratios of the regular 3-D thin shell elements in the RB/FB PE and FE models are 1:1.6 and 1:1.8, respectively. The maximum aspect ratios of the regular 3-D solid brick elements in the PE and FE models are 1:1.6 and 1:3.5, respectively. As described in Reference 2-x, the accuracy of the SASSI2010 program has been verified and validated for models with a maximum aspect ratio of 1:4 for both the 3-D thin shell and 3-D solid brick finite elements. Additionally, the accuracy of using non-uniform irregular elements is also demonstrated in Appendix C by the results of a comparative study.

The analyses of the PE RB/FB model use the DM where all nodes of the excavated volume are specified as interaction nodes to calculate the SSI system impedance matrix. The analyses of the FE RB/FB model use the MSM simplification, where only a selected set of nodes of the excavated volume are specified as interaction nodes. For the FE RB/FB model, all the nodes at the six exterior sides and the one horizontal plane at EL 0.08 m of the excavated

volume are specified as interaction nodes. The selection of interaction nodes is consistent with the MSM benchmarking report Reference 2-t.

The site profiles used for the site-specific SSI analysis of the RB/FB are presented in Tables 4.3-2 through 4.3-4 for the partial column profiles, and in Tables 4.3-5 through 4.3-7 for the full column profiles. They consist of 38 and 41 layers on top of the half-space for the partial and full columns, respectively. The maximum value of Poisson's ratio of all materials in the RB/FB model is 0.48, which is within the range to which the accuracy of the SASSI2010 program has been verified and validated (Reference 2-x). The shear and compression wave velocities are adjusted using the equivalent wave travel time procedure as shown below.

$$Vs_{ave} = \frac{H}{\sum_i d_i / Vs_i} \quad Vp_{ave} = \frac{H}{\sum_i d_i / Vp_i}$$

where, H is the thickness of the adjusted layer and d_i, Vs_i and Vp_i are the thickness, shear wave and compression wave velocities of the layers in the original site profiles, respectively. The unit weight and damping ratios of the adjusted layers are determined as weighted averages with respect to the layer thickness. A graphical comparison between the adjusted soil profiles used in the SSI analyses and the corresponding strain iterated soil profiles from the site response analyses are provided in Figure 4.3-14 and Figure 4.3-15 for shear and compression wave velocities and damping ratios. As shown, there are no differences between the subgrade dynamic properties used as input in the RB/FB SSI analyses soil profiles and those obtained from the equivalent linear site response analyses (Reference 2-e).

The top of the half-space in the RB/FB models is established at DCD elevation -167.3 m (125 ft, NAVD 88). Consistent with the SASSI2010 user's manual (Reference 2-y) recommendations, the half-space simulation consists of an additional ten layers with thickness that varies as function of frequency. The total depth of the site model used for the SSI analyses of the RB/FB exceeds two times the footprint dimension of the analyzed structure. Results of the sensitivity study presented in Appendix H demonstrate that the depth of the lower boundary of the site model does not affect the results of the SSI analysis.

As indicated in Figure 4.3-13, the RB/FB stick model is connected to the side walls at floor EL -11.5 m, -6.4 m, -0.68 m, and 4.5 m by a set of rigid beams. At the base of the model at EL -15.5 m, a rigid link is used to connect all the stick models to the center of the basemat. Figure 4.3-13 shows the connection between the RB/FB stick model and the foundation.

Figures 4.3-6 and 4.3-10 show the 3-D spring elements established at the RB/FB exterior wall/backfill interfaces for the PE and FE models, respectively. Springs are also established at the bottom of the structural (HOUSE) model to calculate reactions at the basemat interface with the underlying Zone III-IV rock. These spring elements are assigned global stiffness properties high enough to ensure they do not affect the dynamic response of the analyzed SSI system, but not so high that they cause numerical sensitivity resulting from significant digit saturation truncation. The interface spring elements provide spring force results that serve as input for calculation of the site-specific wall lateral pressure and foundation bearing pressure

demands. The spring force results also serve as input for the calculation of seismic driving forces for the site-specific stability evaluations.

5. ANALYSIS RESULTS

This section presents the results of the site-specific SSI analyses of the RB/FB models with upper bound stiffness properties and OBE damping values (Cases 1 through 6 in Table 4.2-1) for:

a Acceleration transfer functions for responses at key locations
b Acceleration transfer functions relative to outcrop input motion for responses at the top of the RB/FB, RCCV, Reactor Shield Wall (RSW), Pedestal and VW LMSMs
c Maximum acceleration of floor lumped masses and SDOF oscillator masses
d Maximum forces and moments of stick beam elements
e Maximum relative displacements
f Maximum lateral pressures on below-grade exterior walls
g ISRS for responses at key locations

Plots of amplitudes of the interpolated acceleration transfer function results for responses at RB/FB key locations demonstrate the sufficient accuracy of the interpolated results. The responses obtained from the analyses of different subgrade profiles are compared to evaluate the effects of soil property variations and different embedment configurations on the RB/FB seismic response.

The transfer function results indicate that the effects of variation of rock subgrade stiffness on the seismic response of the RB/FB structure are very small, resulting in insignificant shifts in peak response frequencies. Only the amplitudes of peak responses are affected by the variations of subgrade properties due to different subgrade damping. The comparisons of responses obtained from the analyses of the full and partial column profiles show that the relatively thin strata of saprolite and structural fill located above the top of Zone III rock have a negligible effect on the response of the heavy RB/FB. The differences between the responses obtained from the analyses of partially and fully embedded models are due to the differences in the energy content of the input motions used for the SSI analyses of partial and full column profiles at structural frequencies. The analysis of the UB full column profile mostly yields bounding horizontal responses due to the lower subgrade material damping and the higher energy content of the full column input motion at frequencies close to the structural resonance frequencies. The higher energy content of the full column input motion at these lower frequencies is due to the enhancements made on the design motion spectra to meet the NEI check as described in ISG-017 (Reference 2-q).

5.1 Transfer Function

Figures 5.1-1 through 5.1-6 present plots of the amplitudes of the acceleration transfer functions obtained from the SASSI2010 analyses of the RB/FB models with upper bound stiffness properties and OBE damping values (Cases 1 through 6 in Table 4.2-1) for the responses at the following key locations within the RB/FB:

Location	Node Number	SASSI Models Node Number
RB/FB Refueling Floor	109	190
RCCV Top Slab	208	280
VW Top	701	701
RSW Top	707	707
RPV Top	801	801
RB/FB Basemat	2	20

Figures 5.1-1 (a through f), Figures 5.1-2 (a through f), and Figures 5.1-3 (a through f) present plots of the amplitudes of the acceleration transfer functions from the analyses of the partial column profiles. Figures 5.1-4 (a through f), Figures 5.1-5 (a through f), and Figures 5.1-6 (a through f) present plots of the amplitudes of the acceleration transfer functions from the analyses of the full column profiles. Each figure includes three plots presenting the RB/FB responses in the three orthogonal directions due to the three earthquake components. The computed values of the transfer functions in these plots are depicted with dots. The interpolated values of the transfer functions are depicted by solid lines. The plots generally have no numerical anomalies in the interpolated transfer functions (e.g., sharp narrow spikes) that can potentially impact the accuracy of the frequency domain SSI analyses results. It was determined in Reference 2-cc, by using additional frequencies of analysis, that the isolated apparent anomaly in a few of the transfer function interpolations does not affect the accuracy of the corresponding responses.

The transfer function plots indicate that the co-directional responses (the responses in the direction of the applied earthquake) govern the seismic response of the RB/FB at the NA3 rock site. Figures 5.1-1f, 5.1-2f, and 5.1-3f present the transfer function results from the analyses of the BE, LB, and UB partial column profiles, respectively, for the response of the RB/FB basemat. The most pronounced cross-directional responses of the RB/FB basemat can be observed in the transfer function results in Figure 5.1-2f that are obtained from the analysis of the LB profile, thus indicating that the softer subgrade amplifies the torsional and rocking response of the RB/FB basemat. The comparisons of the amplitudes of the first peaks in the cross-directional response transfer functions indicate that among the cross-directional responses the rocking of the RB/FB basemat in the NS (X) direction is the most significant. The same observations regarding the rocking and torsional response of the RB/FB basemat can be made from the transfer functions plots in Figures 5.1-4f, 5.1-5f, and 5.1-6f that present the results from the SSI analyses of the BE, LB, and UB full column profiles, respectively.

As expected, the horizontal transfer function amplitudes are characterized with large peaks at frequencies that are close to the embedment shear column frequencies listed in Table 3.1-7 and at frequencies where dips occur in the response spectra of the input in-layer acceleration time histories presented in Figures 3.2-1 through 3.2-3. Therefore, these large peaks in the acceleration transfer function amplitudes that represent the response amplifications relative to the in-column input motion are not reflected in the ARS results presented in Section 5.3.

The large peaks at soil column frequencies are not present in the transfer functions representing the structural responses relative to the input outcrop motion making them a better indicator of structural response. These outcrop transfer functions are calculated using the following three steps:

1. FFT is performed on the time histories of in-layer and outcrop ground motion at the bottom of the RB/FB basemat elevation obtained from Reference 2-g.
2. The ratio between the in-layer and outcrop motion Fourier spectra yields transfer functions representing the transformation of the RB/FB design in-layer motion into an outcrop motion.
3. The product of the complex in-layer/outcrop transfer functions and the SASSI2010 calculated complex transfer functions of the structural response relative to the in-column motion provide the outcrop motion transfer functions (i.e., transfer functions of responses relative to the outcrop input motion).

Reference 2-bb documents the calculations of the transfer functions relative to the outcrop motion.

Figure 5.1-7 presents the transfer functions that represent the transformation of the in-layer motion time histories used as input for the SSI analysis of the BE, LB, and UB partial column profiles into horizontal and vertical RB/FB design outcrop motion acceleration time histories. The first valleys in the horizontal partial column motion in-layer/outcrop transfer functions occur at frequencies close to the rock embedment shear column frequencies listed in Table 3.1-7. Figure 5.1-8 presents the transfer functions for the transformation of the in-layer motion for SSI analyses of the BE, LB, and UB full column profiles into full column design outcrop motion. The first valleys in the horizontal full column motion in-layer/outcrop transfer functions occur at frequencies close to the in-situ soil (saprolite) embedment shear column frequencies listed in Table 3.1-7.

Figures 5.1-9 through 5.1-12 present the outcrop transfer function amplitudes for the co-directional responses of the RB/FB top, RCCV top, VW top, and RSW top, respectively, in the NS (X), EW (Y), and vertical (Z) directions. The plots compare the results from the analyses of the six soil profiles where the solid lines represent the results from the analyses of the RB/FB PE model and the dashed lines represent the results from the analyses of the RB/FB FE model. The plots also show the outcrop motion design spectra for the partial column and full column with solid and dashed lines, respectively. The comparisons in Figures 5.1-9 through 5.1-12 show the transfer function peaks at frequencies close to the natural frequencies of structures with negligible shifts in the peak frequencies. The sharp peaks in some of the outcrop function plots are due to the anomaly of the SASSI transfer function interpolation. These transfer function interpolation anomalies do not affect the accuracy of the calculated responses.

The variations of subgrade properties affect only the amplitudes of peak responses with the peaks of transfer function amplitudes obtained for the analyses of the UB subgrade properties

being the largest as a result of the lower damping of subgrade materials. The peaks in the transfer function amplitudes for the horizontal response of the RB/FB, RCCV, and VW are at lower frequencies where the full column input motion spectra exceed the partial column spectra.

The comparisons of outcrop motion transfer functions obtained from the analyses of the six subgrade profiles indicate that the NA3 rock subgrade has a very small effect on the seismic response of the RB/FB. The differences in responses obtained from the analyses of different subgrade profiles are due to the differences in the subgrade material damping and the different energy content of the input motion at natural frequencies of the RB/FB structures. The outcrop motion transfer functions indicate that the analysis of the UB full column profile mostly yields bounding horizontal responses of the RB/FB, RCCV, and VW.

5.2 Maximum Accelerations and Member Forces

Appendix A provides tables that have results for the RB/FB maximum accelerations and member forces from the SSI analysis of the RB/FB model with upper bound stiffness properties and OBE damping values for all six subgrade profiles (Cases 1 through 6 in Table 4.2-1). The plots of maximum accelerations and maximum stick member shear forces and torsional moments are presented herein to illustrate the effect of different subgrade conditions and embedment configurations on the RB/FB maximum responses.

Figures 5.2-1 (a through e) and Figures 5.2-2 (a through e) present comparisons of the results for maximum absolute accelerations at the RB/FB mass locations from the analyses of the RB/FB PE and RB/FB FE models, respectively. Tables 5.2-1 and 5.2-2 compare the maximum vertical and horizontal acceleration results for the RB/FB slab and wall SDOF oscillators obtained from the analyses of the six subgrade profiles. Figures 5.2-3 (a through e) and Figures 5.2-4 (a through e) present comparisons of the maximum shear forces and torsion results obtained from the analyses of the RB/FB PE and RB/FB FE models, respectively. The comparisons of the maximum member force and acceleration results show that the analyses of the UB subgrade profiles typically govern the RB/FB maximum responses.

To illustrate how different embedment configurations affect the RB/FB maximum accelerations and member force responses, Figures 5.2-5 (a through e) and Figures 5.2-6 (a through e) compare the envelope of the maximum response results obtained from the analysis of the RB/FB PE model and RB/FB FE model. As discussed in Section 5.1, the differences between the responses obtained from the analyses of the partially and fully embedded models are primarily due to the differences in the energy content of the input motions used for the SSI analyses of the partial and full column profiles at structural frequencies.

The observations made from the comparisons of maximum acceleration and member force responses are consistent with the outcrop motion transfer function results shown in Section 5.1.

5.3 Acceleration Response Spectra

Comparisons of the 5% damped ARS results are presented for the same selected locations within the RB/FB as the ones listed in Section 5.1 for the transfer functions and some selected slab and wall oscillators which have the largest weight at each elevation.

The following is the procedure used for the development of the floor ISRS:

1. For each of the four outrigger locations (ne, nw, se, sw) at particular floor elevations, three components (X, Y, and Z) of the ARS due to input motion in three directions (X, Y, and Z) are calculated by the SASSI MOTION module to obtain a total of 36 ARS results:

$$\text{Outrigger}^{(ne)} \rightarrow (f_{XX}^{(ne)}, f_{XY}^{(ne)}, f_{XZ}^{(ne)}, f_{YX}^{(ne)}, f_{YY}^{(ne)}, f_{YZ}^{(ne)}, f_{ZX}^{(ne)}, f_{ZY}^{(ne)}, f_{ZZ}^{(ne)})$$

$$\text{Outrigger}^{(nw)} \rightarrow (f_{XX}^{(nw)}, f_{XY}^{(nw)}, f_{XZ}^{(nw)}, f_{YX}^{(nw)}, f_{YY}^{(nw)}, f_{YZ}^{(nw)}, f_{ZX}^{(nw)}, f_{ZY}^{(nw)}, f_{ZZ}^{(nw)})$$

$$\text{Outrigger}^{(se)} \rightarrow (f_{XX}^{(se)}, f_{XY}^{(se)}, f_{XZ}^{(se)}, f_{YX}^{(se)}, f_{YY}^{(se)}, f_{YZ}^{(se)}, f_{ZX}^{(se)}, f_{ZY}^{(se)}, f_{ZZ}^{(se)})$$

$$\text{Outrigger}^{(sw)} \rightarrow (f_{XX}^{(sw)}, f_{XY}^{(sw)}, f_{XZ}^{(sw)}, f_{YX}^{(sw)}, f_{YY}^{(sw)}, f_{YZ}^{(sw)}, f_{ZX}^{(sw)}, f_{ZY}^{(sw)}, f_{ZZ}^{(sw)})$$

Where, f_{ij} represent ARS for response in j-direction due to earthquake in i-direction

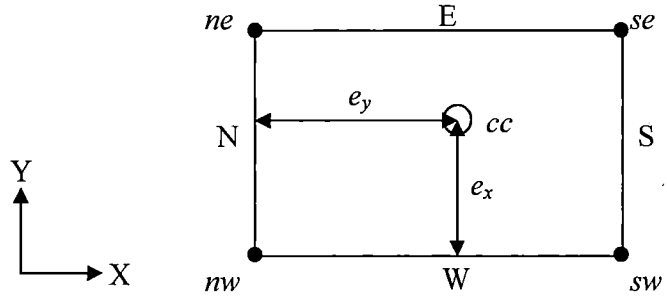

2. The spectra for the nodal responses due to the three input motion components in the X, Y, and Z directions are combined using the SRSS method to obtain a total of 12 ARS of the response of each of the four outrigger nodes (ne, nw, se, sw) in three orthogonal directions (X, Y, and Z):

$$f_X^{(ne)} = \sqrt{f_{XX}^{(ne)2} + f_{YX}^{(ne)2} + f_{ZX}^{(ne)2}} \quad , \quad f_Y^{(ne)} = \sqrt{f_{XY}^{(ne)2} + f_{YY}^{(ne)2} + f_{ZY}^{(ne)2}}$$

$$f_Z^{(ne)} = \sqrt{f_{XZ}^{(ne)2} + f_{YZ}^{(ne)2} + f_{ZZ}^{(ne)2}}$$

$$f_X^{(nw)} = \sqrt{f_{XX}^{(nw)2} + f_{YX}^{(nw)2} + f_{ZX}^{(nw)2}} \quad , \quad f_Y^{(nw)} = \sqrt{f_{XY}^{(nw)2} + f_{YY}^{(nw)2} + f_{ZY}^{(nw)2}}$$

$$f_Z^{(nw)} = \sqrt{f_{XZ}^{(nw)2} + f_{YZ}^{(nw)2} + f_{ZZ}^{(nw)2}}$$

$$f_X^{(se)} = \sqrt{f_{XX}^{(se)2} + f_{YX}^{(se)2} + f_{ZX}^{(se)2}} \quad , \quad f_Y^{(se)} = \sqrt{f_{XY}^{(se)2} + f_{YY}^{(se)2} + f_{ZY}^{(se)2}}$$

$$f_Z^{(se)} = \sqrt{f_{XZ}^{(se)2} + f_{YZ}^{(se)2} + f_{ZZ}^{(se)2}}$$

$$f_X^{(sw)} = \sqrt{f_{XX}^{(sw)2} + f_{YX}^{(sw)2} + f_{ZX}^{(sw)2}} \quad , \quad f_Y^{(sw)} = \sqrt{f_{XY}^{(sw)2} + f_{YY}^{(sw)2} + f_{ZY}^{(sw)2}}$$
$$f_Z^{(sw)} = \sqrt{f_{XZ}^{(sw)2} + f_{YZ}^{(sw)2} + f_{ZZ}^{(sw)2}}$$

3. The ARS calculated for all four outrigger locations are enveloped to obtain the three ARS for the floor response in three orthogonal directions (X, Y, and Z):

$$F_X = max(f_X^{(ne)}, f_X^{(nw)}, f_X^{(se)}, f_X^{(sw)})$$
$$F_Y = max(f_Y^{(ne)}, f_Y^{(nw)}, f_Y^{(se)}, f_Y^{(sw)})$$
$$F_Z = max(f_Z^{(ne)}, f_Z^{(nw)}, f_Z^{(se)}, f_Z^{(sw)})$$

4. The calculations in steps 1 to 3 are performed for each of the six SSI analysis cases considered. The final design ISRS for each orthogonal direction is calculated by broadening the envelope of the ARS results of the six SSI analysis cases as presented in Appendix E.

5. The calculations in steps 1 to 4 are performed for each ISRS damping value.

The following is the procedure for development of ISRS for the out-of-plane responses of flexible slabs and walls:

1. For each SDOF oscillator, the ARS of the SDOF response due to the input motion in three directions (X, Y, and Z) are calculated by the SASSI MOTION module to obtain a total of three ARS results:

   Slabs SDOF $\rightarrow (f_{XZ}, f_{YZ}, f_{ZZ})$

   EW Walls SDOF $\rightarrow (f_{XX}, f_{YX}, f_{ZX})$

   NS Walls SDOF $\rightarrow (f_{XY}, f_{YY}, f_{ZY})$

2. The spectra for the SDOF responses due to the three input motion components in the X, Y, and Z directions are combined for each spectral frequency using the SRSS method to obtain the SDOF ARS:

   Slabs SDOF $\rightarrow \quad f_Z^{(SDOF)} = \sqrt{f_{XZ}^{\ 2} + f_{YZ}^{\ 2} + f_{ZZ}^{\ 2}}$

   EW Walls SDOF $\rightarrow \quad f_X^{(SDOF)} = \sqrt{f_{XX}^{\ 2} + f_{YX}^{\ 2} + f_{ZX}^{\ 2}}$

   NS Walls SDOF $\rightarrow \quad f_Y^{(SDOF)} = \sqrt{f_{XY}^{\ 2} + f_{YY}^{\ 2} + f_{ZY}^{\ 2}}$

3. The calculations in steps 1 to 2 are performed for each of the six SSI analysis cases considered. The final site-specific design SDOF ISRS is calculated by ±15% broadening the envelope of the ARS results of the six SSI analysis cases as presented in Appendix E.

4. The site-specific design SDOF ISRS are enveloped as specified in Sections A.3.3.5.4 and Section A.3.3.8 of Reference 2-k, to obtain the final ISRS for site-specific design of equipment attached to particular slabs and walls, respectively.

Figures 5.3-1 (a through f), Figures 5.3-2 (a through f) and Figures 5.3-3 (a through f), respectively, present the 5% damped ISRS for the response in NS (x), EW (y) and vertical (z) directions at key locations within the RB/FB obtained from the SSI analyses of the RB/FB model with upper bound stiffness properties and OBE damping values (Cases 1 to 6 in Table 4.2-1). The figures in Appendix F present the 5% damped ISRS for the responses of SDOF masses. The figures present the ISRS obtained from the analyses of the PE model with solid lines. The ISRS obtained from the analyses of the FE model are presented with dashed lines. The site-specific ISRS are compared with the corresponding standard design ISRS that are presented with solid black lines.

The comparison of the ISRS results obtained from the different site-specific SSI analysis cases show that the responses obtained from the analyses of the UB subgrade profiles govern the ISRS with the exception of narrow frequency intervals (<25 Hz) where the analyses of the BE and LB profiles can be bounding. The results from the analyses of the full column profiles bound the horizontal ISRS for frequencies between 3 and 8 Hz and in general bound the vertical ISRS for frequencies between 3 and 15 Hz reflecting the higher energy content of the full column input motion at lower frequencies.

The comparisons in Figures 5.3-1 through 5.3-3 indicate that the site-specific ISRS exceed the corresponding standard design ISRS mainly above 10 Hz where the site-specific FIRS exceed the Certified Seismic Design Response Spectra (CSDRS). The peak exceedances occur in the site-specific horizontal ISRS close to the natural frequencies of the containment internal structures (10 to 30 Hz). The site-specific vertical ISRS exceed the standard design ISRS at frequencies above 10 Hz. The exceedances in the SDOF oscillator ISRS presented in Appendix F occur mainly at frequencies corresponding to the frequencies of the oscillators.

The ISRS exceedances are due to the lower OBE structural damping values used for the site-specific SSI analysis versus the SSE damping values used for standard design SSI analyses. The fact that the NA3 site-specific design motion has higher energy content than the standard design CSDRS at frequencies close to the SSI frequencies of the RB/FB structure also explain the exceedances in ISRS.

5.4 Maximum Relative Displacements

The following is the procedure used for development of the maximum floor displacements relative to the free-field motion:

1. For each of the four outrigger locations (ne, nw, se, sw) at particular floor elevations, three components (X, Y, and Z) of maximum relative displacements due to the input motion in three directions (X, Y, and Z) are calculated by the SASSI MOTION module to obtain a total of 36 maximum relative displacement values:

Outrigger$^{(ne)} \rightarrow (d_{XX}^{(ne)}, d_{XY}^{(ne)}, d_{XZ}^{(ne)}, d_{YX}^{(ne)}, d_{YY}^{(ne)}, d_{YZ}^{(ne)}, d_{ZX}^{(ne)}, d_{ZY}^{(ne)}, d_{ZZ}^{(ne)})$

Outrigger$^{(nw)} \rightarrow (d_{XX}^{(nw)}, d_{XY}^{(nw)}, d_{XZ}^{(nw)}, d_{YX}^{(nw)}, d_{YY}^{(nw)}, d_{YZ}^{(nw)}, d_{ZX}^{(nw)}, d_{ZY}^{(nw)}, d_{ZZ}^{(nw)})$

Outrigger$^{(se)} \rightarrow (d_{XX}^{(se)}, d_{XY}^{(se)}, d_{XZ}^{(se)}, d_{YX}^{(se)}, d_{YY}^{(se)}, d_{YZ}^{(se)}, d_{ZX}^{(se)}, d_{ZY}^{(se)}, d_{ZZ}^{(se)})$

Outrigger$^{(sw)} \rightarrow (d_{XX}^{(sw)}, d_{XY}^{(sw)}, d_{XZ}^{(sw)}, d_{YX}^{(sw)}, d_{YY}^{(sw)}, d_{YZ}^{(sw)}, d_{ZX}^{(sw)}, d_{ZY}^{(sw)}, d_{ZZ}^{(sw)})$

Where, d_{ij} represent displacement in j-direction due to earthquake in i-direction

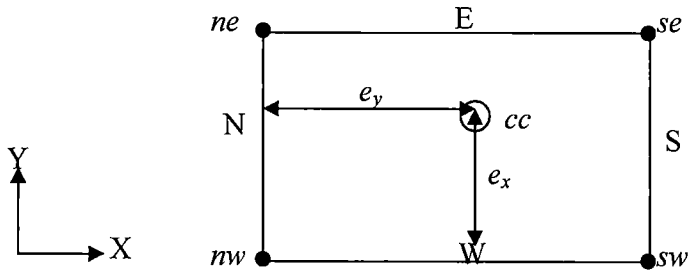

2. The nodal displacements due to the three input motion components in the X, Y, and Z directions are combined using the SRSS method to obtain a total of twelve values of the maximum displacements of each of the four outrigger nodes (ne, nw, se, sw) in three orthogonal directions (X, Y, and Z):

$$d_X^{(ne)} = \sqrt{d_{XX}^{(ne)2} + d_{YX}^{(ne)2} + d_{ZX}^{(ne)2}}, \quad d_Y^{(ne)} = \sqrt{d_{XY}^{(ne)2} + d_{YY}^{(ne)2} + d_{ZY}^{(ne)2}}$$

$$d_Z^{(ne)} = \sqrt{d_{XZ}^{(ne)2} + d_{YZ}^{(ne)2} + d_{ZZ}^{(ne)2}}$$

$$d_X^{(nw)} = \sqrt{d_{XX}^{(nw)2} + d_{YX}^{(nw)2} + d_{ZX}^{(nw)2}}, \quad d_Y^{(nw)} = \sqrt{d_{XY}^{(nw)2} + d_{YY}^{(nw)2} + d_{ZY}^{(nw)2}}$$

$$d_Z^{(nw)} = \sqrt{d_{XZ}^{(nw)2} + d_{YZ}^{(nw)2} + d_{ZZ}^{(nw)2}}$$

$$d_X^{(se)} = \sqrt{d_{XX}^{(se)2} + d_{YX}^{(se)2} + d_{ZX}^{(se)2}}, \quad d_Y^{(se)} = \sqrt{d_{XY}^{(se)2} + d_{YY}^{(se)2} + d_{ZY}^{(se)2}}$$

$$d_Z^{(se)} = \sqrt{d_{XZ}^{(se)2} + d_{YZ}^{(se)2} + d_{ZZ}^{(se)2}}$$

$$d_X^{(sw)} = \sqrt{d_{XX}^{(sw)2} + d_{YX}^{(sw)2} + d_{ZX}^{(sw)2}}, \quad d_Y^{(sw)} = \sqrt{d_{XY}^{(sw)2} + d_{YY}^{(sw)2} + d_{ZY}^{(sw)2}}$$

$$d_Z^{(sw)} = \sqrt{d_{XZ}^{(sw)2} + d_{YZ}^{(sw)2} + d_{ZZ}^{(sw)2}}$$

3. The maximum displacements calculated for all four outrigger locations are enveloped to obtain the maximum displacements of the floor in the X, Y, and Z directions:

$D_X = max(d_X^{(ne)}, d_X^{(nw)}, d_X^{(se)}, d_X^{(sw)})$

$D_Y = max(d_Y^{(ne)}, d_Y^{(nw)}, d_Y^{(se)}, d_Y^{(sw)})$

$D_Z = max(d_Z^{(ne)}, d_Z^{(nw)}, d_Z^{(se)}, d_Z^{(sw)})$

4. The calculations in steps 1 to 3 are performed for each of the six SSI analysis cases considered. The final site-specific values of the design maximum displacements of the floor relative to the free-field motion are obtained as the envelope of the results of the six SSI analysis cases.

Appendix A presents the results of the site-specific SSI analyses of RB/FB models with upper bound stiffness properties and OBE damping values (Cases 1 through 6 in Table 4.2-1) for maximum relative displacements between RB/FB key locations and the displacements of RB/FB floors relative to the free-field motion. Tables 5.4-1 and 5.4-2 present the maximum displacements of slab and wall oscillators relative to the free-field motion.

5.5 Maximum Lateral Pressures on Below-Grade Exterior Walls

As discussed in Section 4.3, spring elements between "double nodes" are installed on the foundation and soil/rock interfaces to calculate the SSI forces. The lateral seismic pressures on the RB/FB below-grade walls are calculated from the SASSI analysis results for the spring forces installed between the shells on the sides of the embedded portion of the RB/FB model and the surrounding near-field elements. The calculations are performed in the following steps:

1. The time histories of the spring forces are extracted from each SASSI run for each contact spring element.
2. The absolute value of the co-directional spring force magnitudes obtained from the analyses of the three orthogonal input earthquake motion components are combined absolutely in the time domain.
3. The maximum lateral forces normal to the wall plane are obtained at all contact spring elements.
4. The absolute values of the maximum lateral forces for all spring elements at the same elevations are summed up to obtain the total maximum lateral forces at the respective elevations for the four RB/FB below-grade exterior walls separately.
5. The total maximum lateral forces are divided by the tributary area for each node group at the same elevation to obtain the soil pressure distribution for the four exterior walls.

Figure 5.5-1 provides plots of the results of the site-specific SSI analysis of the RB/FB models with upper bound stiffness properties and OBE damping values (Cases 1 through 6 in Table 4.2-1) for the maximum seismic lateral pressures on the RB/FB below-grade exterior walls. The comparison of the results obtained from different analyses show that the variation of the soil properties has a very small effect on the calculated dynamic pressures on the exterior walls. Very small differences can be observed between the lateral pressures

calculated from the analysis of the BE, LB, and UB profiles. The results obtained from the analyses of full column profiles show that the pressures on the RB/FB exterior walls from the structural fill/saprolite are small relative to those from the concrete fill/Zone III rock. The analyses of both embedment configurations yield maximum lateral pressures at the top of the Zone III rock (elevation -0.68 m) and bottom of the RB/FB basemat (elevation -15.5 m).

In the site specific RB/FB stability evaluation report (Reference 2-s), the dynamic lateral pressure results obtained from the site-specific SSI analysis documented in this report are combined with site-specific static pressures to develop the total site-specific lateral load demands on the RB/FB below-grade exterior walls. These total site-specific lateral loads are compared with the corresponding standard design loads in order to determine exceedances of the NA3 site-specific lateral loads demands relative to the standard design.

5.6 Base Reactions and Contact Pressures

The results of the SSI analyses for contact spring forces are also used to calculate the time histories of the seismic driving forces used as input for the sliding stability evaluations and dynamic bearing pressure calculations documented in Reference 2-s. The time histories of the horizontal and vertical driving seismic forces in the three orthogonal directions are calculated as the algebraic sum of the spring forces in the three directions at each time step from all contact spring elements located at the interfaces between the RB/FB and the surrounding soil.

The contact spring elements located at the bottom of the RB/FB basemat provide the input needed for the calculation of the dynamic bearing pressures in Reference 2-s. The calculations of the dynamic bearing pressures are based on the time histories of:

- The overturning base moments calculated for both the horizontal directions by summing algebraically the moments generated by each contact spring reaction at the bottom of the RB/FB basemat
- The vertical driving seismic forces calculated as the algebraic sum of the vertical spring forces at each time step from all contact spring elements located at the interface between the bottom of the RB/FB basemat and the rock

The time histories of the vertical spring forces obtained from the contact springs located at the bottom of the RB/FB basemat are also used to develop the base contact pressure plots that are used to calculate the minimum base contact area. These calculations are performed in the following steps:

1. Extract the RB/FB basemat bottom contact spring vertical forces $P_{jZ}^{i}(t)$ at each time step from the SASSI runs, where j =*X, Y* and *Z* is the input excitation direction and *i* is the contact spring element number.

   The vertical forces of the spring element *i* that consider the response due to phasing differences of the input, or the input direction reversal can be obtained as

$$S^i_{jZ}(t) = (-1)^q P^i_{jZ}(t)$$

Where, $q=2$ when the input j is along the positive j direction, and $q=1$ when input direction is reversed.

Calculate the total vertical seismic base reaction as:

$$S_Z(t) = \sum_{i=1}^{N} \left(S^i_{XZ}(t) + S^i_{YZ}(t) + S^i_{ZZ}(t) \right)$$

where, N is the total number of the contact spring elements located at the RB/FB basemat bottom.

2. Calculates the total vertical base reaction:

$$R_V(t) = D - B - S_Z(t)$$

where, D is RB/FB seismic weight and B is groundwater buoyancy force.

3. Calculate the overturning moments toward the NS and EW direction induced by the vertical seismic base reactions as follows:

$$M_{NS}(t) = \sum_{i=1}^{N} \left(S^i_{XZ}(t) + S^i_{YZ}(t) + S^i_{ZZ}(t) \right) * X_i$$

$$M_{EW}(t) = \sum_{i=1}^{N} \left(S^i_{XZ}(t) + S^i_{YZ}(t) + S^i_{ZZ}(t) \right) * Y_i$$

where, *Xi* and *Yi* are the NS and EW directional coordinates of the contact spring location in the coordinate system with origin at the geometrical center of the basemat, respectively.

4. Calculate the time histories of base vertical reaction eccentricity as:

$$Ecc(t) = \frac{1}{R_V(t)} \sqrt{M_{NS}(t)^2 + M_{EW}(t)^2}$$

5. The critical time step (t_c), when the maximum uplift of the RB/FB basemat occurs, is determined as the time instance when the value of the base vertical reaction eccentricity *Ecc(t)* is the largest.

6. The plot of the base contact area is developed using the base spring force results at the critical time step that yields the maximum value for base vertical reaction eccentricity.

7. The base contact pressures on the tributary area of the spring element *i* are calculated by dividing the base spring forces by its tributary area and then subtracting the uniform static pressure due to the effective weight of the building (the RB/FB seismic weight minus the ground water buoyancy) as follows:

$$\sigma_{iZ} = \frac{S^i_{XZ}(t_c) + S^i_{YZ}(t_c) + S^i_{ZZ}(t_c)}{A_i} - \frac{D - B}{A}$$

where, A is the footprint area of the basemat and A_i is the tributary area of the spring element *i*. The positive value of σ_{iZ} indicates that the tributary area is in tension (or uplifted).

8. The contact area of the foundation is determined as the total area (ΣA_i) where the value of the contact pressure σ_{iZ} is negative.

According to the guidance in SRP Acceptance Criteria 3.7.2.II.4 (Reference 2-p), uplift for non-symmetric structures may be more affected by the phasing between the three directions of input motions. There are a total of eight possible combinations of the three orthogonal seismic input directions if reversal of each of the input is considered for input phasing effects. Since the RB/FB is symmetrical with respect to NS (X) direction vertical plane, the direction of the input motion in the EW (Y) direction has a negligible phasing effect on the calculated uplift area. The only significant eccentricity of the building is with respect to the EW direction vertical plane. Therefore, the number of the combinations considered in the contact ratio (uplift) evaluation is reduced to the following four (4) listed below:

a) $R_D+R_B+Ex+Ey+Ez$

b) $R_D+R_B+Ex-Ey-Ez$

c) $R_D+R_B-Ex+Ey+Ez$

d) $R_D+R_B-Ex-Ey-Ez$

where, $+Ej$ represent the effect of vertical spring forces $S'_{jZ}(t)=P'_{jZ}(t)$ when $q=2$; and $-Ej$ represents the effect of vertical spring forces $S'_{jZ}(t)=(-1)P'_{jZ}(t)$ when $q=1$, as defined in Step 1. above;

R_D *and* R_B, respectively, are the effects of dead weight and groundwater buoyancy on the base contact pressures.

Figure 5.6-1 presents the time histories of the eccentricities of vertical base reactions obtained from the set of six SSI analyses performed on the RB/FB model with upper bound stiffness properties and OBE damping (analysis Cases 1 to 6 in Table 4.2-1). The critical instances of time when the eccentricity of the vertical base reaction has maximum value are identified with red lines. Table 5.6-1 that summarizes the calculations of maximum base reaction eccentricities and associated minimum contact ratios shows that the analysis of the UB full column subgrade profile yields the minimum base contact ratio.

Figures 5.6-2a and 5.6-2b, respectively, present contour plots of the SASSI2010 base contact pressure results for the critical partial and full column subgrade profiles for the critical instances of time (t = 3.225 sec for the UB partial column profile and the UB full column profile) when the uplift of RB/FB basemat is the largest. The grid lines in Figures 5.6-2a and 5.6-2b schematically show the mesh of the basemat shell elements. The positive values of the contact pressures in Figures 5.6-2a a) and 5.6-2b a) represent tension of the base contact springs. The negative values in the figures represent compression of the base contact springs

and are used to determine the portion of the basemat that is in contact with the underlying subgrade.

Note that, in Figures 5.6-2a a) and 5.6-2b a), there are concentrated tension zones presented in the area immediately adjacent to the node that connects the rigid beam element and the basemat shell elements. These concentrated tension zones are due to the structural modeling simplification where the LMSM is connected with the basemat shell elements through only one node that is close to the center of the basemat. Figure 4.3-13 of this report shows the connection between the LMSM and the basemat which is consistent with the modeling approach used for the standard design analyses described in Section 8.3 of Reference 2-k. In order to account for the effects of this modeling simplification on the foundation uplift results, the contact pressures calculated in Step 7 are adjusted by redistributing the total tension force in the rigid beam element uniformly to all the contact spring elements at the bottom of the RB/FB basemat. Plots b) in Figures 5.6-2a and 5.6-2b show the adjusted contact area results. In the figures, the shaded areas are the uplifted areas representing the tributary areas of the contact springs with tension force.

The results of the uplift evaluation in Table 5.6-1 and the plots in Figure 5.6-2 show that the contact area between the RB/FB basemat and the underlying subgrade remains larger than 80% which, per guidance of SRP 3.7.2 (Reference 2-p), ensures that the possible uplift of the RB/FB basemat has a negligible effect on the RB/FB seismic response and on the results of site-specific RB/FB SSI analyses documented in this report that are performed on linear elastic models.

Appendix J presents the alternative uplift calculations that are performed to further address uncertainties related to the modeling of the basemat stiffness in the RB/FB dynamic model used for the SSI analyses. As shown in Figures 4.3-8 and 4.3-12, which present the RB/FB complex dynamic models used for the SSI analyses of partial and full column profiles, respectively, shell elements are used to model the basemat and the below-grade exterior walls. Stick elements are used to represent the stiffness of the interior walls below grade elevations and all above grade walls. These stick elements only represent the overall stiffness of the walls for the purpose of calculating floor responses and, unlike the shells modeling the in-plane stiffness of exterior walls, do not capture the contribution of the inner walls and the RPV pedestal to the overall stiffness of the RB/FB complex basemat. Therefore, the RB/FB dynamic model underestimates the stiffness of the basemat, which in turn affects the distribution of base pressures used for calculations of the minimum foundation contact area.

In order to address the effect of basemat stiffness on the RB/FB foundation uplift calculations, alternative calculations are performed in Appendix J that consider the bounding case of an absolutely rigid foundation. These alternative calculations are performed for the two critical UB partial column and UB full column analysis cases. The results of the alternative foundation uplift calculations in Appendix J demonstrate that the uncertainties related to the RB/FB complex foundation stiffness do not affect the conclusions of the SASSI2010 uplift analyses presented in Figure 5.6-2.

6. ENVELOPING SEISMIC RESPONSES

The results from the site-specific SSI analyses of the RB/FB models with upper bound stiffness properties and OBE damping values (Cases 1 through 6 in Table 4.2-1) are enveloped and compared with the corresponding standard design envelopes documented in Reference 2-k in order to determine the exceedances of the NA3 site-specific seismic demands relative to the corresponding standard design seismic demands. The site-specific enveloping seismic responses presented in this report form the basis for seismic design and evaluation of the RB/FB at the NA3 site.

6.1 Enveloping Structural Load Demands

The site-specific seismic structural loads representative of the seismic demands on the RB/FB structure are developed following the methodology used to develop the standard design enveloping maximum structural loads presented in Reference 2-k. The horizontal load demands on the RB/FB structures are developed from the diagrams of the maximum enveloping shear forces and maximum enveloping torsional moments obtained as the envelope of the member force results from the analyses of the six subgrade profiles. The vertical site-specific seismic load demands on the RB/FB structures are developed from the diagrams of the maximum enveloping vertical floor mass accelerations obtained as the envelope of the maximum acceleration results from the analyses of the six subgrade profiles. The maximum enveloping bending moments are also used for the structural evaluation of the RB/FB to account for the effects of floor rocking on the wall axial forces. The results for maximum enveloping vertical accelerations of the SDOF oscillator masses are used to develop the local out-of-plane load demands on the RB/FB flexible slabs and walls.

Tables 6.1-1 (a through f) present the seismic shear forces and moments obtained as the envelope of the results from the site-specific SSI analyses of all six subsurface profiles and compares them with the corresponding standard design loads. The torsional moments in these tables and similar tables in the appendices are the calculated results from the SSI analyses. They need to be combined with the accidental torsion in the structural evaluation. Tables 6.1-2 (a through e) present the comparison of envelopes of site-specific maximum accelerations at floor lumped mass locations with the corresponding standard design enveloping accelerations. The comparisons of the diagrams of the site-specific horizontal and vertical load demands with the corresponding seismic loads used for standard design are illustrated in Figures 6.1-1 (a through e) and Figures 6.1-2 (a through e). Figures 6.1-1 compare the shear force and torsion diagrams that define the horizontal seismic load demands on the RB/FB structures. Figures 6.1-2 compare the maximum vertical accelerations and bending moment diagrams that define the vertical seismic load demands on the RB/FB structures.

Table 6.1-3 presents the site-specific enveloping out-of-plane load demands on the RB/FB flexible slabs obtained as the envelope of the results of the SSI analysis of the RB/FB model with the upper bound stiffness properties and the OBE damping values (Cases 1 through 6 in Table 4.2-1). Table 6.1-4 presents the site-specific out-of-plane load demands on the RB/FB flexible walls enveloping the results obtained from Cases 1 through 6. Tables 6.1-3 and 6.1-4

compare the site-specific enveloping out-of-plane load demands on the RB/FB flexible slabs and walls with the magnitudes of the corresponding loads used in Reference 2-1 for the standard design of the RB/FB structures.

The weighted average out-of-plane accelerations presented in Tables 6.1-3 and 6.1-4 represent the total site-specific seismic load demands on the flexible slabs and walls that include the contribution of both:

- The flexible modes of vibration represented by the maximum accelerations of the SDOF oscillators
- The rigid modes of vibration represented by the maximum accelerations of the floor lumped masses

Appendix D describes the methodology used for the calculation of the site-specific out-of-plane loads on the flexible slabs and walls that is identical to the methodology used in Reference 2-1 for the standard design of the RB/FB structures. The site-specific out-of-plane load demands on flexible slabs and walls are calculated using the SSI analysis results for the maximum accelerations of the floor lumped masses presented in Appendix A and the maximum accelerations of SDOF oscillator masses presented in Tables 5.2-1 and 5.2.2.

Table 6.1-5 presents the site-specific enveloping relative displacements and reactions for the RPV stabilizer and the D/F.

The comparisons presented in Figure 6.1-1, Figure 6.1-2, and Tables 6.1-1 through 6.1-4 indicate that the enveloping site-specific load demands can exceed the corresponding loads used for the standard design of the RB/FB structures. The comparisons in Figure 6.1-1 and Table 6.1-1 indicate that the NA3 site-specific horizontal load demands on the RB/FB walls are enveloped by the standard design with exception to the NS shear load demands on the VW and RSW that exceed the corresponding standard design loads at elevations above 7.5 m. Comparisons in Figure 6.1-2 indicate larger exceedances in vertical loads at higher elevations above 8.0 m can increase the axial stress demands and reduce the capacity of the reinforced concrete members. The most significant exceedances can be observed for the local out-of-plane loads on the flexible walls and the slabs located at elevations of 17.5 m and above. The maximum exceedance of 58% is calculated for the out-of-plane vertical load on the M/S tunnel slab.

Site-specific evaluations of the RB/FB structures are performed to address these exceedances in the sites-specific load demands and calculate the available margins of RB/FB structures at the NA3 site. These site-specific evaluations use site-specific seismic loads that are developed based on the results obtained from the site-specific SSI analysis of the RB/FB presented in this report.

6.2 Enveloping Maximum Displacements

Table 6.2-1 presents comparisons of the site-specific enveloping maximum relative displacement between RB/FB key locations with the corresponding standard design

enveloping relative displacements. Table 6.2-2 presents the site specific enveloping maximum displacements of RB/FB floor locations relative to free-field motion and compares them with the corresponding standard design displacements. The comparisons of the site-specific enveloping displacements with the corresponding standard design values show that the NA3 high frequency design motion results in displacements that are enveloped by the standard design in general but with few exceedances, as indicated in Table 6.2-1. The exceedance will be incorporated into the site-specific evaluation.

The site-specific enveloping maximum displacements of slab and floor SDOF oscillators are presented in Tables 5.4-1 and 5.4-2. Table 5.4-1 shows that only the NA3 envelope of vertical relative displacement of Node 9103 exceeds corresponding standard design vertical displacement (1.38 cm vs. 1.27 cm). However, the maximum vertical displacements of the roof oscillators (nodes 9101 through 9108) are enveloped for design consideration. Therefore, the enveloping NA3 vertical displacement of the roof is 1.38 cm which is much smaller than 4.99 cm of the standard design.

6.3 Site-Specific Design ISRS

Appendix E presents figures of site-specific enveloping ISRS for critical damping ratios 2, 3, 4, 5, 7, 10, and 20% at all locations in the RB/FB that are peak broadened by $\pm$15% and valley filled. These ISRS represent the envelope of ISRS results from the site-specific SSI analyses of the RB/FB model with upper bound stiffness properties and OBE damping (analysis Cases 1 to 6 in Table 4.2-1). These serve as the basis for the site-specific design and qualification of the RB/FB equipment and components.

7. CONCLUSIONS

The following are conclusions from the results of the NA3 site-specific SSI analyses of the RB/FB structures and components:

- Site-specific seismic demands slightly exceed the seismic demands used for the standard design of the RB/FB structures and components.
- The site-specific evaluation of the RB/FB structures and components use input seismic loads that are based on the site-specific enveloping loads presented in Section 6.1. In order to address the effects of structural stiffness variation, the enveloping loads presented in Section 6.1 are amplified as described in Section B.5 of Appendix B to bound the effects of concrete cracking. Reference 2-n presents these enhanced bounding seismic structural loads used as input for the site-specific evaluations of the RB/FB structures and components and compares them with the corresponding seismic loads used for the standard design.
- Site-specific enveloping ISRS presented in Appendix E are developed for all damping values and locations of the RB/FB based on the analyses of the RB/FB models with upper bound stiffness properties and OBE damping. In order to address the effects of structural stiffness variation, the site-specific evaluations of the

spent/new fuel storage racks, PCCS condensers, drywell head, GDCS pool structure, upper/lower personnel airlocks, upper/lower drywell equipment hatches and wetwell equipment hatch use ISRS that are enhanced as described in Appendix B. Reference 2-n presents these enhanced bounding ISRS used as input for the site-specific evaluations of the above structures and components.

- Reference 2-n also presents the enhanced bounding ISRS for the response of the RB/FB at the key floor locations listed in Section 5.1. Other ISRS shall also be enhanced as described in Appendix B and Reference 2-n.

Table 3.1-1 BE In-Situ Strain Compatible Dynamic Subsurface Properties

Layer #	Thickness (m)	Top-Depth (m)	Unit Weight (t/m^3)	V_s (m/s)	V_p (m/s)	Damping (%)
1	0.61	0.00	2.00	277	678	2.07
2	0.76	0.61	2.00	267	761	3.38
3	0.76	1.37	2.00	267	761	3.38
4	0.76	2.13	2.08	397	1667	2.89
5	0.76	2.90	2.08	397	1667	2.89
6	0.76	3.66	2.08	575	1549	2.50
7	0.76	4.42	2.08	575	1549	2.50
8	0.91	5.18	2.32	1318	3229	0.58
9	0.91	6.10	2.32	1318	3229	0.58
10	0.91	7.01	2.32	1318	3229	0.58
11	0.91	7.92	2.32	1318	3229	0.58
12	0.91	8.84	2.32	1318	3229	0.58
13	0.91	9.75	2.32	1318	3229	0.58
14	0.91	10.67	2.32	1318	3229	0.58
15	0.61	11.58	2.32	1318	3229	0.58
16	0.91	12.19	2.32	1318	3229	0.58
17	0.91	13.11	2.32	1318	3229	0.58
18	0.91	14.02	2.32	1318	3229	0.58
19	1.22	14.94	2.32	1318	3229	0.58
20	0.91	16.15	2.32	1318	3229	0.58
21	0.91	17.07	2.32	1318	3229	0.58
22	0.91	17.98	2.32	1318	3229	0.58
23	1.22	18.90	2.32	1318	3229	0.58
24	0.91	20.12	2.61	1661	4068	1.00
25	1.22	21.03	2.61	1661	4068	1.00
26	1.22	22.25	2.61	1661	4068	1.00
27	1.22	23.47	2.61	1661	4068	1.00
28	1.22	24.69	2.61	1661	4068	1.00
29	1.22	25.91	2.61	1578	3866	1.00
30	1.22	27.13	2.61	1578	3866	1.00
31	1.22	28.35	2.61	1578	3866	1.00
32	1.22	29.57	2.61	1578	3866	1.00
33	1.52	30.78	2.61	1578	3866	1.00
34	1.22	32.31	2.63	2682	4779	1.00
35	1.52	33.53	2.63	2682	4779	1.00
36	1.52	35.05	2.63	2682	4779	1.00
37	1.52	36.58	2.63	2682	4779	1.00
38	1.52	38.10	2.63	2682	4779	1.00
39	1.52	39.62	2.63	2682	4779	1.00
40	1.52	41.15	2.63	2682	4779	1.00
41	1.52	42.67	2.63	2682	4779	1.00
42	1.52	44.20	2.63	2682	4779	1.00
43	1.52	45.72	2.63	2682	4779	1.00
44	-	47.24	2.63	2804	4996	1.00

Table 3.1-2 LB In-Situ Strain Compatible Dynamic Subsurface Properties

Layer #	Thickness (m)	Top-Depth (m)	Unit Weight (t/m^3)	V_s (m/s)	V_p (m/s)	Damping (%)
1	0.61	0.00	2.00	188	460	3.50
2	0.76	0.61	2.00	163	464	7.02
3	0.76	1.37	2.00	163	464	7.02
4	0.76	2.13	2.08	248	1265	5.52
5	0.76	2.90	2.08	248	1265	5.52
6	0.76	3.66	2.08	384	1463	4.40
7	0.76	4.42	2.08	384	1463	4.40
8	0.91	5.18	2.32	979	2398	1.02
9	0.91	6.10	2.32	979	2398	1.02
10	0.91	7.01	2.32	979	2398	1.02
11	0.91	7.92	2.32	979	2398	1.02
12	0.91	8.84	2.32	979	2398	1.02
13	0.91	9.75	2.32	979	2398	1.02
14	0.91	10.67	2.32	979	2398	1.02
15	0.61	11.58	2.32	979	2398	1.02
16	0.91	12.19	2.32	979	2398	1.02
17	0.91	13.11	2.32	979	2398	1.02
18	0.91	14.02	2.32	979	2398	1.02
19	1.22	14.94	2.32	979	2398	1.02
20	0.91	16.15	2.32	979	2398	1.02
21	0.91	17.07	2.32	979	2398	1.02
22	0.91	17.98	2.32	979	2398	1.02
23	1.22	18.90	2.32	979	2398	1.02
24	0.91	20.12	2.61	1230	3014	1.82
25	1.22	21.03	2.61	1230	3014	1.82
26	1.22	22.25	2.61	1230	3014	1.82
27	1.22	23.47	2.61	1230	3014	1.82
28	1.22	24.69	2.61	1230	3014	1.82
29	1.22	25.91	2.61	1058	2591	1.82
30	1.22	27.13	2.61	1058	2591	1.82
31	1.22	28.35	2.61	1058	2591	1.82
32	1.22	29.57	2.61	1058	2591	1.82
33	1.52	30.78	2.61	1058	2591	1.82
34	1.22	32.31	2.63	2190	3902	1.82
35	1.52	33.53	2.63	2190	3902	1.82
36	1.52	35.05	2.63	2190	3902	1.82
37	1.52	36.58	2.63	2190	3902	1.82
38	1.52	38.10	2.63	2190	3902	1.82
39	1.52	39.62	2.63	2190	3902	1.82
40	1.52	41.15	2.63	2190	3902	1.82
41	1.52	42.67	2.63	2190	3902	1.82
42	1.52	44.20	2.63	2190	3902	1.82
43	1.52	45.72	2.63	2190	3902	1.82
44	-	47.24	2.63	2290	4079	1.82

Table 3.1-3 UB In-Situ Strain Compatible Dynamic Subsurface Properties

Layer #	Thickness (m)	Top-Depth (m)	Unit Weight (t/m^3)	V_s (m/s)	V_p (m/s)	Damping (%)
1	0.61	0.00	2.00	408	999	1.22
2	0.76	0.61	2.00	437	1248	1.63
3	0.76	1.37	2.00	437	1248	1.63
4	0.76	2.13	2.08	634	2666	1.52
5	0.76	2.90	2.08	634	2666	1.52
6	0.76	3.66	2.08	862	2321	1.42
7	0.76	4.42	2.08	862	2321	1.42
8	0.91	5.18	2.32	1774	4346	0.33
9	0.91	6.10	2.32	1774	4346	0.33
10	0.91	7.01	2.32	1774	4346	0.33
11	0.91	7.92	2.32	1774	4346	0.33
12	0.91	8.84	2.32	1774	4346	0.33
13	0.91	9.75	2.32	1774	4346	0.33
14	0.91	10.67	2.32	1774	4346	0.33
15	0.61	11.58	2.32	1774	4346	0.33
16	0.91	12.19	2.32	1774	4346	0.33
17	0.91	13.11	2.32	1774	4346	0.33
18	0.91	14.02	2.32	1774	4346	0.33
19	1.22	14.94	2.32	1774	4346	0.33
20	0.91	16.15	2.32	1774	4346	0.33
21	0.91	17.07	2.32	1774	4346	0.33
22	0.91	17.98	2.32	1774	4346	0.33
23	1.22	18.90	2.32	1774	4346	0.33
24	0.91	20.12	2.61	2242	5492	0.55
25	1.22	21.03	2.61	2242	5492	0.55
26	1.22	22.25	2.61	2242	5492	0.55
27	1.22	23.47	2.61	2242	5492	0.55
28	1.22	24.69	2.61	2242	5492	0.55
29	1.22	25.91	2.61	2354	5767	0.55
30	1.22	27.13	2.61	2354	5767	0.55
31	1.22	28.35	2.61	2354	5767	0.55
32	1.22	29.57	2.61	2354	5767	0.55
33	1.52	30.78	2.61	2354	5767	0.55
34	1.22	32.31	2.63	3285	5852	0.55
35	1.52	33.53	2.63	3285	5852	0.55
36	1.52	35.05	2.63	3285	5852	0.55
37	1.52	36.58	2.63	3285	5852	0.55
38	1.52	38.10	2.63	3285	5852	0.55
39	1.52	39.62	2.63	3285	5852	0.55
40	1.52	41.15	2.63	3285	5852	0.55
41	1.52	42.67	2.63	3285	5852	0.55
42	1.52	44.20	2.63	3285	5852	0.55
43	1.52	45.72	2.63	3285	5852	0.55
44	-	47.24	2.63	3434	6119	0.55

Table 3.1-4 BE Dynamic Properties of Structural and Concrete Fill Materials

Layer #	Thickness (m)	Top-Depth (m)	Unit Weight (t/m^3)	V_s (m/s)	V_p (m/s)	Damping (%)
1	0.61	0.00	2.08	224	418	2.18
2	0.76	0.61	2.08	198	370	4.24
3	0.76	1.37	2.08	198	370	4.24
4	0.76	2.13	2.08	216	1103	5.13
5	0.76	2.90	2.08	216	1103	5.13
6	0.76	3.66	2.08	224	1144	5.80
7	0.76	4.42	2.08	224	1144	5.80
Concrete Fill		5.18	2.32	2134	3325	1.00

Table 3.1-5 LB Dynamic Properties of Structural and Concrete Fill Materials

Layer #	Thickness (m)	Top-Depth (m)	Unit Weight (t/m^3)	Vs (m/s)	Vp (m/s)	Damping (%)
1	0.61	0.00	2.08	162	303	3.12
2	0.76	0.61	2.08	127	238	7.00
3	0.76	1.37	2.08	127	238	7.00
4	0.76	2.13	2.08	135	690	8.45
5	0.76	2.90	2.08	135	690	8.45
6	0.76	3.66	2.08	143	729	9.40
7	0.76	4.42	2.08	143	729	9.40
Concrete Fill		5.18	2.32	1829	2850	1.80

Table 3.1-6 UB Dynamic Properties of Structural and Concrete Fill Materials

Layer #	Thickness (m)	Top-Depth (m)	Unit Weight (t/m^3)	V_s (m/s)	V_p (m/s)	Damping (%)
1	0.61	0.00	2.08	309	578	1.52
2	0.76	0.61	2.08	307	574	2.57
3	0.76	1.37	2.08	307	574	2.57
4	0.76	2.13	2.08	346	1463	3.11
5	0.76	2.90	2.08	346	1463	3.11
6	0.76	3.66	2.08	352	1463	3.58
7	0.76	4.42	2.08	352	1463	3.58
Concrete Fill		5.18	2.32	2438	3800	0.55

Table 3.1-7 Comparisons of the Average Strain-Compatible Shear Wave Velocities and Shear Column Frequencies of the Fill and In-Situ Materials

Soil Case	Concrete Fill/ Zone III Rock Embedment					Structural Fill/ Saprolite Embedment				
	Depth	Backfill		In-Situ		Depth	Backfill		In-Situ	
	m	$V_{s\text{-}ave}$ m/s	f_{sc} Hz	$V_{s\text{-}ave}$ m/s	f_{sc} Hz	m	$V_{s\text{-}ave}$ m/s	f_{sc} Hz	$V_{s\text{-}ave}$ m/s	f_{sc} Hz
LB	14.8	1829	30.9	979	16.5	5.2	137	6.6	228	11.0
BE		2134	36.0	1318	22.3		213	10.3	360	17.4
UB		2438	41.2	1774	30.0		331	16.0	566	27.3

Table 4.1-1 Damping Values for Dynamic Analysis

Components	Percent of Critical Damping		OBE Reference
	SSE[1]	OBE	
Reinforced concrete structures	7.0	4.0	2-v
Vent Wall/Diaphragm Floor:			
0% concrete stiffness contribution[2] [5]	4.0	--	
50% concrete stiffness contribution [3] [5]	5.0[4]	--	
100% concrete stiffness contribution [2]	--	3.0	2-v
Reactor Shield Wall[2]	4.0	3.0	2-v
Reactor Pressure Vessel (RPV) [2]	4.0	2.0	2-d
Separator / Chimney / Shroud[2]	4.0	2.0	2-d
Fuel			
– horizontal	6.0	6.0	2-d
– vertical	6.0	4.0	2-d
Control Rod Drive Housing (CRDH)	2.0	1.0	2-d
RPV and Shroud support[2]	4.0	2.0	2-d
CRDH support (CRD restraint) [2]	4.0	2.0	2-d
Shroud support[2]	4.0	2.0	2-d

Notes:
(1) SSE damping values are obtained from Table 3.7-1 of Reference 2-dd, unless noted otherwise.
(2) This component is considered a welded steel assembly/structure for selection of damping value.
(3) This component is considered a steel-concrete (SC) structure for selection of damping value.
(4) Value obtained from Reference 2-ee for SC structures.
(5) SSE damping determined as a function of in-fill concrete contribution to the stiffness of concrete-filled steel structures

Table 4.2-1 RB/FB Site-Specific SSI Analysis Cases, Passing, and Cut-off Frequencies

Case No.	Computer Program	Structural Model Properties*	Subgrade Profile		Method	Control Motion El.	Frequency (Hz)		Captured Motion Energy		
							Passing	Cut-off	X	Y	Z
1	SASSI 2010	UC100	Partial Column	LB	DM	224 ft	62	62	99%	98%	96%
2				BE			83	70	100%	100%	100%
3				UB			112	70	99%	99%	100%
4			Full Column	LB	MSM		33	33	82%	82%	88%
5				BE			50	50	96%	96%	94%
6				UB			78	70	99%	99%	100%
Sensitivity Analyses for Evaluations of Stiffness Variation Effects in Appendix B											
S1	SASSI 2010	CR50	Partial Column	LB	DM	224 ft	62	62	99%	98%	96%
S2				BE			83	70	100%	100%	100%
S3				UB			112	70	99%	99%	100%
S4			Full Column	LB	MSM		33	33	82%	82%	88%
S5	ACS SASSI			BE			50	50	96%	96%	94%
S6				UB			78	70	99%	99%	100%
S7	SASSI 2010	CR00	Partial Column	LB	DM	224 ft	62	62	99%	98%	96%
S8				BE			83	70	100%	100%	100%
S9				UB			112	70	99%	99%	100%
S10			Full Column	LB	MSM		33	33	82%	82%	88%
S11	ACS SASSI			BE			50	50	96%	96%	94%
S12				UB			78	70	99%	99%	100%
Point Radius Validation (Appendix C)											
P1	SASSI 2010	UC100 R=3.40m	Full Column	UB	MSM	224 ft	78	70	99%	99%	100%
P2		UC100 R=0.86m					78	70	99%	99%	100%
P3		UC100 UM **)					50	50	95%	94%	99%
ACS SASSI Verification Analyses in Appendix I											
V1	ACS SASSI	UC100	Full Column	UB	MSM	224 ft	78	70	99%	99%	100%

*Structural Properties:

UC100 – Uncracked reinforced concrete and 100% in-fill concrete contribution to the stiffness of concrete-filled steel structures and OBE damping values

CR50 – Cracked reinforced concrete and 50% in-fill concrete contribution to the stiffness of concrete-filled steel structures and SSE damping values

CR00 – Cracked reinforced concrete and 0% in-fill concrete contribution to stiffness of concrete-filled steel structures and SSE damping values

**) Uniform Mesh Model

Table 4.2-2 List of Frequencies of Analysis

Freq. No.	Freq. (Hz)					
	Partial Column			Full Column		
	BE	UB	LB	BE	UB	LB
1	0.0244	0.0244	0.0244	0.0244	0.0244	0.0244
41	1.0010	1.0010	1.0010	1.0010	1.0010	1.0010
82	2.0020	2.0020	2.0020	2.0020	2.0020	2.0020
102	2.4902	2.4902	2.4902	2.4902	2.4902	2.4902
123	3.0029	3.0029	3.0029	3.0029	3.0029	3.0029
143	3.4912	3.4912	3.4912	3.4912	3.4912	3.4912
164	4.0039	4.0039	4.0039	4.0039	4.0039	4.0039
184	4.4922	4.4922	4.4922	4.4922	4.4922	4.4922
205	5.0049	5.0049	5.0049	5.0049	5.0049	5.0049
225	5.4932	5.4932	5.4932	5.4932	5.4932	5.4932
246	6.0059	6.0059	6.0059	6.0059	6.0059	6.0059
266	6.4941	6.4941	6.4941	6.4941	6.4941	6.4941
287	7.0068	7.0068	7.0068	7.0068	7.0068	7.0068
307	7.4951	7.4951	7.4951	7.4951	7.4951	7.4951
328	8.0078	8.0078	8.0078	8.0078	8.0078	8.0078
348	8.4961	8.4961	8.4961	8.4961	8.4961	8.4961
369	9.0088	9.0088	9.0088	9.0088	9.0088	9.0088
389	9.4971	9.4971	9.4971	9.4971	9.4971	9.4971
410	10.010	10.010	10.010	10.010	10.010	10.010
430	10.498	10.498	10.498	10.498	10.498	10.498
451	11.011	11.011	11.011	11.011	11.011	11.011
471	11.499	11.499	11.499	11.499	11.499	11.499
492	12.012	12.012	12.012	12.012	12.012	12.012
512	12.500	12.500	12.500	12.500	12.500	12.500
532	12.988	12.988	12.988	12.988	12.988	12.988
573	13.989	13.989	13.989	13.989	13.989	13.989
614	14.990	14.990	14.990	14.990	14.990	14.990
655	15.991	15.991	15.991	15.991	15.991	15.991
696	16.992	16.992	16.992	16.992	16.992	16.992
737	17.993	17.993	17.993	17.993	17.993	17.993
778	18.994	18.994	18.994	18.994	18.994	18.994
819	19.995	19.995	19.995	19.995	19.995	19.995
860	20.996	20.996	20.996	20.996	20.996	20.996
901	21.997	21.997	21.997	21.997	21.997	21.997
942	22.998	22.998	22.998	22.998	22.998	22.998
983	23.999	23.999	23.999	23.999	23.999	23.999
1024	25.000	25.000	25.000	25.000	25.000	25.000
1065	26.001	26.001	26.001	26.001	26.001	26.001
1106	27.002	27.002	27.002	27.002	27.002	27.002
1147	28.003	28.003	28.003	28.003	28.003	28.003
1188	29.004	29.004	29.004	29.004	29.004	29.004
1229	30.005	30.005	30.005	30.005	30.005	30.005
1270	31.006	31.006	31.006	31.006	31.006	31.006
1311	32.007	32.007	32.007	32.007	32.007	32.007
1352	33.008	33.008	33.008	33.008	33.008	33.008
1393	34.009	34.009	34.009	34.009	34.009	
1434	35.010	35.010	35.010	35.010	35.010	

Table 4.2-2 List of Frequencies of Analysis (Continued)

Freq. No.	Freq. (Hz)					
	Partial Column			Full Column		
	BE	UB	LB	BE	UB	LB
1475	36.011	36.011	36.011	36.011	36.011	
1516	37.012	37.012	37.012	37.012	37.012	
1557	38.013	38.013	38.013	38.013	38.013	
1598	39.014	39.014	39.014	39.014	39.014	
1639	40.015	40.015	40.015	40.015	40.015	
1680	41.016	41.016	41.016	41.016	41.016	
1721	42.017	42.017	42.017	42.017	42.017	
1762	43.018	43.018	43.018	43.018	43.018	
1803	44.019	44.019	44.019	44.019	44.019	
1844	45.020	45.020	45.020	45.020	45.020	
1885	46.021	46.021	46.021	46.021	46.021	
1926	47.022	47.022	47.022	47.022	47.022	
1966	47.998	47.998	47.998	47.998	47.998	
2007	48.999	48.999	48.999	48.999	48.999	
2048	50.000	50.000	50.000	50.000	50.000	
2089	51.001	51.001	51.001		51.001	
2130	52.002	52.002	52.002		52.002	
2171	53.003	53.003	53.003		53.003	
2212	54.004	54.004	54.004		54.004	
2233	54.517	54.517	54.517		54.517	
2253	55.005	55.005	55.005		55.005	
2294	56.006	56.006	56.006		56.006	
2335	57.007	57.007	57.007		57.007	
2376	58.008	58.008	58.008		58.008	
2417	59.009	59.009	59.009		59.009	
2458	60.010	60.010	60.010		60.010	
2499	61.011	61.011	61.011		61.011	
2540	62.012	62.012	62.012		62.012	
2581	63.013	63.013			63.013	
2622	64.014	64.014			64.014	
2663	65.015	65.015			65.015	
2703	65.991	65.991			65.991	
2744	66.992	66.992			66.992	
2785	67.993	67.993			67.993	
2826	68.994	68.994			68.994	
2867	69.995	69.995			69.995	

Table 4.3-1 Lateral Extent of Structural Fill around RB/FB

North	3.13 m (10.27 ft)	One-half the distance between RB/FB and Turbine Building 0.5 x 6.26 m (20.54 ft)
South	3.13 m (10.27 ft)	Minimum distance to inside face of Sheet Piling adjacent to RB/FB
East	6.975 m (22.88 ft)	One-half the distance between RB/FB and Control Building 0.5 x 13.95 m (45.77 ft)
West	3.13 m (10.27 ft)	Minimum distance to inside face of Sheet Piling adjacent to RB/FB
Minimum Distance	**3.13 m (10.27 ft)**	RB/FB lateral extent of backfill

Table 4.3-2 Subsurface Properties for SSI Analysis of RB/FB PE (BE profile)

EL	Soil						Backfill					
	Unit Weight	Vs	Vp	Damping	Highest Frequency	Poisson's	Unit Weight	Vs	Vp	Damping	Highest Frequency	Poisson's
[m]	[t/m^3]	[m/sec]	[m/sec]	[%]	[Hz]	ratio	[t/m^3]	[m/sec]	[m/sec]	[%]	[Hz]	ratio
-0.68	2.32	1318	3229	0.58	82.8	0.400	2.32	2134	3325	1.00	134.2	0.150
-3.54												
-3.54	2.32	1318	3229	0.58	82.8	0.400	2.32	2134	3325	1.00	134.2	0.150
-6.40												
-6.40	2.32	1318	3229	0.58	82.8	0.400	2.32	2134	3325	1.00	134.2	0.150
-8.95												
-8.95	2.32	1318	3229	0.58	82.8	0.400	2.32	2134	3325	1.00	134.2	0.150
-11.50												
-11.50	2.32	1318	3229	0.58	82.8	0.400	2.32	2134	3325	1.00	134.2	0.150
-13.50												
-13.50	2.32	1318	3229	0.58	82.8	0.400	2.32	2134	3325	1.00	134.2	0.150
-15.50												
-15.50	2.60	1644	4025	0.98	111.4	0.400						
-18.45												
-18.45	2.61	1661	4068	1.00	112.2	0.400						
-21.41												
-21.41	2.61	1578	3865	1.00	98.6	0.400						
-24.61												
-24.61	2.61	1578	3865	1.00	98.6	0.400						
-27.81												
-27.81	2.63	2682	4779	1.00	107.9	0.270						
-32.78												
-32.78	2.63	2682	4779	1.00	107.7	0.270						
-37.76												
-37.76	2.63	2682	4779	1.00	107.7	0.270						
-42.74												
-42.74	2.63	2804	4996	1.00		0.270						
-												

Note: The soil properties of the adjusted layer, shown in the red box, are evaluated from the original properties shown below.

Original data

-15.50	2.32	1318	3229	0.58		0.400	
-15.62							
-15.62	2.61	1661	4068	1.00		0.400	
-18.45							

Vs and Vp are determined using the equivalent wave travel time procedure.
Example: 1644=(18.45-15.5)/(0.12/1318+2.83/1661)
Damping ratio is determined using the thickness weighted average procedure.
Example: 0.98=(0.58x(15.62-15.50)+1.00x(18.45-15.62))/(0.12+2.83)

Table 4.3-3 Subsurface Properties for SSI Analysis of RB/FB PE (LB profile)

EL	Soil						Backfill					
	Unit Weight	Vs	Vp	Damping	Highest Frequency	Poisson's	Unit Weight	Vs	Vp	Damping	Highest Frequency	Poisson's
[m]	[t/m^3]	[m/sec]	[m/sec]	[%]	[Hz]	ratio	[t/m^3]	[m/sec]	[m/sec]	[%]	[Hz]	ratio
-0.68	2.32	979	2398	1.02	61.5	0.400	2.32	1829	2850	1.80	115.0	0.150
-3.54												
-3.54	2.32	979	2398	1.02	61.5	0.400	2.32	1829	2850	1.80	115.0	0.150
-6.40												
-6.40	2.32	979	2398	1.02	61.5	0.400	2.32	1829	2850	1.80	115.0	0.150
-8.95												
-8.95	2.32	979	2398	1.02	61.5	0.400	2.32	1829	2850	1.80	115.0	0.150
-11.50												
-11.50	2.32	979	2398	1.02	61.5	0.400	2.32	1829	2850	1.80	115.0	0.150
-13.50												
-13.50	2.32	979	2398	1.02	61.5	0.400	2.32	1829	2850	1.80	115.0	0.150
-15.50												
-15.50	2.60	1217	2983	1.79	82.5	0.400						
-18.45												
-18.45	2.61	1230	3014	1.82	83.1	0.400						
-21.41												
-21.41	2.61	1058	2591	1.82	66.1	0.400						
-24.61												
-24.61	2.61	1058	2591	1.82	66.1	0.400						
-27.81												
-27.81	2.63	2190	3902	1.82	88.1	0.270						
-32.78												
-32.78	2.63	2190	3902	1.82	87.9	0.270						
-37.76												
-37.76	2.63	2190	3902	1.82	87.9	0.270						
-42.74												
-42.74	2.63	2290	4079	1.82		0.270						
-												

Note: The soil properties of the adjusted layer, shown in the red box, are evaluated from the original properties shown below.

Original data

-15.50	2.32	979	2398	1.02		0.400
-15.62						
-15.62	2.61	1230	3014	1.82		0.400
-18.45						

Vs and Vp are determined using the equivalent wave travel time procedure.

Example: 1217=(18.45-15.5)/(0.12/979+2.83/1230)

Damping ratio is determined using the thickness weighted average procedure.

Example: 1.79=(1.02x(15.62-15.50)+1.82x(18.45-15.62))/(0.12+2.83)

Table 4.3-4 Subsurface Properties for SSI Analysis of RB/FB PE (UB profile)

EL	Soil						Backfill					
	Unit Weight	Vs	Vp	Damping	Highest Frequency	Poisson's	Unit Weight	Vs	Vp	Damping	Highest Frequency	Poisson's
[m]	[t/m^3]	[m/sec]	[m/sec]	[%]	[Hz]	ratio	[t/m^3]	[m/sec]	[m/sec]	[%]	[Hz]	ratio
-0.68	2.32	1774	4346	0.33	111.5	0.400	2.32	2438	3800	0.55	153.3	0.150
-3.54												
-3.54	2.32	1774	4346	0.33	111.5	0.400	2.32	2438	3800	0.55	153.3	0.150
-6.40												
-6.40	2.32	1774	4346	0.33	111.5	0.400	2.32	2438	3800	0.55	153.3	0.150
-8.95												
-8.95	2.32	1774	4346	0.33	111.5	0.400	2.32	2438	3800	0.55	153.3	0.150
-11.50												
-11.50	2.32	1774	4346	0.33	111.5	0.400	2.32	2438	3800	0.55	153.3	0.150
-13.50												
-13.50	2.32	1774	4346	0.33	111.5	0.400	2.32	2438	3800	0.55	153.3	0.150
-15.50												
-15.50	2.60	2218	5434	0.54	150.3	0.400						
-18.45												
-18.45	2.61	2242	5492	0.55	151.4	0.400						
-21.41												
-21.41	2.61	2354	5767	0.55	147.1	0.400						
-24.61												
-24.61	2.61	2354	5767	0.55	147.1	0.400						
-27.81												
-27.81	2.63	3285	5852	0.55	132.1	0.270						
-32.78												
-32.78	2.63	3285	5852	0.55	131.9	0.270						
-37.76												
-37.76	2.63	3285	5852	0.55	131.9	0.270						
-42.74												
-42.74	2.63	3434	6119	0.55		0.270						
-												

Note: The soil properties of the adjusted layer, shown in the red box, are evaluated from the original properties shown below.

Original data

-15.50	2.32	1774	4346	0.33		0.400
-15.62						
-15.62	2.61	2242	5492	0.55		0.400
-18.45						

Vs and Vp are determined using the equivalent wave travel time procedure.
Example: 2218=(18.45-5.5)/(0.12/1774+2.83/2242)
Damping ratio is determined using the thickness weighted average procedure.
Example: 0.54=(0.33x(15.62-15.50)+0.55x(18.45-15.62))/(0.12+2.83)

Table 4.3-5 Subsurface Properties for SSI Analysis of RB/FB FE (BE profile)

EL	Soil						Backfill					
	Unit Weight	Vs	Vp	Damping	Highest Frequency	Poisson's	Unit Weight	Vs	Vp	Damping	Highest Frequency	Poisson's
[m]	[t/m^3]	[m/sec]	[m/sec]	[%]	[Hz]	ratio	[t/m^3]	[m/sec]	[m/sec]	[%]	[Hz]	ratio
4.50	2.00	277	678	2.07	56.9	0.400	2.08	224	418	2.18	56.9	0.299
3.89												
3.89	2.00	267	761	3.38	54.9	0.430	2.08	198	370	4.24	50.3	0.299
3.13												
3.13	2.00	267	761	3.38	54.9	0.430	2.08	198	370	4.24	50.3	0.299
2.37												
2.37	2.08	397	1668	2.89	81.6	0.470	2.08	216	1103	5.13	54.9	0.480
1.61												
1.61	2.08	397	1668	2.89	81.6	0.470	2.08	216	1103	5.13	54.9	0.480
0.84												
0.84	2.08	575	1549	2.50	118.2	0.420	2.08	224	1144	5.80	56.9	0.480
0.08												
0.08	2.08	575	1549	2.50	118.2	0.420	2.08	224	1144	5.80	56.9	0.480
-0.68												
-0.68	2.32	1318	3229	0.58	135.5	0.400	2.32	2134	3325	1.00	272.7	0.150
-2.00												
-2.00	2.32	1318	3229	0.58	67.7	0.400	2.32	2134	3325	1.00	136.3	0.150
-4.50												
-4.50	2.32	1318	3229	0.58	67.7	0.400	2.32	2134	3325	1.00	136.3	0.150
-6.40												
-6.40	2.32	1318	3229	0.58	67.7	0.400	2.32	2134	3325	1.00	136.3	0.150
-8.40												
-8.40	2.32	1318	3229	0.58	67.7	0.400	2.32	2134	3325	1.00	136.3	0.150
-10.40												
-10.40	2.32	1318	3229	0.58	67.7	0.400	2.32	2134	3325	1.00	136.3	0.150
-11.50												
-11.50	2.32	1318	3229	0.58	67.7	0.400	2.32	2134	3325	1.00	136.3	0.150
-13.50												
-13.50	2.32	1318	3229	0.58	67.7	0.400	2.32	2134	3325	1.00	136.3	0.150
-15.50												
-15.50	2.60	1644	4025	0.98	84.5	0.400						
-18.45												
-18.45	2.61	1661	4068	1.00	85.4	0.400						
-21.41												
-21.41	2.61	1578	3865	1.00	81.1	0.400						
-23.41												
-23.41	2.61	1578	3865	1.00	81.1	0.400						
-25.61												
-25.61	2.61	1578	3865	1.00	81.1	0.400						
-27.81												
-27.81	2.63	2682	4779	1.00	107.9	0.270						
-32.78												
-32.78	2.63	2682	4779	1.00	107.7	0.270						
-37.76												
-37.76	2.63	2682	4779	1.00	107.7	0.270						
-42.74												
-42.74	2.63	2804	4996	1.00		0.270						
-												

Note: The soil properties of the adjusted layer, shown in the red box, are evaluated from the original properties shown below.

Original data

-15.50	2.32	1318	3229	0.58		0.400
-15.62						
-15.62	2.61	1661	4068	1.00		0.400
-18.45						

Vs and Vp are determined using the equivalent wave travel time procedure.
Example: 1644=(18.45-15.5)/(0.12/1318+2.83/1661)
Damping ratio is determined using the thickness weighted average procedure.
Example: 0.98=(0.58x(15.62-15.50)+1.00x(18.45-15.62))/(0.12+2.83)

Table 4.3-6 Subsurface Properties for SSI Analysis of RB/FB FE (LB profile)

EL	Soil						Backfill					
	Unit Weight	Vs	Vp	Damping	Highest Frequency	Poisson's	Unit Weight	Vs	Vp	Damping	Highest Frequency	Poisson's
[m]	[t/m^3]	[m/sec]	[m/sec]	[%]	[Hz]	ratio	[t/m^3]	[m/sec]	[m/sec]	[%]	[Hz]	ratio
4.50	2.00	188	460	3.50	38.6	0.400	2.08	162	303	3.12	41.1	0.300
3.89												
3.89	2.00	163	464	7.02	33.5	0.430	2.08	127	238	7.00	32.2	0.301
3.13												
3.13	2.00	163	464	7.02	33.5	0.430	2.08	127	238	7.00	32.2	0.301
2.37												
2.37	2.08	248	1266	5.52	51.0	0.480	2.08	135	689	8.45	34.3	0.480
1.61												
1.61	2.08	248	1266	5.52	51.0	0.480	2.08	135	689	8.45	34.3	0.480
0.84												
0.84	2.08	384	1463	4.40	78.9	0.463	2.08	143	729	9.40	36.3	0.480
0.08												
0.08	2.08	384	1463	4.40	78.9	0.463	2.08	143	729	9.40	36.3	0.480
-0.68												
-0.68	2.32	979	2398	1.02	100.6	0.400	2.32	1829	2850	1.80	233.7	0.150
-2.00												
-2.00	2.32	979	2398	1.02	50.3	0.400	2.32	1829	2850	1.80	116.8	0.150
-4.50												
-4.50	2.32	979	2398	1.02	50.3	0.400	2.32	1829	2850	1.80	116.8	0.150
-6.40												
-6.40	2.32	979	2398	1.02	50.3	0.400	2.32	1829	2850	1.80	116.8	0.150
-8.40												
-8.40	2.32	979	2398	1.02	50.3	0.400	2.32	1829	2850	1.80	116.8	0.150
-10.40												
-10.40	2.32	979	2398	1.02	50.3	0.400	2.32	1829	2850	1.80	116.8	0.150
-11.50												
-11.50	2.32	979	2398	1.02	50.3	0.400	2.32	1829	2850	1.80	116.8	0.150
-13.50												
-13.50	2.32	979	2398	1.02	50.3	0.400	2.32	1829	2850	1.80	116.8	0.150
-15.50												
-15.50	2.60	1217	2983	1.79	62.6	0.400						
-18.45												
-18.45	2.61	1230	3014	1.82	63.2	0.400						
-21.41												
-21.41	2.61	1058	2591	1.82	54.4	0.400						
-23.41												
-23.41	2.61	1058	2591	1.82	54.4	0.400						
-25.61												
-25.61	2.61	1058	2591	1.82	54.4	0.400						
-27.81												
-27.81	2.63	2190	3902	1.82	88.1	0.270						
-32.78												
-32.78	2.63	2190	3902	1.82	87.9	0.270						
-37.76												
-37.76	2.63	2190	3902	1.82	87.9	0.270						
-42.74												
-42.74	2.63	2290	4079	1.82		0.270						
-												

Note: The soil properties of the adjusted layer, shown in the red box, are evaluated from the original properties shown below.

Original data

-15.50	2.32	979	2398	1.02		0.400
-15.62						
-15.62	2.61	1230	3014	1.82		0.400
-18.45						

Vs and Vp are determined using the equivalent wave travel time procedure.
Example: 1217=(18.45-15.5)/(0.12/979+2.83/1230)
Damping ratio is determined using the thickness weighted average procedure.
Example: 1.79=(1.02x(15.62-15.50)+1.82x(18.45-15.62))/(0.12+2.83)

Table 4.3-7 Subsurface Properties for SSI Analysis of RB/FB FE (UB profile)

EL	Soil						Backfill					
	Unit Weight	Vs	Vp	Damping	Highest Frequency	Poisson's	Unit Weight	Vs	Vp	Damping	Highest Frequency	Poisson's
[m]	[t/m^3]	[m/sec]	[m/sec]	[%]	[Hz]	ratio	[t/m^3]	[m/sec]	[m/sec]	[%]	[Hz]	ratio
4.50	2.00	408	999	1.22	83.9	0.400	2.08	309	578	1.52	78.5	0.300
3.89												
3.89	2.00	437	1248	1.63	89.8	0.430	2.08	307	574	2.57	78.0	0.300
3.13												
3.13	2.00	437	1248	1.63	89.8	0.430	2.08	307	574	2.57	78.0	0.300
2.37												
2.37	2.08	634	2665	1.52	130.4	0.470	2.08	346	1463	3.11	87.9	0.470
1.61												
1.61	2.08	634	2665	1.52	130.4	0.470	2.08	346	1463	3.11	87.9	0.470
0.84												
0.84	2.08	862	2321	1.42	177.3	0.420	2.08	352	1463	3.58	89.5	0.469
0.08												
0.08	2.08	862	2321	1.42	177.3	0.420	2.08	352	1463	3.58	89.5	0.469
-0.68												
-0.68	2.32	1774	4346	0.33	182.4	0.400	2.32	2438	3800	0.55	311.5	0.150
-2.00												
-2.00	2.32	1774	4346	0.33	91.2	0.400	2.32	2438	3800	0.55	155.7	0.150
-4.50												
-4.50	2.32	1774	4346	0.33	91.2	0.400	2.32	2438	3800	0.55	155.7	0.150
-6.40												
-6.40	2.32	1774	4346	0.33	91.2	0.400	2.32	2438	3800	0.55	155.7	0.150
-8.40												
-8.40	2.32	1774	4346	0.33	91.2	0.400	2.32	2438	3800	0.55	155.7	0.150
-10.40												
-10.40	2.32	1774	4346	0.33	91.2	0.400	2.32	2438	3800	0.55	155.7	0.150
-11.50												
-11.50	2.32	1774	4346	0.33	91.2	0.400	2.32	2438	3800	0.55	155.7	0.150
-13.50												
-13.50	2.32	1774	4346	0.33	91.2	0.400	2.32	2438	3800	0.55	155.7	0.150
-15.50												
-15.50	2.60	2218	5434	0.54	114.0	0.400						
-18.45												
-18.45	2.61	2242	5492	0.55	115.2	0.400						
-21.41												
-21.41	2.61	2354	5767	0.55	121.0	0.400						
-23.41												
-23.41	2.61	2354	5767	0.55	121.0	0.400						
-25.61												
-25.61	2.61	2354	5767	0.55	121.0	0.400						
-27.81												
-27.81	2.63	3285	5852	0.55	132.1	0.270						
-32.78												
-32.78	2.63	3285	5852	0.55	131.9	0.270						
-37.76												
-37.76	2.63	3285	5852	0.55	131.9	0.270						
-42.74												
-42.74	2.63	3434	6119	0.55		0.270						
-												

Note: The soil properties of the adjusted layer, shown in the red box, are evaluated from the original properties shown below.

Original data

-15.50	2.32	1774	4346	0.33		0.400
-15.62						
-15.62	2.61	2242	5492	0.55		0.400
-18.45						

Vs and Vp are determined using the equivalent wave travel time procedure.
Example: 2218=(18.45-15.5)/(0.12/1774+2.83/2242)
Damping ratio is determined using the thickness weighted average procedure.
Example: 0.54=(0.33x(15.62-15.50)+0.55x(18.45-15.62))/(0.12+2.83)

Table 5.2-1 Maximum Accelerations of Slab SDOF Oscillators

SDOF Oscillator		Vertical Acceleration (g)							Standard Design
Elev. (m)	Node No.	Full Column			Partial Column			NA3 Envelope	
		LB	BE	UB	LB	BE	UB		
52.40	9101	*0.33*	0.33	0.32	0.30	0.30	0.30	0.33	1.20
	9102	*1.33*	1.29	1.28	0.80	0.79	0.77	1.33	1.82
	9103	3.90	5.58	*6.27*	2.91	4.11	4.79	6.27	3.14
	9104	2.02	2.38	*2.62*	1.89	2.01	2.26	2.62	2.45
	9105	1.60	2.27	*2.42*	1.62	2.10	2.17	2.42	2.32
	9106	2.44	3.09	3.52	2.11	3.06	*3.74*	3.74	2.99
	9107	1.42	2.31	*3.22*	1.59	2.08	3.08	3.22	2.80
	9108	1.12	1.69	*2.50*	1.24	1.49	2.09	2.50	2.61
34.00	9091	0.94	1.42	*1.61*	0.79	1.03	1.29	1.61	1.29
	9092	0.88	1.11	*1.61*	0.85	1.07	1.34	1.61	1.08
27.00	9081	1.15	1.36	*1.60*	1.00	1.10	1.26	1.60	1.16
	9082	0.89	1.17	*1.52*	0.76	0.93	1.26	1.52	0.99
	9083	0.78	1.06	*1.30*	0.74	0.84	1.06	1.30	1.09
	9084	0.73	1.25	*1.67*	0.90	0.99	1.42	1.67	1.32
	9085	0.86	1.14	*1.46*	0.72	0.89	1.19	1.46	0.97
22.50	9071	*1.15*	1.15	1.15	0.64	0.65	0.67	1.15	1.60
	9072	*1.79*	1.70	1.64	1.12	1.07	1.03	1.79	1.31
	9073	2.37	3.56	*4.47*	1.84	2.57	3.13	4.47	2.03
	9074	0.93	1.24	*1.53*	0.87	1.07	1.25	1.53	1.31
	9075	1.04	1.29	*1.51*	0.98	1.08	1.32	1.51	1.16
17.50	9061	1.97	3.00	*3.65*	1.61	2.30	2.90	3.65	1.79
	9062	1.15	1.57	2.40	1.37	1.68	*2.62*	2.62	1.49
	9063	0.77	0.96	*1.13*	0.64	0.82	0.98	1.13	0.82
	9064	1.14	1.38	*1.53*	0.93	1.07	1.17	1.53	1.84
	9065	0.59	1.00	*1.28*	0.80	0.93	1.24	1.28	1.42
13.57	9051	0.74	0.95	*1.11*	0.64	0.82	0.96	1.11	0.81
	9052	0.59	0.94	*1.25*	0.75	0.89	1.22	1.25	1.46
9.06	9041	0.83	0.84	*0.95*	0.69	0.76	0.82	0.95	0.88
	9042	0.61	0.94	*1.26*	0.70	0.85	1.19	1.26	1.42
4.65	9031	0.84	1.42	*1.62*	0.98	1.41	1.59	1.62	1.17
	9032	0.79	0.86	*0.89*	0.69	0.74	0.84	0.89	0.97
	9033	0.78	0.93	*1.12*	0.78	0.85	0.98	1.12	1.02
	9034	0.60	1.20	*1.73*	1.10	1.16	1.81	1.81	1.51
	9035	0.57	0.87	*1.07*	0.69	0.77	1.05	1.07	1.38
-1.00	9021	0.92	0.86	*0.97*	0.88	0.84	0.92	0.97	1.12
	9022	1.26	1.60	1.90	0.99	1.64	*2.07*	2.07	1.45
	9023	0.80	0.92	*0.98*	0.75	0.79	0.89	0.98	1.01
	9024	0.72	0.98	*1.12*	0.67	0.94	1.03	1.12	0.89
	9025	0.55	1.00	1.14	0.75	0.85	*1.21*	1.21	1.34
	9026	0.54	1.06	1.38	1.06	1.22	*1.63*	1.63	1.57
	9027	0.55	0.65	0.67	0.54	0.57	*0.68*	0.68	0.88
-6.40	9011	0.77	0.76	*0.84*	0.73	0.76	0.84	0.84	0.92
	9012	0.68	1.03	*1.17*	0.76	1.05	1.13	1.17	0.92
	9013	0.71	0.88	1.35	0.68	0.93	*1.52*	1.52	1.35

Note: The shaded values in the table show exceedance from standard design.
The values shown in Italic are governing case.

Table 5.2-2 Maximum Accelerations of Wall SDOF Oscillators

SDOF Oscillator			Horizontal Acceleration (g)							
Elev. (m)	Node No.	Dir.	Full Column			Partial Column			NA3 Envelope	Standard Design
			LB	BE	UB	LB	BE	UB		
42.00	99981	NS (X)	1.73	2.32	*2.66*	1.45	1.93	2.20	2.66	1.54
	99982		1.07	1.46	*1.54*	0.93	1.22	1.53	1.54	1.00
13.57	99971		1.19	1.66	*2.11*	1.21	1.51	1.81	2.11	1.38
	99972		1.57	1.46	2.00	1.84	1.90	*2.29*	2.29	1.37
	99973		0.73	1.19	1.35	0.91	1.26	*1.88*	1.88	1.15
	99974		0.64	0.74	1.04	0.59	0.81	*1.10*	1.10	1.00
42.00	99983	EW (Y)	1.27	1.45	*1.86*	1.09	1.26	1.59	1.86	1.71
	99984		0.98	0.89	*1.02*	0.75	0.99	1.00	1.02	1.56
	99985		0.88	0.89	*1.00*	0.68	0.75	0.85	1.00	1.25
13.57	99975		1.10	1.50	1.66	1.38	1.74	*2.16*	2.16	1.28
	99976		0.43	0.64	0.78	0.53	0.69	*0.92*	0.92	1.00

Note: The shaded values in the table show exceedance from standard design.
The values shown in Italic are governing case.

Table 5.4-1 Maximum Displacements of Slab SDOF Oscillators Relative to Free-Field

Elev. (m)	Node No.	Vertical Displacement (cm)							
		Full Column			Partial Column			NA3 Envelope.	Standard Design
		LB	BE	UB	LB	BE	UB		
52.40	9101	1.03	1.03	1.02	0.96	0.96	0.95	1.03	4.99
	9102	1.15	1.13	1.10	0.64	0.63	0.62	1.15	2.08
	9103	0.91	1.25	1.38	0.68	0.93	1.06	1.38	1.27
	9104	0.35	0.38	0.43	0.28	0.29	0.32	0.43	1.27
	9105	0.30	0.30	0.32	0.24	0.24	0.25	0.32	1.26
	9106	0.31	0.32	0.34	0.24	0.27	0.29	0.34	1.26
	9107	0.27	0.29	0.31	0.21	0.23	0.24	0.31	1.26
	9108	0.26	0.27	0.30	0.20	0.21	0.22	0.30	1.26
34.00	9091	0.24	0.25	0.27	0.19	0.19	0.20	0.27	1.23
	9092	0.23	0.24	0.26	0.18	0.18	0.19	0.26	1.20
27.00	9081	0.25	0.24	0.27	0.20	0.20	0.21	0.27	1.14
	9082	0.22	0.23	0.25	0.17	0.17	0.18	0.25	1.14
	9083	0.21	0.22	0.23	0.16	0.17	0.17	0.23	1.16
	9084	0.20	0.21	0.22	0.16	0.16	0.16	0.22	1.18
	9085	0.22	0.22	0.24	0.17	0.17	0.18	0.24	1.14
22.50	9071	1.02	1.02	1.01	0.56	0.57	0.57	1.02	1.74
	9072	0.99	0.91	0.89	0.56	0.54	0.52	0.99	1.36
	9073	0.49	0.70	0.84	0.38	0.50	0.60	0.84	1.31
	9074	0.19	0.22	0.23	0.15	0.17	0.18	0.23	1.28
	9075	0.18	0.20	0.20	0.14	0.15	0.16	0.20	1.27
17.50	9061	0.42	0.58	0.69	0.34	0.47	0.56	0.69	1.13
	9062	0.15	0.16	0.17	0.12	0.13	0.15	0.17	1.10
	9063	0.18	0.18	0.20	0.14	0.14	0.15	0.20	1.11
	9064	0.23	0.26	0.28	0.18	0.19	0.20	0.28	1.18
	9065	0.16	0.16	0.19	0.12	0.12	0.12	0.19	1.11
13.57	9051	0.16	0.17	0.18	0.13	0.13	0.13	0.18	1.12
	9052	0.14	0.14	0.15	0.11	0.11	0.11	0.15	1.12
9.06	9041	0.15	0.14	0.15	0.12	0.12	0.12	0.15	1.11
	9042	0.13	0.12	0.12	0.10	0.09	0.09	0.13	1.11
4.65	9031	0.09	0.11	0.10	0.08	0.09	0.09	0.11	1.13
	9032	0.12	0.11	0.11	0.10	0.10	0.10	0.12	1.08
	9033	0.16	0.15	0.15	0.13	0.13	0.12	0.16	1.17
	9034	0.09	0.07	0.08	0.06	0.06	0.07	0.09	1.13
	9035	0.11	0.10	0.09	0.08	0.08	0.07	0.11	1.07
-1.00	9021	0.09	0.08	0.08	0.08	0.08	0.07	0.09	1.11
	9022	0.09	0.08	0.08	0.06	0.07	0.07	0.09	1.11
	9023	0.10	0.09	0.09	0.08	0.08	0.08	0.10	1.03
	9024	0.11	0.12	0.12	0.09	0.09	0.09	0.12	1.17
	9025	0.09	0.07	0.07	0.06	0.06	0.06	0.09	1.02
	9026	0.07	0.06	0.05	0.05	0.05	0.05	0.07	1.11
	9027	0.11	0.10	0.09	0.08	0.07	0.07	0.11	1.16
-6.40	9011	0.11	0.09	0.08	0.08	0.08	0.07	0.11	1.17
	9012	0.10	0.09	0.09	0.07	0.07	0.07	0.10	1.17
	9013	0.08	0.06	0.06	0.05	0.05	0.05	0.08	1.01

Note: The shaded values in the table show the governing case.

Table 5.4-2 Maximum Displacements of Walls SDOF Oscillators Relative to Free-Field

Elev. (m)	Node No.	Dir.	Horizontal Displacement (cm)							
			Full Column			Partial Column			NA3 Envelope	Standard Design
			LB	BE	UB	LB	BE	UB		
42.00	99981	NS	1.05	1.13	1.09	0.80	0.84	0.85	1.13	-
	99982		0.94	1.02	0.97	0.73	0.78	0.76	1.02	-
13.57	99971		0.47	0.54	0.55	0.42	0.44	0.46	0.55	-
	99972		0.40	0.41	0.39	0.36	0.37	0.36	0.41	-
	99973		0.35	0.36	0.33	0.30	0.29	0.31	0.36	-
	99974		0.35	0.36	0.33	0.30	0.29	0.29	0.36	-
42.00	99983	EW	1.24	1.07	1.16	0.88	0.81	0.88	1.24	-
	99984		1.17	1.02	1.07	0.82	0.76	0.81	1.17	-
	99985		1.14	0.99	1.04	0.80	0.75	0.79	1.14	-
13.57	99975		0.50	0.44	0.45	0.44	0.50	0.52	0.52	-
	99976		0.37	0.31	0.31	0.27	0.33	0.32	0.37	-

Note: The shaded values in the table show the governing case.

Table 5.6-1 Summary of Maximum Base Reaction Eccentricity and Minimum Contact Ratio Results

Combination of Input Direction	Analysis	Full Column			Partial Column		
		BE	UB	LB	BE	UB	LB
+Ex+Ey+Ez	Max. Eccentricity (m)	9.24	8.58	7.47	9.03	9.07	8.25
	Min. Contact Ratio	93.1 %	93.1 %	95.3 %	94.7 %	94.1 %	95.5 %
	at Time (s)	3.645	3.625	4.320	4.310	4.070	4.315
+Ex-Ey-Ez	Max. Eccentricity (m)	8.37	8.51	7.51	8.44	9.44	7.23
	Min. Contact Ratio	92.0 %	89.2 %	95.7 %	92.8 %	90.4 %	96.1 %
	at Time (s)	3.235	3.225	3.465	3.225	3.225	3.460
-Ex+Ey+Ez	Max. Eccentricity (m)	7.22	6.63	7.53	7.17	7.53	6.86
	Min. Contact Ratio	95.9 %	92.2 %	93.5 %	94.1 %	93.7 %	94.5 %
	at Time (s)	3.460	3.625	3.470	4.425	3.350	4.430
-Ex-Ey-Ez	Max. Eccentricity (m)	9.99	9.24	9.37	9.12	10.65	7.86
	Min. Contact Ratio	91.4 %	90.9 %	92.5 %	93.5 %	91.3 %	93.6 %
	at Time (s)	3.150	3.145	3.155	7.080	7.075	3.155

Note: The shaded values in the table show the governing case.

Table 6.1-1a Enveloping Maximum Structural Force and Moment Demands on RB/FB

Element		Standard Design					NA3 Enveloping Demands					Difference/Exceedance				
Elev. (m)	Node No.	Shear (MN)		Bending (MN-m)		Torsion (MN-m)	Shear (MN)		Bending (MN-m)		Torsion (MN-m)	Shear		Bending		Torsion
		NS	EW	NS*)	EW*)		NS	EW	NS*)	EW*)		NS	EW	NS*)	EW*)	
52.40	110	151.9	158.2	1642	1808	1379	192.2	140.0	2724	2142	1284	27%	-12%	66%	18%	-7%
	109			4303	4465				5838	4488				36%	1%	
34.00	109	191.7	153.0	5585	5522	2405	173.2	113.9	8196	5821	1938	-10%	-26%	47%	5%	-19%
	108			6477	6317				8719	6389				35%	1%	
27.00	108	425.4	400.7	7685	7106	3333	396.0	259.4	9400	7162	2799	-7%	-35%	22%	1%	-16%
	107			8964	8596				9599	7958				7%	-7%	
22.50	107	483.7	464.0	9905	9193	6093	436.4	291.8	11216	8328	4678	-10%	-37%	13%	-9%	-23%
	106			11464	11297				11424	9227				0%	-18%	
17.5	106	532.9	555.4	12386	11935	5068	438.4	343.5	12105	9408	4023	-18%	-38%	-2%	-21%	-21%
	105			13778	13867				12349	10195				-10%	-26%	
13.57	105	569.2	599.9	14298	14377	5245	450.7	363.7	12839	10255	4211	-21%	-39%	-10%	-29%	-20%
	104			16593	16740				13651	11216				-18%	-33%	
9.06	104	610.1	654.3	16966	17191	5985	454.6	383.4	13904	11338	4694	-25%	-41%	-18%	-34%	-22%
	103			19378	19672				15231	12506				-21%	-36%	
4.65	103	839.8	872.2	19064	20192	11425	454.7	360.1	9392	6302	5248	-46%	-59%	-51%	-69%	-54%
	102			23163	24272				10952	7759				-53%	-68%	
-1.00	102	871.4	938.5	23673	24948	11523	240.0	226.6	6545	4819	2718	-72%	-76%	-72%	-81%	-76%
	101			27655	29263				7303	5358				-74%	-82%	
-6.40	101	933.6	1029.7	28126	30038	11690	237.7	200.4	4748	3351	2079	-75%	-81%	-83%	-89%	-82%
-11.5	2			32235	35275				5053	3356				-84%	-90%	

Note: The shaded values in the table show exceedance from standard design.

*) NS and EW represent moments for bending in NS or EW direction, respectively.

Table 6.1-1b Enveloping Maximum Structural Force and Moment Demands on RCCV

Element		Standard Design					NA3 Enveloping Demands					Difference/Exceedance				
Elev. (m)	Node No.	Shear (MN)		Bending (MN-m)		Torsion (MN-m)	Shear (MN)		Bending (MN-m)		Torsion (MN-m)	Shear		Bending		Torsion
		NS	EW	NS*)	EW*)		NS	EW	NS*)	EW*)		NS	EW	NS*)	EW*)	
34.00	209	137.0	183.2	195	581	36	130.9	133.2	230	510	29	-4%	-27%	18%	-12%	-19%
	208			1057	1496				1029	1160				-3%	-22%	
27.00	208	164.9	248.5	1708	2532	1814	141.1	151.9	2162	2303	1489	-14%	-39%	27%	-9%	-18%
	207			2959	4368				2938	3071				-1%	-30%	
17.50	206	230.2	290.2	3315	4715	1982	184.1	158.4	3259	3667	1591	-20%	-45%	-2%	-22%	-20%
	205			4147	5761				3691	3904				-11%	-32%	
13.57	205	263.4	326.2	4327	5949	2186	207.9	173.4	3817	4203	1762	-21%	-47%	-12%	-29%	-19%
	204			5404	7264				4389	4491				-19%	-38%	
9.06	204	304.2	365.8	5628	7519	2616	225.4	201.2	4481	4853	2062	-26%	-45%	-20%	-35%	-21%
	203			6785	8909				5190	5203				-24%	-42%	
4.65	203	227.3	289.4	6992	9171	2870	109.2	125.7	5523	5470	1439	-52%	-57%	-21%	-40%	-50%
	202			7958	10581				5740	5824				-28%	-45%	
-1.00	202	272.4	330.6	8076	10738	2926	67.6	68.1	6008	6066	690	-75%	-79%	-26%	-44%	-76%
	201			9417	12523				5924	6035				-37%	-52%	
-6.40	201	261.7	303.5	9534	12651	1962	70.7	55.1	6053	6141	349	-73%	-82%	-37%	-51%	-82%
-11.50	2			10836	14200				5961	6127				-45%	-57%	

Note: The shaded values in the table show exceedance from standard design.

*) NS and EW represent moments for bending in NS or EW direction, respectively.

Table 6.1-1c Enveloping Maximum Structural Force and Moment Demands on Vent Wall

Element		Standard Design					NA3 Enveloping Demands					Difference/Exceedance				
Elev. (m)	Node No.	Shear (MN)		Bending (MN-m)		Torsion (MN-m)	Shear (MN)		Bending (MN-m)		Torsion (MN-m)	Shear		Bending		Torsion
		NS	EW	NS*)	EW*)		NS	Ew	NS*)	EW*)		NS	EW	NS*)	EW*)	
17.50	701	35.0	37.0	78	85	116	47.9	32.4	74	56	107	37%	-12%	-5%	-34%	-8%
	702			114	136				139	107				22%	-21%	
14.50	702	36.4	39.3	119	148	118	47.1	32.4	139	113	108	29%	-18%	17%	-24%	-8%
	703			226	260				279	204				23%	-22%	
11.50	703	37.0	41.8	229	269	120	45.8	35.1	280	207	111	24%	-16%	22%	-23%	-8%
	704			340	390				411	301				21%	-23%	
8.50	704	37.8	44.7	341	396	122	44.7	36.5	411	302	112	18%	-18%	21%	-24%	-8%
	705			379	438				458	338				21%	-23%	
7.4625	705	40.7	40.5	359	438	101	39.1	29.4	440	352	92	-4%	-27%	23%	-20%	-9%
4.65	706, 303			456	525				513	427				13%	-19%	

Note: The shaded values in the table show exceedance from standard design.

*) NS and EW represent moments for bending in NS or EW direction, respectively.

Table 6.1-1d Enveloping Maximum Structural Force and Moment Demands on Pedestal

Element		Standard Design					NA3 Enveloping Demands					Difference/Exceedance				
Elev. (m)	Node No.	Shear (MN)		Bending (MN-m)		Torsion (MN-m)	Shear (MN)		Bending (MN-m)		Torsion (MN-m)	Shear		Bending		Torsion
		NS	EW	NS*)	EW*)		NS	EW	NS*)	EW*)		NS	EW	NS*)	EW*)	
4.65	303	32.8	44.8	581	621	142	20.5	16.9	667	496	71	-38%	-62%	15%	-20%	-50%
	377			599	667				651	502				9%	-25%	
2.42	377	48.1	66.3	732	817	172	30.9	25.4	793	614	86	-36%	-62%	8%	-25%	-50%
	302			778	922				754	631				-3%	-32%	
-1.00	302	65.6	81.4	839	959	146	22.1	15.7	691	571	34	-66%	-81%	-18%	-40%	-77%
	376			928	1050				658	555				-29%	-47%	
-2.75	376	66.0	81.7	928	1050	146	21.8	16.1	658	555	34	-67%	-80%	-29%	-47%	-77%
	301			1116	1330				594	524				-47%	-61%	
-6.40	301	104.4	121.2	1149	1346	118	29.8	22.4	555	518	21	-71%	-82%	-52%	-62%	-82%
-11.50	2			1655	1963				553	514				-67%	-74%	

Note: The shaded values in the table show exceedance from standard design.

*) NS and EW represent moments for bending in NS or EW direction, respectively.

Table 6.1-1e Enveloping Maximum Structural Force and Moment Demands on Reactor Shield Wall

Element		Standard Design					NA3 Enveloping Demands					Difference/Exceedance				
Elev. (m)	Node No.	Shear (MN)		Bending (MN-m)		Torsion (MN-m)	Shear (MN)		Bending (MN-m)		Torsion (MN-m)	Shear		Bending		Torsion
		NS	EW	NS*)	EW*)		NS	EW	NS*)	EW*)		NS	EW	NS*)	EW*)	
24.18	707	3.0	2.7	2.1	1.7	0.4	4.2	3.0	2.5	2.2	0.5	40%	11%	19%	29%	25%
	708			13.2	12.4				18.9	13.8				43%	11%	
20.20	708	14.6	12.3	18.4	16.8	1.4	20.8	10.4	25.8	19.8	1.7	42%	-15%	40%	18%	21%
	709			79.0	68.4				113.5	59.2				44%	-13%	
15.775	709	17.3	14.4	81.9	71.0	1.9	24.4	11.9	116.7	61.3	2.4	41%	-17%	42%	-14%	26%
	710			158.4	133.6				224.1	113.9				41%	-15%	
11.35	710	19.9	16.6	159.1	136.4	2.4	27.1	12.7	227.6	116.1	3.0	36%	-23%	43%	-15%	25%
	711			236.2	198.7				331.9	165.6				41%	-17%	
7.4625	711	41.1	35.6	197.0	183.6	23.4	22.4	16.8	99.3	77.7	21.4	-45%	-53%	-50%	-58%	-9%
	712			292.4	251.3				141.3	119.0				-52%	-53%	
4.65	712	14.3	19.5	125.1	133.0	30.3	8.9	7.4	147.6	108.1	15.2	-38%	-62%	18%	-19%	-50%
	713			133.0	150.9				139.8	110.8				5%	-27%	
2.4615	713	1.5	1.3	3.6	3.2	0.2	1.4	1.1	3.9	2.9	0.1	-7%	-15%	8%	-9%	-50%
1.96	714			2.9	2.7				3.2	2.3				10%	-15%	
1.96	714	0.9	0.7	2.7	2.4	0.1	0.9	0.7	2.8	2.1	0.1	0%	0%	4%	-13%	0%
-0.8	715			0.5	0.5				0.7	0.6				40%	20%	

Note: The shaded values in the table show exceedance from standard design.

*) NS and EW represent moments for bending in NS or EW direction, respectively.

Table 6.1-1f Enveloping Maximum Load Demands on RPV

Component	Node No.	Elem. No.	Standard Design					NA3 Enveloping Demands					Difference				
			Axial (MN)	Shear (MN)		Moment (MN-m)		Axial (MN)	Shear (MN)		Moment (MN-m)		Axial	Shear		Moment	
				NS	EW	NS*)	EW*)		NS	EW	NS*)	EW*)		NS	EW	NS*)	EW*)
Shroud Bottom	845	844	8.58	7.2	7.0	16.2	14.3	9.10	18.6	6.7	29.9	10.3	6%	158%	-4%	85%	-28%
	846					21.3	17.3				44.5	14.8				109%	-14%
Fuel Top	847	845	0.05	1.2	1.1	0.0	0.0	0.05	0.8	0.8	0.0	0.0	0%	-33%	-27%	-	-
	848					0.1	0.1				0.1	0.1				0%	0%
Fuel Middle	848	846	0.44	1.0	1.0	0.1	0.1	0.46	1.0	0.8	0.1	0.1	5%	0%	-20%	0%	0%
	849					0.8	0.8				0.8	0.6				0%	-25%
Fuel Middle	849	847	1.15	0.6	0.6	0.8	0.8	1.20	0.6	0.5	0.8	0.6	4%	0%	-17%	0%	-25%
	850					1.2	1.3				1.2	0.9				0%	-31%
Fuel Middle	850	848	1.86	0.2	0.2	1.2	1.3	1.93	0.4	0.3	1.2	0.9	4%	100%	50%	0%	-31%
	851					1.2	1.3				1.1	0.9				-8%	-31%
Fuel Middle	851	849	2.56	0.6	0.6	1.2	1.3	2.63	0.7	0.5	1.1	0.9	3%	17%	-17%	-8%	-31%
	852					0.8	0.8				0.7	0.7				-13%	-13%
Fuel Middle	852	850	3.24	1.0	1.0	0.8	0.8	3.31	0.9	0.8	0.7	0.7	2%	-10%	-20%	-13%	-13%
	853					0.1	0.1				0.1	0.1				0%	0%
Fuel Bottom	853	851	3.56	1.1	1.1	0.1	0.1	3.64	1.0	0.9	0.1	0.1	2%	-9%	-18%	0%	0%
	854					0.0	0.0				0.0	0.0				-	-
RPV Support	815	871	25.3	18.6	17.9	144	136	23.3	29.8	16.8	183	113	-8%	60%	-6%	27%	-17%
	711					141	137				177	109				26%	-20%

Note: The shaded values in the table show exceedance from standard design.

*) NS and EW represent moments for bending in NS or EW direction, respectively.

Table 6.1-2a Enveloping Maximum Accelerations for RB/FB

Elev. (m)	Node No.	Acceleration (g)						Difference		
		Standard Design			NA3 Enveloping					
		NS	EW	Vert.	NS	EW	Vert.	NS	EW	Vert.
52.40	110	1.68	1.78	1.27	2.13	1.55	1.56	27%	-13%	23%
34.00	109	1.18	1.15	0.83	1.02	0.81	1.20	-14%	-30%	45%
27.00	108	0.99	1.02	0.73	0.96	0.69	1.02	-3%	-32%	40%
22.50	107	0.98	0.91	0.73	0.83	0.73	0.92	-15%	-20%	26%
17.50	106	0.98	0.84	0.73	0.80	0.65	0.80	-18%	-23%	10%
13.57	105	0.97	0.77	0.74	0.79	0.62	0.72	-19%	-19%	-3%
9.06	104	0.84	0.73	0.73	0.76	0.54	0.62	-10%	-26%	-15%
4.65	103	0.73	0.68	0.78	0.76	0.56	0.56	4%	-18%	-28%
-1.00	102	0.68	0.63	0.76	0.62	0.51	0.57	-9%	-19%	-25%
-6.40	101	0.61	0.62	0.68	0.50	0.43	0.50	-18%	-31%	-26%
-11.50	2	0.60	0.55	0.63	0.43	0.37	0.47	-28%	-33%	-25%
-15.50	1	0.51	0.51	0.51	0.44	0.37	0.46	-14%	-27%	-10%

Note: The presented values are the maximum accelerations at floor lumped mass locations.
The shaded values in the table show exceedance from standard design.

Table 6.1-2b Enveloping Maximum Accelerations for RCCV

Elev. (m)	Node No.	Acceleration (g)						Difference		
		Standard Design			NA3 Enveloping					
		NS	EW	Vert.	NS	EW	Vert.	NS	EW	Vert.
34.00	209	1.18	1.15	0.90	1.02	0.81	1.20	-14%	-30%	33%
27.00	208	0.98	1.02	0.88	0.96	0.69	1.12	-2%	-32%	27%
17.50	206	0.98	0.85	0.73	0.80	0.66	0.91	-18%	-22%	25%
13.57	205	0.97	0.78	0.78	0.79	0.63	0.82	-19%	-19%	5%
9.06	204	0.84	0.74	0.65	0.76	0.54	0.72	-10%	-27%	11%
4.65	203	0.73	0.69	0.70	0.76	0.55	0.65	4%	-20%	-7%
-1.00	202	0.68	0.63	0.59	0.59	0.52	0.58	-13%	-17%	-2%
-6.40	201	0.61	0.60	0.59	0.50	0.44	0.50	-18%	-27%	-15%

Note: The presented values are the maximum accelerations at floor lumped mass locations.
The shaded values in the table show exceedance from standard design.

Table 6.1-2c Enveloping Maximum Accelerations for Vent Wall and Pedestal

Elev. (m)	Node No.	Acceleration (g)						Difference		
		Standard Design			NA3 Enveloping					
		NS	EW	Vert.	NS	EW	Vert.	NS	EW	Vert.
17.50	701	0.98	0.85	1.10	0.80	0.66	0.82	-18%	-22%	-25%
14.50	702	1.40	1.06	1.04	0.77	0.61	0.77	-45%	-42%	-26%
11.50	703	1.42	1.14	0.92	0.77	0.55	0.71	-46%	-52%	-23%
8.50	704	0.98	0.86	0.77	0.74	0.53	0.68	-24%	-38%	-12%
7.4625	705	0.85	0.77	0.70	0.75	0.52	0.67	-12%	-32%	-4%
4.65	706, 303	0.73	0.69	0.67	0.76	0.55	0.65	4%	-20%	-3%
-1.00	302	0.68	0.63	0.59	0.59	0.52	0.59	-13%	-17%	0%
-6.40	301	0.61	0.60	0.50	0.50	0.44	0.49	-18%	-27%	-2%

Note: The presented values are the maximum accelerations at mass center.
The shaded values in the table show exceedance from standard design.

Table 6.1-2d Enveloping Maximum Accelerations for Reactor Shield Wall

Elev. (m)	Node No.	Acceleration (g)						Difference		
		Standard Design			NA3 Enveloping					
		NS	EW	Vert.	NS	EW	Vert.	NS	EW	Vert.
24.18	707	2.51	2.38	0.97	3.61	2.51	1.19	44%	5%	23%
20.20	708	2.13	1.90	0.94	2.81	1.82	1.14	32%	-4%	21%
15.775	709	1.74	1.39	0.84	1.77	1.23	0.99	2%	-12%	18%
11.35	710	1.29	0.95	0.76	1.01	0.69	0.78	-22%	-27%	3%
7.4625	711	0.85	0.77	0.70	0.75	0.52	0.67	-12%	-32%	-4%
4.65	712	0.73	0.69	0.67	0.76	0.55	0.65	4%	-20%	-3%
2.4615	713	0.74	0.66	0.64	0.69	0.55	0.64	-7%	-17%	0%
1.96	714	0.75	0.66	0.64	0.70	0.57	0.64	-7%	-14%	0%
-0.80	715	0.86	0.72	0.65	0.83	0.65	0.64	-3%	-10%	-2%

Note: The presented values are the maximum accelerations at mass center.
The shaded values in the table show exceedance from standard design.

Table 6.1-2e Enveloping Maximum Accelerations for Fuel

Elev. (m)	Node No.	Standard Design			NA3 Enveloping Demands			Difference		
		NS (g)	EW (g)	Vert. (g)	NS (g)	EW (g)	Vert. (g)	NS	EW	Vert.
7.896	847	1.09	1.00	1.41	2.06	0.92	1.49	89%	-8%	6%
7.8071	848	1.06	0.98	1.41	1.91	0.86	1.49	80%	-12%	6%
7.111	849	0.91	0.92	1.41	1.00	0.49	1.47	10%	-47%	4%
6.401	850	0.98	0.91	1.39	0.62	0.64	1.45	-37%	-30%	4%
5.691	851	0.91	0.98	1.36	0.85	0.74	1.41	-7%	-24%	4%
4.981	852	1.20	1.12	1.33	1.61	1.15	1.36	34%	3%	2%
4.2713	853	1.65	1.42	1.28	2.52	1.74	1.31	53%	23%	2%
4.1784	854	1.73	1.52	1.27	2.63	1.81	1.30	52%	19%	2%

Note: The presented values are the maximum accelerations at mass center.
The shaded values in the table show exceedance from standard design.

Table 6.1-3 Enveloping Maximum Out-of-Plane Loads on RB/FB Flexible Slabs

Elev. (m)	Location	Slab Equivalent Out-of-Plane Acceleration Load (g)								Difference
		Partial Column			Full Column			NA3 Envelope	Standard Design[1)]	
		BE	UB	LB	BE	UB	LB			
52.40	RB Roof	1.07	1.23	0.87	1.35	*1.51*	1.07	1.51	1.64	-8%
34.00	RB-RCCV	0.83	0.98	0.71	1.01	*1.23*	0.84	1.23	0.90	37%
	RCCV	0.87	1.05	0.74	1.01	*1.30*	0.84	1.30	0.93	40%
27.00	Top Slab	0.89	1.09	0.77	1.14	*1.37*	0.91	1.37	0.98	40%
	RB-RCCV	0.70	0.81	0.59	0.86	*1.06*	0.69	1.06	0.77	38%
	M/S tunnel roof	0.73	0.88	0.62	0.90	*1.13*	0.69	1.13	0.82	38%
22.50	FB Roof	0.79	0.86	0.74	1.24	*1.31*	1.17	1.31	1.47	-11%
17.50	M/S tunnel slab	1.14	1.47	0.88	1.38	*1.74*	0.99	1.74	1.10	58%
	RB-RCCV	0.64	0.76	0.55	0.77	*0.94*	0.62	0.94	0.78	21%
	DF	1.07	1.17	0.93	1.38	*1.53*	1.14	1.53	1.84	-17%
13.57	RB-RCCV	0.63	0.78	0.54	0.72	*0.89*	0.59	0.89	0.84	6%
9.06	RB-RCCV	0.59	0.69	0.53	0.67	*0.79*	0.61	0.79	0.82	-4%
4.65	FB	0.91	1.10	0.72	0.92	*1.11*	0.60	1.11	1.03	8%
	RB-RCCV	0.70	0.81	0.64	0.81	*0.87*	0.72	0.87	0.95	-8%
	RCCV-Pedestal	0.63	0.71	0.55	0.70	*0.82*	0.61	0.82	0.80	2%
-1.00	FB	0.61	*0.71*	0.51	0.60	*0.71*	0.52	0.71	0.88	-19%
	RB-RCCV	0.59	0.70	0.52	0.64	*0.73*	0.55	0.73	0.85	-14%
	RCCV-Pedestal	0.57	0.65	0.46	0.61	*0.70*	0.55	0.70	0.71	-1%
-6.40	RCCV-Pedestal	0.48	0.55	0.41	0.54	*0.60*	0.51	0.60	0.63	-5%
	RB-RCCV	0.46	0.56	0.38	0.50	*0.57*	0.46	0.57	0.71	-20%

Note: 1) Values from Table 6.2.3.9-20 in Reference 2.1
The shaded values in the table show exceedance from standard design.
The values shown in Italic are governing case.

Table 6.1-4 Enveloping Maximum Out-of-Plane Loads on RB/FB Flexible Walls

Elev. (m)	Location	Wall Equivalent Out-of-Plane Acceleration Load (g)								Difference
		Partial Column			Full Column			NA3 Envelop.	Stand. Design[1)]	
		BE	UB	LB	BE	UB	LB			
42.00	R1 and R7 walls	1.56	1.80	1.23	1.88	*2.10*	1.47	2.10	1.48	42%
	RB and RF walls	1.02	1.14	0.84	1.07	*1.27*	1.02	1.27	1.52	-16%
13.75	F3 wall	1.16	1.39	0.98	1.15	*1.48*	0.93	1.48	1.19	24%
	FA and FF walls	1.25	*1.55*	0.98	1.08	1.21	0.80	1.55	1.09	42%

Note: 1) Values from Table 6.2.3.9-25 in Reference 2.1
The shaded values in the table show exceedance from standard design.
The values shown in Italic are governing case.

Table 6.1-5 Enveloping Maximum Spring Forces and Displacements

(a) RPV Stabilizer Spring Reaction

Dir.	Node No.		Standard Design		NA3 Enveloping Demands		Difference	
	i	j	Rel. Displ. (cm)	Reaction (MN)	Rel. Displ. (cm)	Reaction (MN)	Relative Displacement	Reaction
NS	808	708	0.13	7.85	0.20	12.12	54%	54%
EW	808	708	0.14	8.48	0.12	7.64	-14%	-10%

Note: The shaded values in the table show exceedance from standard design.

(b) D/F Spring Reactions

Elem No.	Standard Design		NA3 Enveloping Demands		Difference	
	Rel. Displ. (cm)	Reaction (MN)	Rel. Displ. (cm)	Reaction (MN)	Relative Displacement	Reaction
9064	-	-	0.21	25.96	-	-
9164	-	-	0.24	30.28	-	-

Table 6.2-1 RB/FB Enveloping Maximum Relative Displacements

Location	Displacement (cm)							
	Nodes No.		NA3 Enveloping			Standard Design		
	i	j	NS	EW	Vert.	NS	EW	Vert.
Fuel top to fuel center	847	850	0.64	0.42	0.00	0.49	0.56	0.00
Fuel center to fuel bottom	850	853	0.56	0.39	0.01	0.58	0.58	0.01
Core plate to vessel bottom	844	828	0.18	0.10	0.02	0.27	0.58	0.02
Top guide to vessel	838	816	0.38	0.10	0.04	0.15	0.12	0.04
Top guide to vessel bottom	838	828	0.41	0.20	0.03	0.55	1.20	0.03
Fuel center to vessel bottom	850	828	0.68	0.47	0.01	0.79	1.07	0.01
CRD housing to bottom head	868	828	0.28	0.19	0.00	0.22	0.42	0.00
CRD housing to bottom head	867	827	0.28	0.19	0.00	0.28	0.55	0.00
RCCV - RPV	206	807	0.60	0.30	0.04	0.48	0.71	0.43
RCCV - Lower part in the VW	206	706	0.35	0.29	0.06	0.90	1.97	0.54
RPV - Lower part in the VW	807	706	0.75	0.44	0.03	1.23	2.66	0.90

Note: The shaded values in the table show exceedance from standard design.

Table 6.2-2 RB/FB Enveloping Maximum Displacements Relative to Free-Field

(a) RB/FB

Elev. (m)	Node No.	Displacement (cm)					
		NA3 Enveloping			Standard Design		
		NS	EW	Vert.	NS	EW	Vert.
52.40	110	1.26	1.57	0.80	7.18	12.34	1.26
34.00	109	0.84	1.04	0.69	5.98	9.42	1.25
27.00	108	0.70	0.87	0.58	5.52	8.34	1.18
22.50	107	0.57	0.73	0.50	5.21	7.58	1.27
17.50	106	0.45	0.57	0.41	4.87	6.84	1.09
13.57	105	0.36	0.46	0.35	4.60	6.23	1.07
9.06	104	0.27	0.34	0.31	4.29	5.54	1.07
4.65	103	0.19	0.22	0.18	3.99	4.85	1.12
-1.00	102	0.12	0.13	0.14	3.63	4.02	1.10
-6.40	101	0.08	0.08	0.12	3.29	3.24	1.15
-11.50	2	0.06	0.06	0.10	2.99	2.60	0.98
-15.50	1	0.06	0.05	0.10	2.80	2.24	1.02

Table 6.2-2 RB/FB Enveloping Maximum Displacements Relative to Free-Field (Continued)

(b) RCCV

Elev. (m)	Node No.	Displacement (cm)					
		NA3 Enveloping			Standard Design		
		NS	EW	Vert.	NS	EW	Vert.
34.00	209	0.83	1.02	0.45	5.98	9.42	1.19
27.00	208	0.69	0.85	0.42	5.52	8.34	1.14
17.50	206	0.44	0.55	0.34	4.87	6.85	1.13
13.57	205	0.36	0.44	0.31	4.60	6.25	1.16
9.06	204	0.27	0.33	0.28	4.29	5.56	1.15
4.65	203	0.19	0.21	0.24	3.99	4.88	1.15
-1.00	202	0.12	0.12	0.18	3.63	4.04	1.15
-6.40	201	0.08	0.08	0.13	3.29	3.25	1.15

Table 6.2-2 RB/FB Enveloping Maximum Displacements Relative to Free-Field (Continued)

(c) Vent Wall and Pedestal

Elev. (m)	Node No.	Displacement (cm)					
		NA3 Enveloping			Standard Design		
		NS	EW	Vert.	NS	EW	Vert.
17.50	701	0.44	0.51	0.24	4.87	6.86	1.18
14.50	702	0.37	0.43	0.23	4.67	6.40	1.18
11.50	703	0.31	0.36	0.22	4.46	5.94	1.18
8.50	704	0.25	0.28	0.21	4.25	5.47	1.18
7.4625	705	0.23	0.26	0.21	4.18	5.31	1.18
4.65	706, 303	0.18	0.20	0.19	3.99	4.88	1.18
-1.00	302	0.12	0.12	0.14	3.63	4.04	1.17
-6.40	301	0.08	0.08	0.10	3.29	3.25	1.17

Table 6.2-2 RB/FB Enveloping Maximum Displacements Relative to Free-Field (Continued)

(d) RSW

Elev. (m)	Node No.	Displacement (cm)					
		NA3 Enveloping			Standard Design		
		NS	EW	Vert.	NS	EW	Vert.
24.18	707	0.82	0.62	0.21	5.32	7.86	1.18
20.20	708	0.67	0.54	0.20	5.05	7.26	1.18
15.78	709	0.47	0.43	0.20	4.75	6.58	1.18
11.35	710	0.32	0.33	0.18	4.44	5.90	1.18
7.46	711	0.23	0.25	0.16	4.18	5.31	1.18
4.65	712	0.18	0.19	0.15	3.99	4.88	1.18
2.46	713	0.16	0.16	0.14	3.84	4.55	1.17
1.96	714	0.15	0.15	0.14	3.81	4.48	1.17
-0.80	715	0.12	0.12	0.14	3.65	4.09	1.17

Table 6.2-2 RB/FB Enveloping Maximum Displacements Relative to Free-Field (Continued)

(e) RPV

Node No.	Displacement (cm)					
	NA3 Enveloping			Standard Design		
	NS	EW	Vert.	NS	EW	Vert.
801	1.21	0.78	0.14	5.60	8.44	1.18
806	0.91	0.64	0.24	5.22	7.61	1.18
807	0.88	0.62	0.23	5.19	7.54	1.18
809	0.74	0.55	0.23	5.03	7.18	1.18
810	0.62	0.49	0.22	4.87	6.83	1.18
813	0.42	0.37	0.20	4.54	6.10	1.18
814	0.35	0.32	0.18	4.40	5.79	1.18
815	0.29	0.28	0.17	4.26	5.48	1.18
827	0.29	0.21	0.16	3.78	4.34	1.18
828	0.29	0.22	0.15	3.73	4.21	1.18
831	0.76	0.79	2.09	5.23	7.36	1.18
832	0.61	0.48	0.28	4.87	6.83	1.18
833	0.59	0.47	0.28	4.81	6.69	1.18
834	0.56	0.43	0.27	4.69	6.41	1.18
844	0.34	0.24	0.19	3.98	4.79	1.18
846	0.29	0.22	0.18	3.88	4.58	1.18
847	0.48	0.29	0.18	4.24	5.39	1.18
851	0.48	0.57	0.39	4.28	5.05	1.18
854	0.34	0.24	0.17	3.98	4.79	1.18
867	0.14	0.13	0.58	3.53	3.80	1.18

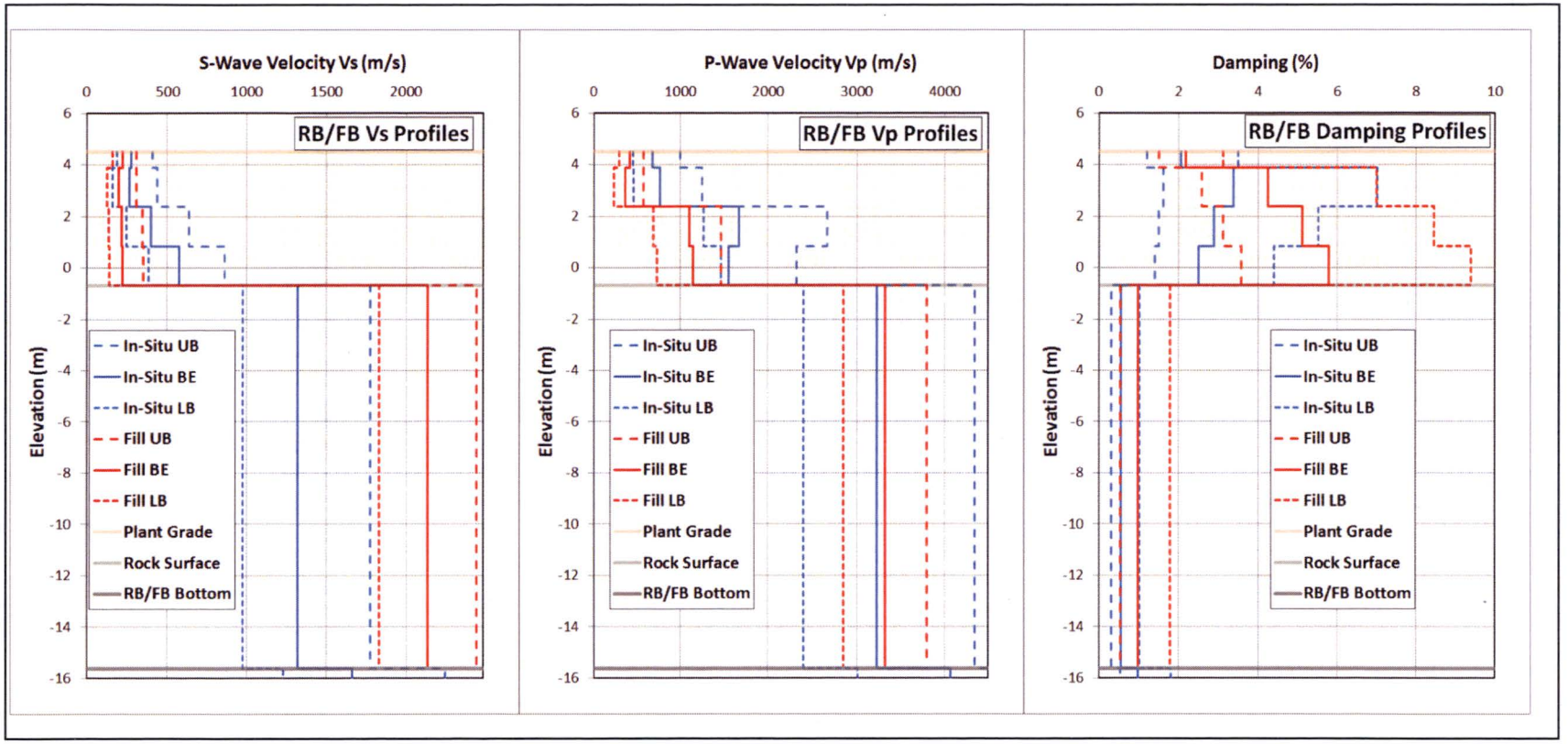

Figure 3.1-1 Comparisions Between Shear Wave Velocity and Damping Ratio of Structural Fill and In-Situ Saprolite

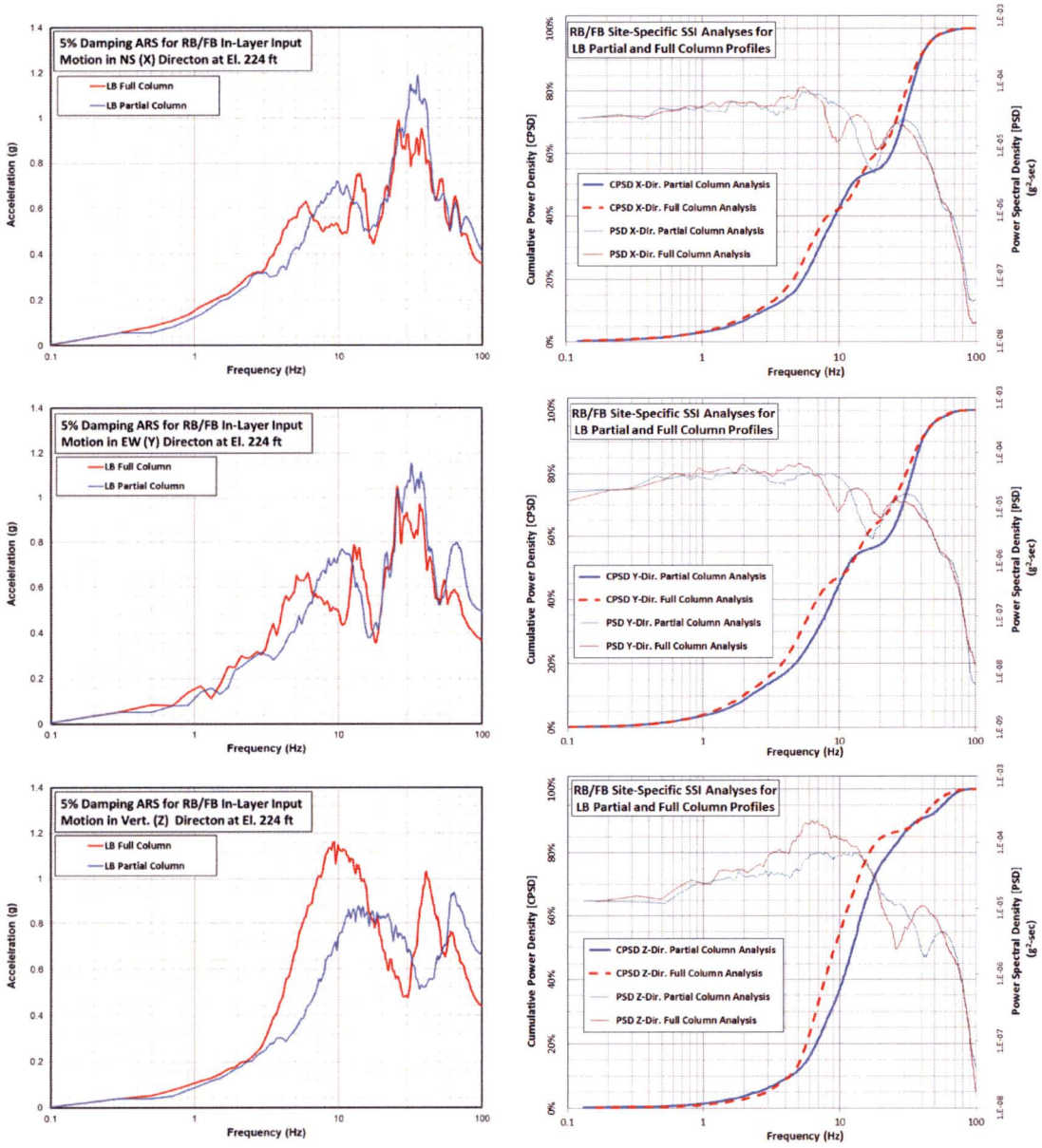

Figure 3.2-1 5% Damped ARS, PSD and CPSD of the RB/FB Input Acceleration Time Histories for Analyses of LB Subgrade Profiles

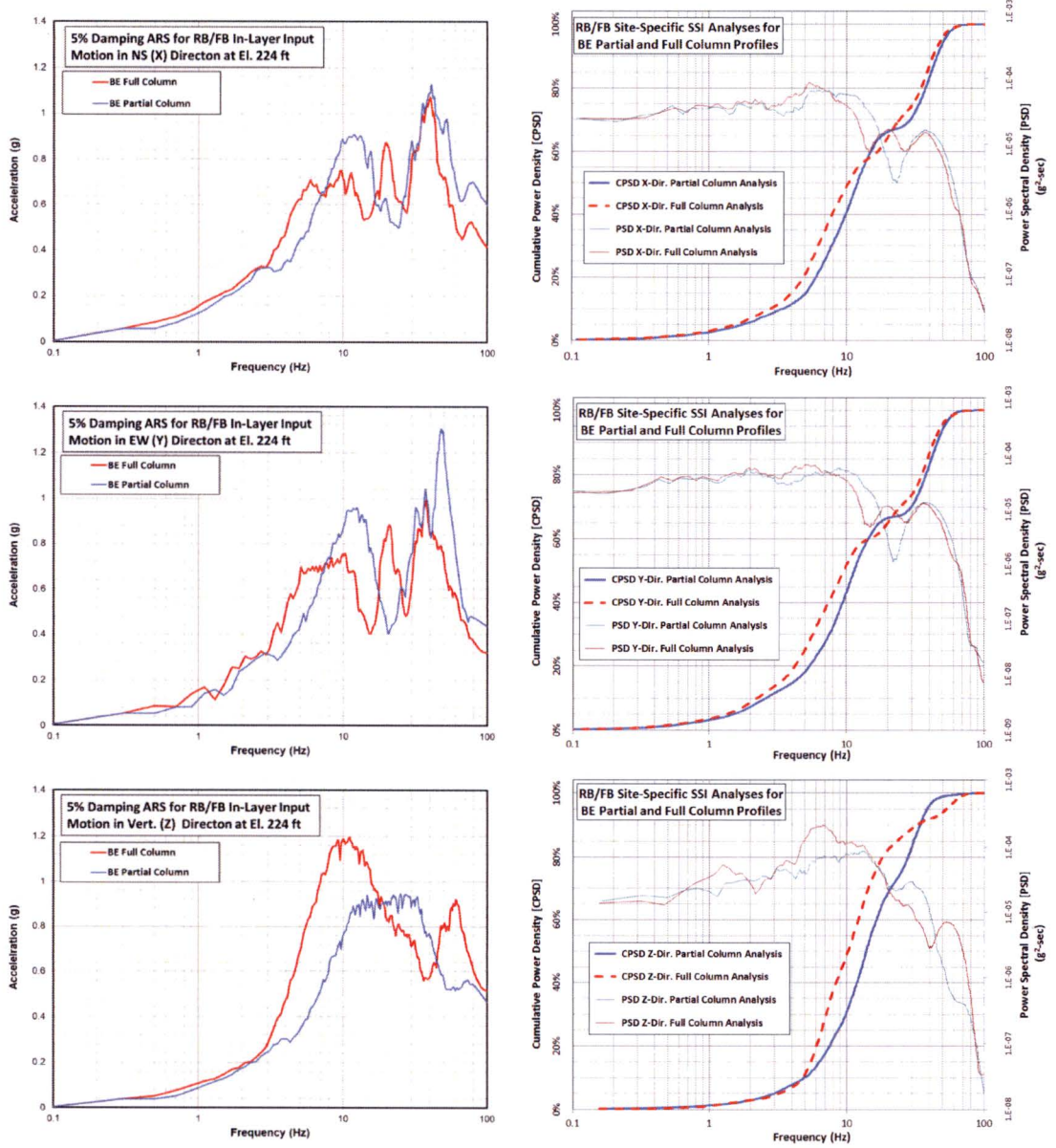

Figure 3.2-2 5% Damped ARS, PSD and CPSD of the RB/FB Input Acceleration Time Histories for Analyses of BE Subgrade Profiles

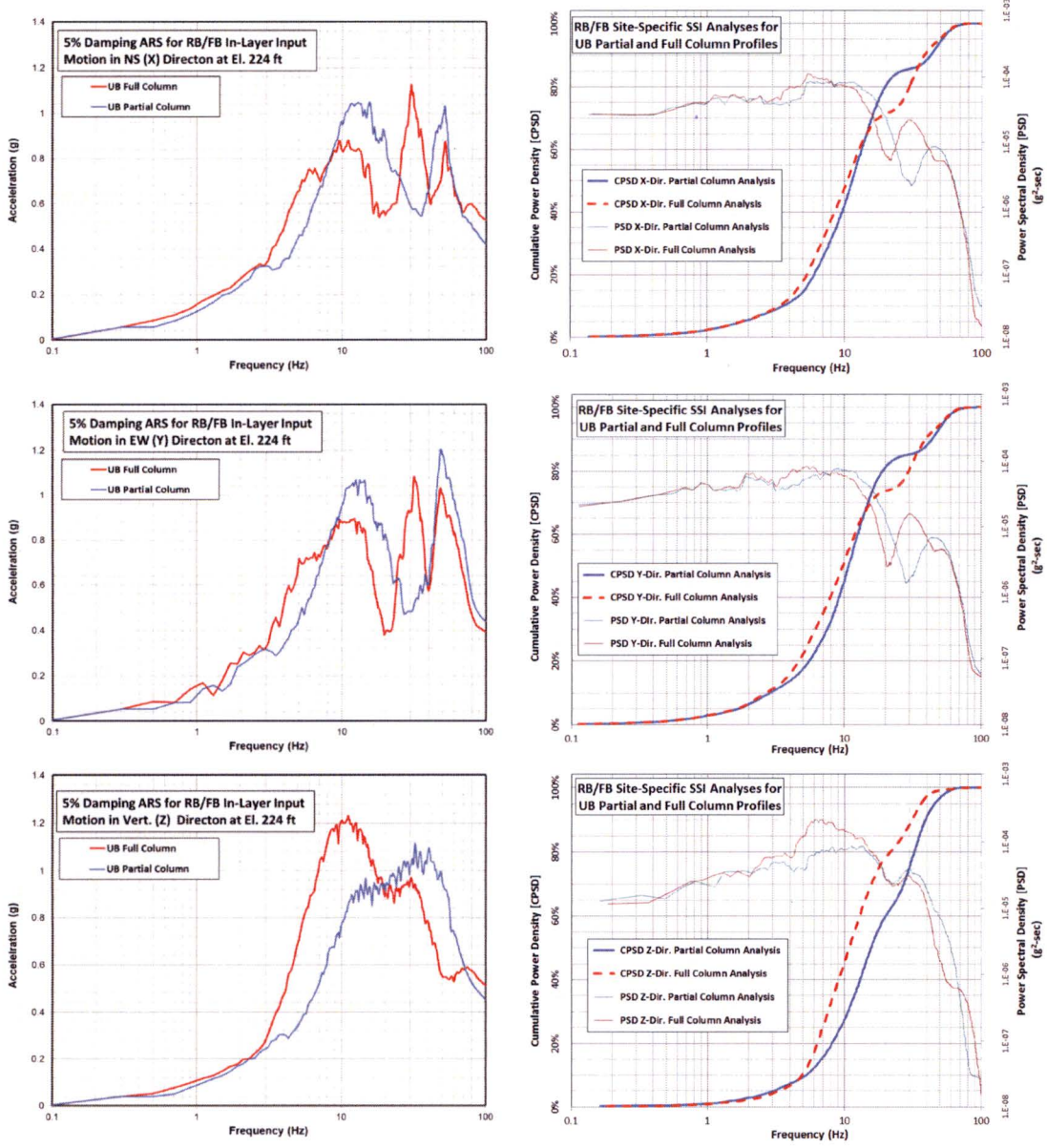

Figure 3.2-3 5% Damped ARS, PSD and CPSD of the RB/FB Input Acceleration Time Histories for Analyses of UB Subgrade Profiles

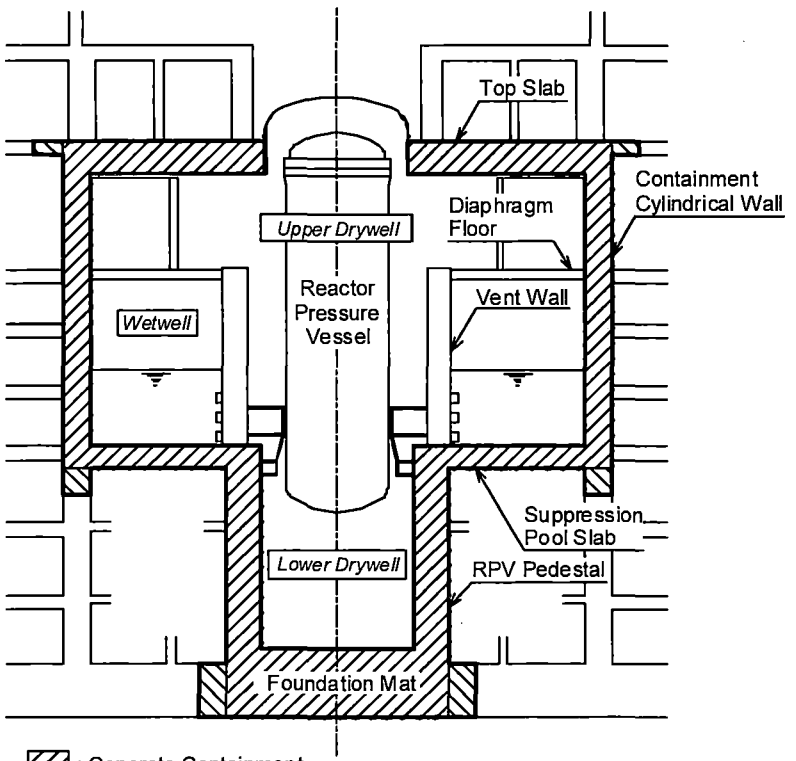

Figure 4.3-1 Major Structural Components Inside Containment

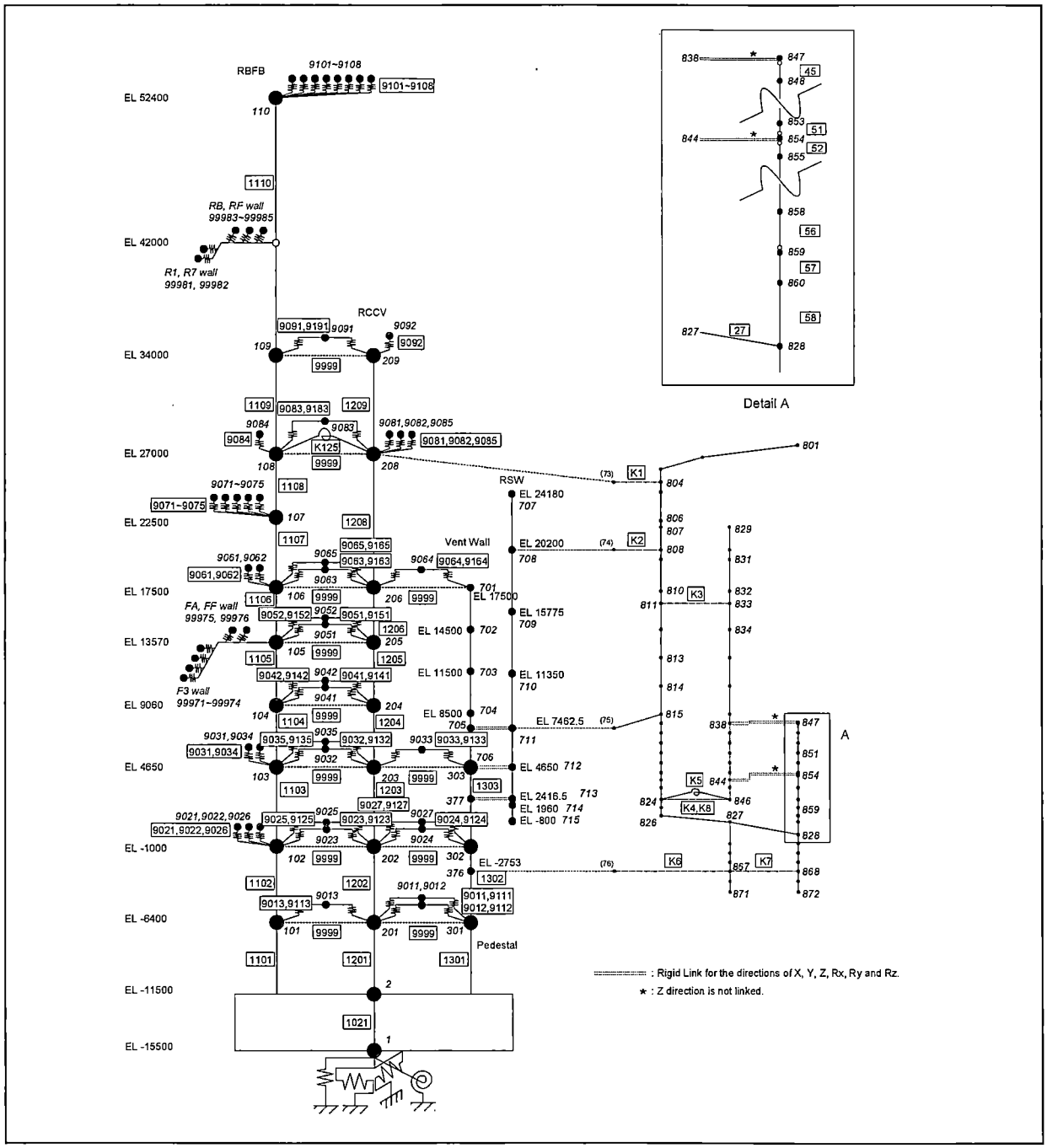

Figure 4.3-2 RB/FB Complex Seismic Analysis Stick Model

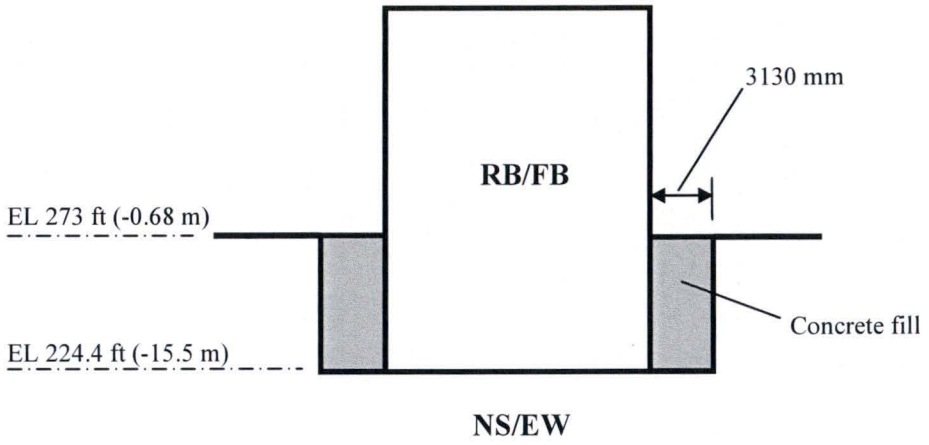

Figure 4.3-3 RB/FB SSI Stand-alone Partially Embedded Model

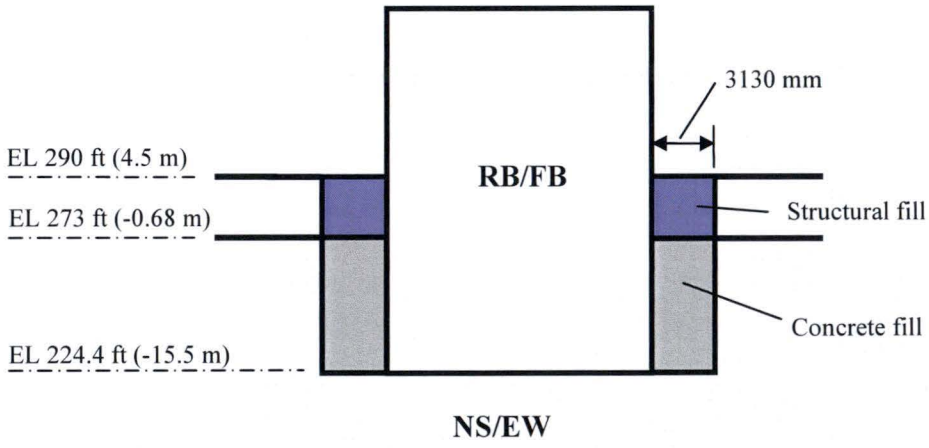

Figure 4.3-4 RB/FB SSI Stand-alone Fully Embedded Model

NOTE: Figures 4.3-3 and 4.3-4 are for illustrative purposes. Metric values in parentheses represent the standard plant elevation.

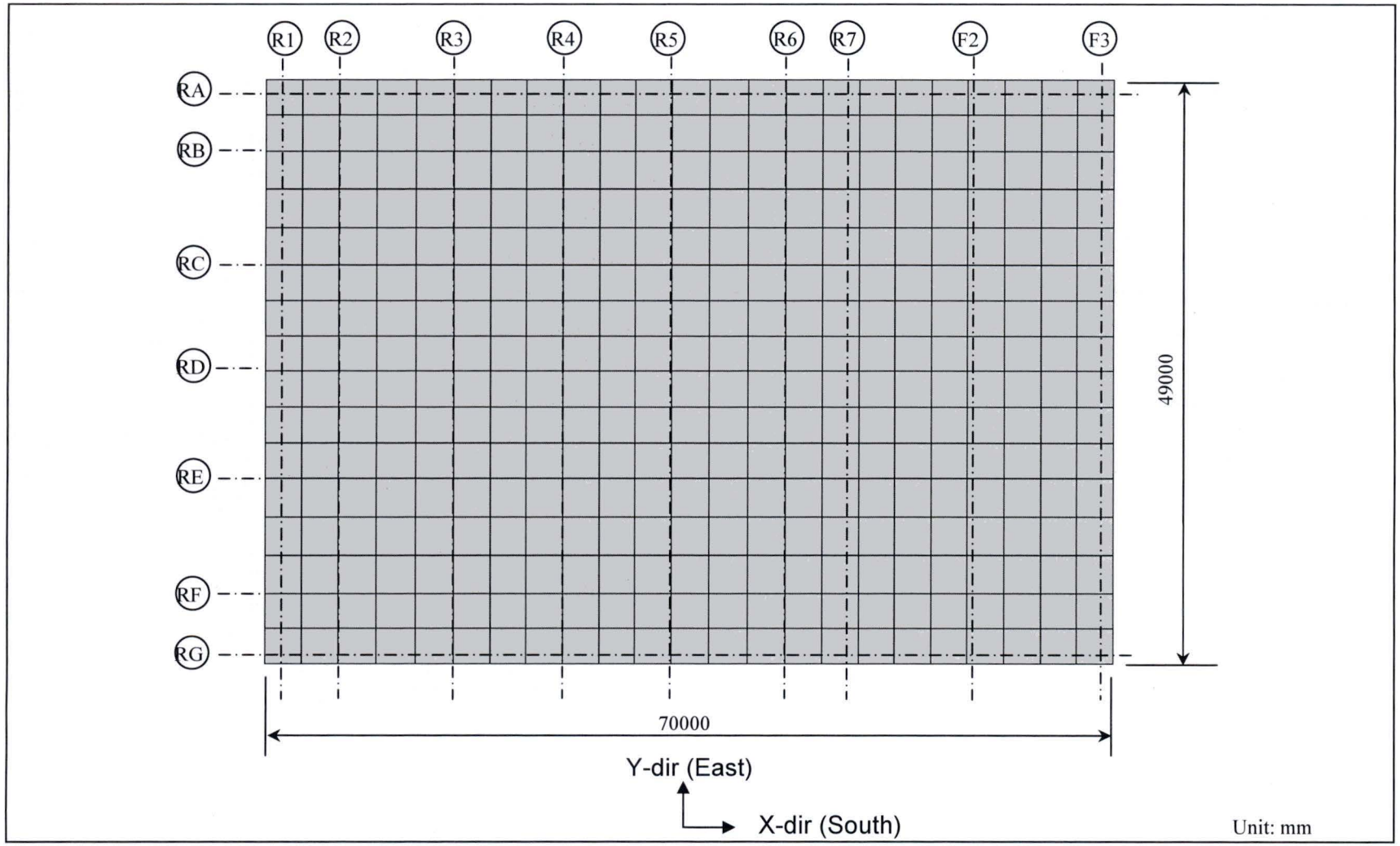

Figure 4.3-5 SASSI2010 Plate Elements for RB/FB Basemat in the Partially Embedded Mode

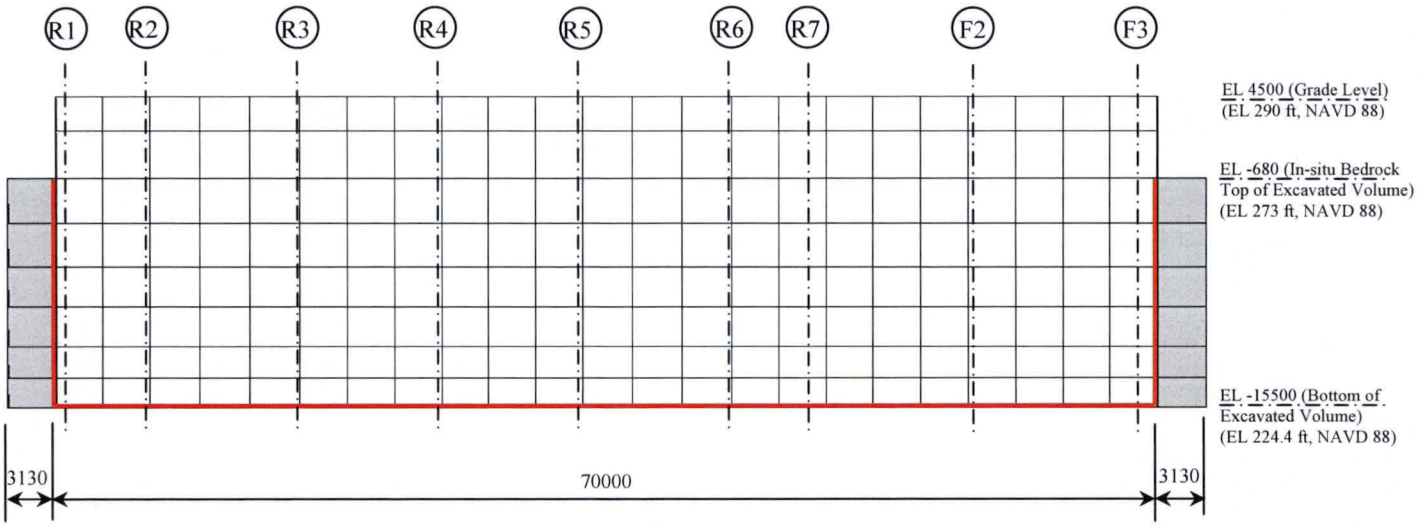

(a) Walls on Column Rows RA and RG

Unit: mm

Note: The extent of double nodes used at the structural/soil interfaces is shown in red lines.

Figure 4.3-6 SASSI2010 Plate Elements for RB/FB Exterior Walls in the Partially Embedded Model

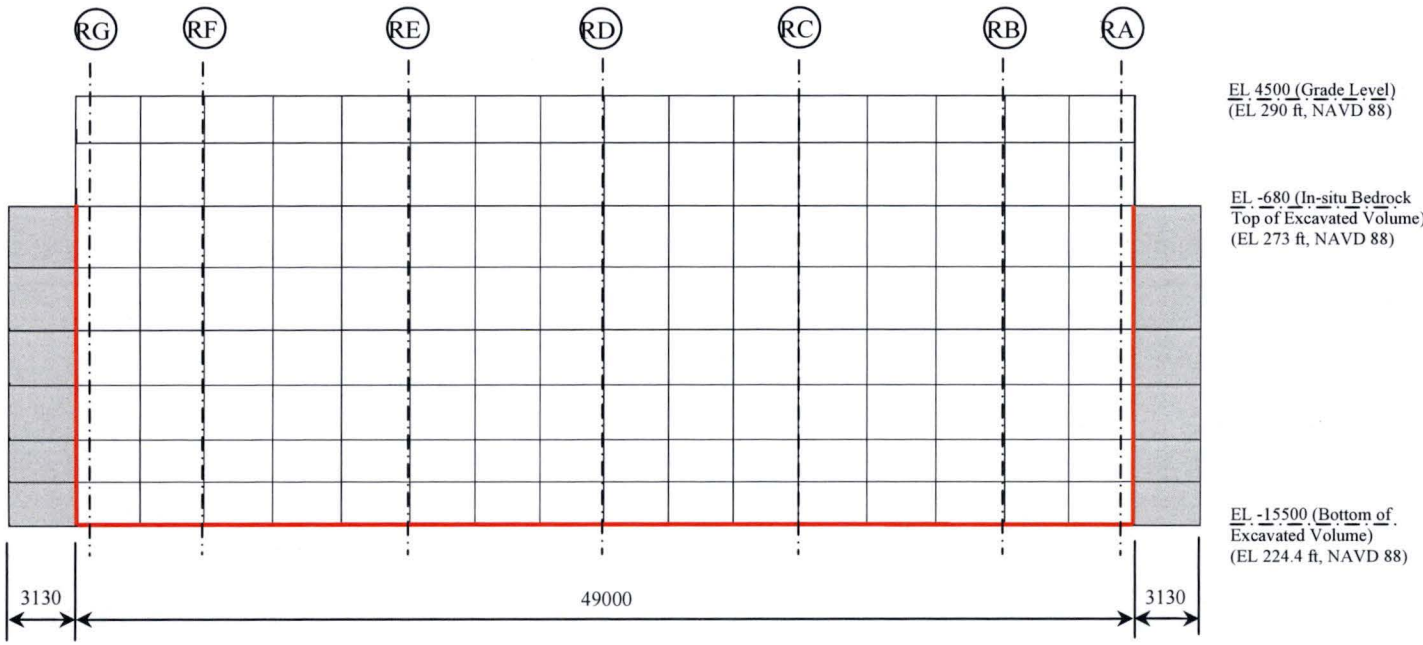

(b) Walls on Column Rows R1 and F3

Unit: mm

Note: The extent of double nodes used at the structural/soil interfaces is shown in red lines.

Figure 4.3-6 SASSI2010 Plate Elements for RB/FB Exterior Walls in the Partially Embedded Model (Continued)

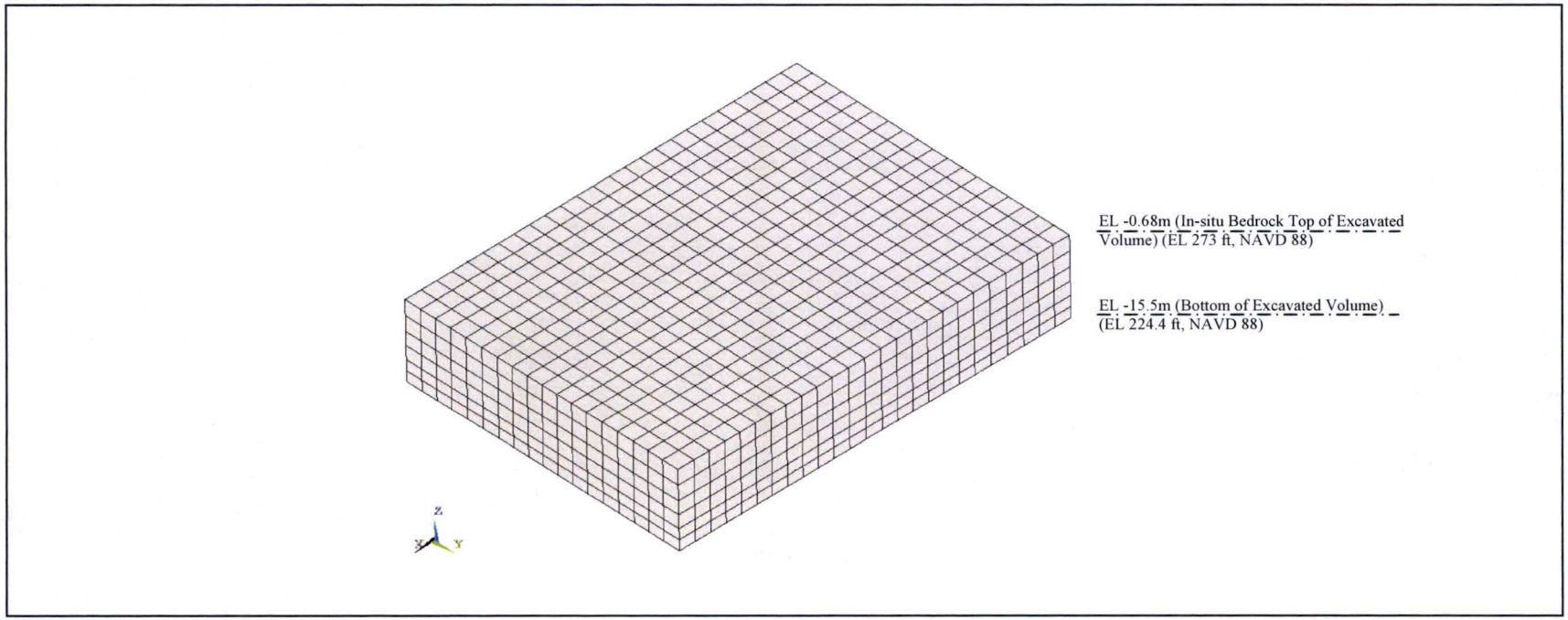

Figure 4.3-7 SASSI2010 Excavated Volume Solid Elements for the RB/FB Partially Embedded Model

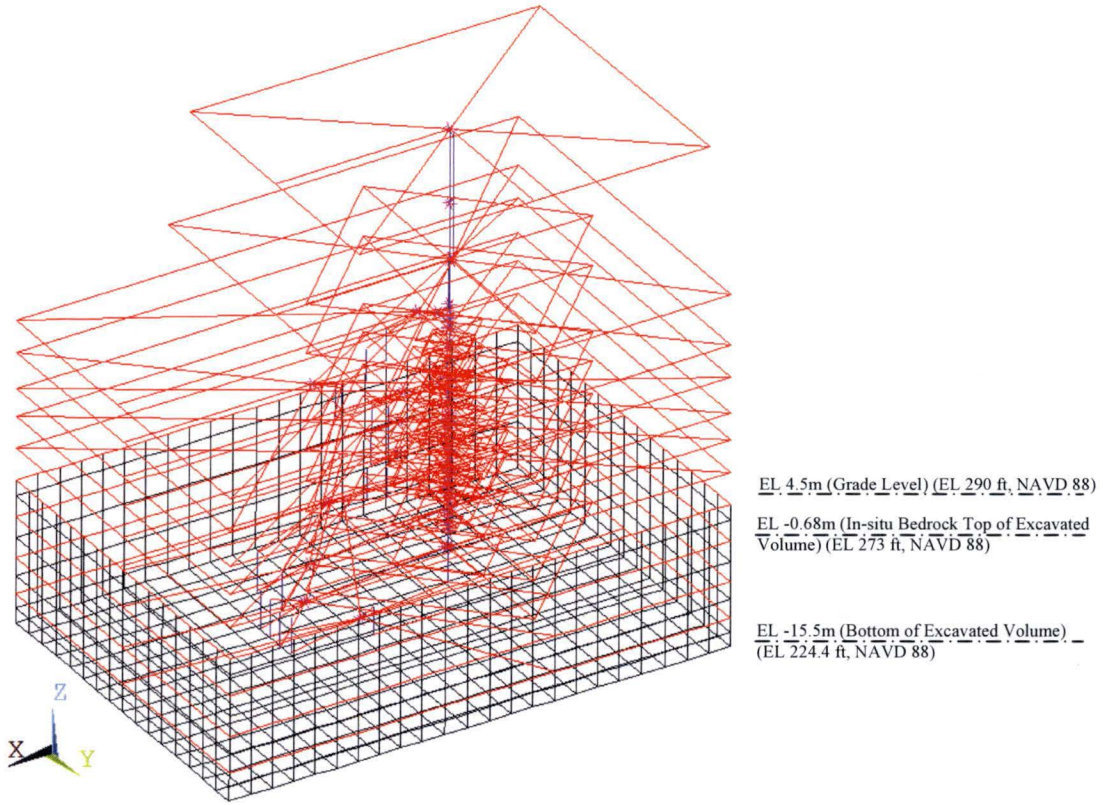

(a) Overview without Concrete Fill and Excavated Volume

Note: 1) Wall and basemat are modeled with shell elements.
2) Rigid beams indicated in red are installed at the floor levels.

Figure 4.3-8 Overview of SASSI2010 SSI RB/FB Partially Embedded Model

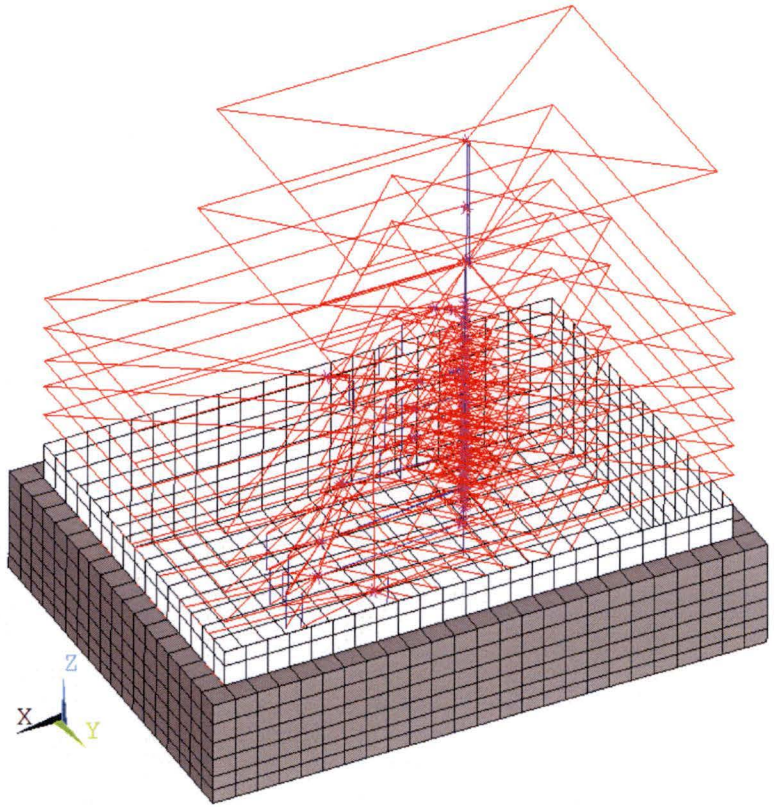

(b) Overview with Concrete Fill and without Excavated Volume

Note: 1) Wall and basemat are modeled with shell elements.
2) Rigid beams indicated in red are installed at the floor levels.

Figure 4.3-8 Overview of SASSI2010 SSI RB/FB Partially Embedded Model (Continued)

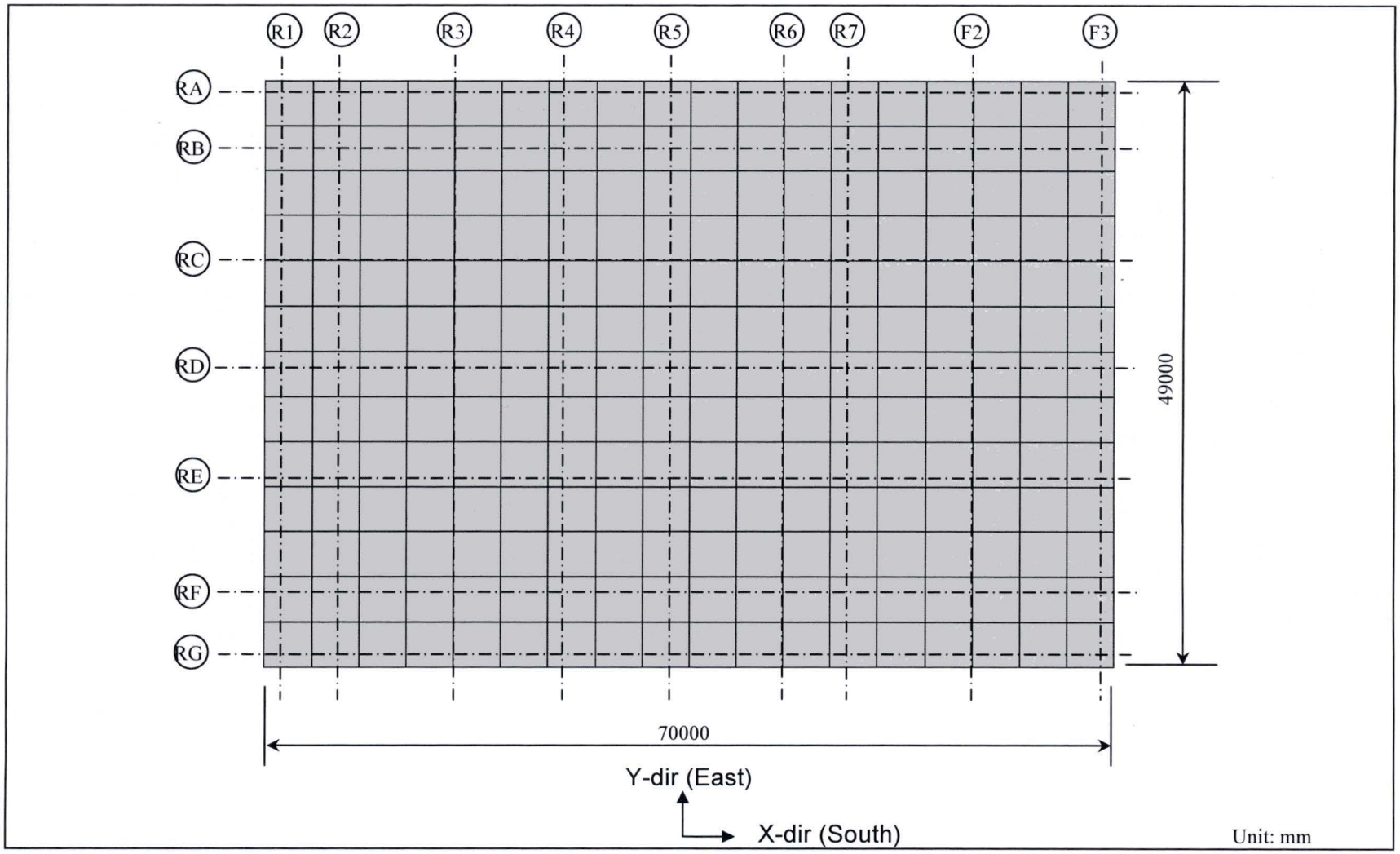

Figure 4.3-9 SASSI2010 Plate Elements for RB/FB Basemat in the Fully Embedded Model

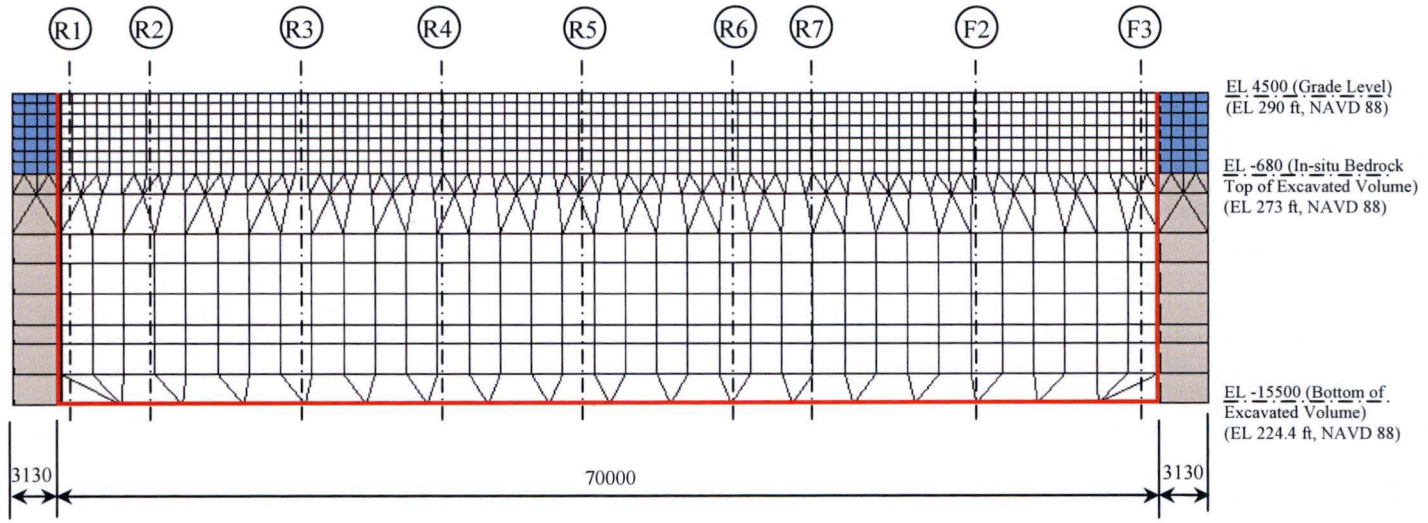

(a) Walls on Column Rows RA and RG

Unit: mm

Note: The extent of double nodes used at the structural/soil interfaces is shown in red lines.

Figure 4.3-10 SASSI2010 Plate Elements for RB/FB Exterior Walls in the Fully Embedded Model

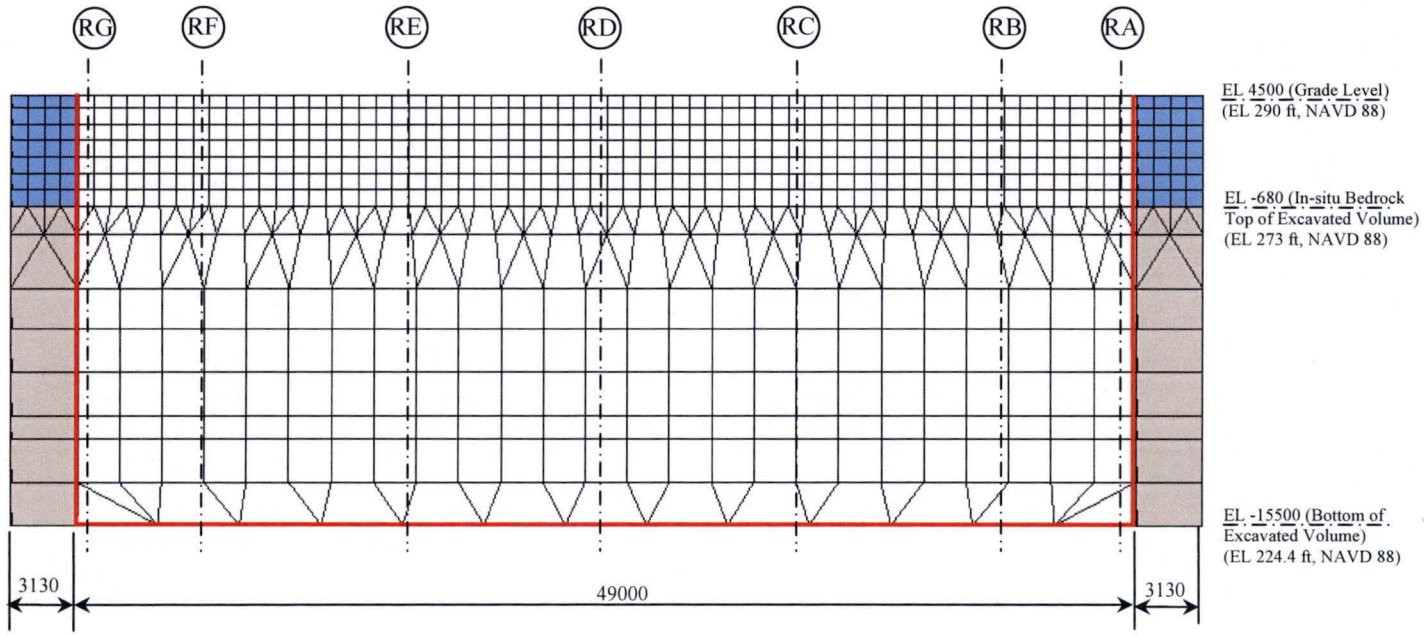

(b) Walls on Column Rows R1 and F3

Unit: mm

Note: The extent of double nodes used at the structural/soil interfaces is shown in red lines.

Figure 4.3-10 SASSI2010 Plate Elements for RB/FB Exterior Walls in the Fully Embedded Model (Continued)

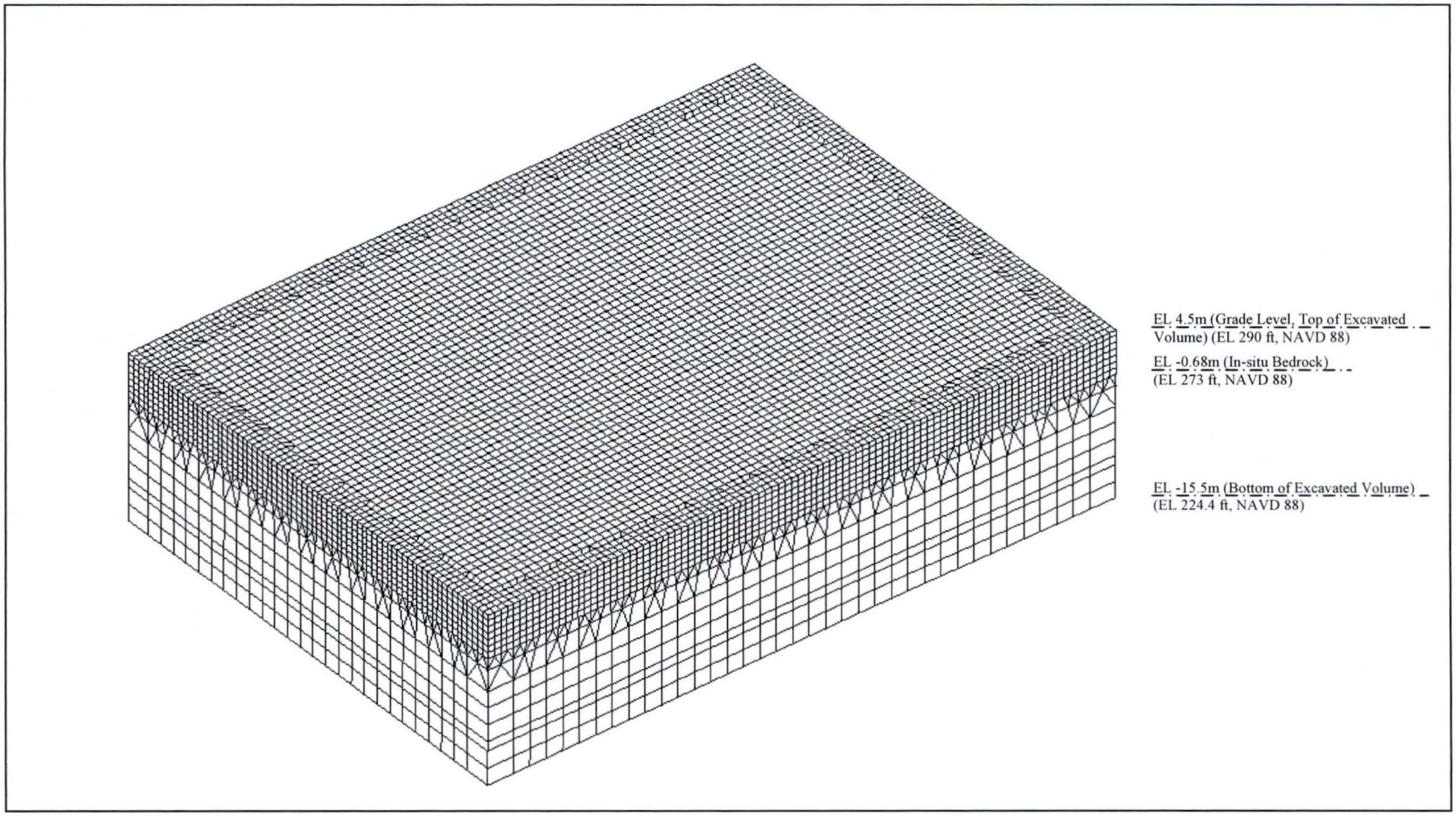

Figure 4.3-11 SASSI2010 Excavated Volume Solid Elements for the RB/FB Fully Embedded Model

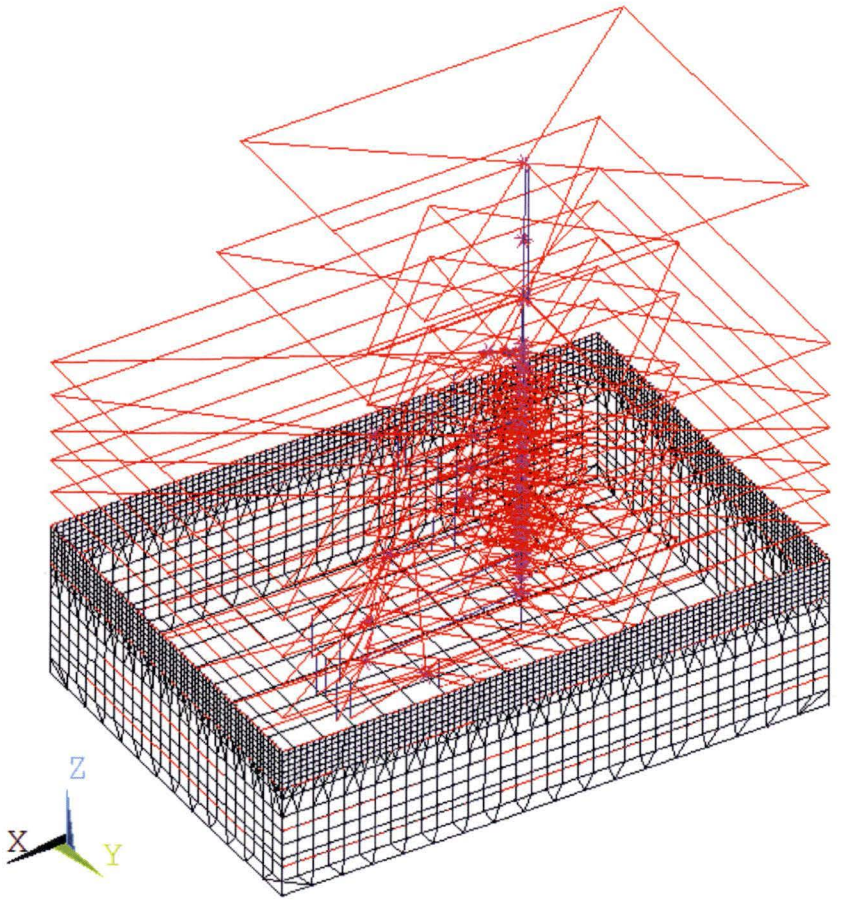

EL 4.5m (Grade Level, Top of Excavated Volume) (EL 290 ft, NAVD 88)

EL -0.68m (In-situ Bedrock (EL 273 ft, NAVD 88)

EL -15.5m (Bottom of Excavated Volume) (EL 224.4 ft, NAVD 88)

(a) Overview without Concrete Fill and Excavated Volume

Note: 1) Wall and basemat are modeled with shell elements.
2) Rigid beams indicated in red are installed at the floor levels.

Figure 4.3-12 Overview of SASSI2010 SSI RB/FB Fully Embedded Model

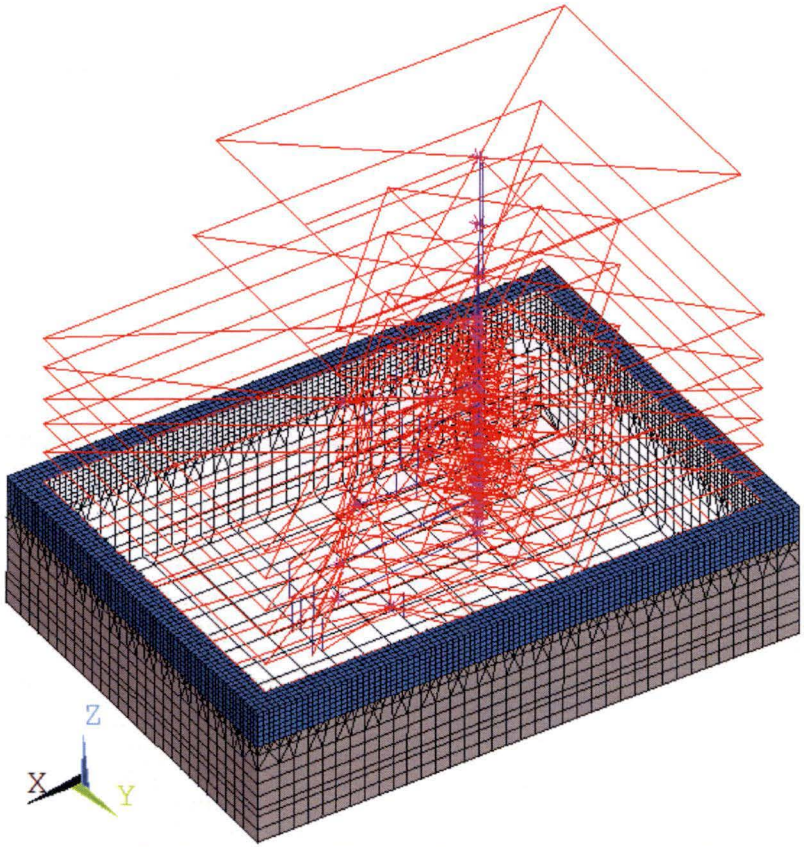

EL. 4.5m (Grade Level) (EL 290 ft, NAVD 88)

EL. -0.68m (In-situ Bedrock Top of Excavated Volume) (EL 273 ft, NAVD 88)

EL. -15.5m (Bottom of Excavated Volume) (EL 224.4 ft, NAVD 88)

(b) Overview with Concrete Fill and without Excavated Volume

Note: 1) Wall and basemat are modeled with shell elements.
2) Rigid beams indicated in red are installed at the floor levels.

Figure 4.3-12 Overview of SASSI2010 SSI RB/FB Fully Embedded Model (Continued)

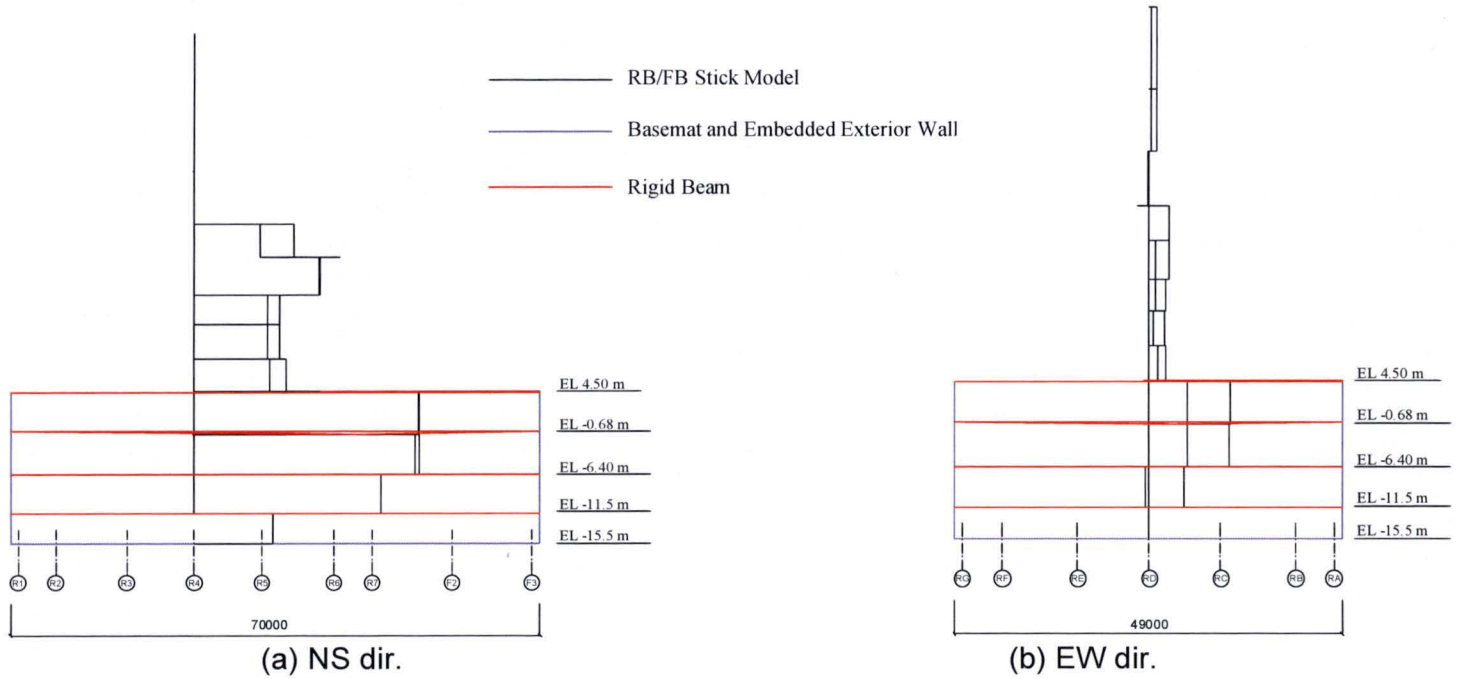

Note: Outriggers installed to the RB/FB stick are not shown in the figures.

Figure 4.3-13 Connection between RB/FB Stick Model and Foundation

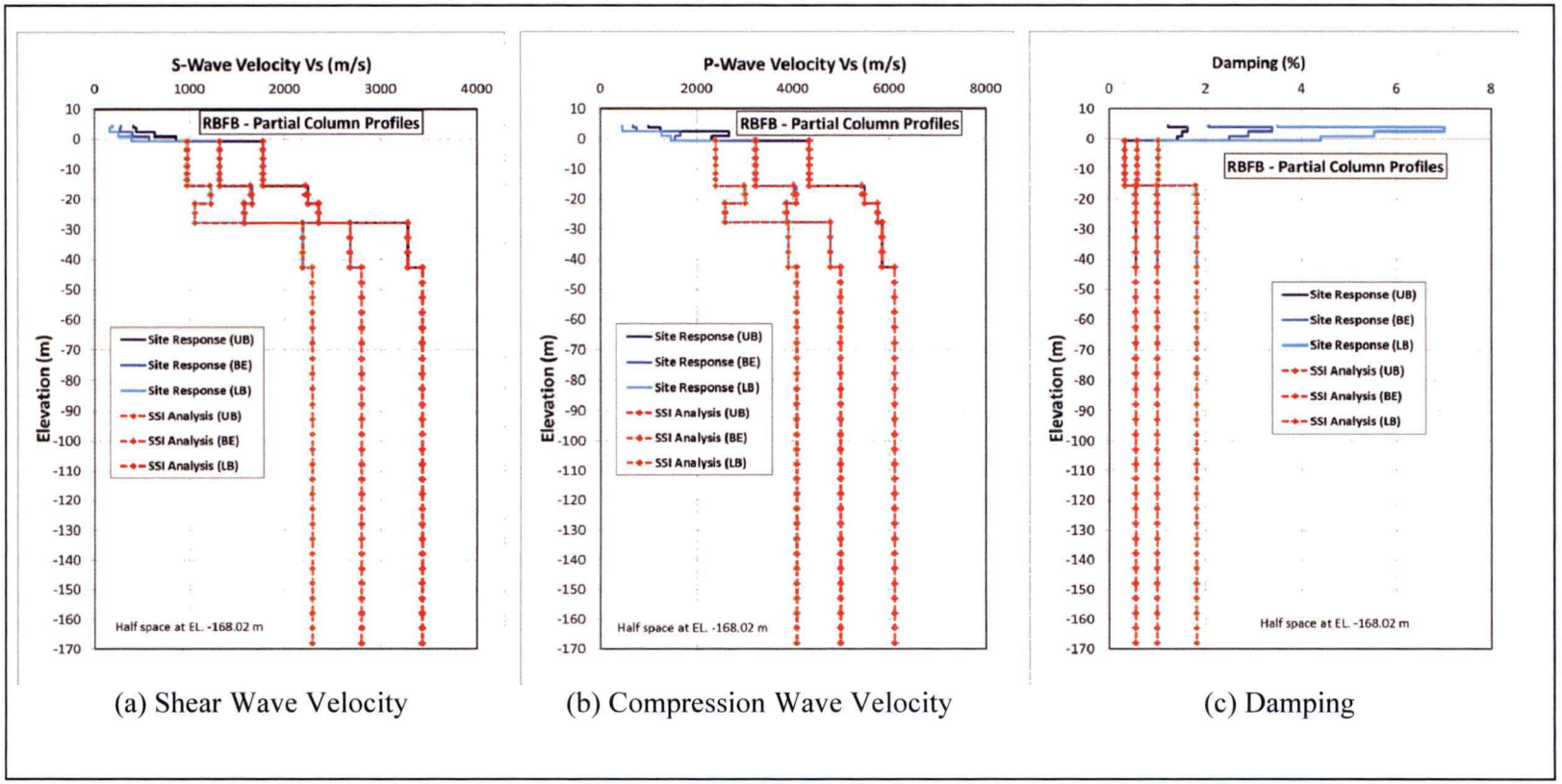

(a) Shear Wave Velocity (b) Compression Wave Velocity (c) Damping

Figure 4.3-14 SSI Input Strain Compatible Subgrade Properties - Partial Column Profiles

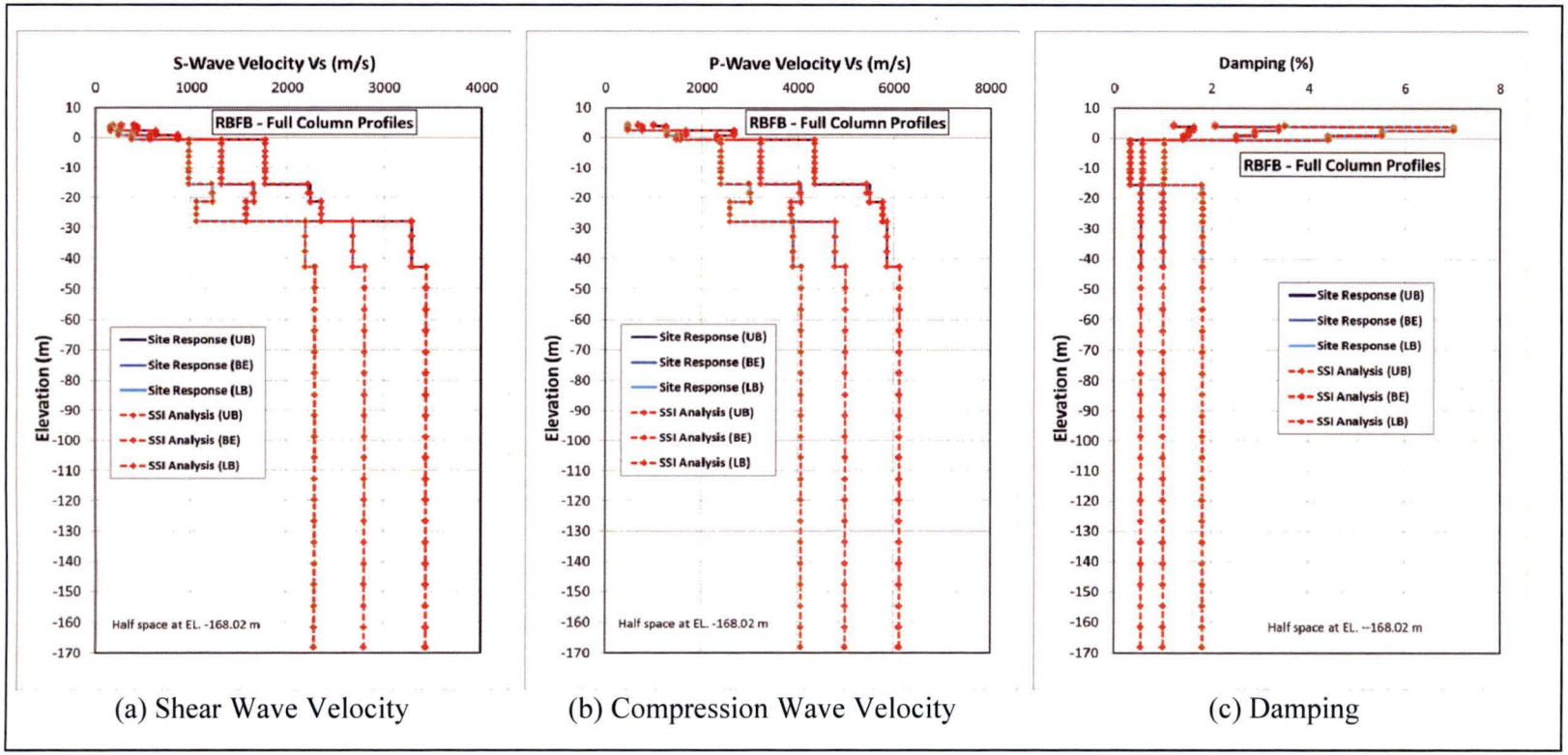

(a) Shear Wave Velocity (b) Compression Wave Velocity (c) Damping

Figure 4.3-15 SSI Input Strain Compatible Subgrade Properties - Full Column Profiles

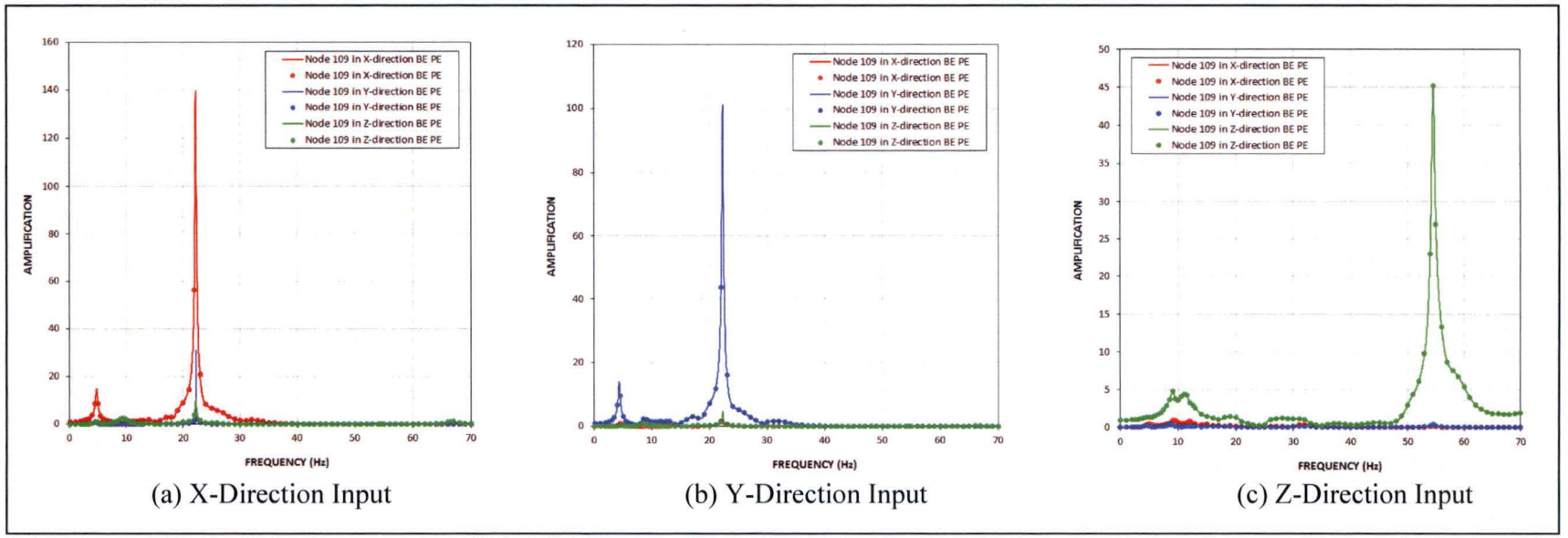

(a) X-Direction Input (b) Y-Direction Input (c) Z-Direction Input

Figure 5.1-1a Transfer Functions of RB/FB Refueling Floor Response from Analysis of BE Partial Column Profile

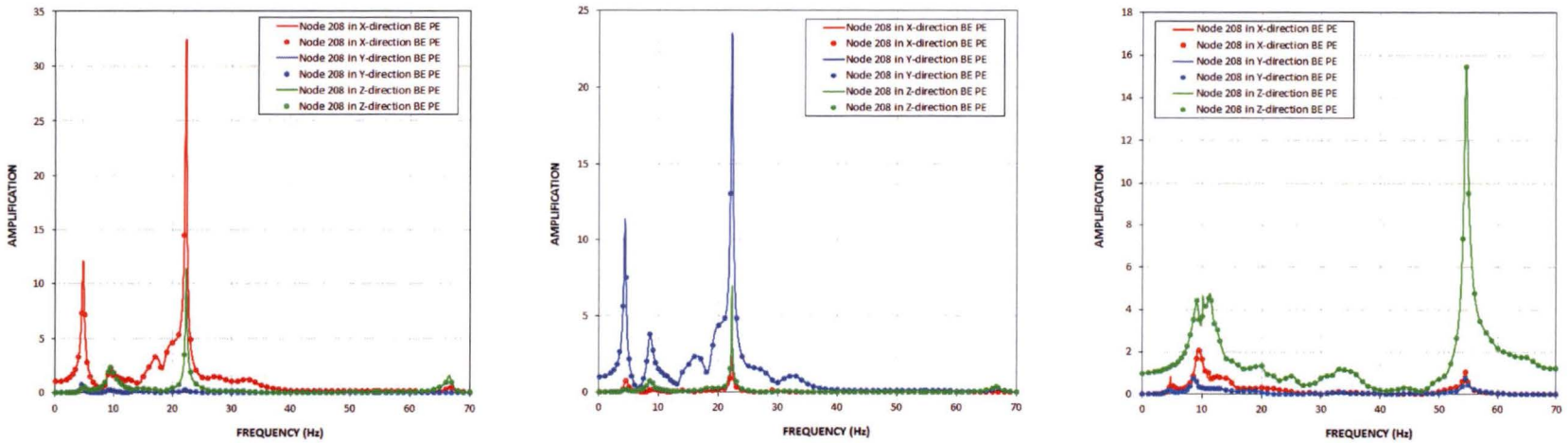

(a) X-Direction Input (b) Y-Direction Input (c) Z-Direction Input

Figure 5.1-1b Transfer Functions of RCCV Top Slab Response from Analysis of BE Partial Column Profile

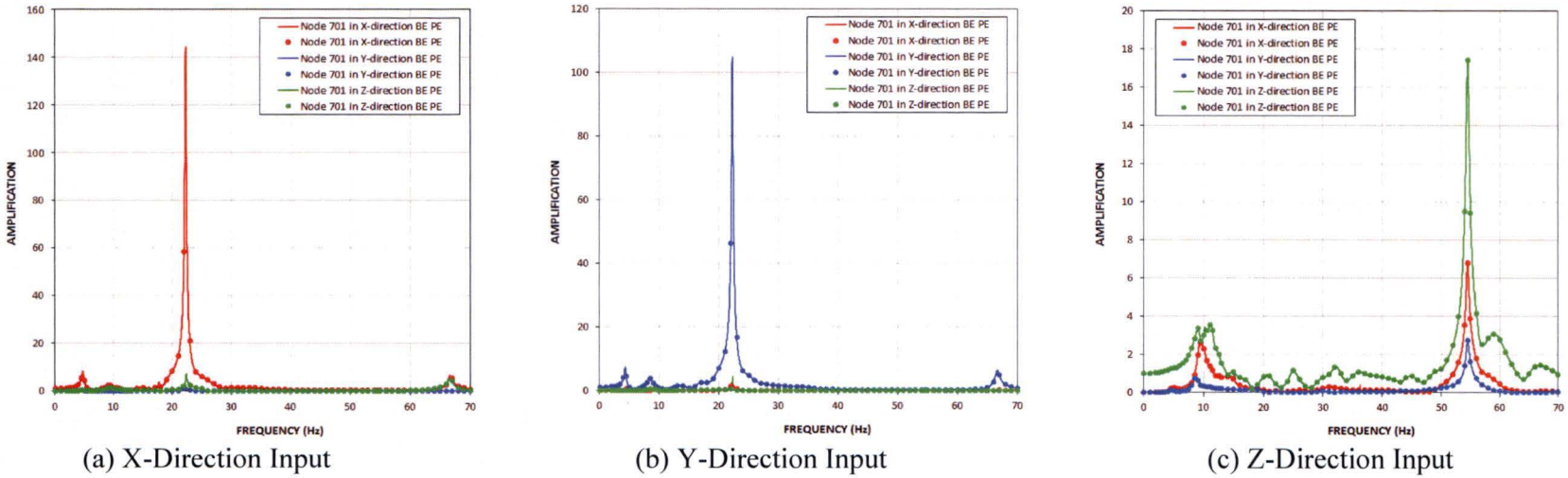

(a) X-Direction Input (b) Y-Direction Input (c) Z-Direction Input

Figure 5.1-1c Transfer Functions of Vent Wall Top Response from Analysis of BE Partial Column Profile

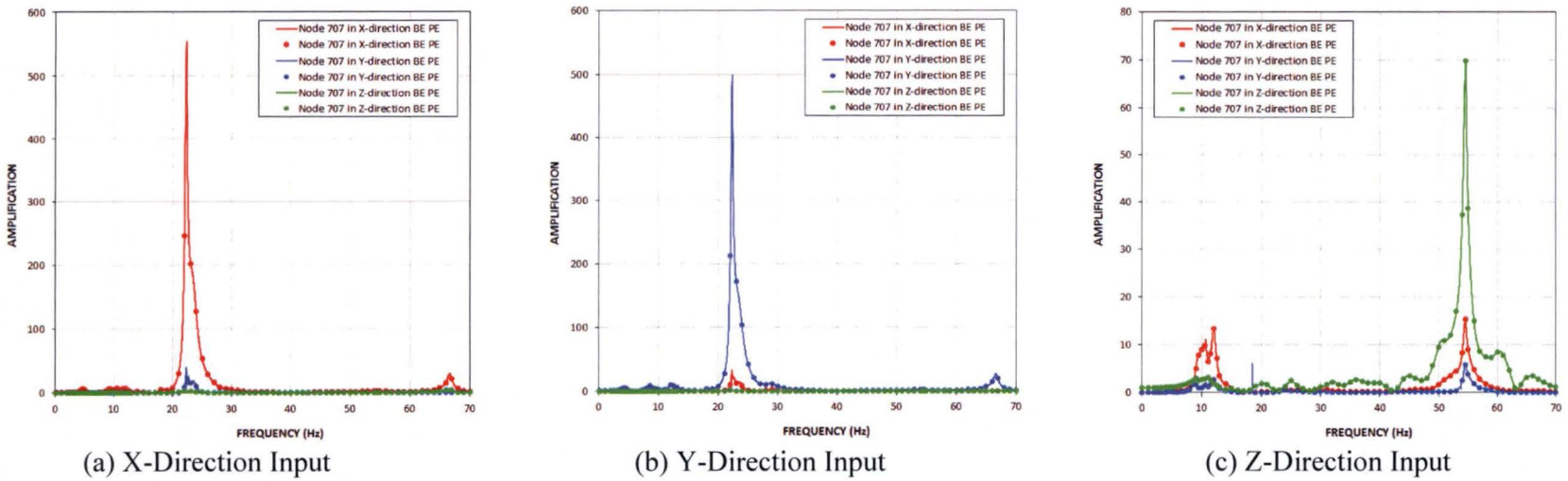

(a) X-Direction Input (b) Y-Direction Input (c) Z-Direction Input

Figure 5.1-1d Transfer Functions of RSW Top Response from Analysis of BE Partial Column Profile

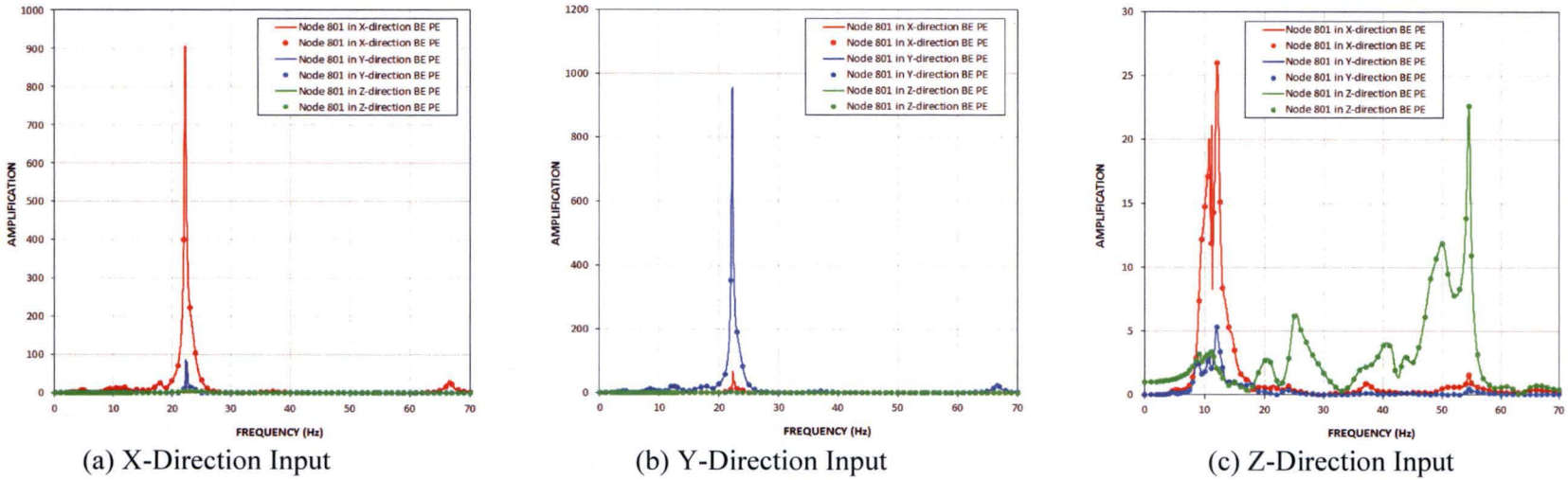

(a) X-Direction Input (b) Y-Direction Input (c) Z-Direction Input

Figure 5.1-1e Transfer Functions of RPV Top Response from Analysis of BE Partial Column Profile

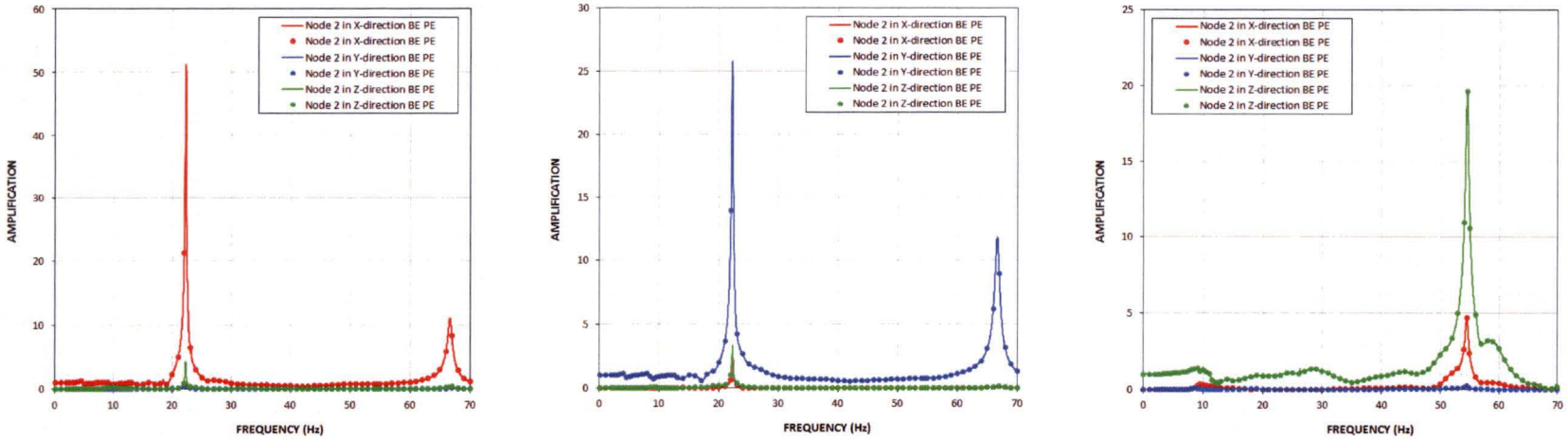

(a) X-Direction Input (b) Y-Direction Input (c) Z-Direction Input

Figure 5.1-1f Transfer Functions of RB/FB Basemat Response from Analysis of BE Partial Column Profile

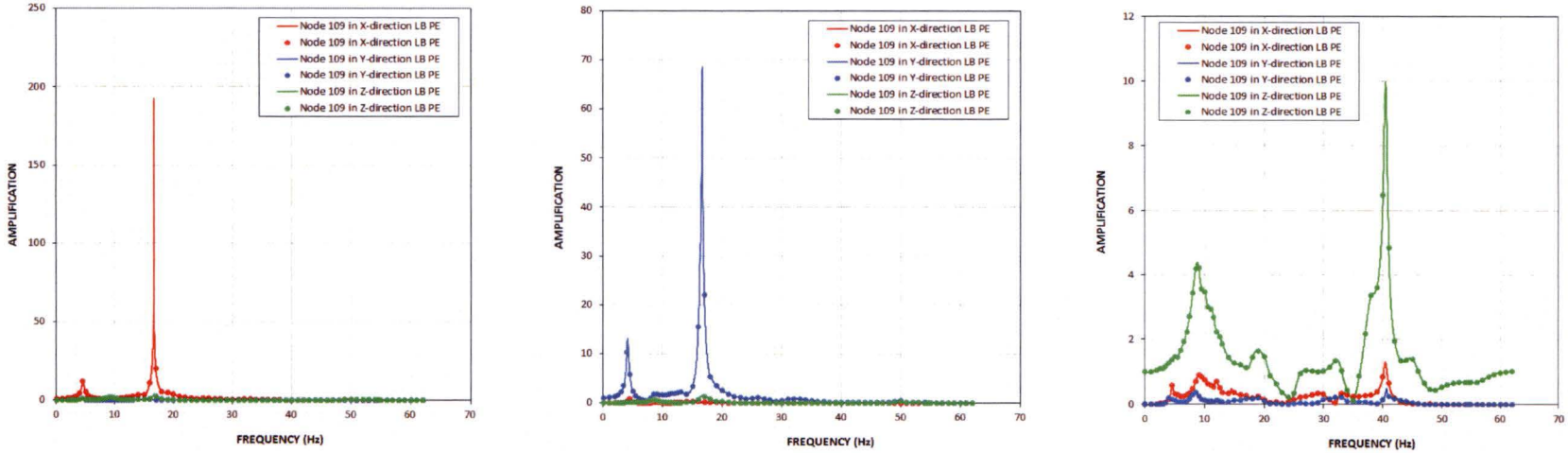

(a) X-Direction Input (b) Y-Direction Input (c) Z-Direction Input

Figure 5.1-2a Transfer Functions of RB/FB Refueling Floor Response from Analysis of LB Partial Column Profile

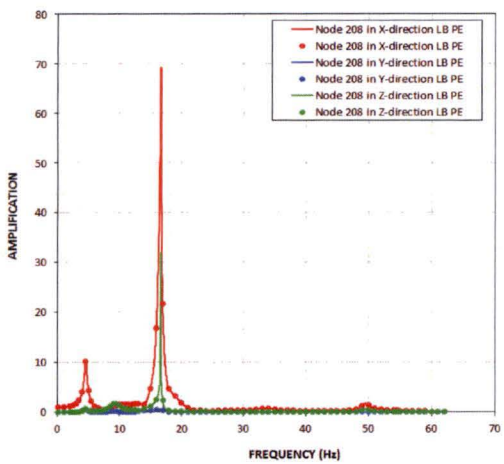

(a) X-Direction Input

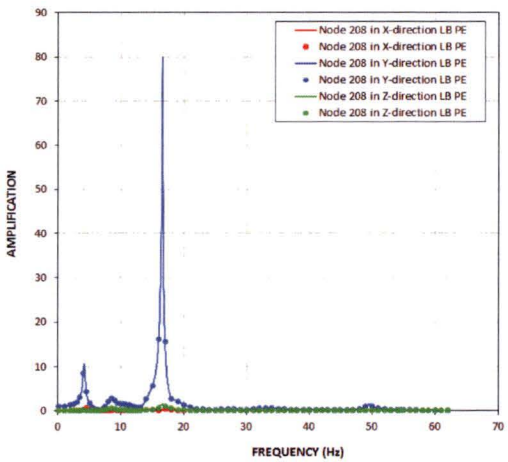

(b) Y-Direction Input

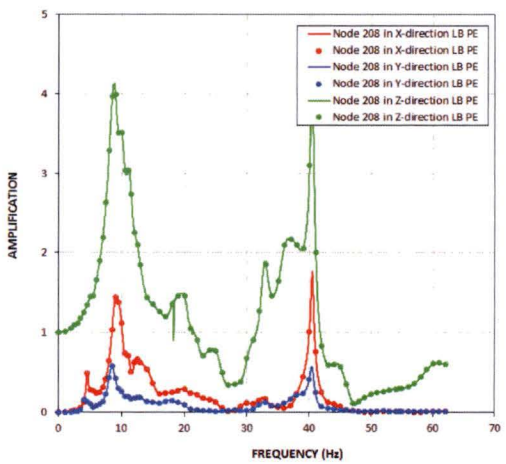

(c) Z-Direction Input

Figure 5.1-2b Transfer Functions of RCCV Top Slab Response from Analysis of LB Partial Column Profile

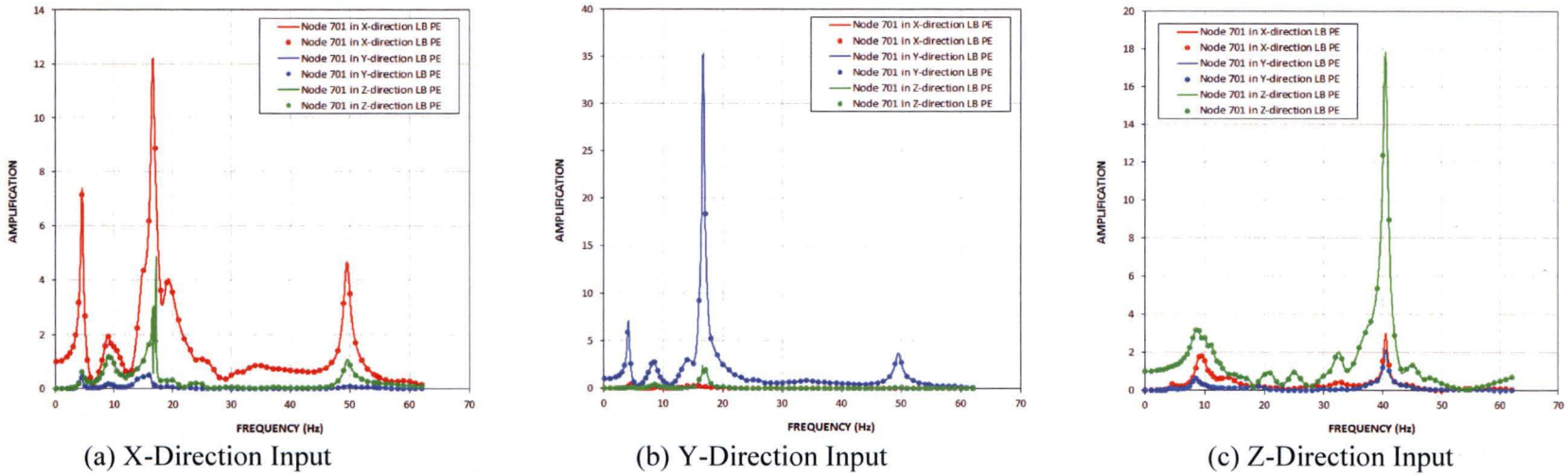

(a) X-Direction Input (b) Y-Direction Input (c) Z-Direction Input

Figure 5.1-2c Transfer Functions of Vent Wall Top Response from Analysis of LB Partial Column Profile

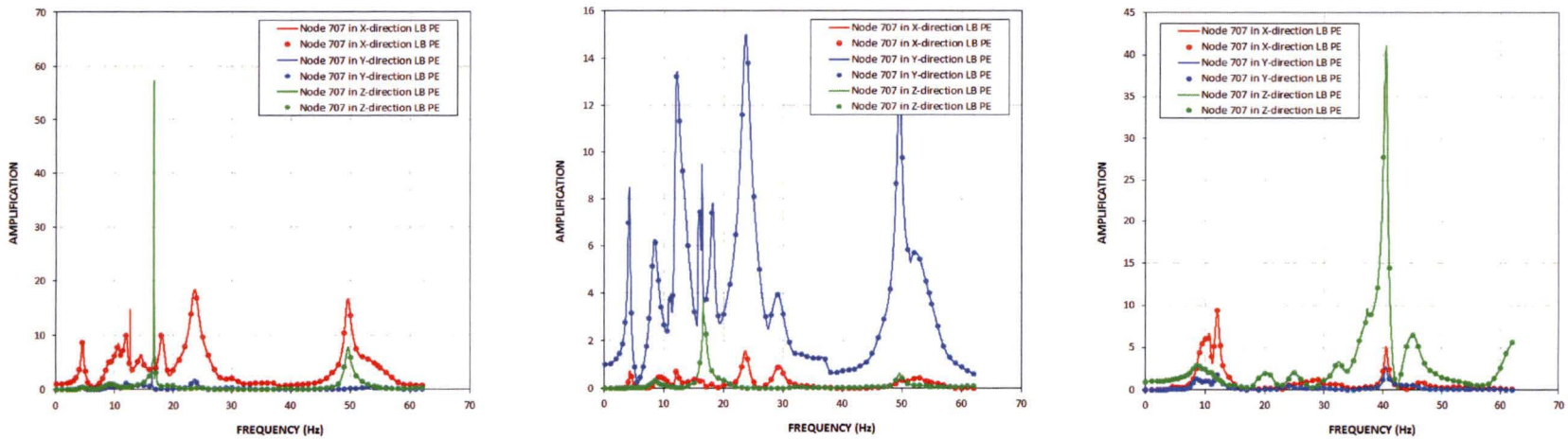

(a) X-Direction Input (b) Y-Direction Input (c) Z-Direction Input

Figure 5.1-2d Transfer Functions of RSW Top Response from Analysis of LB Partial Column Profile

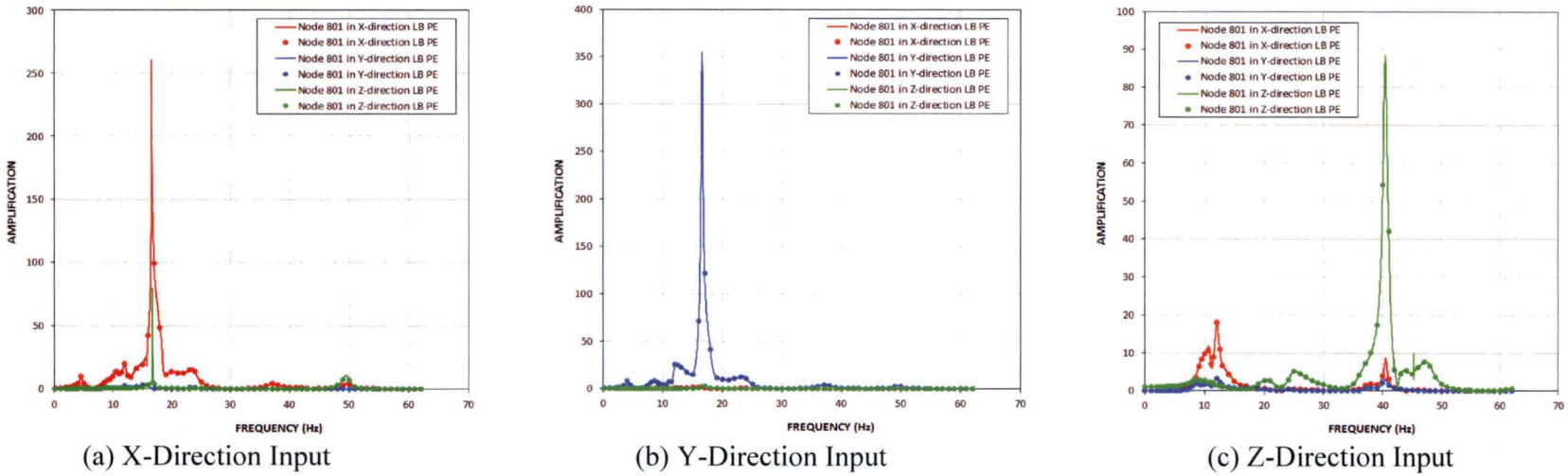

(a) X-Direction Input (b) Y-Direction Input (c) Z-Direction Input

Figure 5.1-2e Transfer Functions of RPV Top Response from Analysis of LB Partial Column Profile

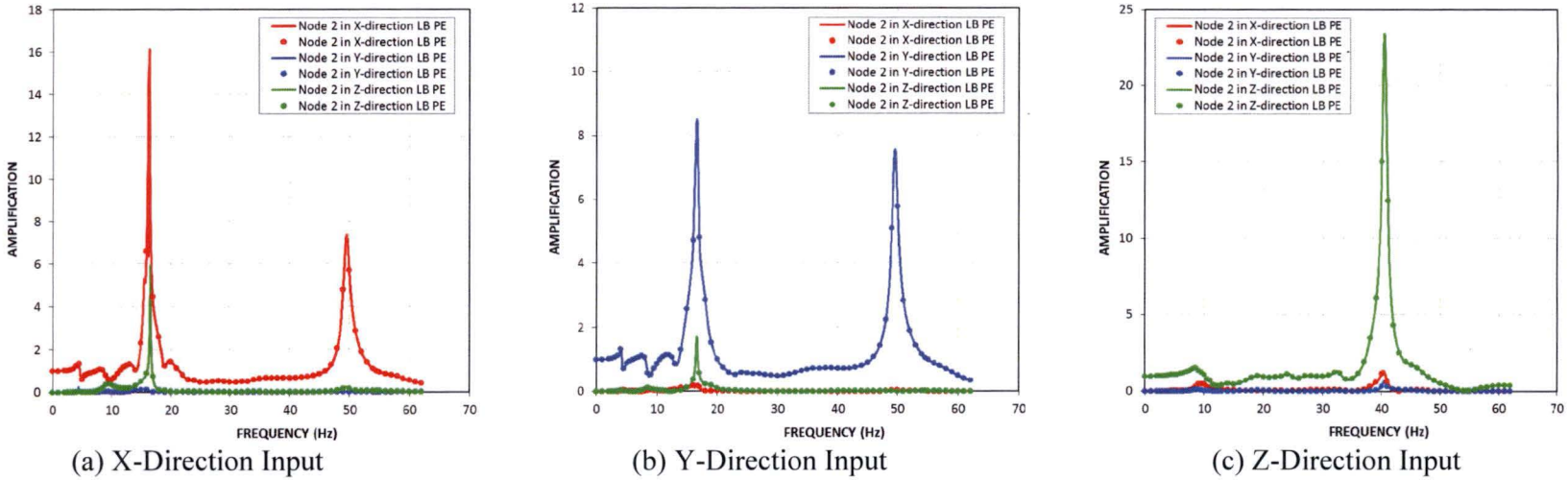

(a) X-Direction Input (b) Y-Direction Input (c) Z-Direction Input

Figure 5.1-2f Transfer Functions of RB/FB Basemat Response from Analysis of LB Partial Column Profile

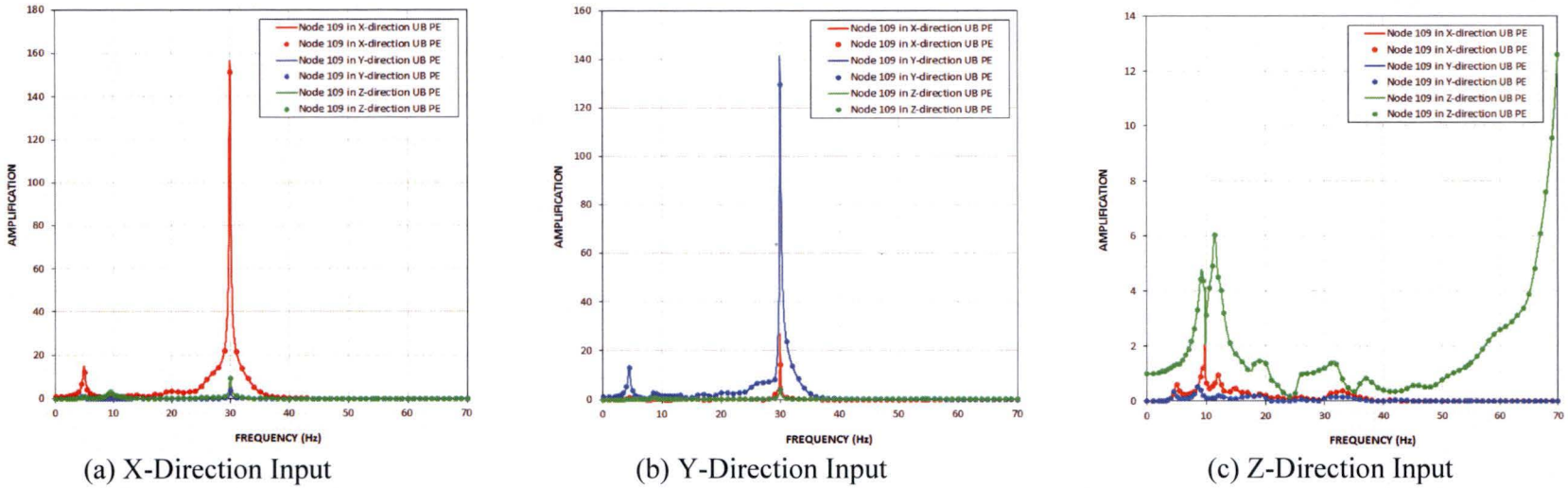

(a) X-Direction Input (b) Y-Direction Input (c) Z-Direction Input

Figure 5.1-3a Transfer Functions of RB/FB Refueling Floor Response from Analysis of UB Partial Column Profile

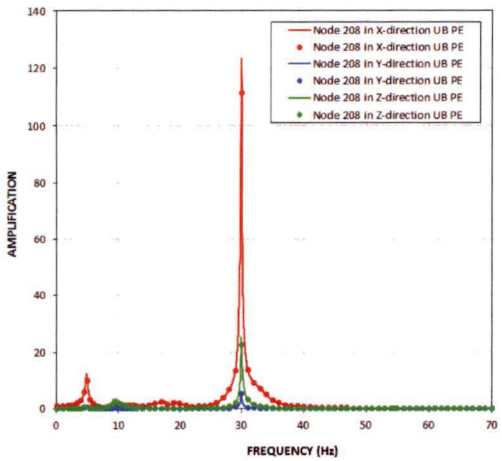

(a) X-Direction Input

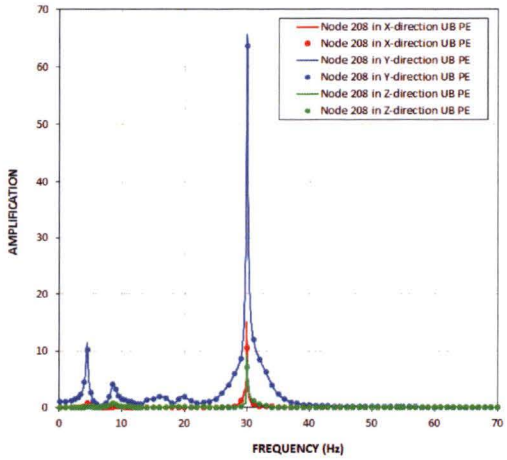

(b) Y-Direction Input

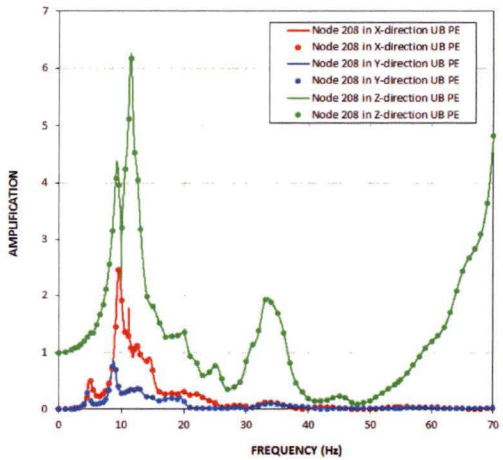

(c) Z-Direction Input

Figure 5.1-3b Transfer Functions of RCCV Top Slab Response from Analysis of UB Partial Column Profile

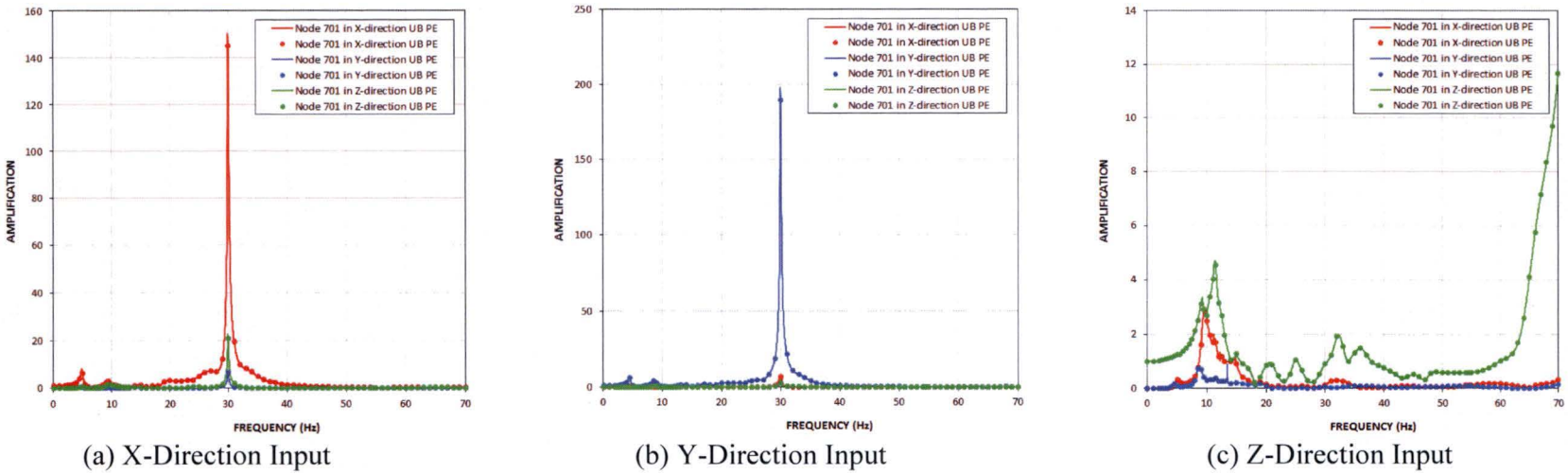

(a) X-Direction Input (b) Y-Direction Input (c) Z-Direction Input

Figure 5.1-3c Transfer Functions of Vent Wall Top Response from Analysis of UB Partial Column Profile

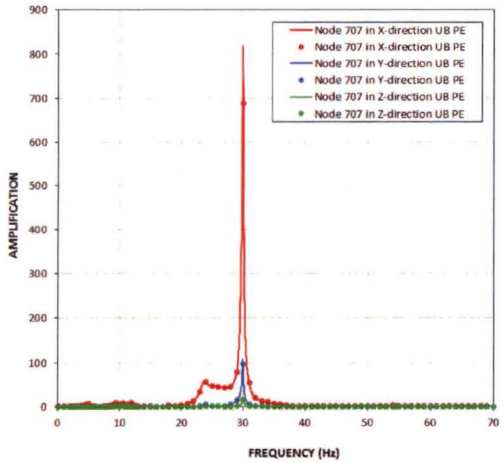

(a) X-Direction Input

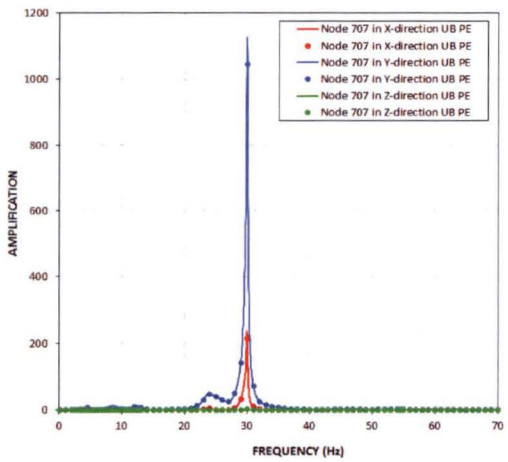

(b) Y-Direction Input

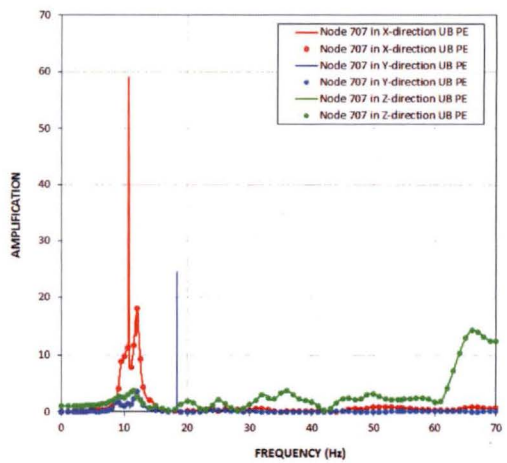

(c) Z-Direction Input

Figure 5.1-3d Transfer Functions of RSW Top Response from Analysis of UB Partial Column Profile

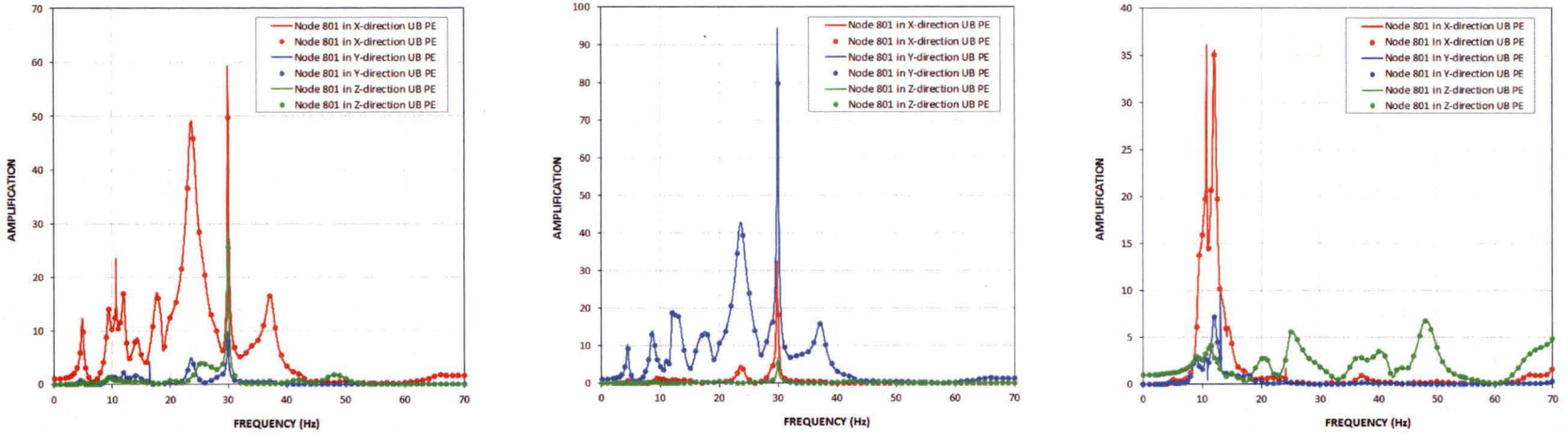

(a) X-Direction Input (b) Y-Direction Input (c) Z-Direction Input

Figure 5.1-3e Transfer Functions of RPV Top Response from Analysis of UB Partial Column Profile

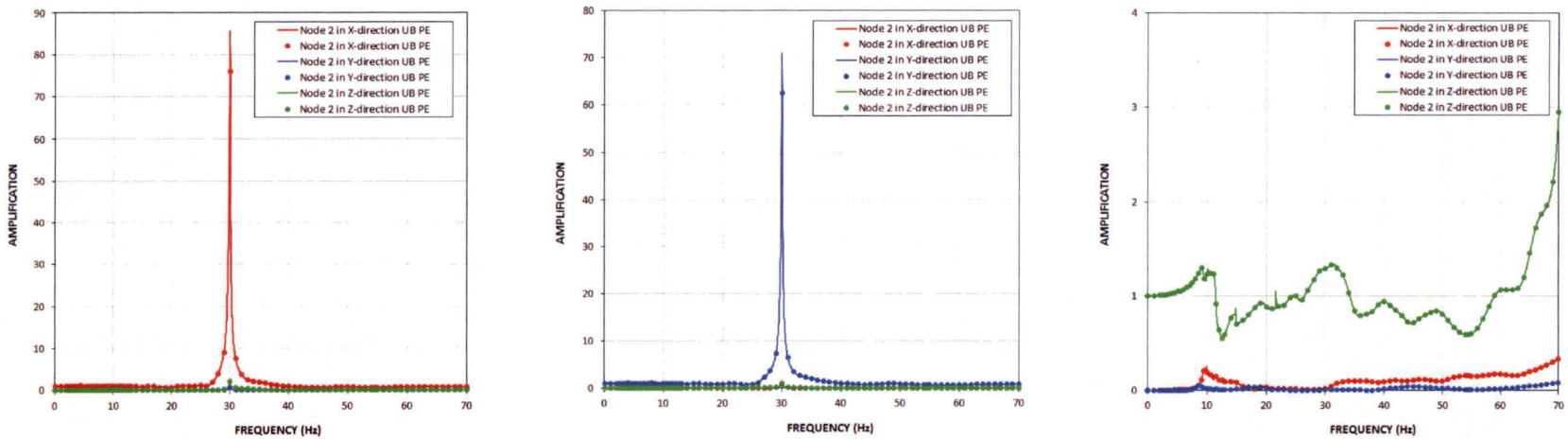

(a) X-Direction Input (b) Y-Direction Input (c) Z-Direction Input

Figure 5.1-3f Transfer Functions of RB/FB Basemat Response from Analysis of UB Partial Column Profile

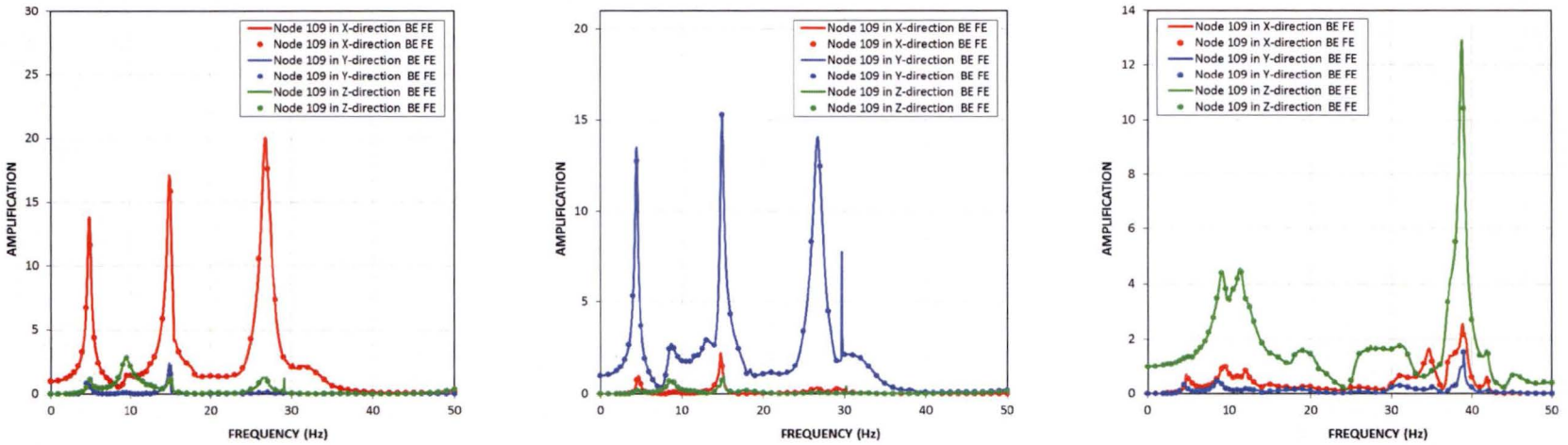

(a) X-Direction Input (b) Y-Direction Input (c) Z-Direction Input

Figure 5.1-4a Transfer Functions of RB/FB Refueling Floor Response from Analysis of BE Full Column Profile

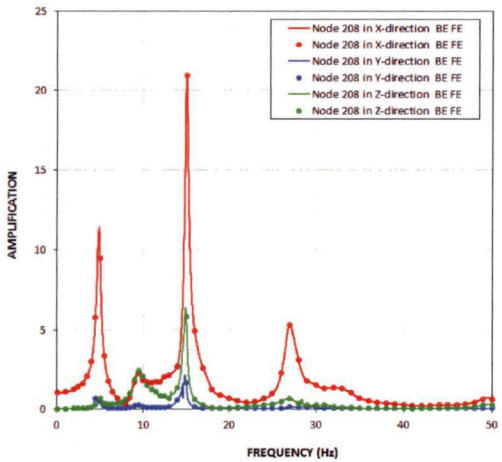

(a) X-Direction Input

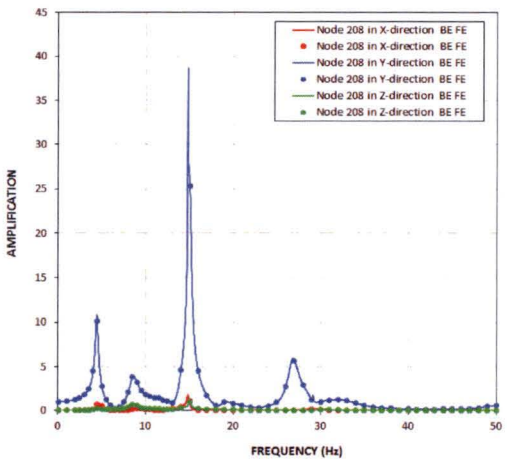

(b) Y-Direction Input

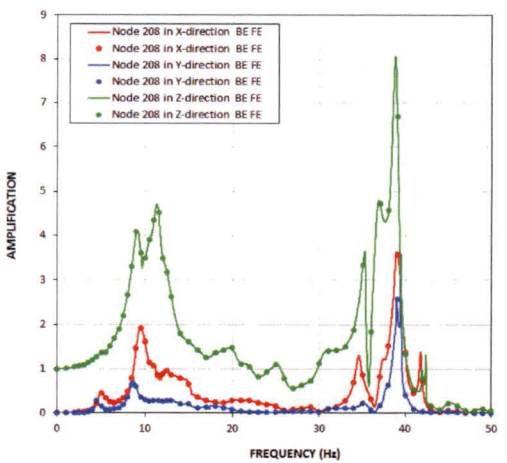

(c) Z-Direction Input

Figure 5.1-4b Transfer Functions of RCCV Top Slab Response from Analysis of BE Full Column Profile

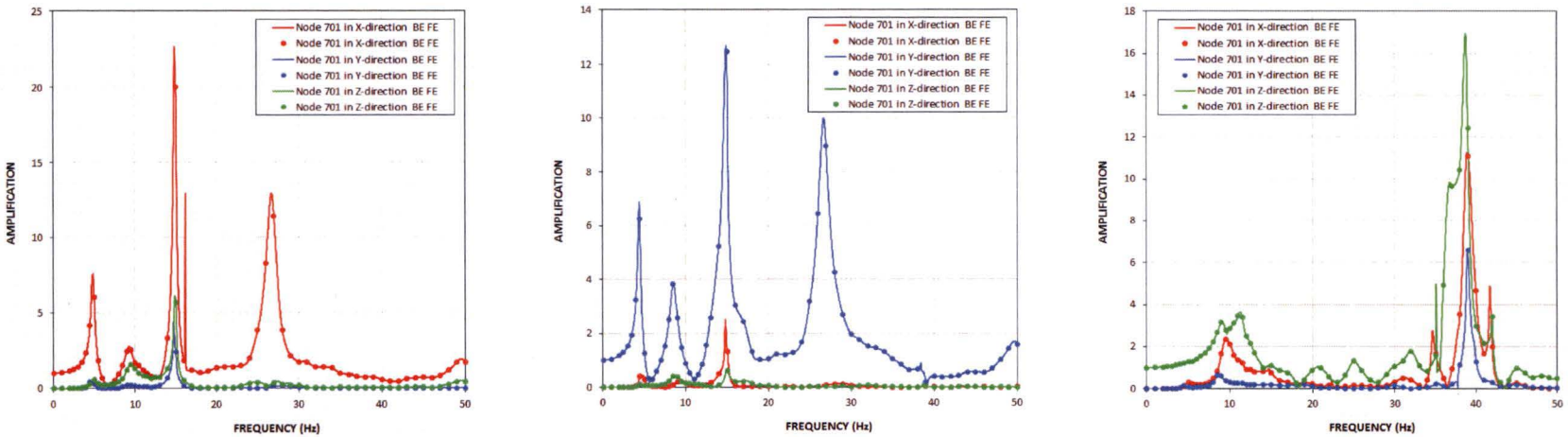

(a) X-Direction Input (b) Y-Direction Input (c) Z-Direction Input

Figure 5.1-4c Transfer Functions of Vent Wall Top Response from Analysis of BE Full Column Profile

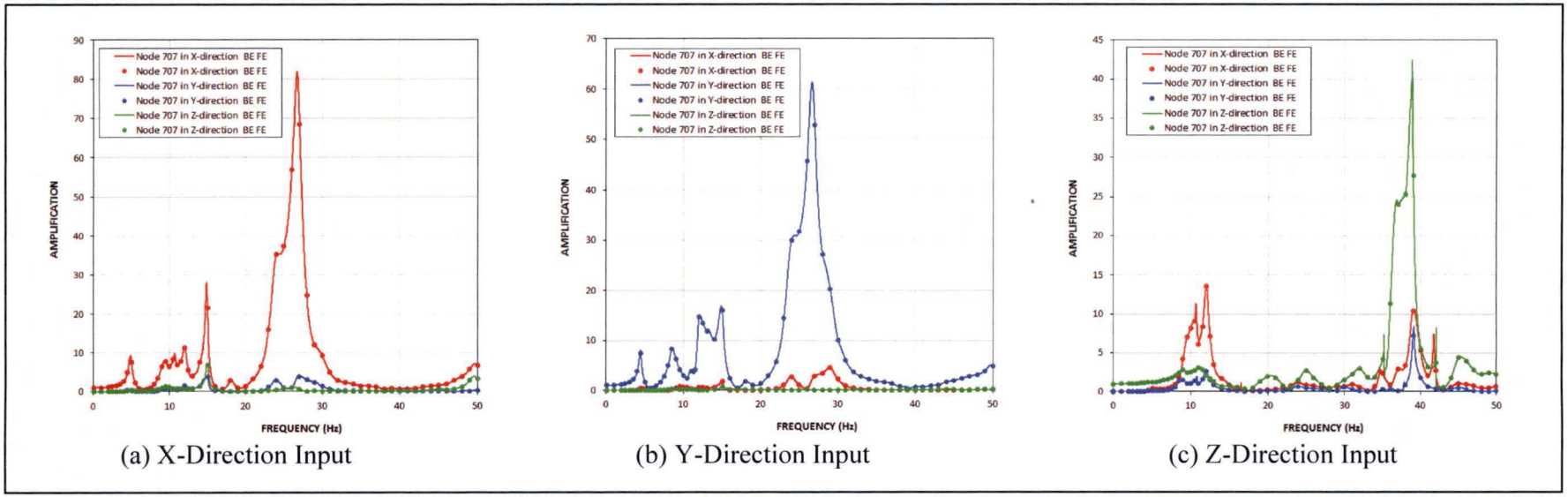

(a) X-Direction Input (b) Y-Direction Input (c) Z-Direction Input

Figure 5.1-4d Transfer Functions of RSW Top Response from Analysis of BE Full Column Profile

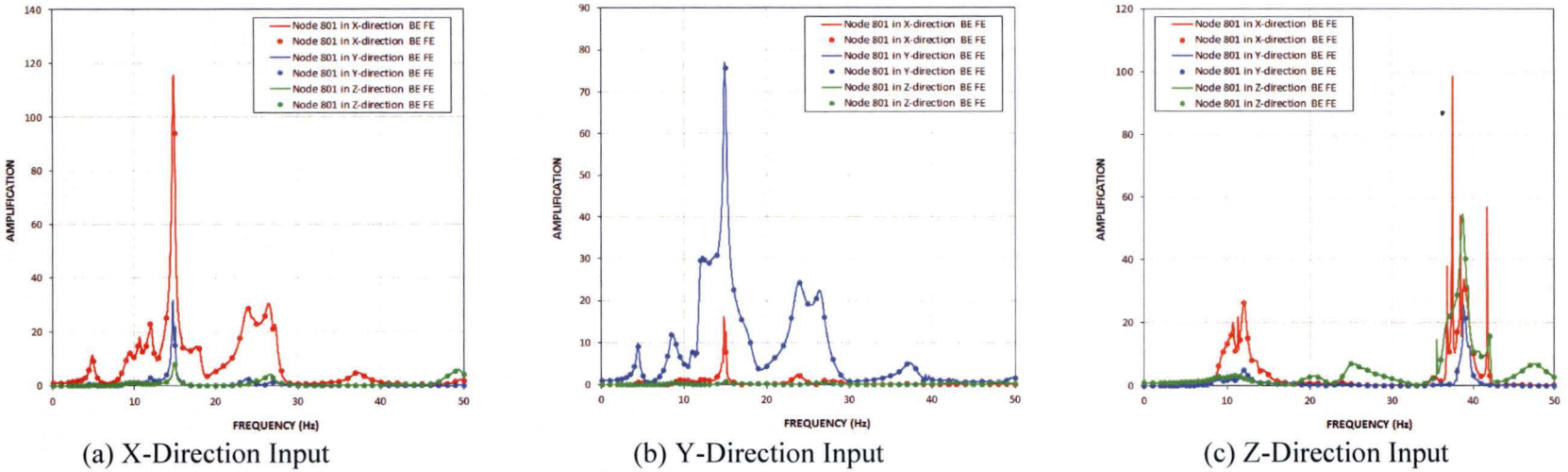

(a) X-Direction Input (b) Y-Direction Input (c) Z-Direction Input

Figure 5.1-4e Transfer Functions of RPV Top Response from Analysis of BE Full Column Profile

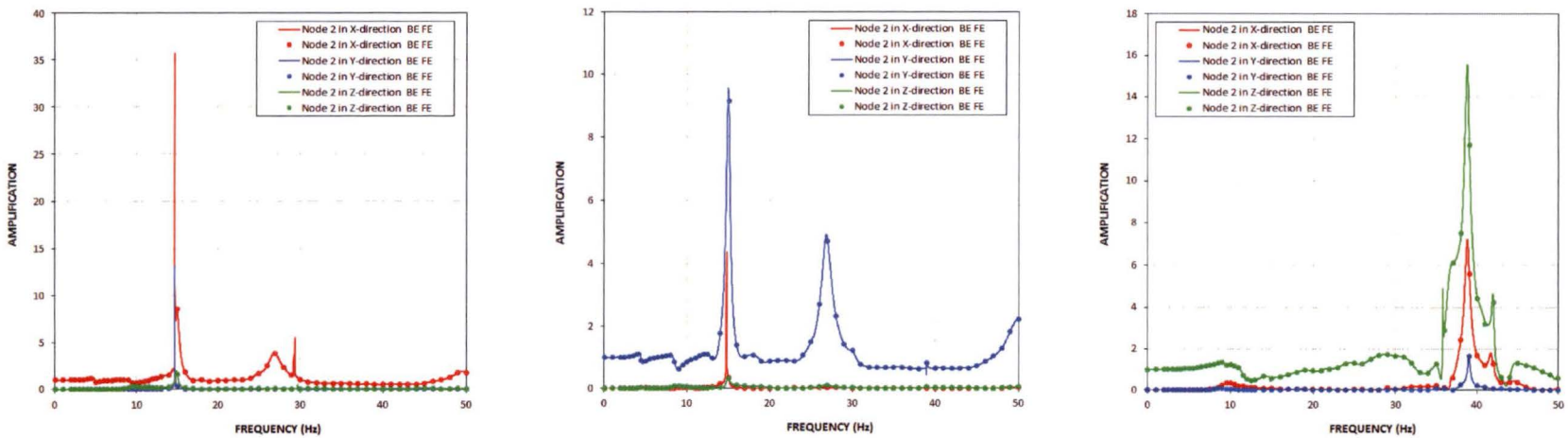

(a) X-Direction Input (b) Y-Direction Input (c) Z-Direction Input

Figure 5.1-4f Transfer Functions of RB/FB Basemat Response from Analysis of BE Full Column Profile

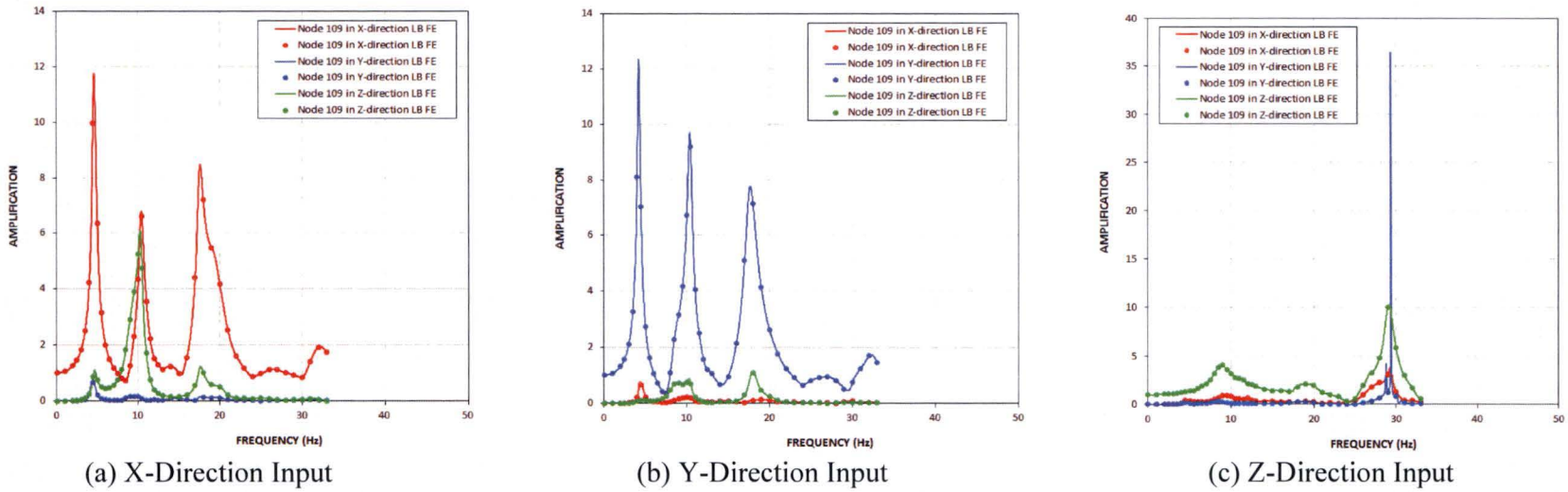

(a) X-Direction Input (b) Y-Direction Input (c) Z-Direction Input

Figure 5.1-5a Transfer Functions of RB/FB Refueling Floor Response from Analysis of LB Full Column Profile

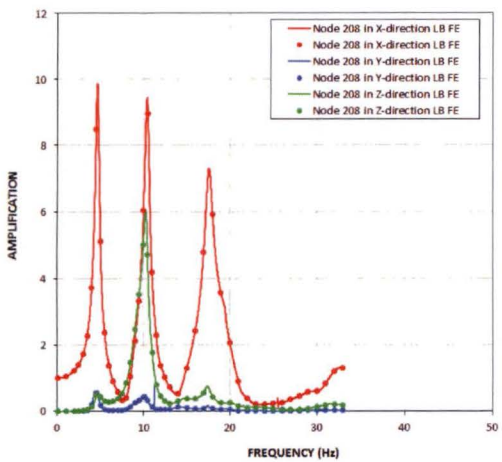

(a) X-Direction Input

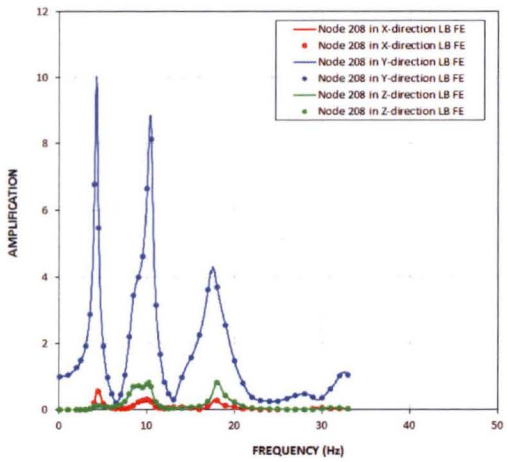

(b) Y-Direction Input

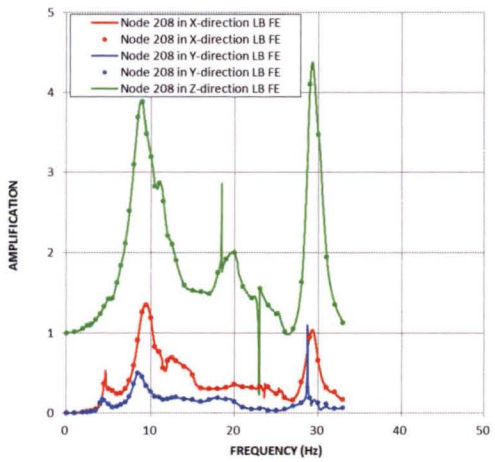

(c) Z-Direction Input

Figure 5.1-5b Transfer Functions of RCCV Top Slab Response from Analysis of LB Full Column Profile

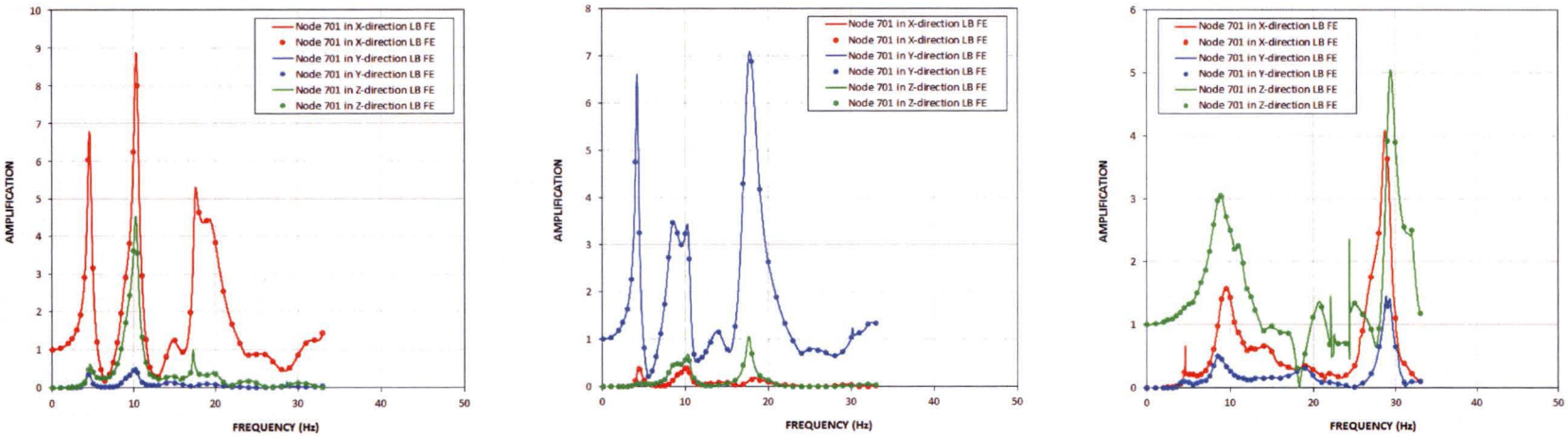

(a) X-Direction Input (b) Y-Direction Input (c) Z-Direction Input

Figure 5.1-5c Transfer Functions of Vent Wall Top Response from Analysis of LB Full Column Profile

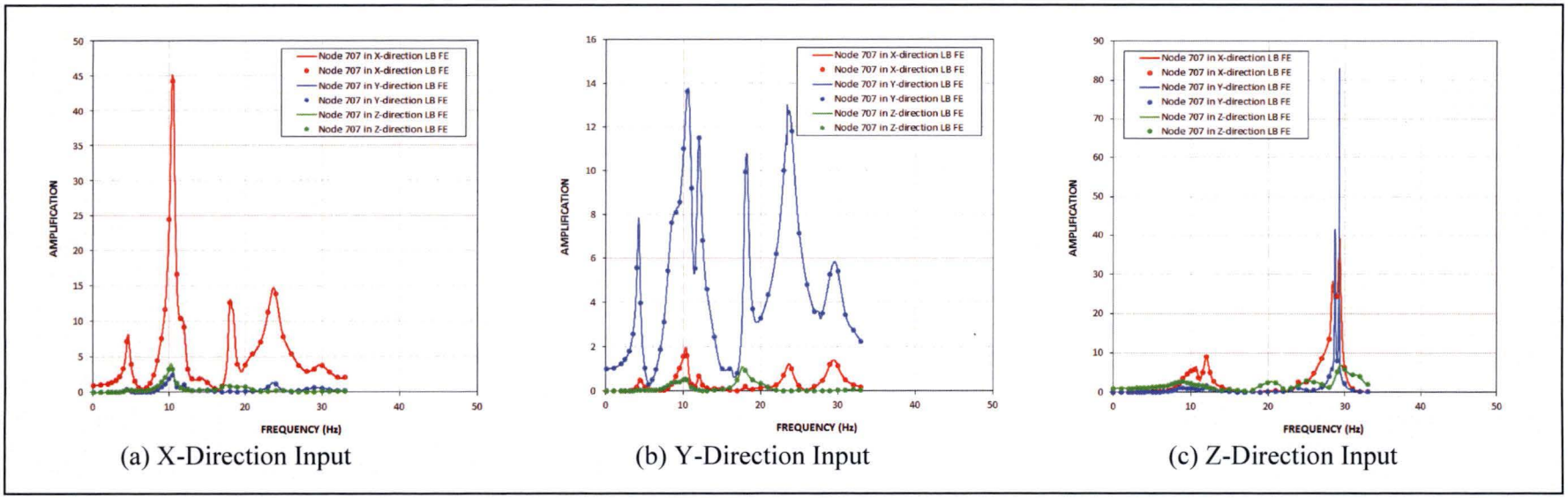

(a) X-Direction Input (b) Y-Direction Input (c) Z-Direction Input

Figure 5.1-5d Transfer Functions of RSW Top Response from Analysis of LB Full Column Profile

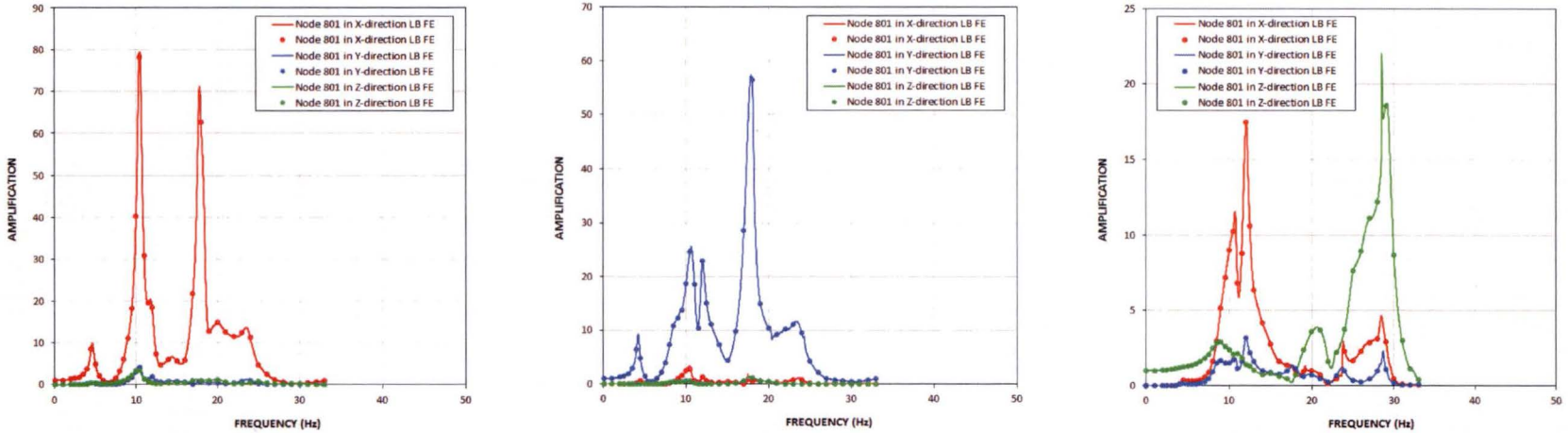

(a) X-Direction Input (b) Y-Direction Input (c) Z-Direction Input

Figure 5.1-5e Transfer Functions of RPV Top Response from Analysis of LB Full Column Profile

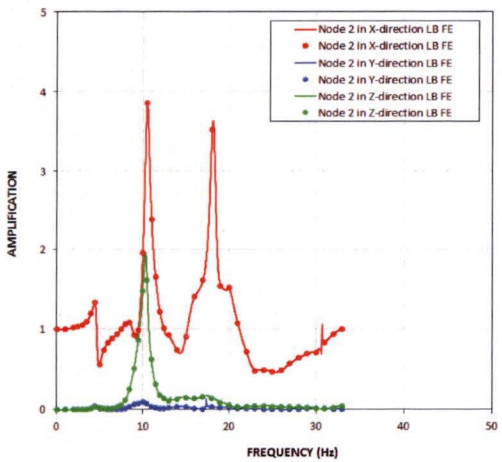

(a) X-Direction Input

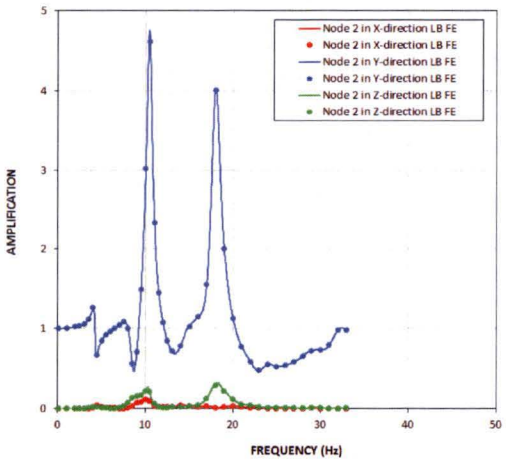

(b) Y-Direction Input

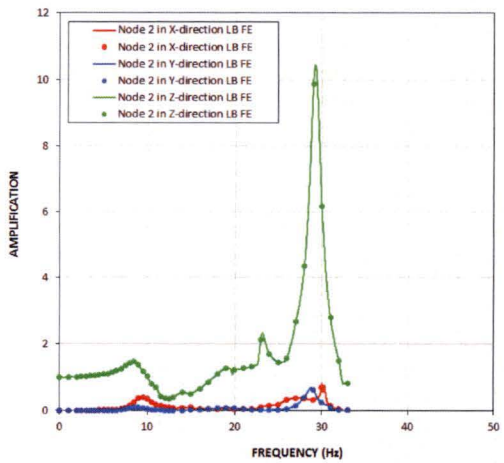

(c) Z-Direction Input

Figure 5.1-5f Transfer Functions of RB/FB Basemat Response from Analysis of LB Full Column Profile

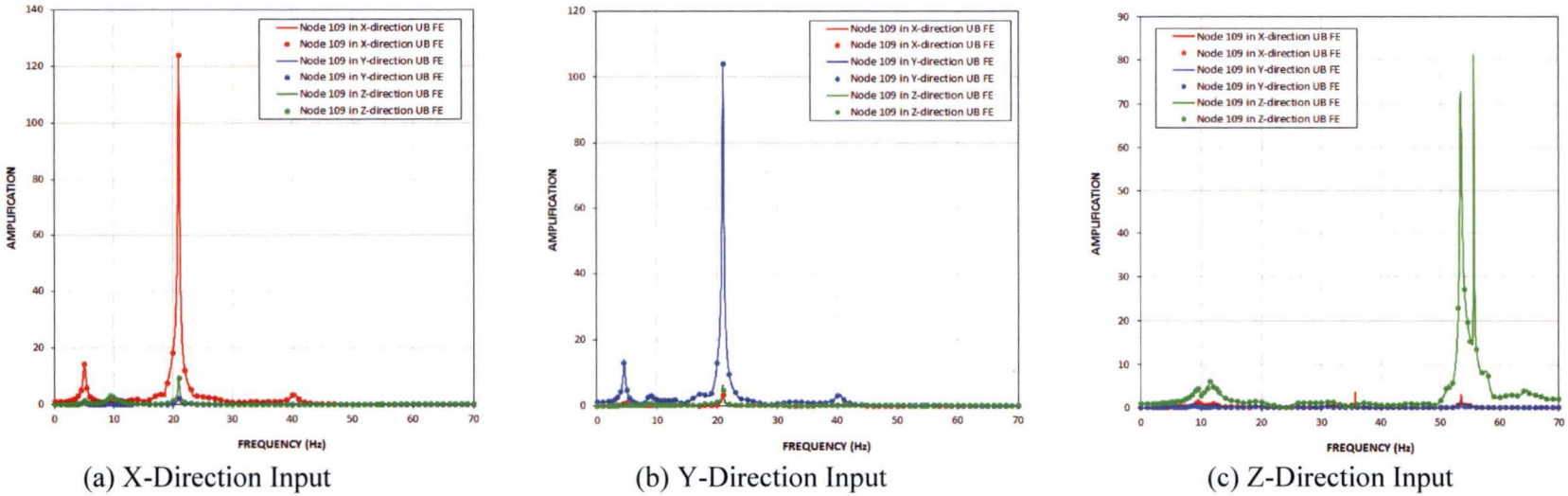

(a) X-Direction Input (b) Y-Direction Input (c) Z-Direction Input

Figure 5.1-6a Transfer Functions of RB/FB Refueling Floor Response from Analysis of UB Full Column Profile

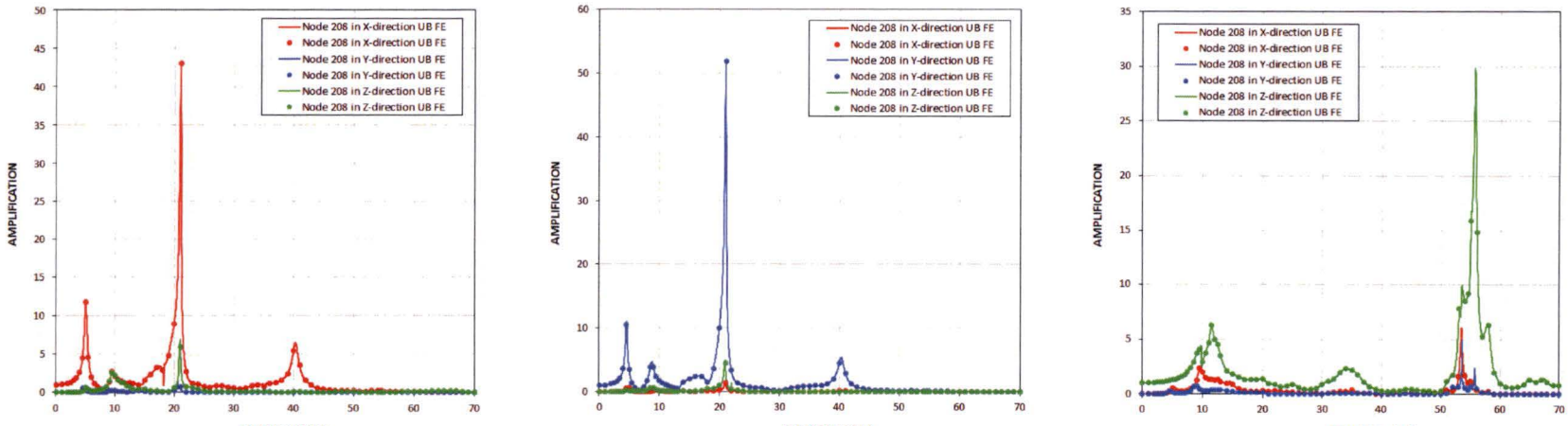

(a) X-Direction Input (b) Y-Direction Input (c) Z-Direction Input

Figure 5.1-6b Transfer Functions of RCCV Top Slab Response from Analysis of UB Full Column Profile

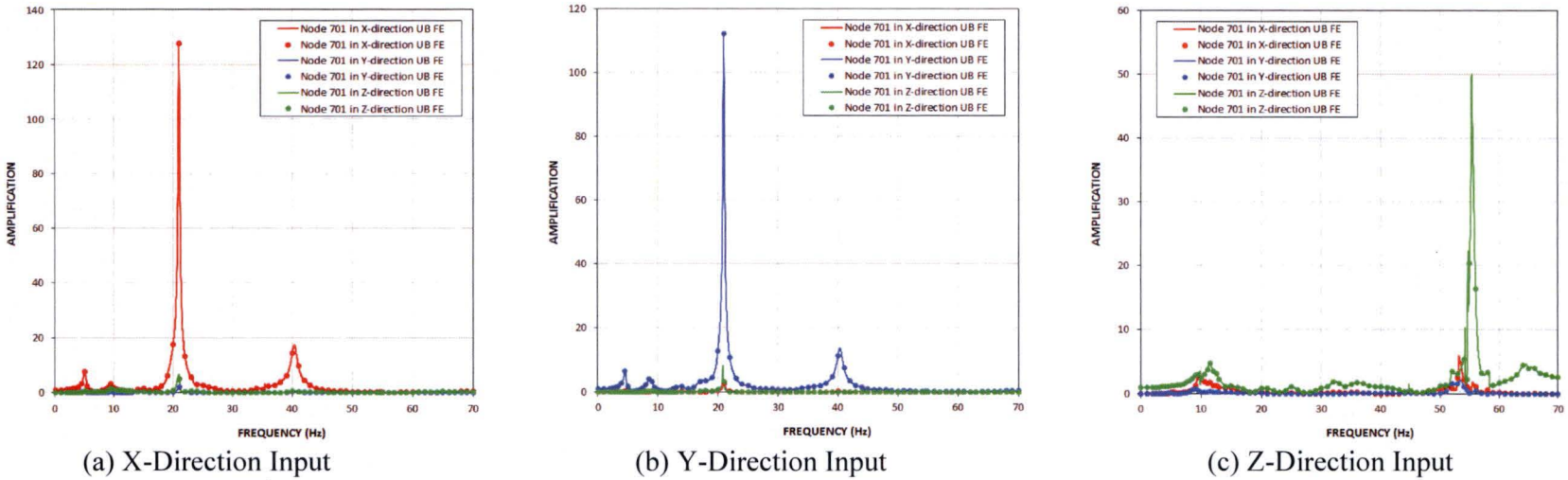

(a) X-Direction Input (b) Y-Direction Input (c) Z-Direction Input

Figure 5.1-6c Transfer Functions of Vent Wall Top Response from Analysis of UB Full Column Profile

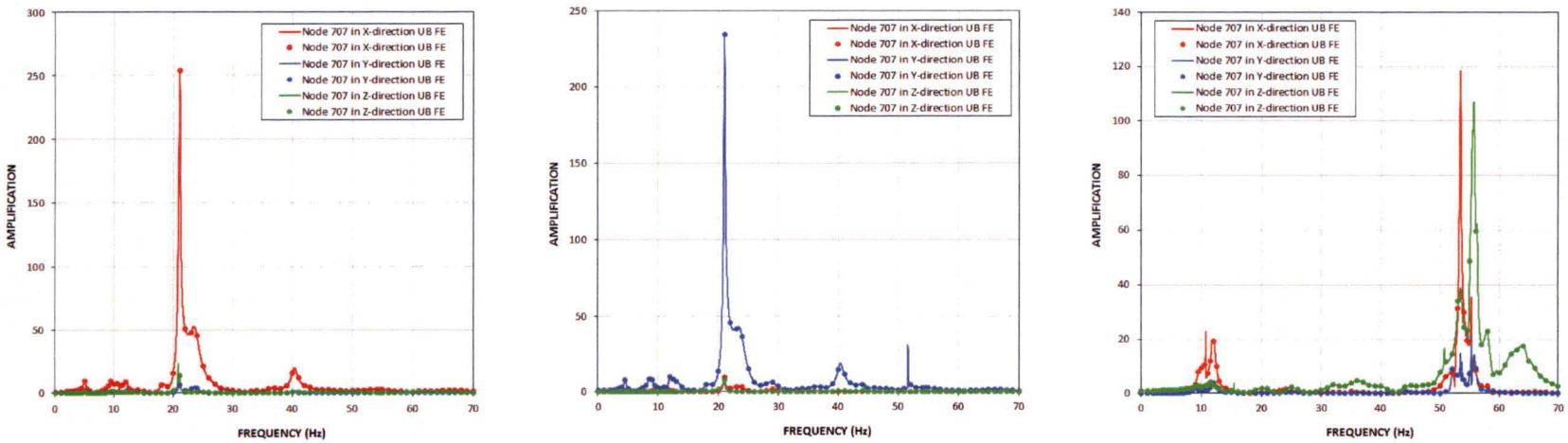

(a) X-Direction Input (b) Y-Direction Input (c) Z-Direction Input

Figure 5.1-6d Transfer Functions of RSW Top Response from Analysis of UB Full Column Profile

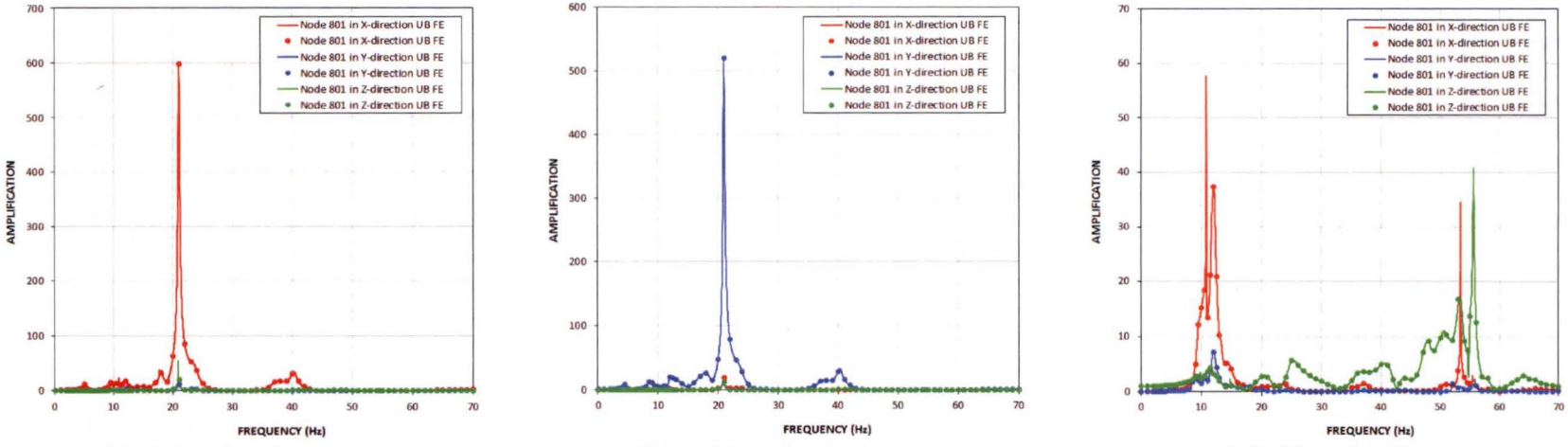

(a) X-Direction Input (b) Y-Direction Input (c) Z-Direction Input

Figure 5.1-6e Transfer Functions of RPV Top Response from Analysis of UB Full Column Profile

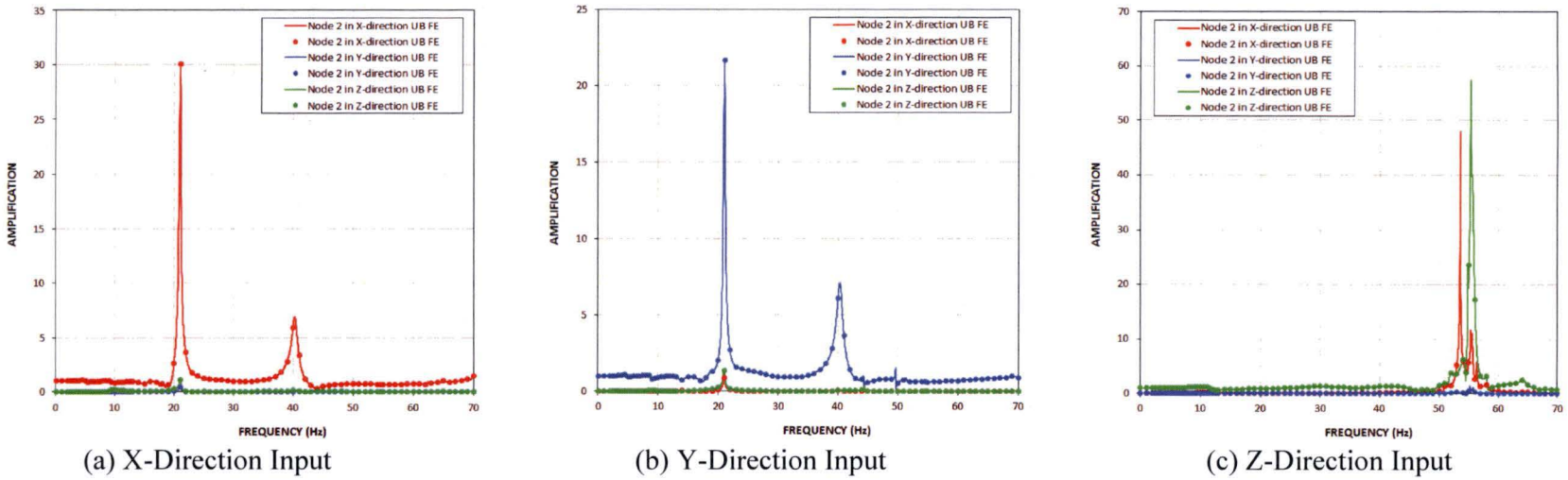

(a) X-Direction Input (b) Y-Direction Input (c) Z-Direction Input

Figure 5.1-6f Transfer Functions of RB/FB Basemat Response from Analysis of UB Full Column Profile

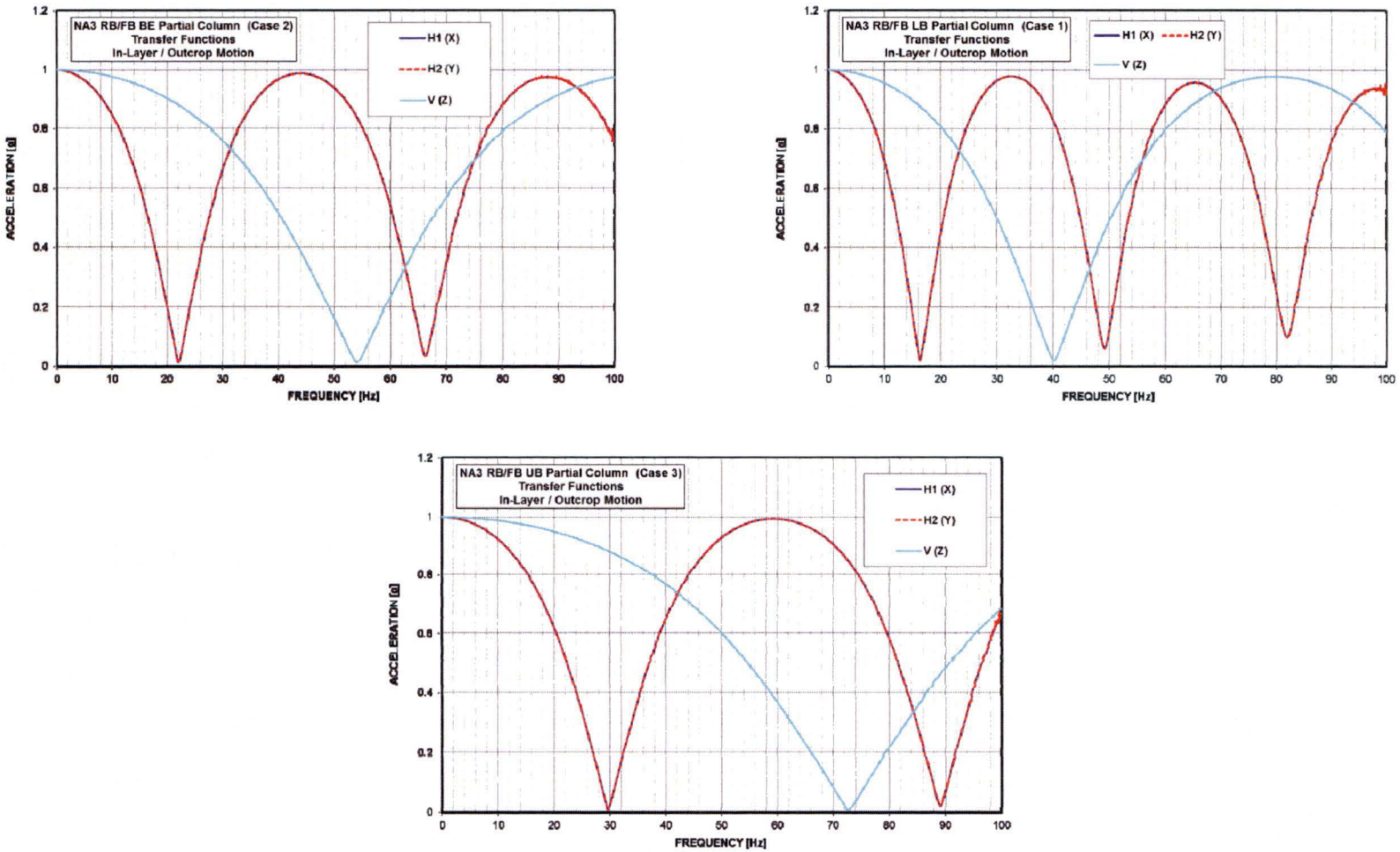

Figure 5.1-7 Transfer Functions for Transformation of RB/FB Partial Column In-Layer Motion into Outcrop Motion

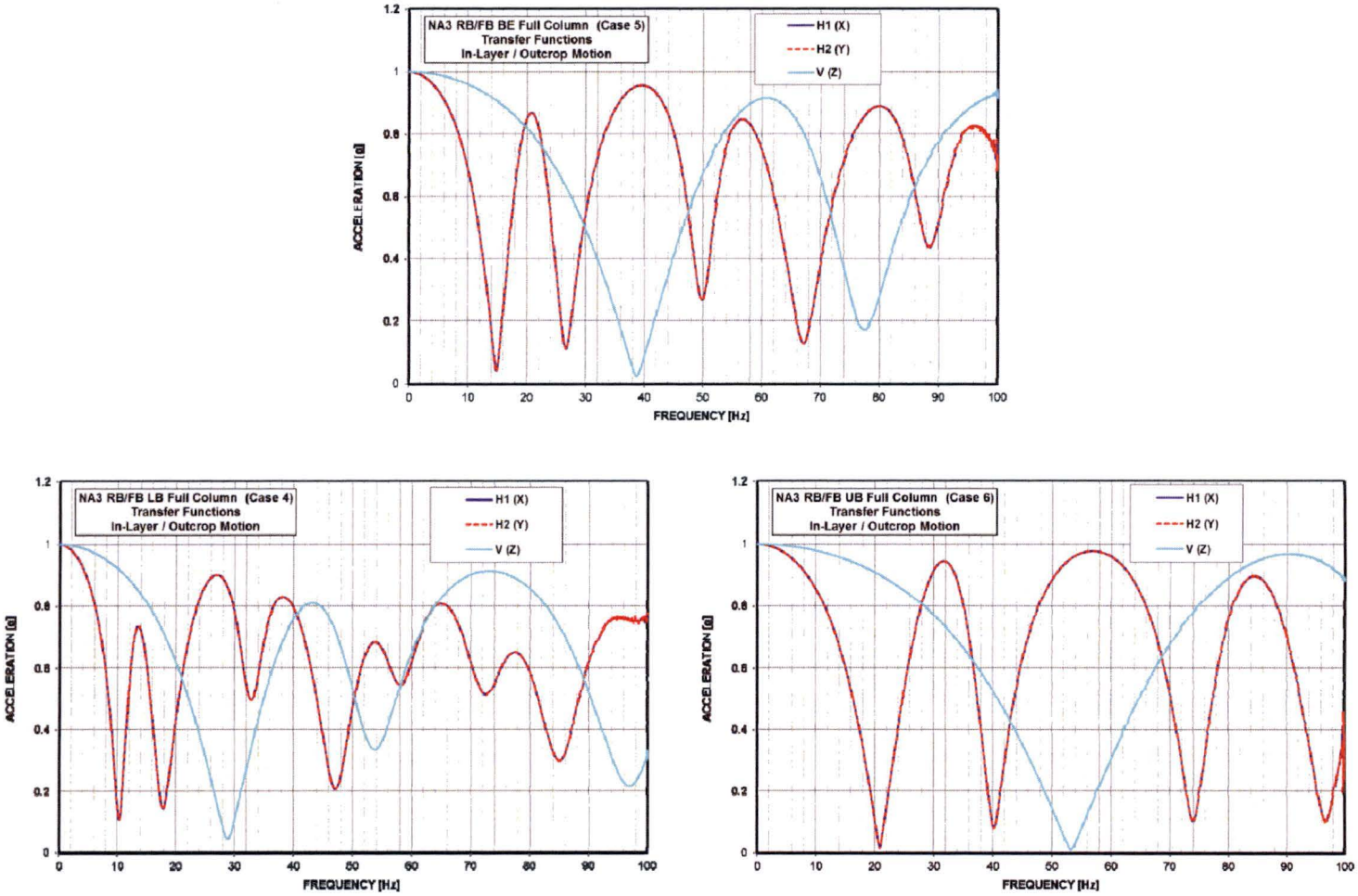

Figure 5.1-8 Transfer Functions for Transformation of RB/FB Full Column In-Layer Motion into Outcrop Motion

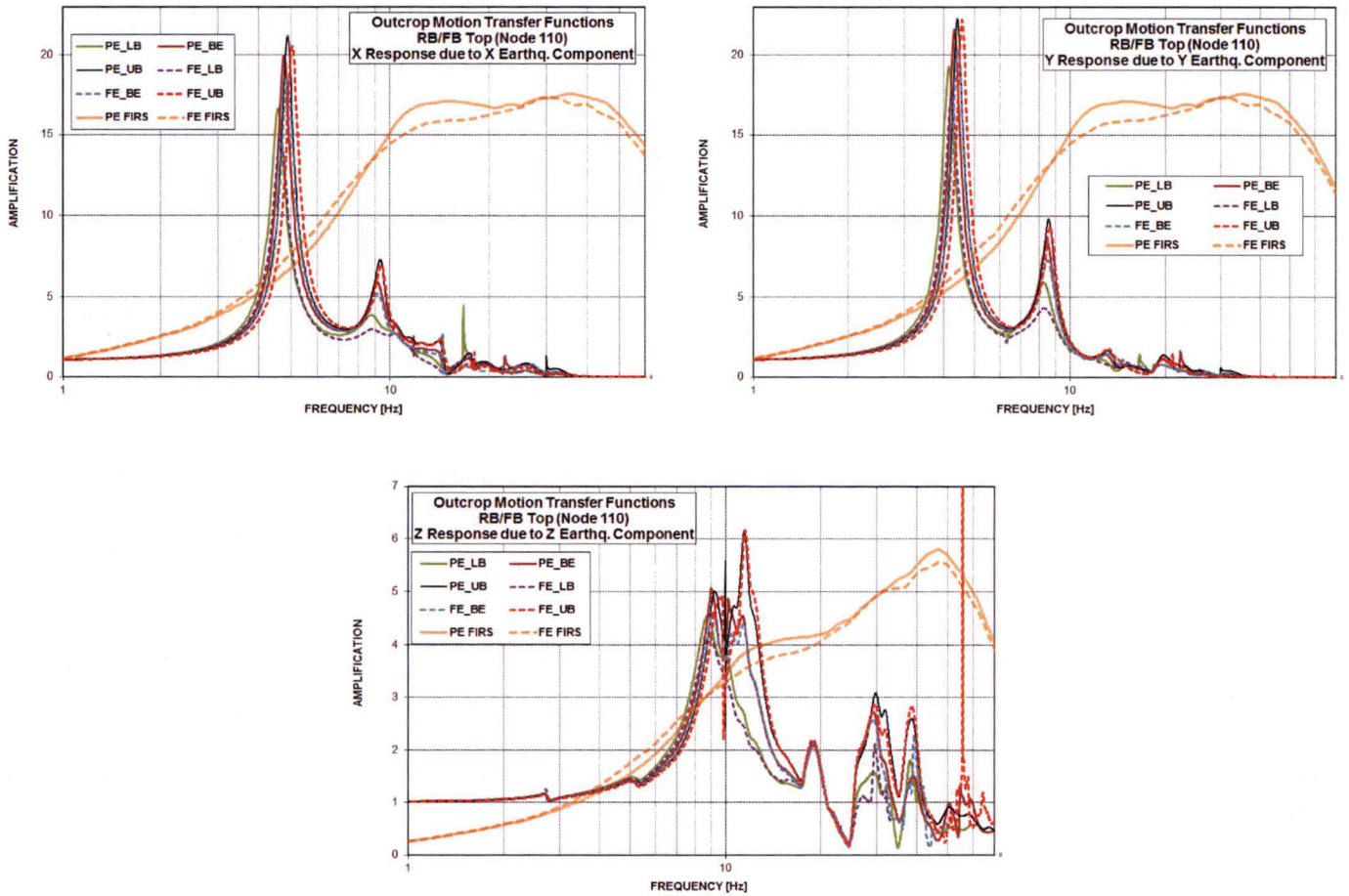

Figure 5.1-9 Outcrop Transfer Functions for Response of RB/FB Top

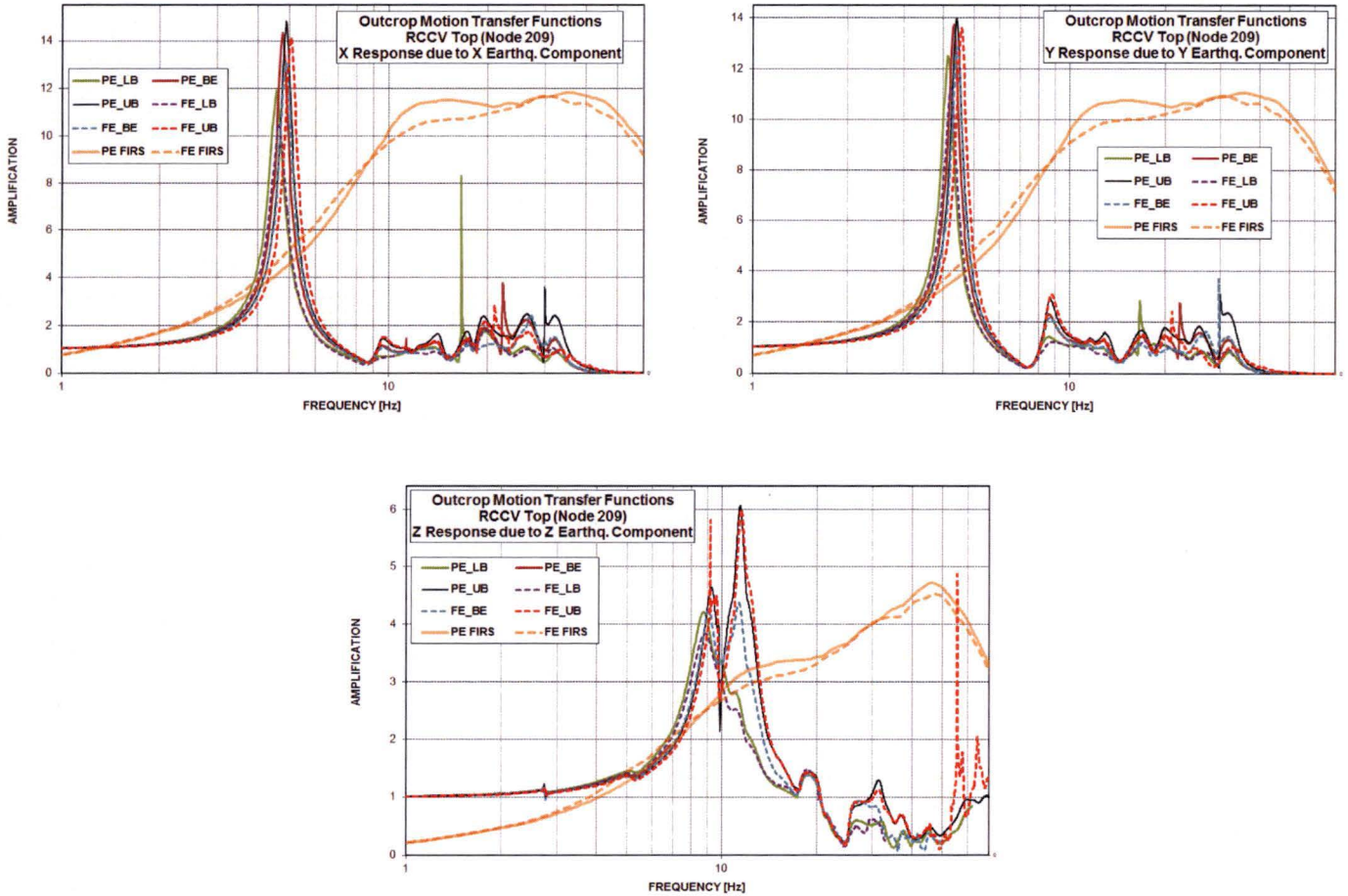

Figure 5.1-10 Outcrop Transfer Functions for Response of RCCV Top

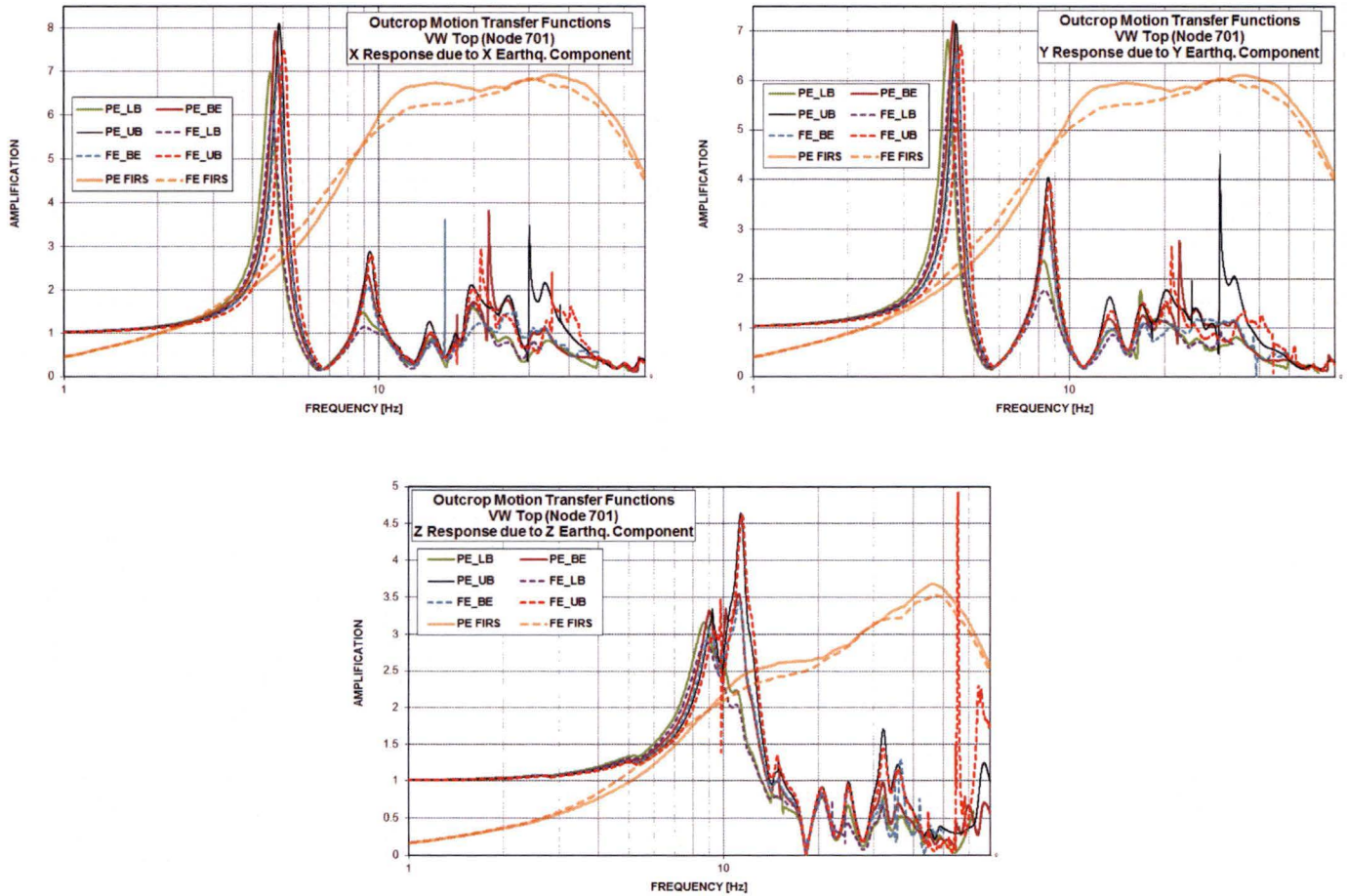

Figure 5.1-11 Outcrop Transfer Functions for Response of VW Top

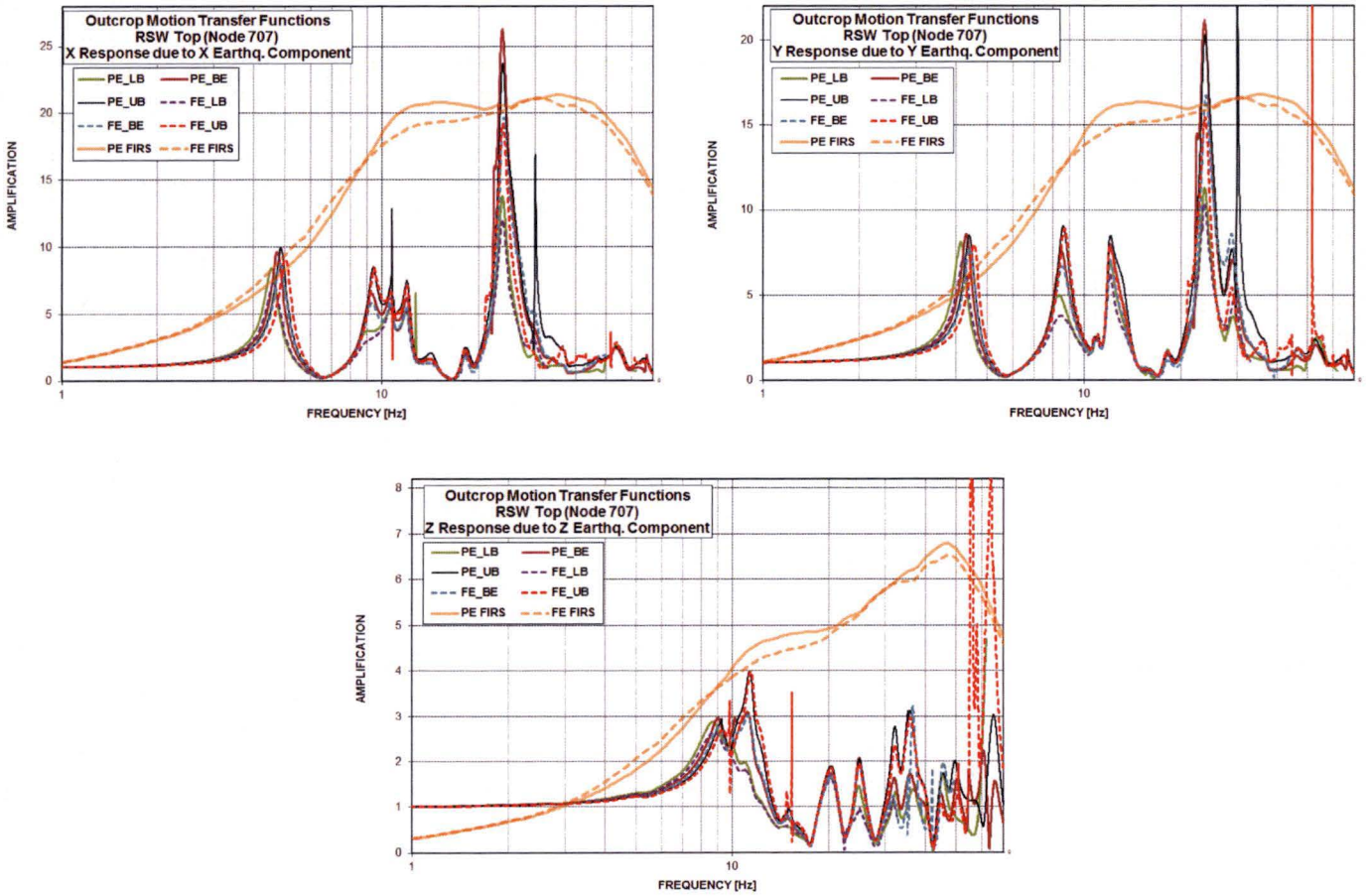

Figure 5.1-12 Outcrop Transfer Functions for Response of RSW Top

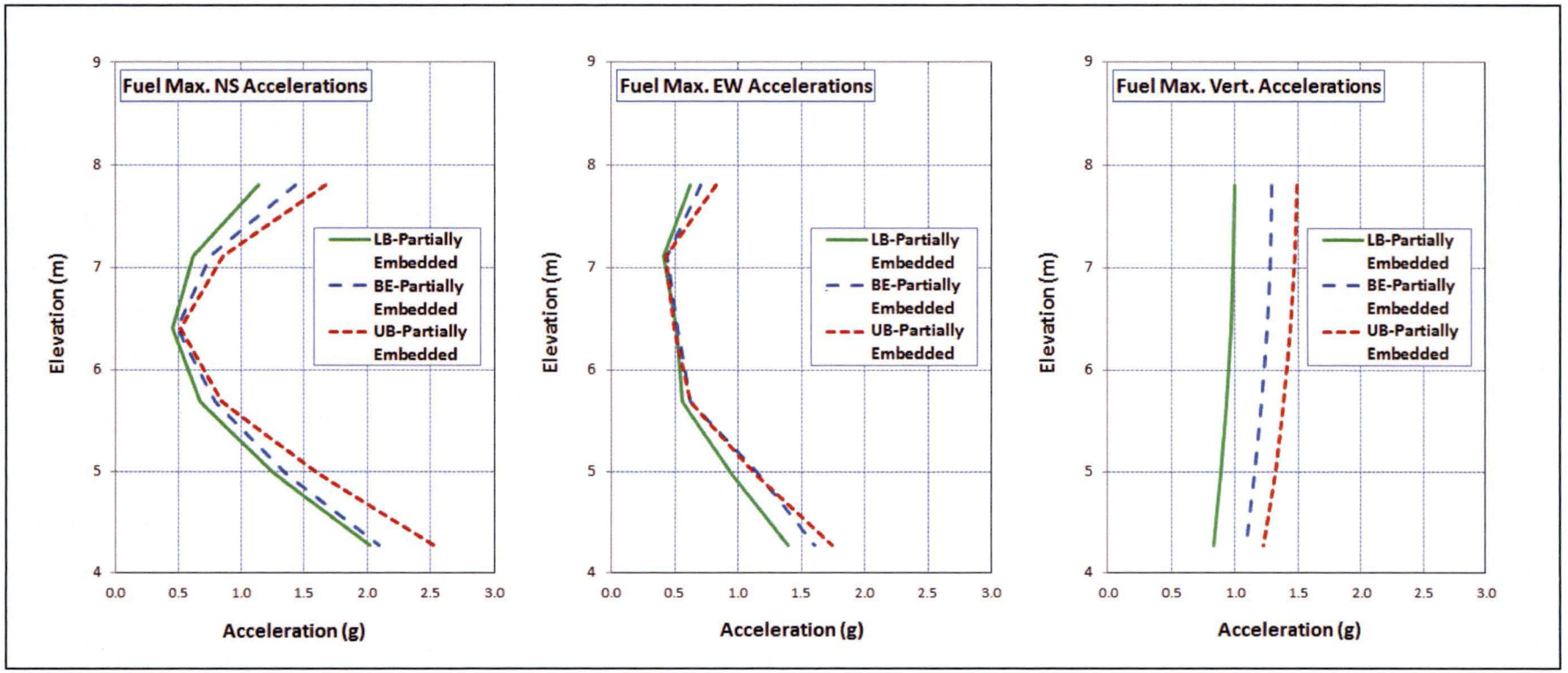

Figure 5.2-1a Maximum Acceleration Results from Analyses of Fuel PE Model

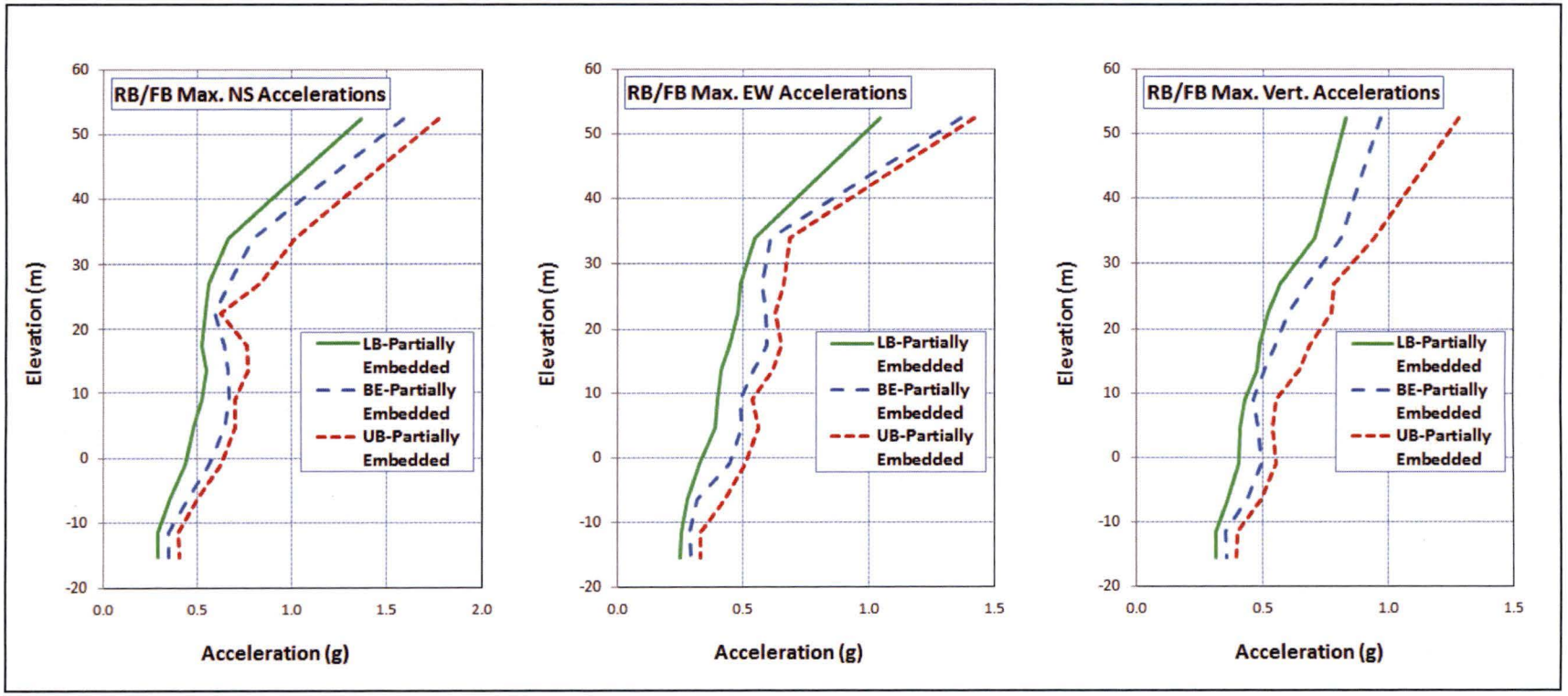

Figure 5.2-1b Maximum Acceleration Results from Analyses of RB/FB PE Model

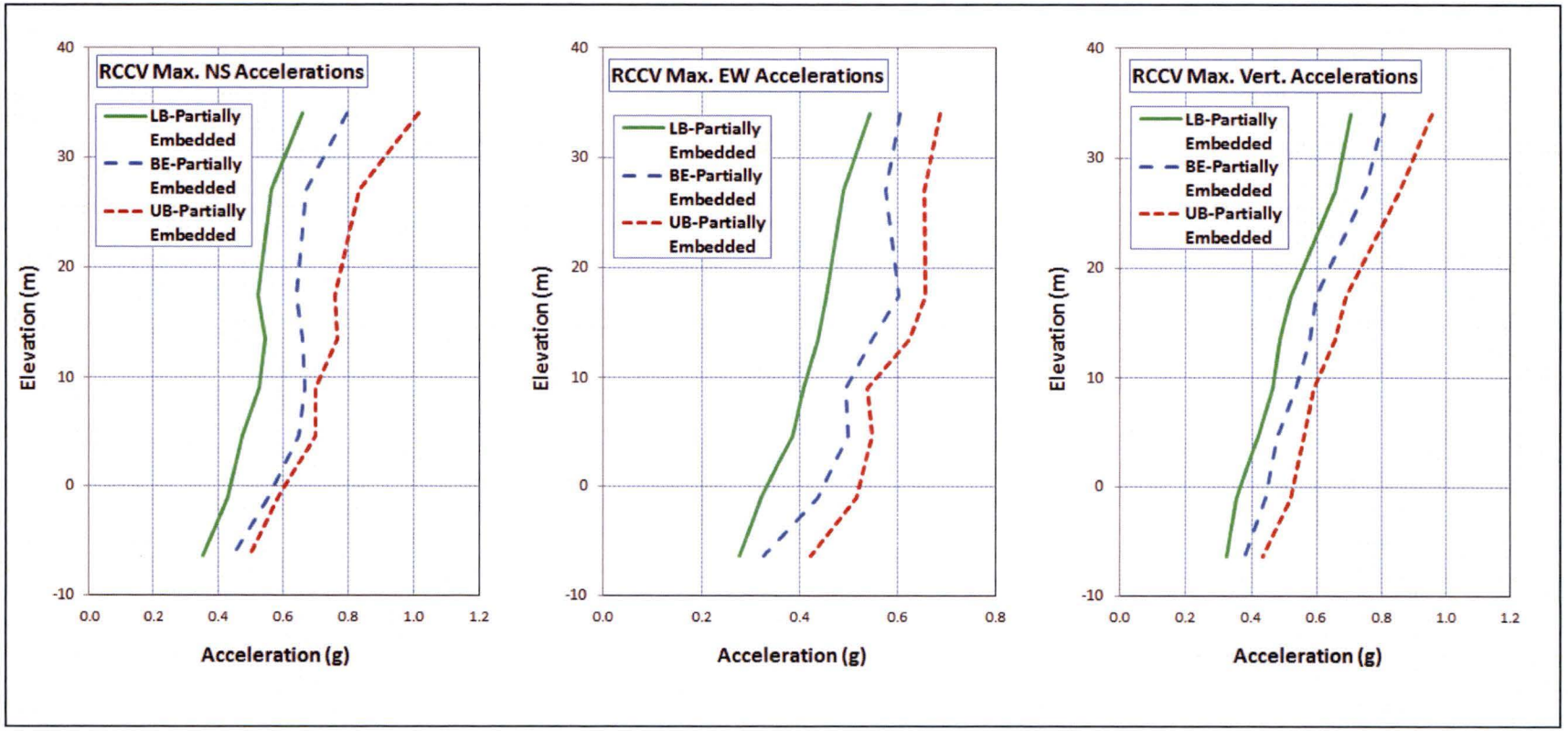

Figure 5.2-1c Maximum Acceleration Results from Analyses of RCCV PE Model

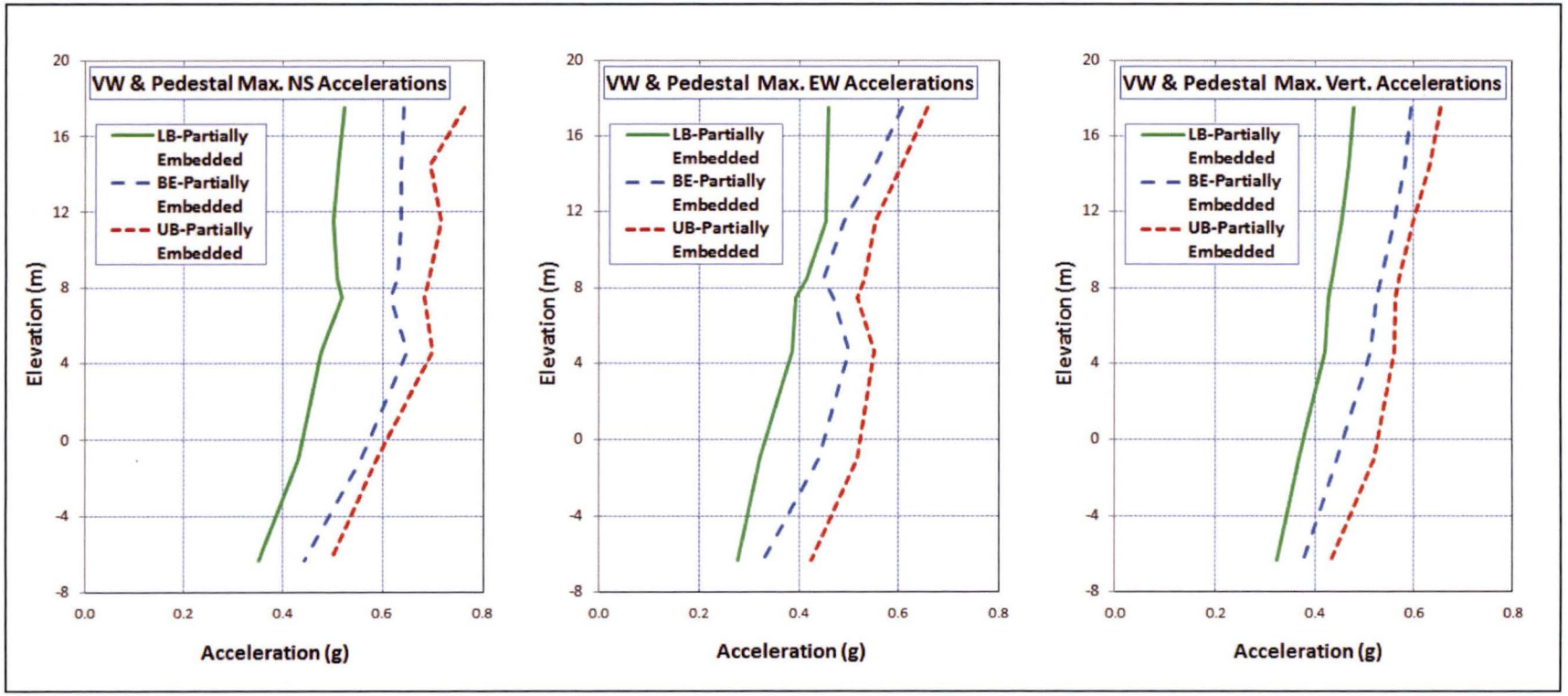

Figure 5.2-1d Maximum Acceleration Results from Analyses of Vent Wall/Pedestal PE Model

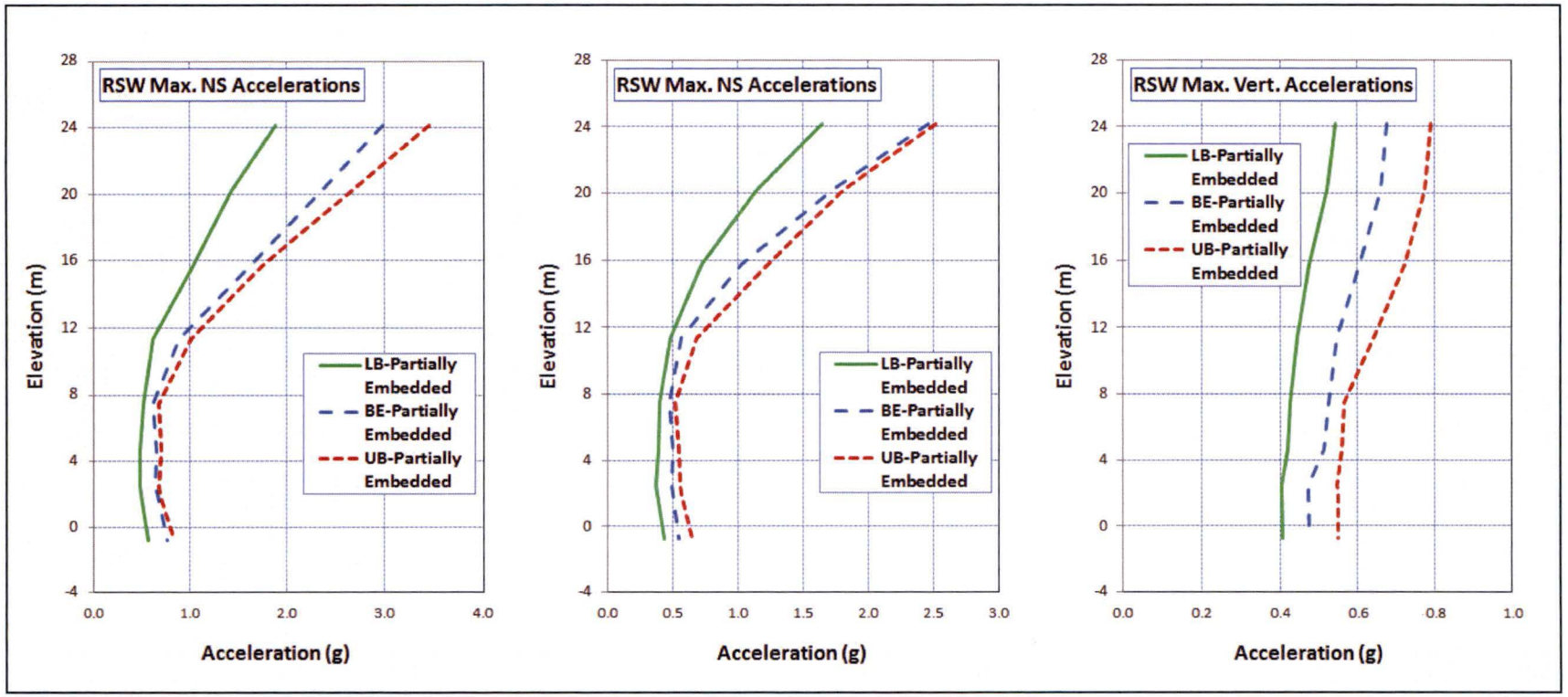

Figure 5.2-1e Maximum Acceleration Results from Analyses of Reactor Shield Wall PE Model

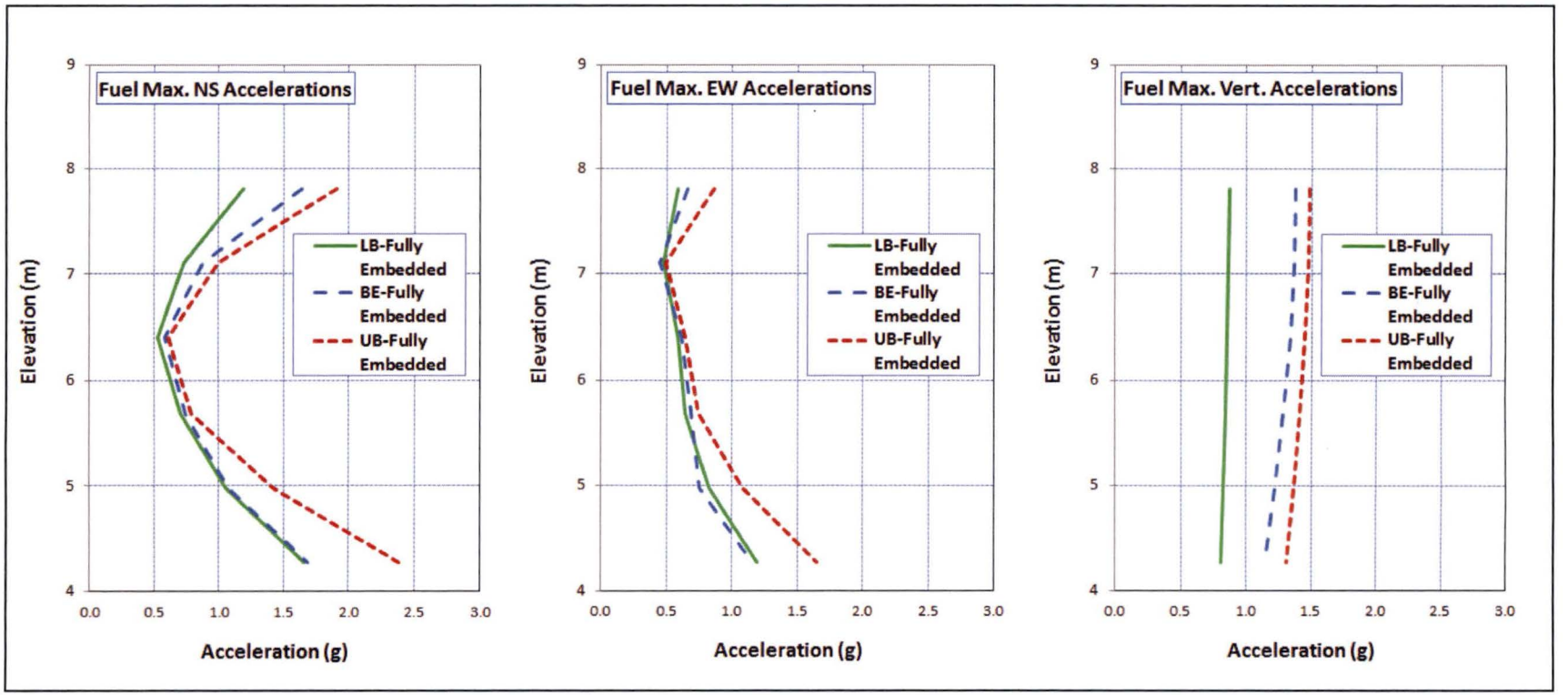

Figure 5.2-2a Maximum Acceleration Results from Analyses of Fuel FE Model

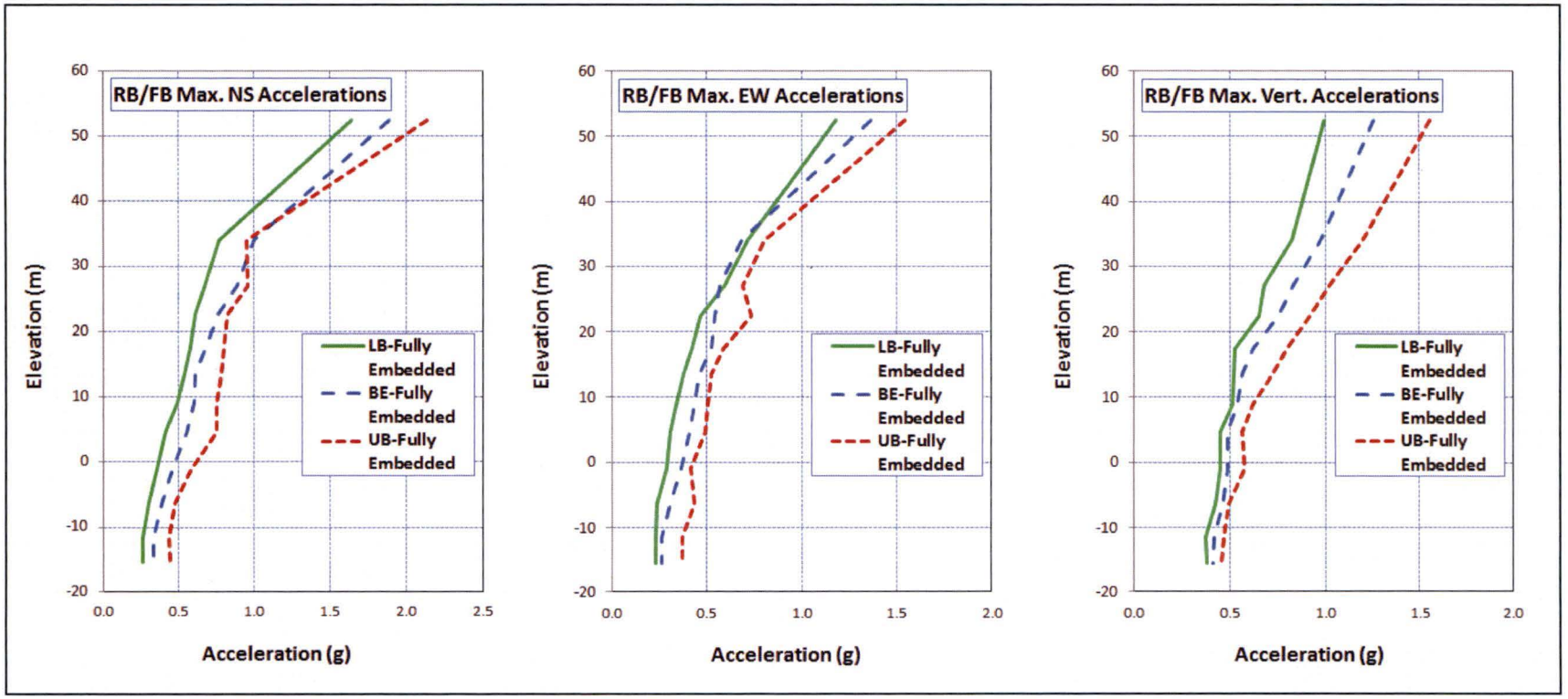

Figure 5.2-2b Maximum Acceleration Results from Analyses of RB/FB FE Model

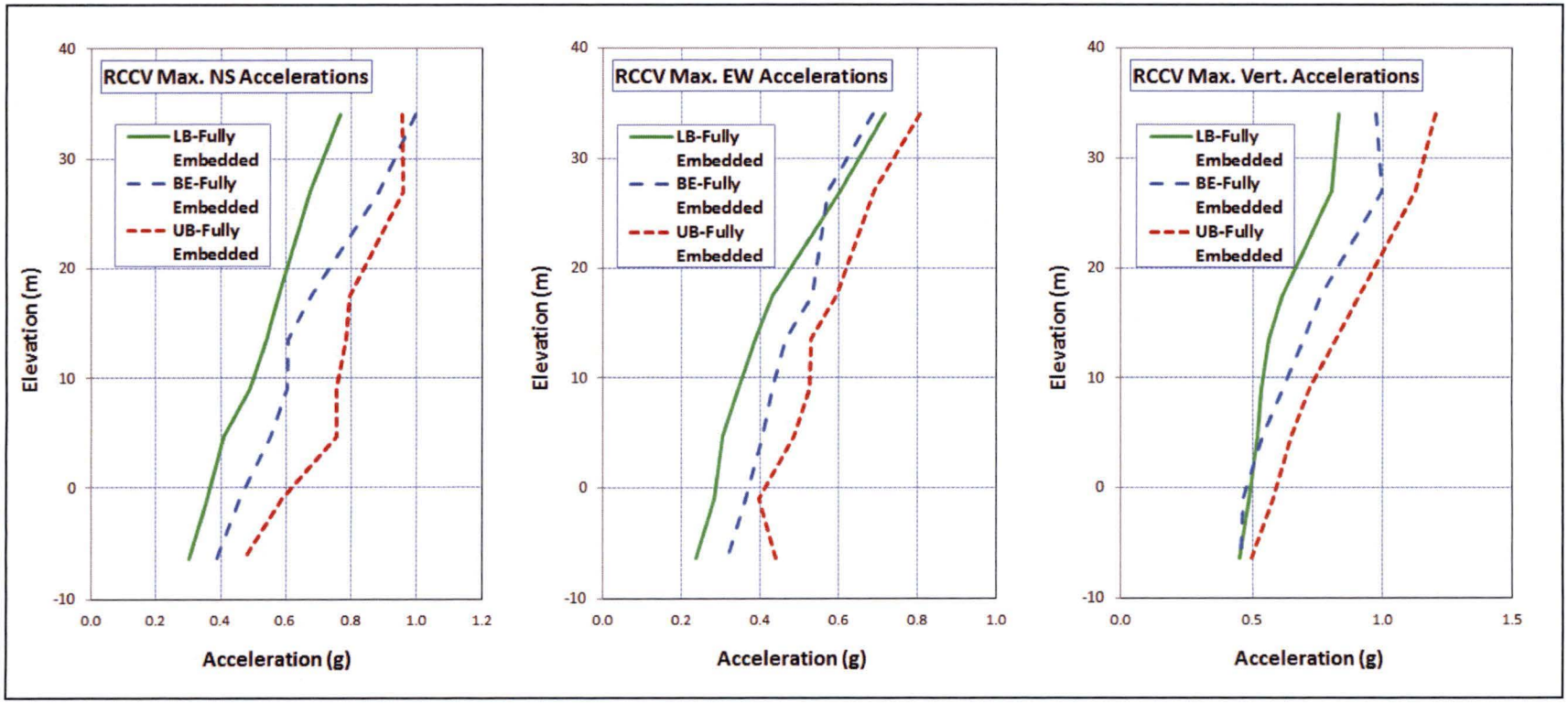

Figure 5.2-2c Maximum Acceleration Results from Analyses of RCCV FE Model

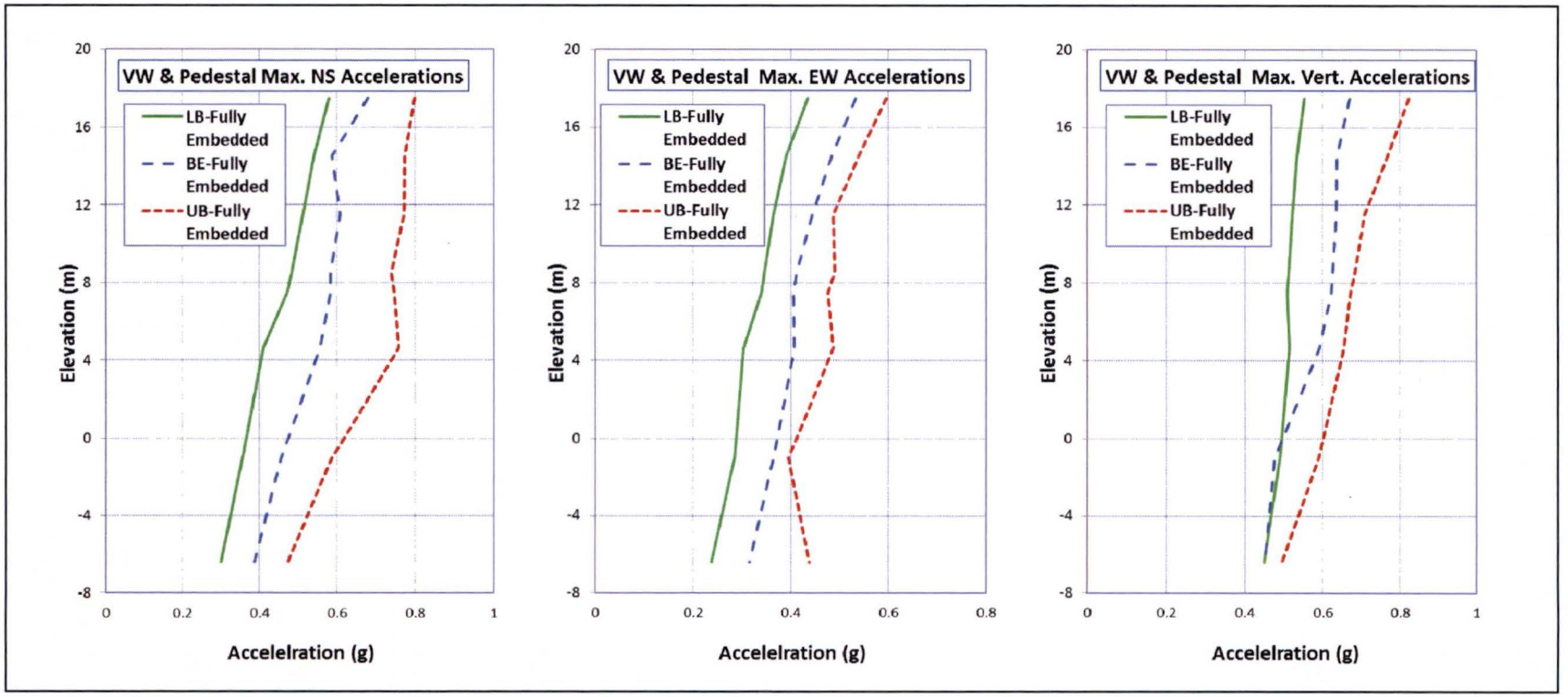

Figure 5.2-2d Maximum Acceleration Results from Analyses of Vent Wall/Pedestal FE Model

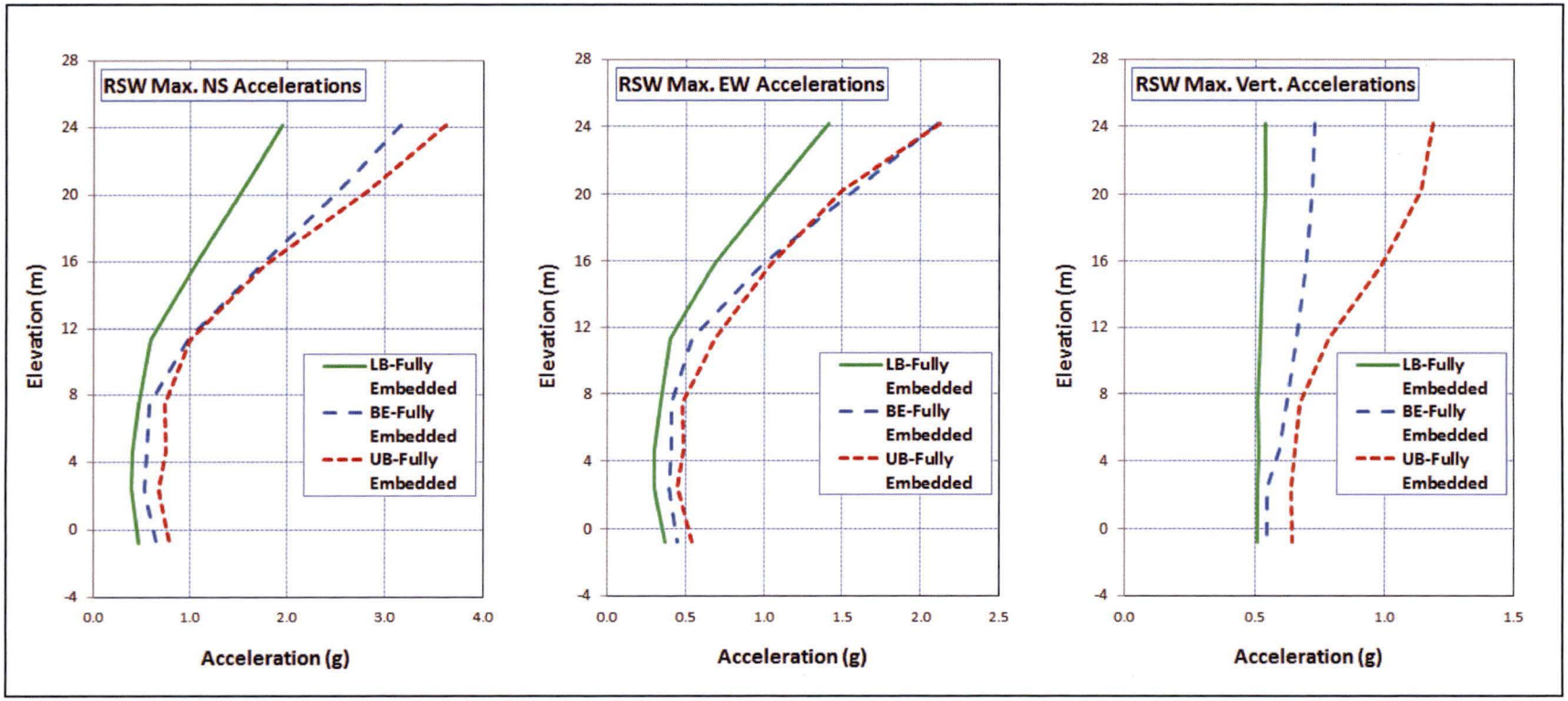

Figure 5.2-2e Maximum Acceleration Results from Analyses of Reactor Shield Wall FE Model

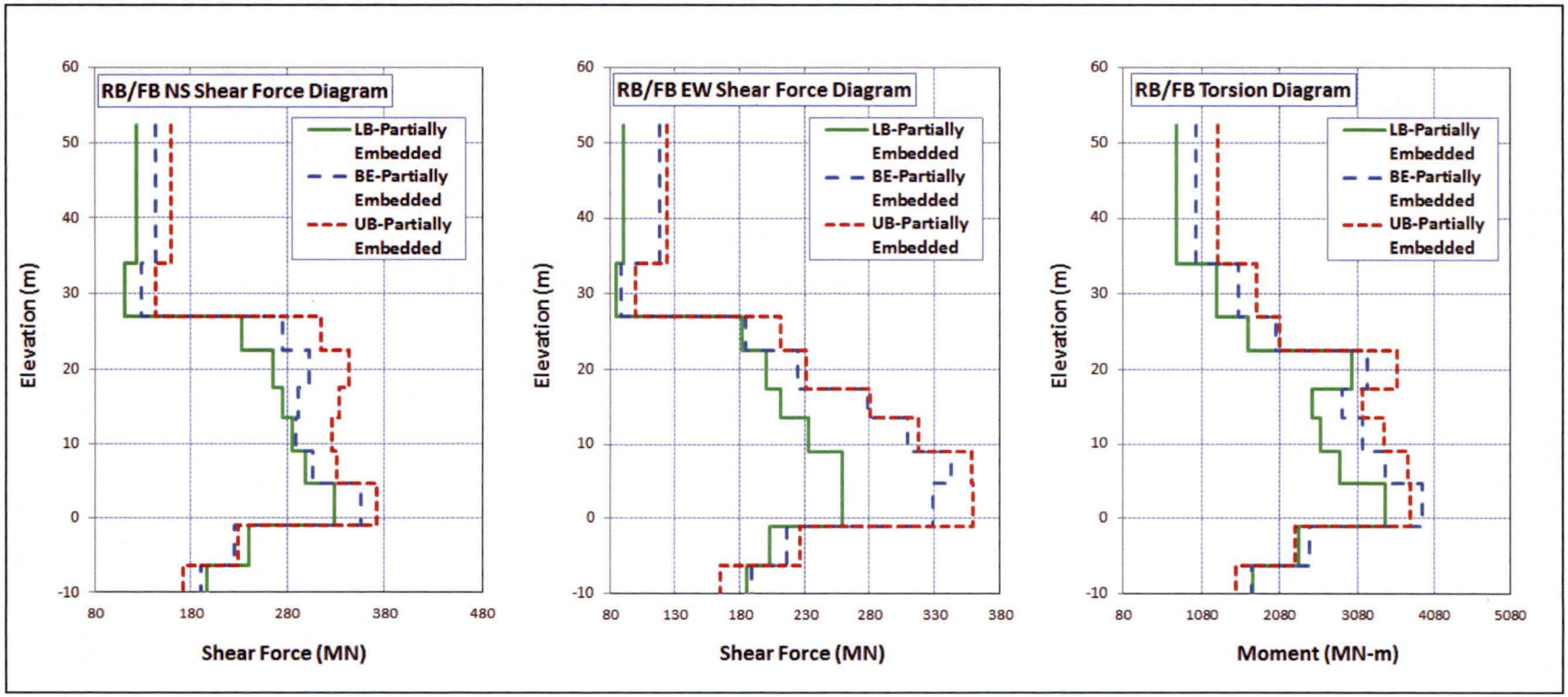

Figure 5.2-3a Maximum Shear Forces and Torsion Results from Analyses of RB/FB PE Model

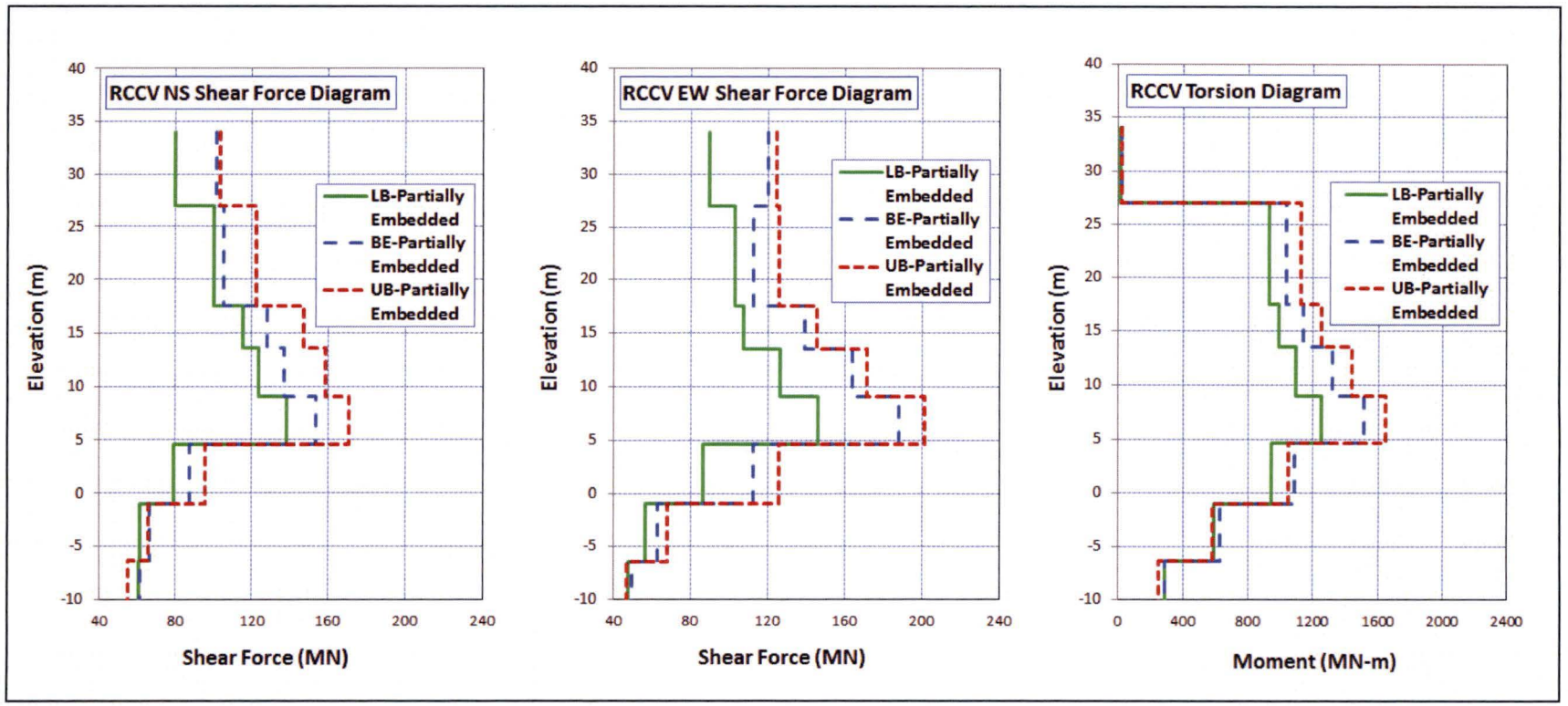

Figure 5.2-3b Maximum Shear Forces and Torsion Results from Analyses of RCCV PE Model

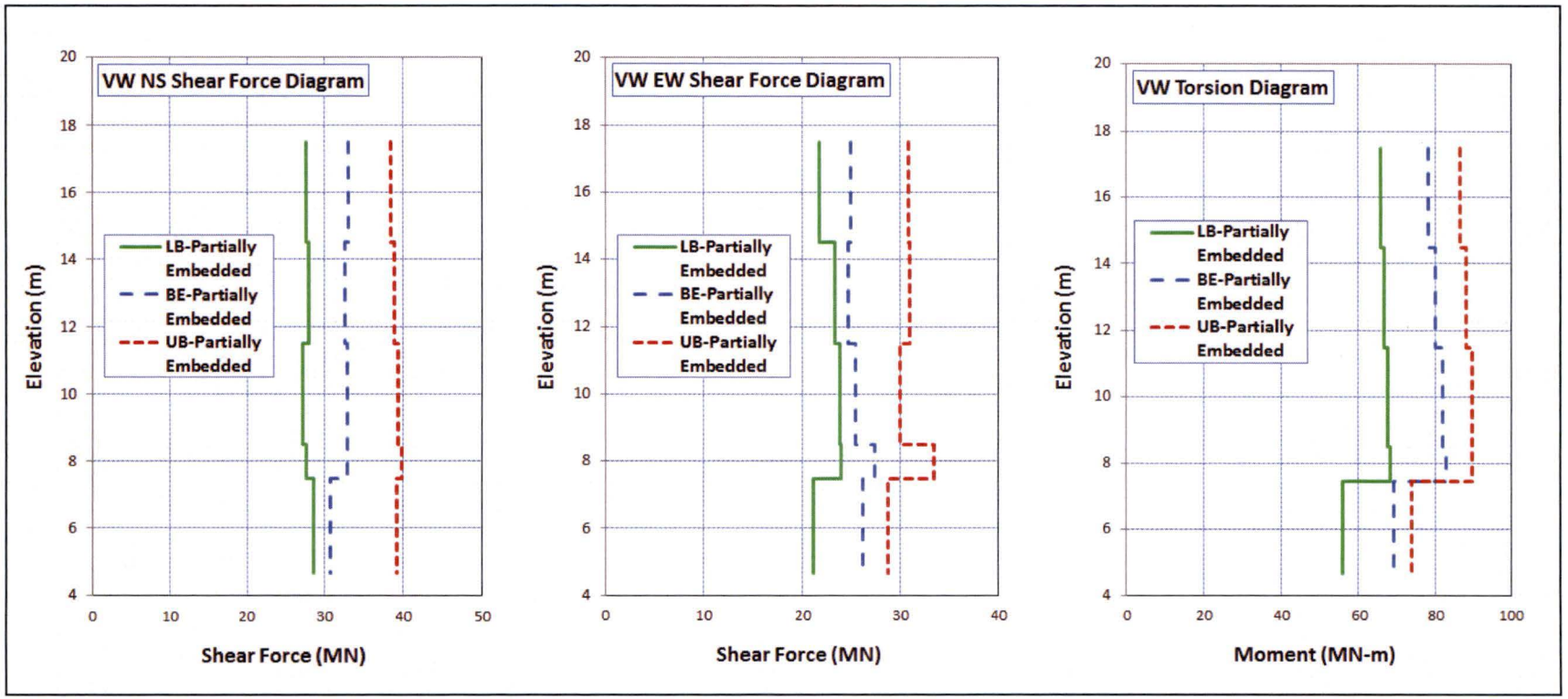

Figure 5.2-3c Maximum Shear Forces and Torsion Results from Analyses of Vent Wall PE Model

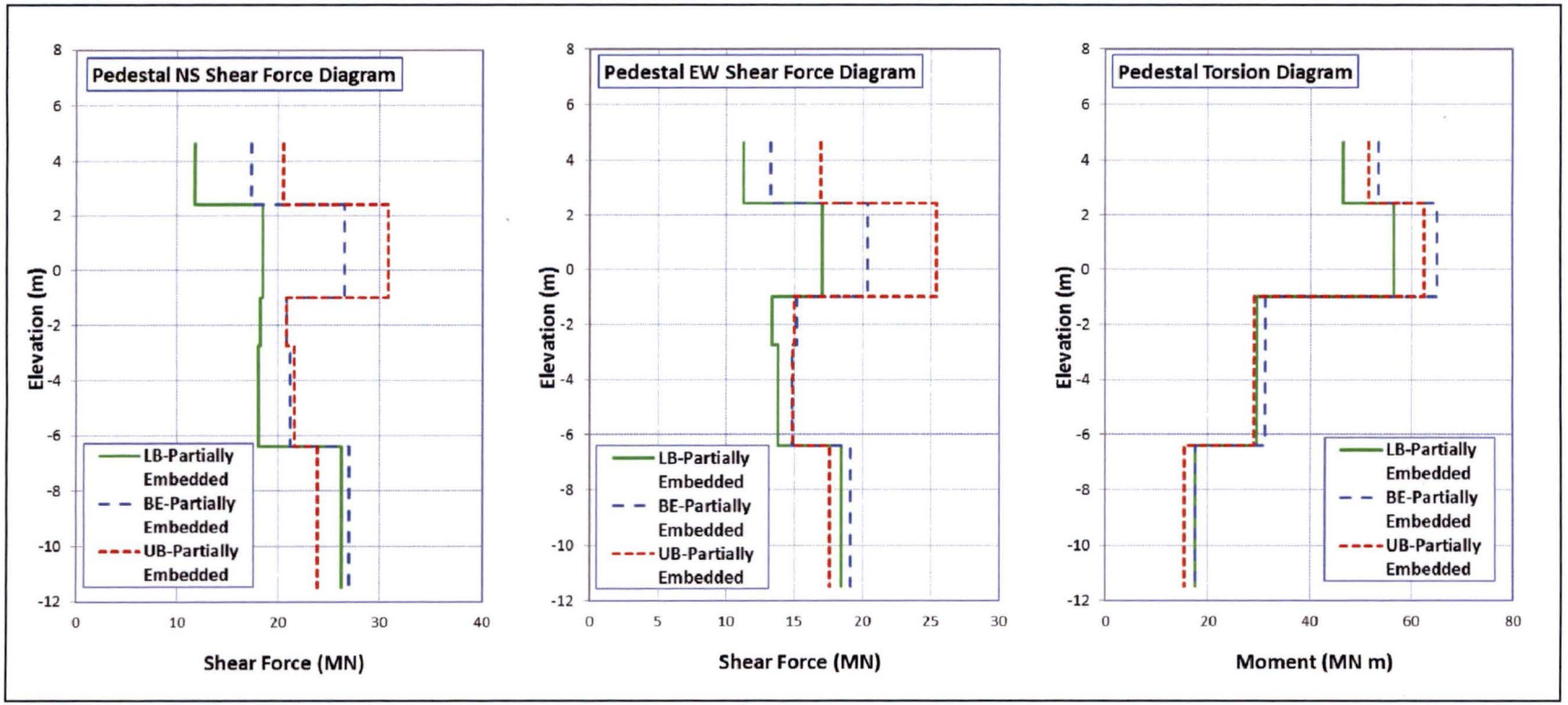

Figure 5.2-3d Maximum Shear Forces and Torsion Results from Analyses of Pedestal PE Model

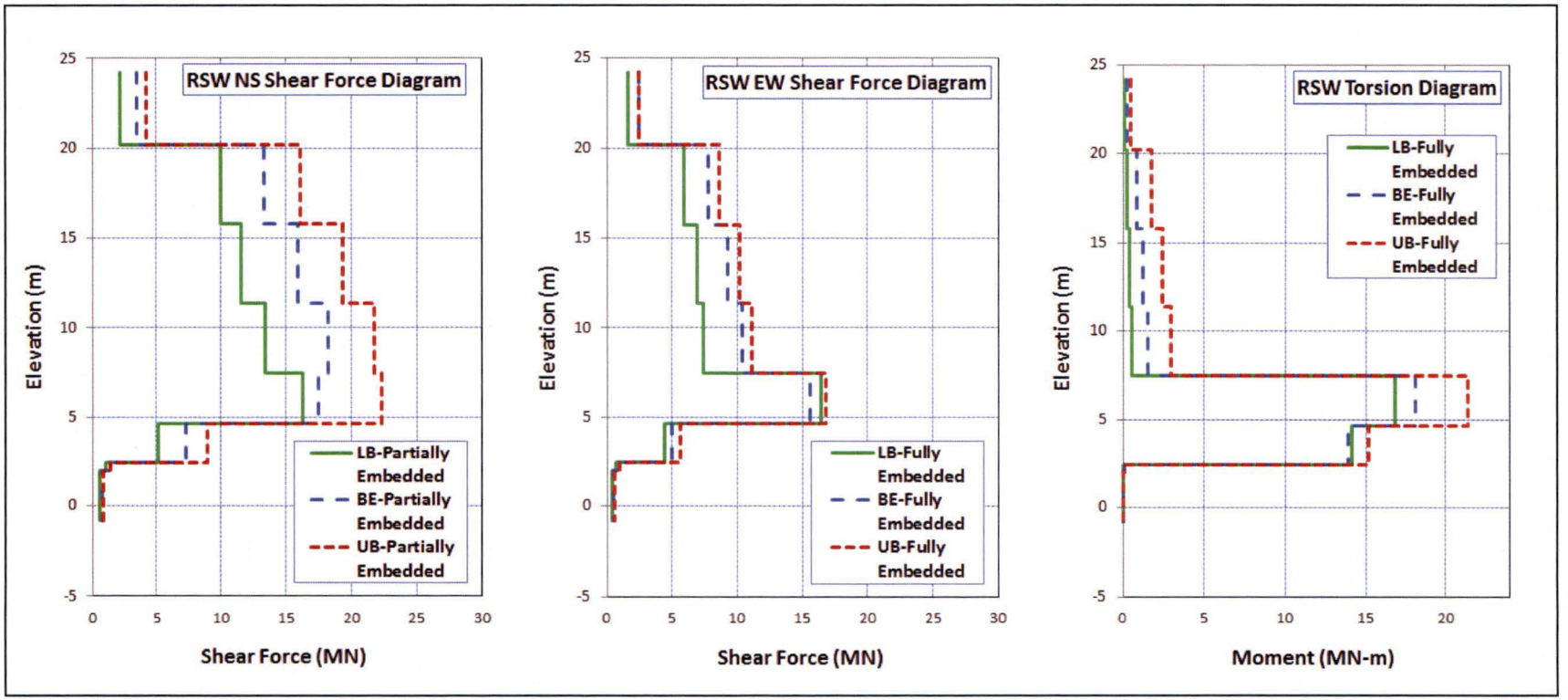

Figure 5.2-3e Maximum Shear Forces and Torsion Results from Analyses of Reactor Shield Wall PE Model

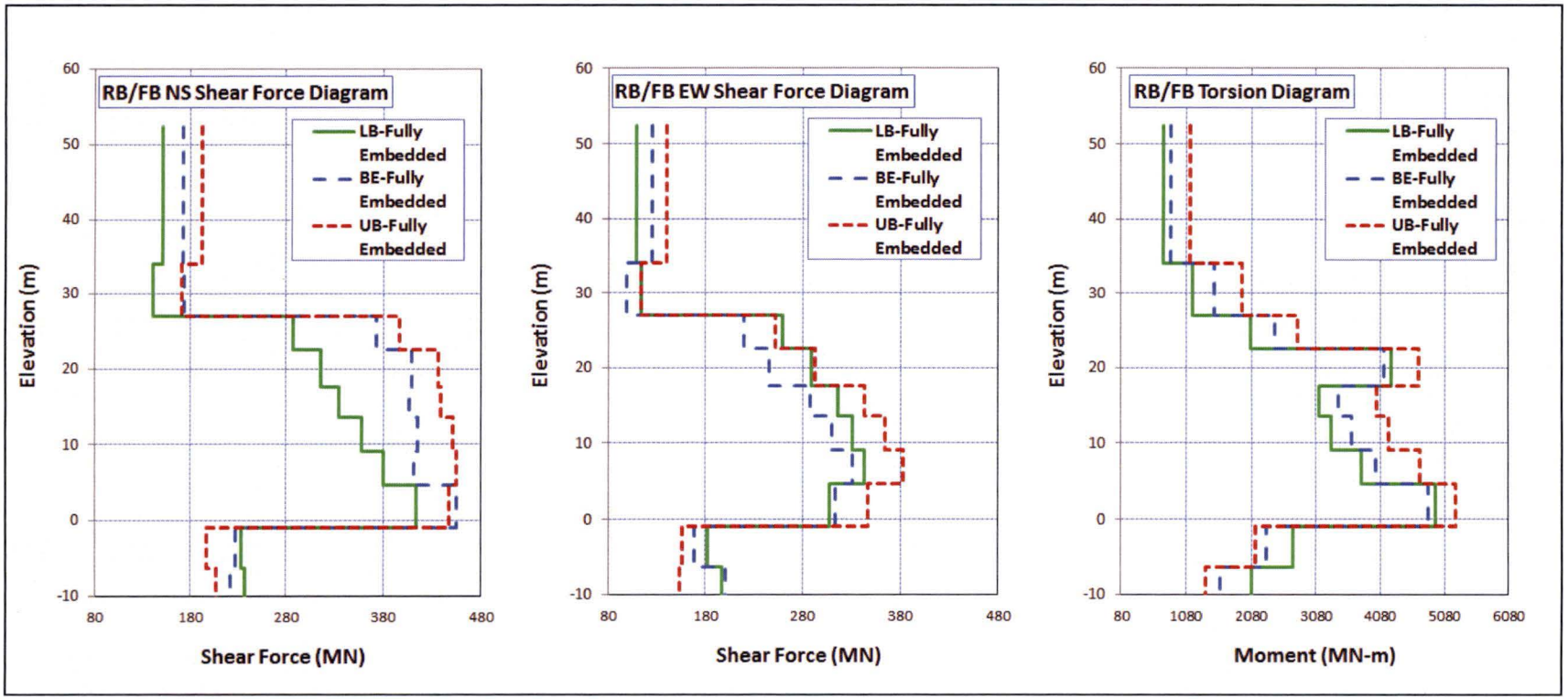

Figure 5.2-4a Maximum Shear Forces and Torsion Results from Analyses of RB/FB FE Model

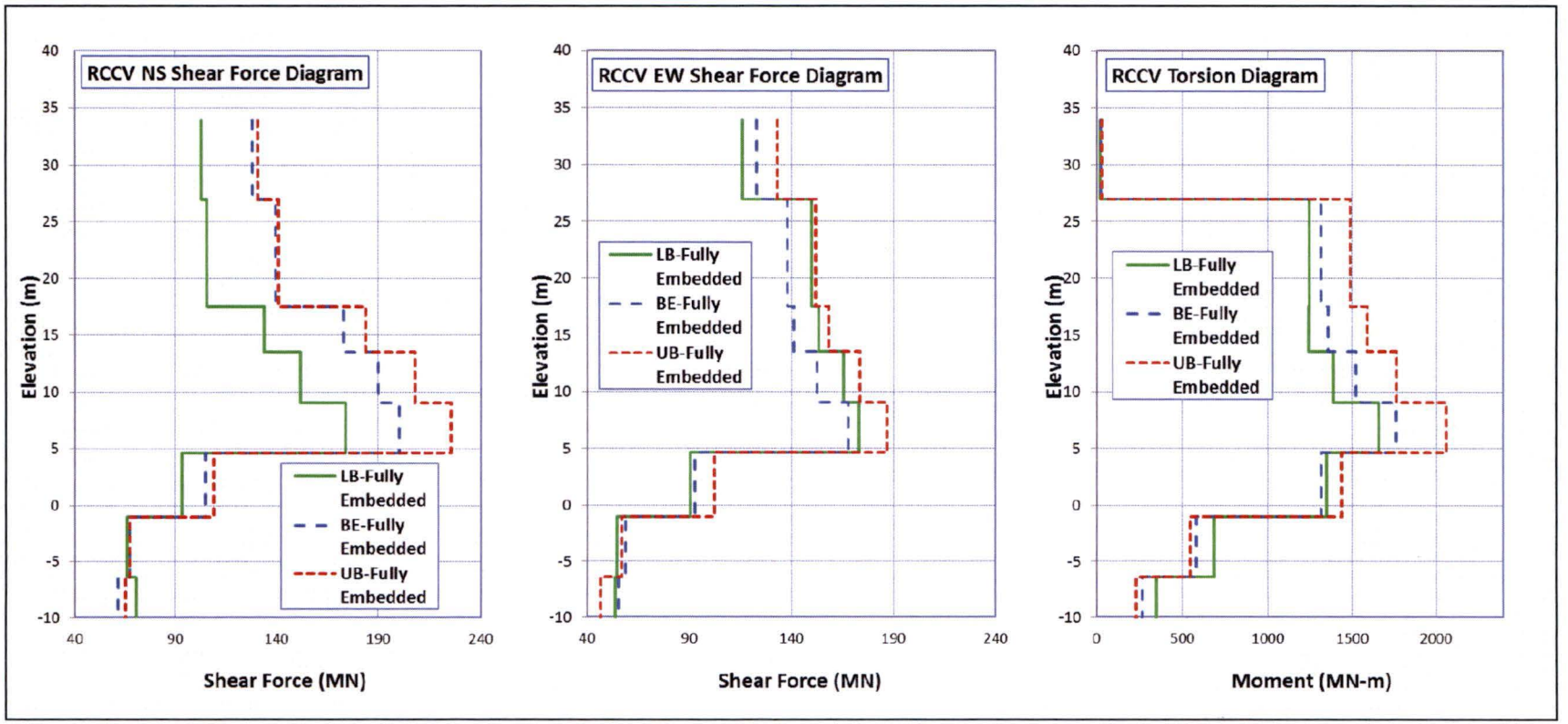

Figure 5.2-4b Maximum Shear Forces and Torsion Results from Analyses of RCCV FE Model

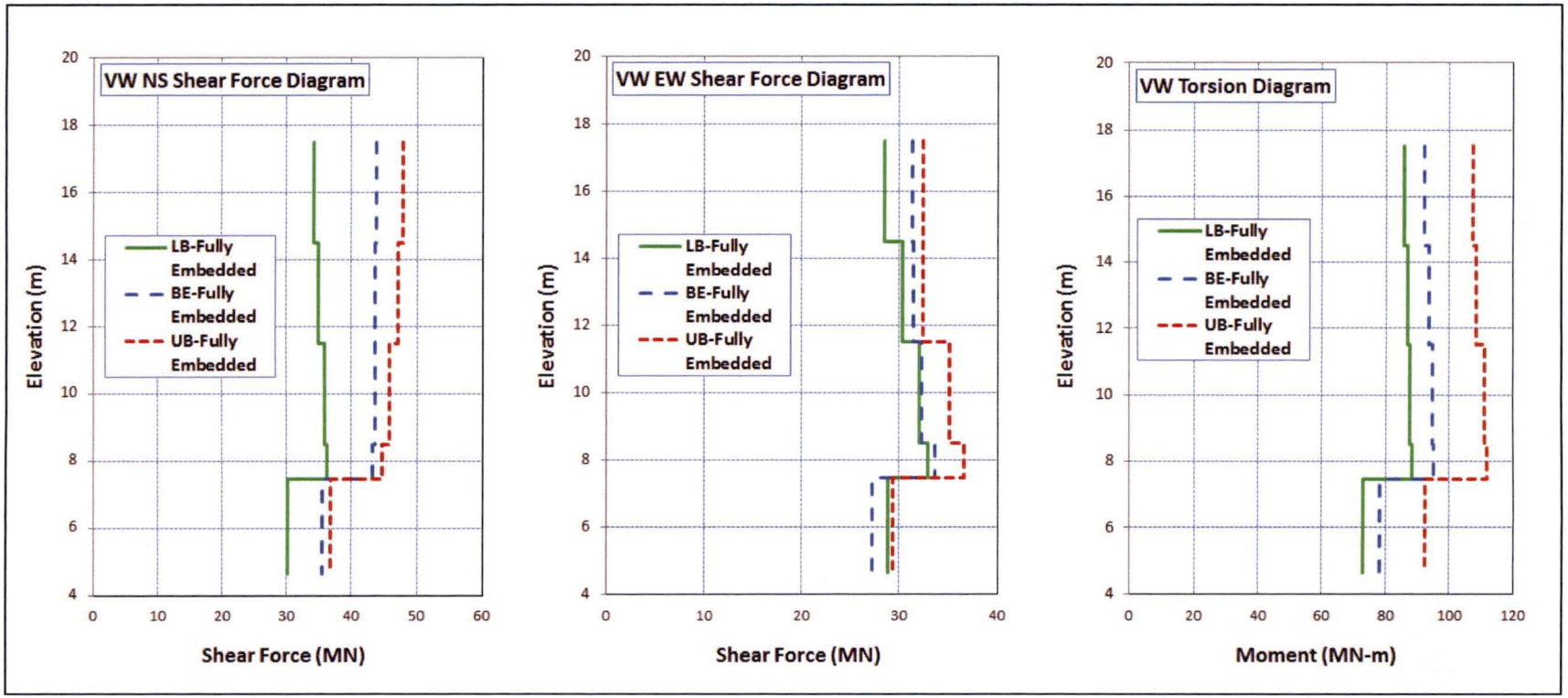

Figure 5.2-4c Maximum Shear Forces and Torsion Results from Analyses of Vent Wall FE Model

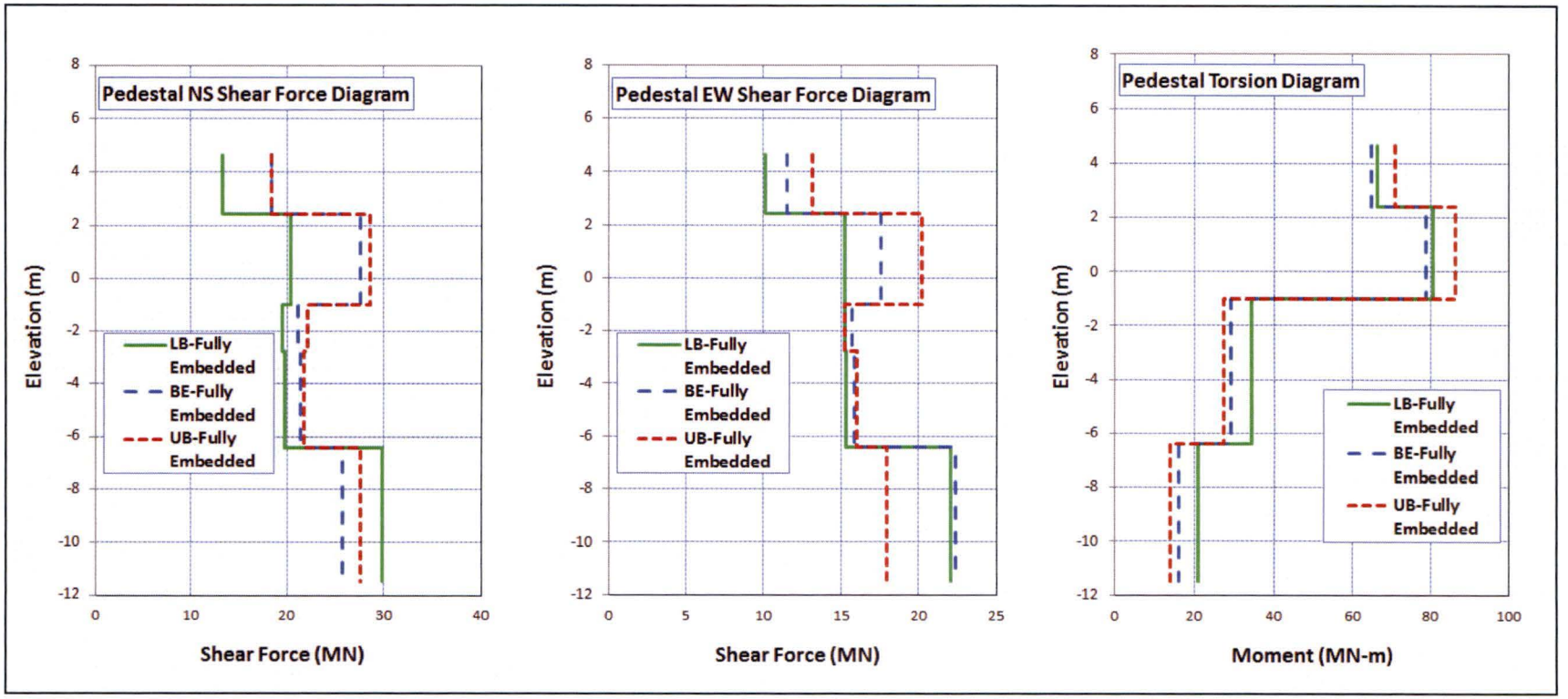

Figure 5.2-4d Maximum Shear Forces and Torsion Results from Analyses of Pedestal FE Model

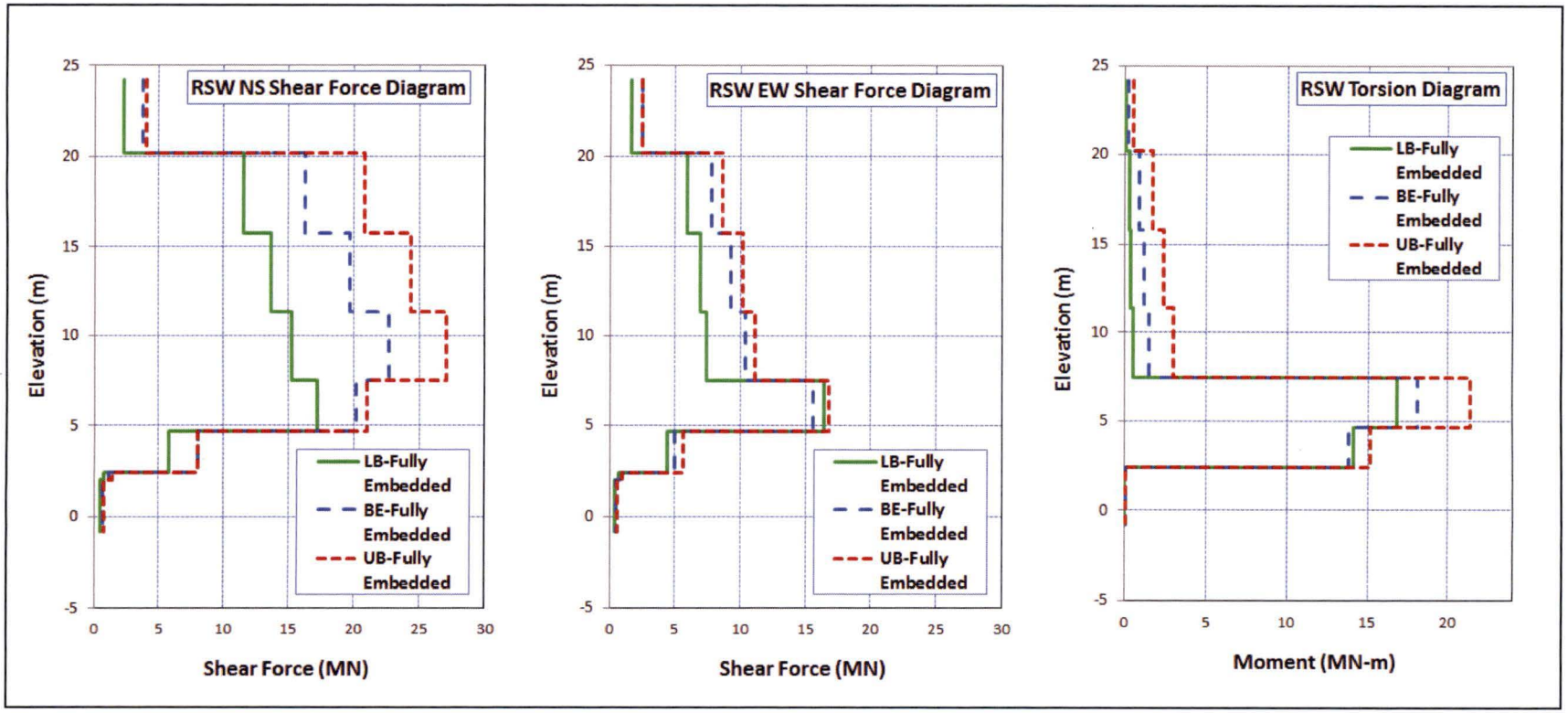

Figure 5.2-4e Maximum Shear Forces and Torsion Results from Analyses of Reactor Shield Wall FE Model

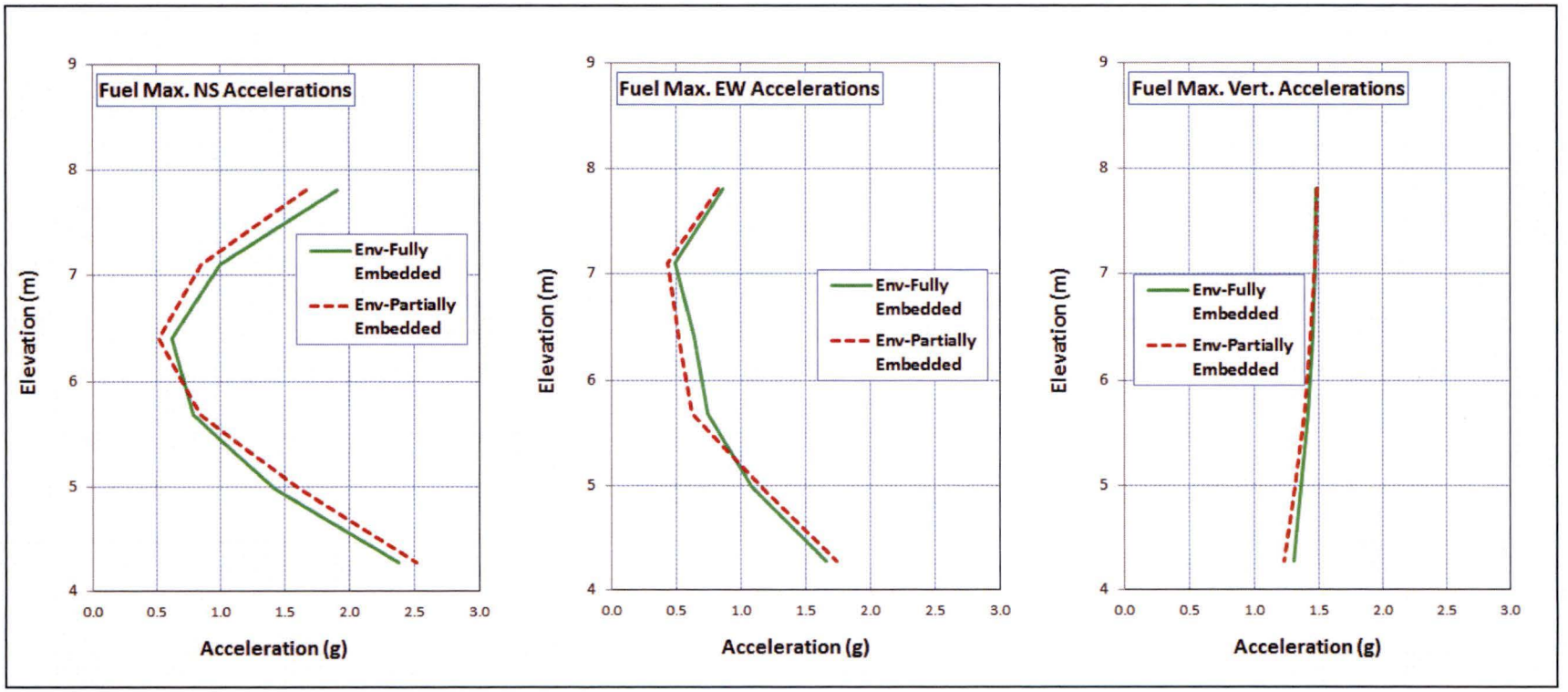

Figure 5.2-5a Effects of Embedment Configuration on Fuel Maximum Accelerations

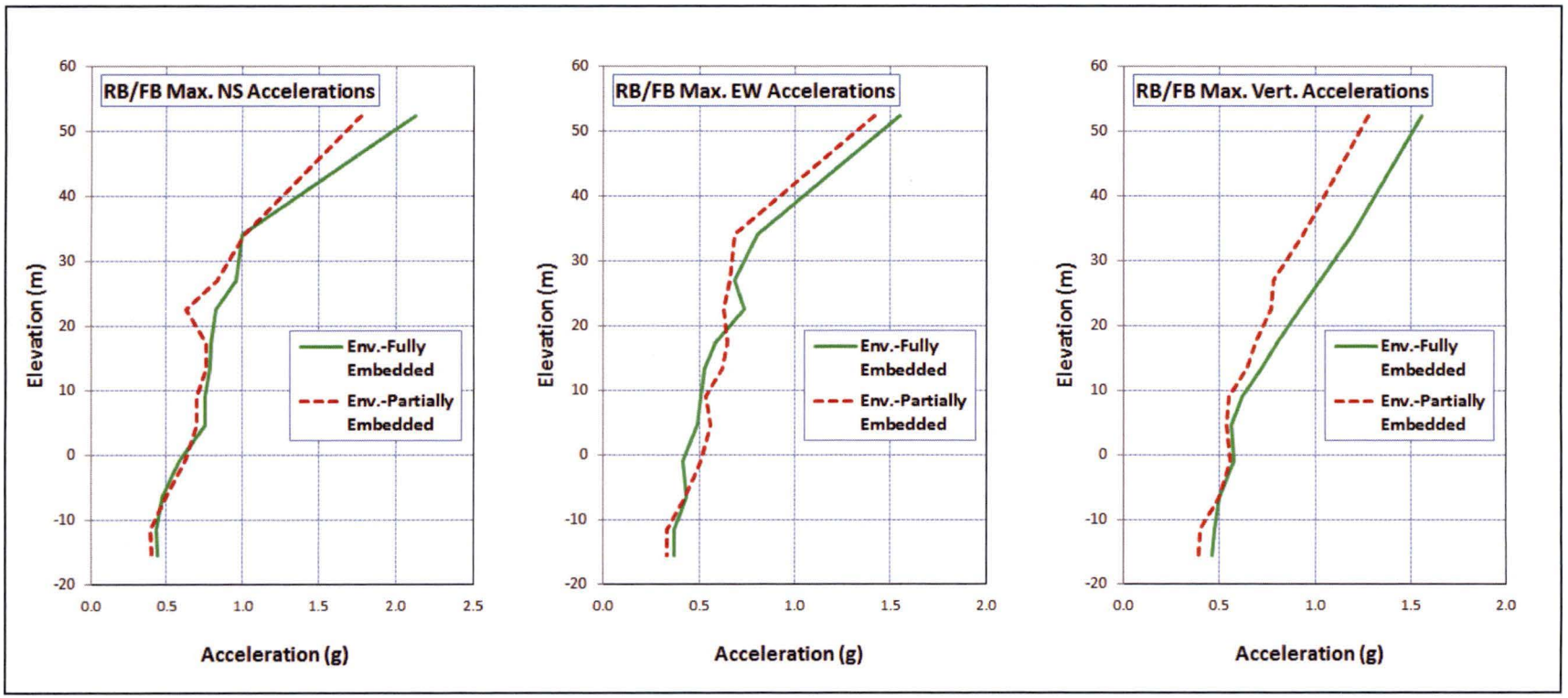

Figure 5.2-5b Effects of Embedment Configuration on RB/FB Maximum Accelerations

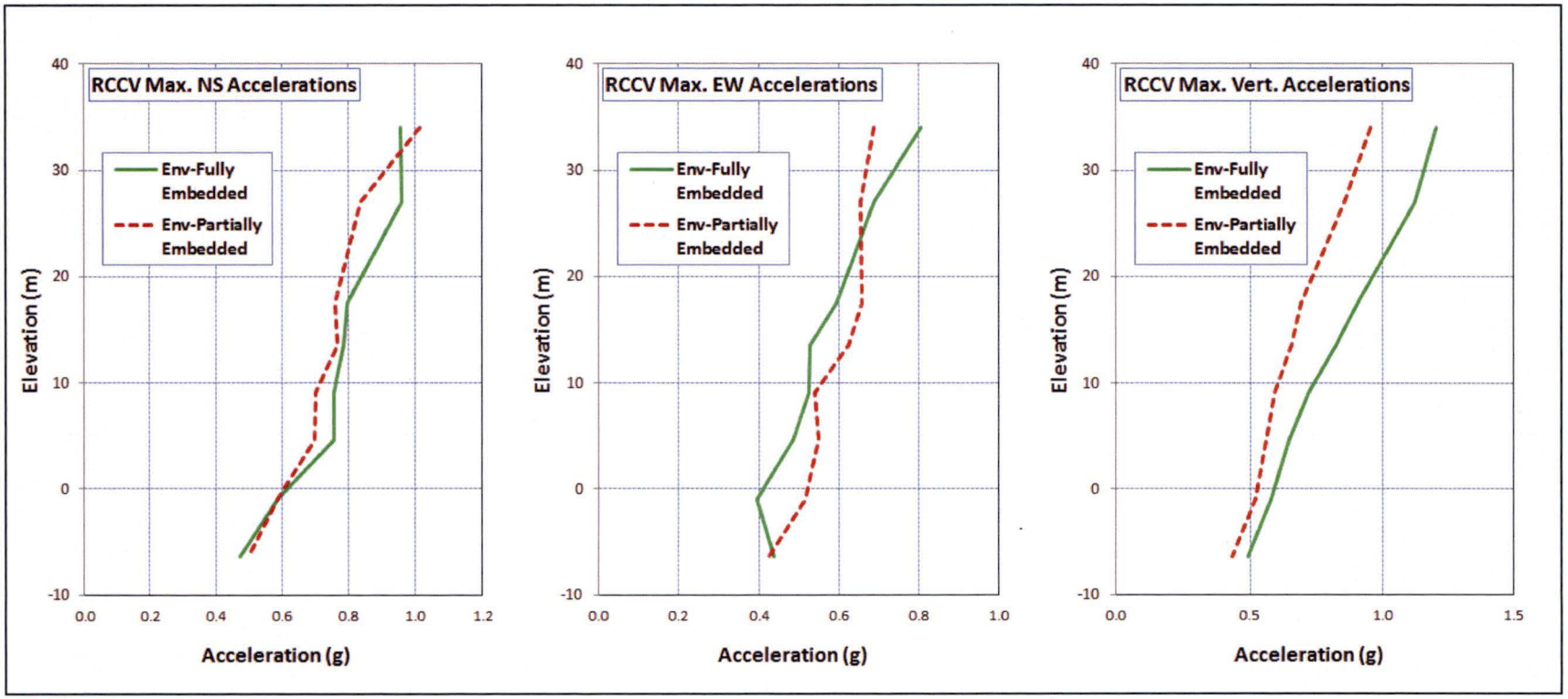

Figure 5.2-5c Effects of Embedment Configuration on RCCV Maximum Accelerations

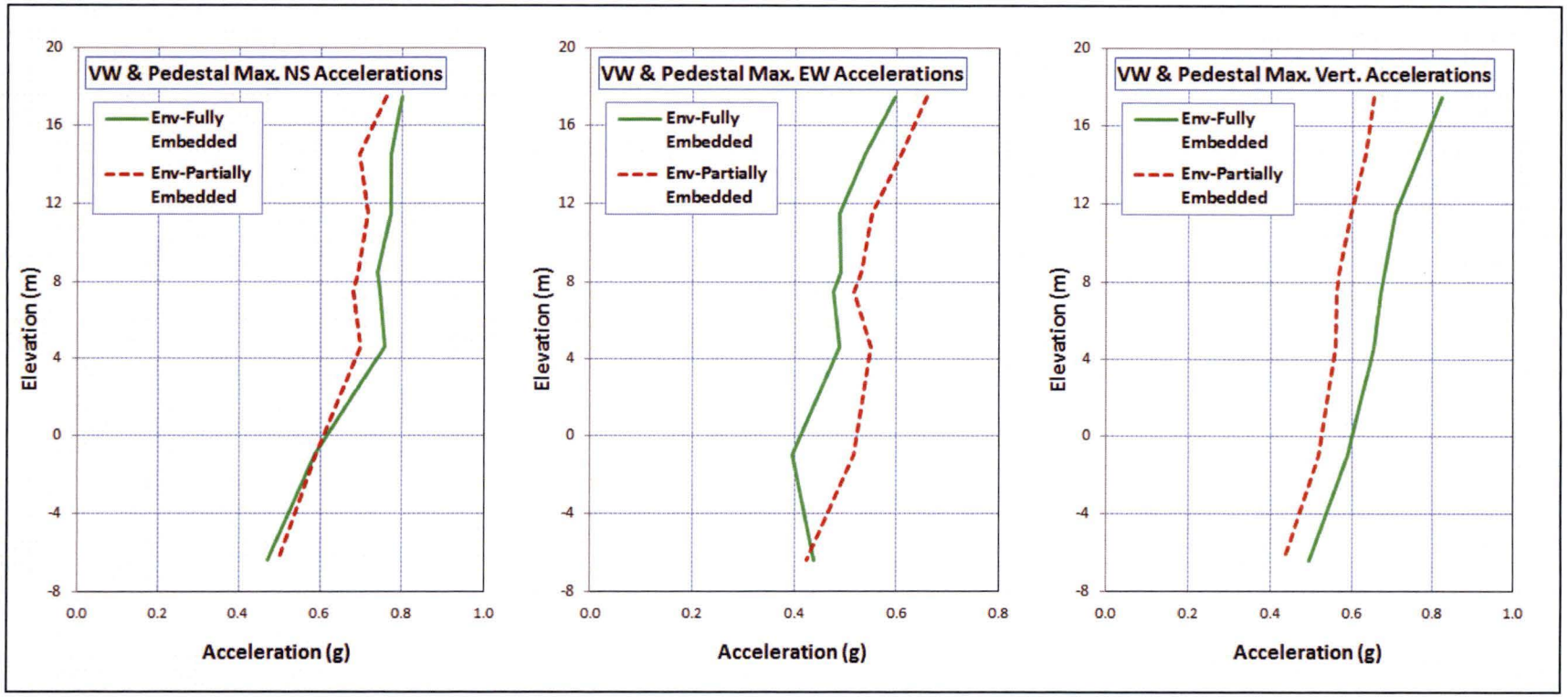

Figure 5.2-5d Effects of Embedment Configuration on Vent Wall/Pedestal Maximum Accelerations

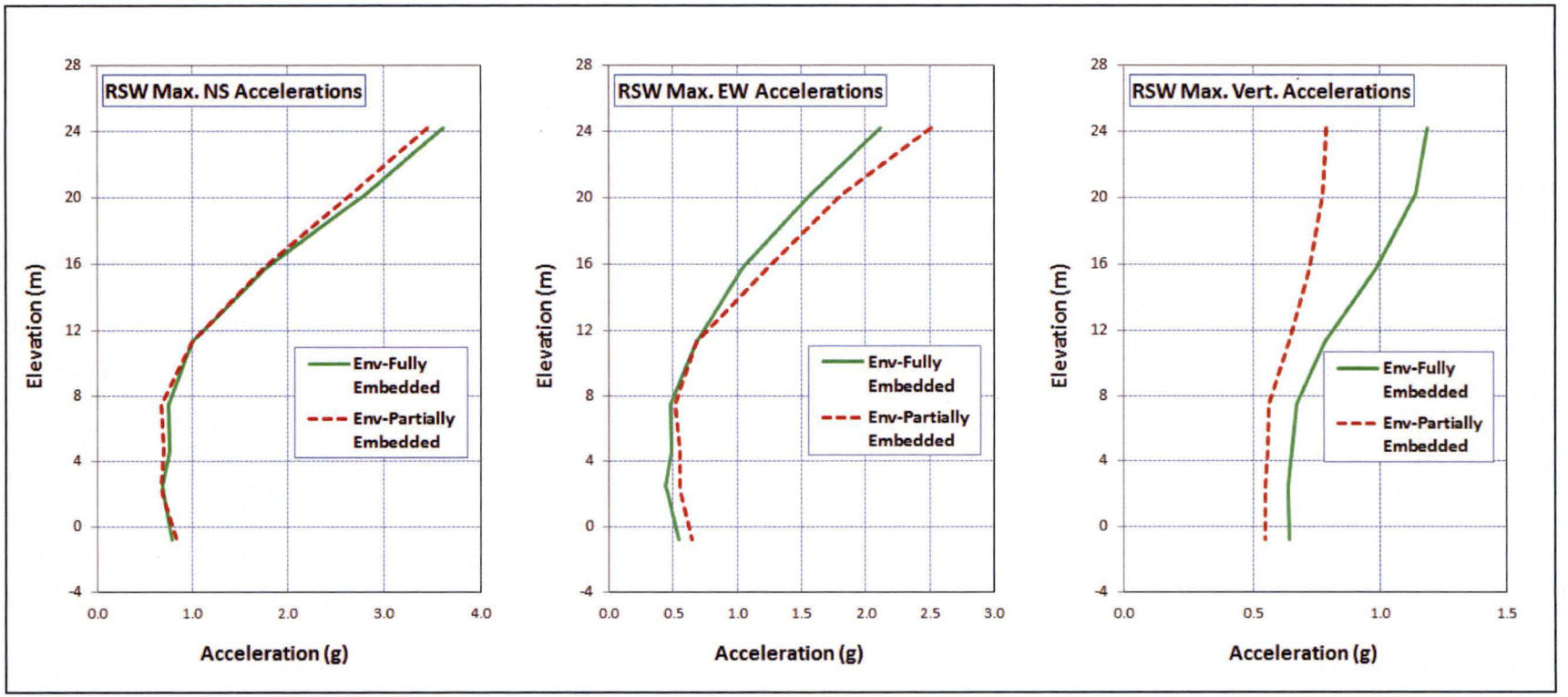

Figure 5.2-5e Effects of Embedment Configuration on Reactor Shield Wall Maximum Accelerations

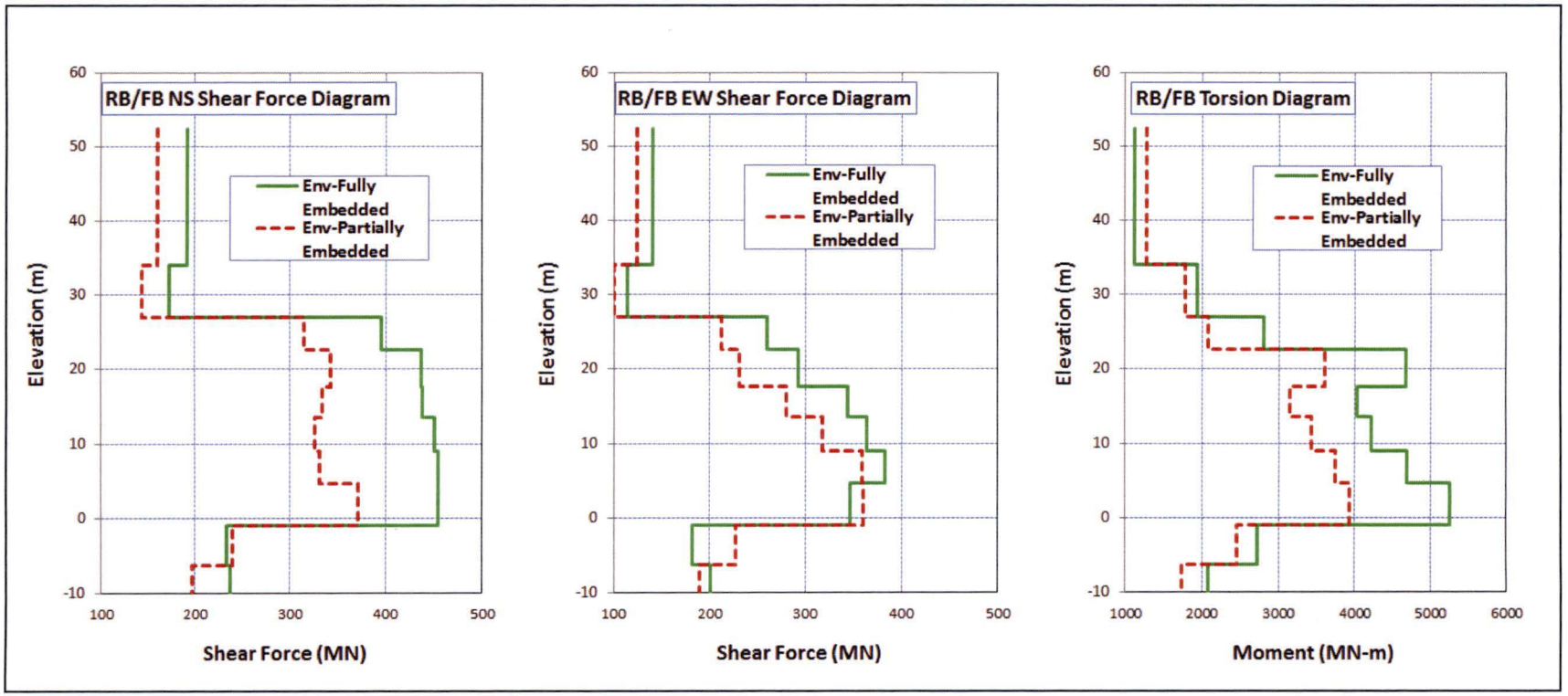

Figure 5.2-6a Effects of Embedment Configuration on RB/FB Maximum Force Results

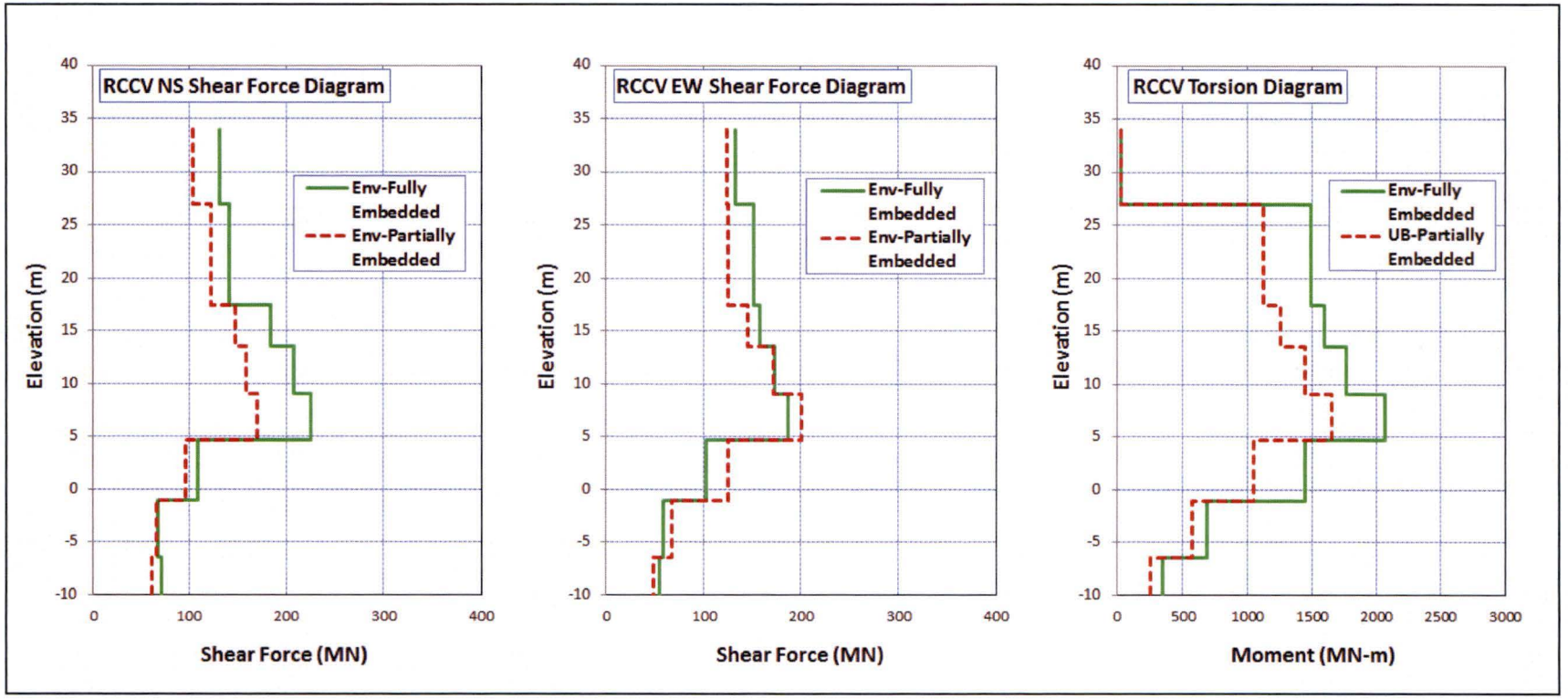

Figure 5.2-6b Effects of Embedment Configuration on RCCV Maximum Force Results

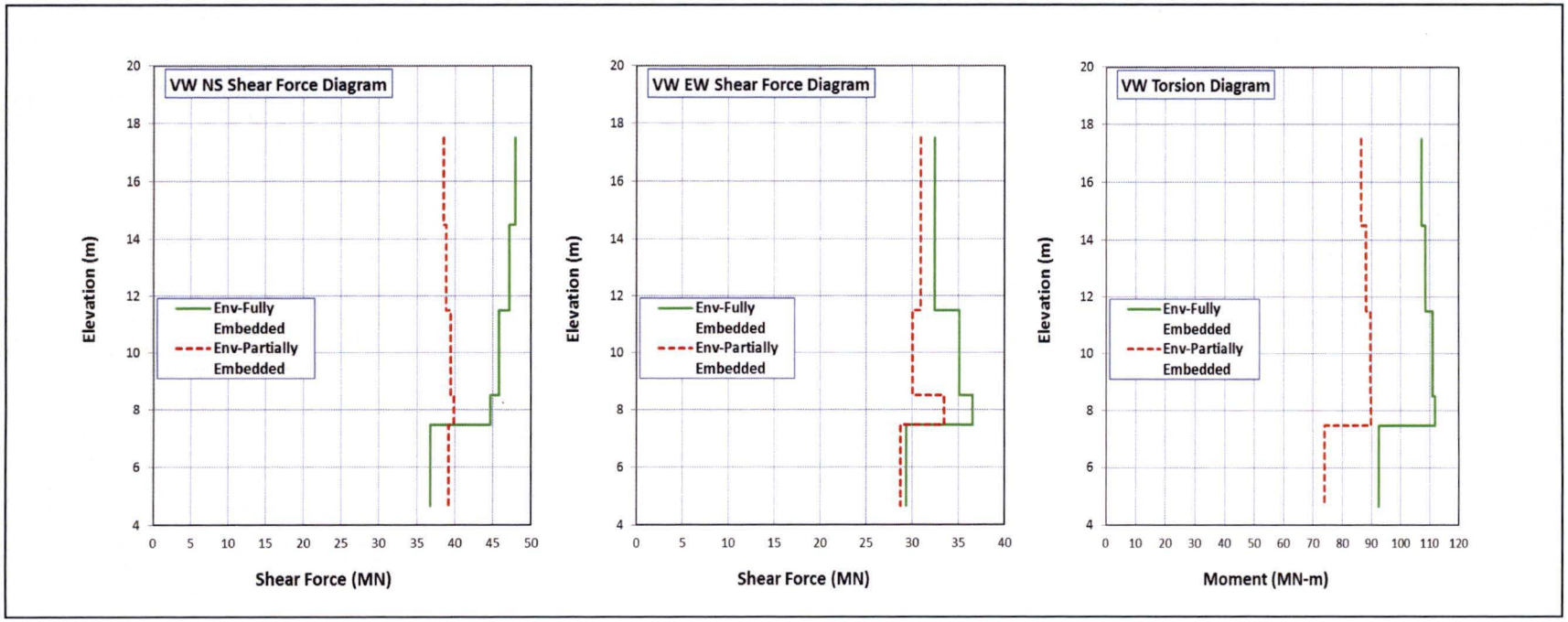

Figure 5.2-6c Effects of Embedment Configuration on Vent Wall Maximum Force Results

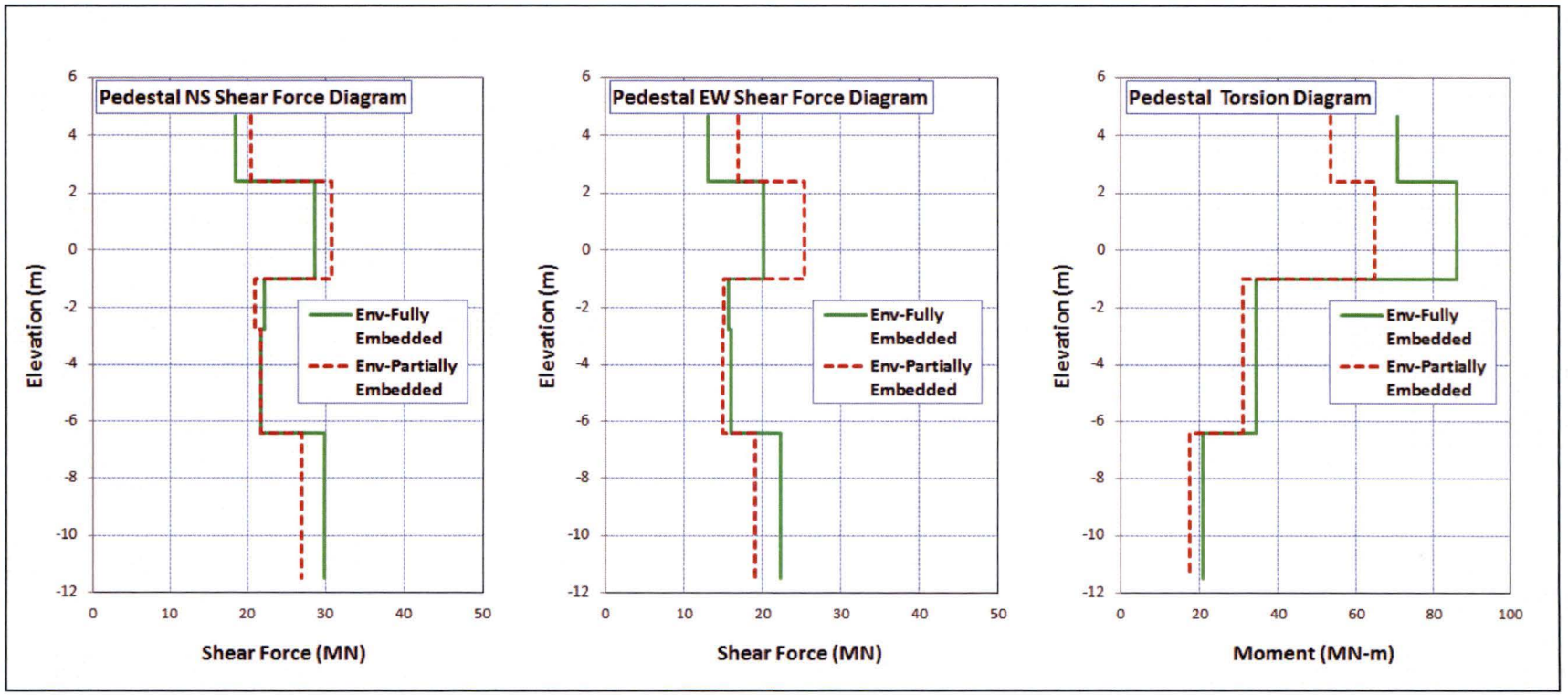

Figure 5.2-6d Effects of Embedment Configuration on Pedestal Maximum Force Results

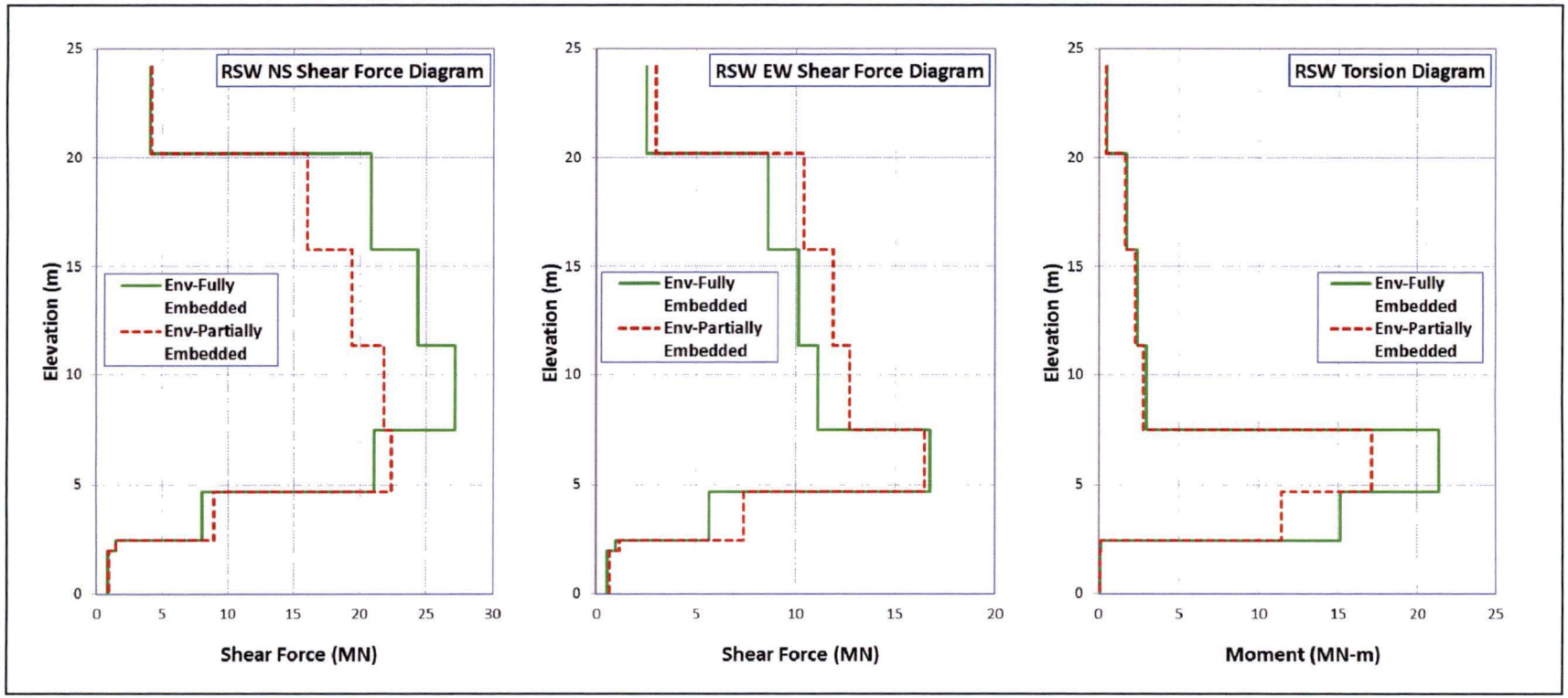

Figure 5.2-6e Effects of Embedment Configuration on Reactor Shield Wall Maximum Force Results

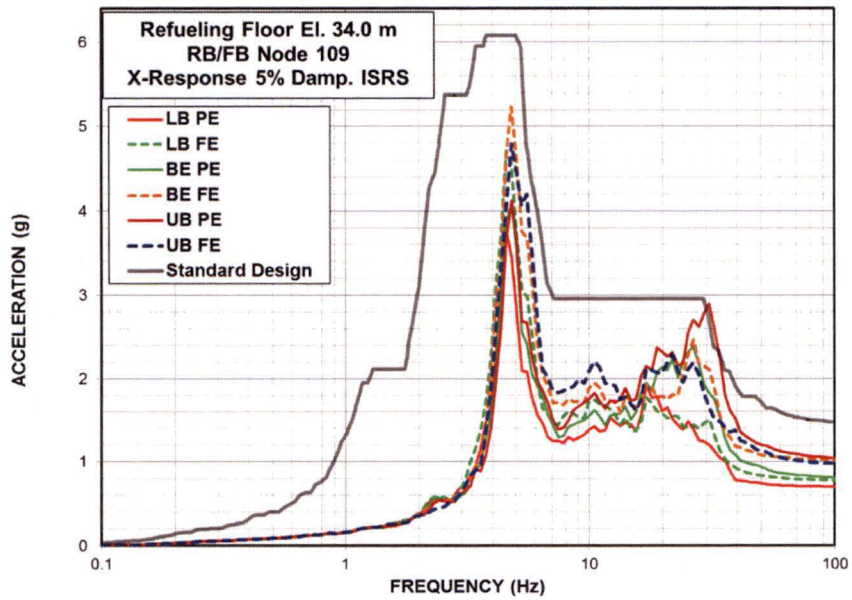

Figure 5.3-1a Comparison of ISRS – RB/FB Refueling Floor in X-Direction

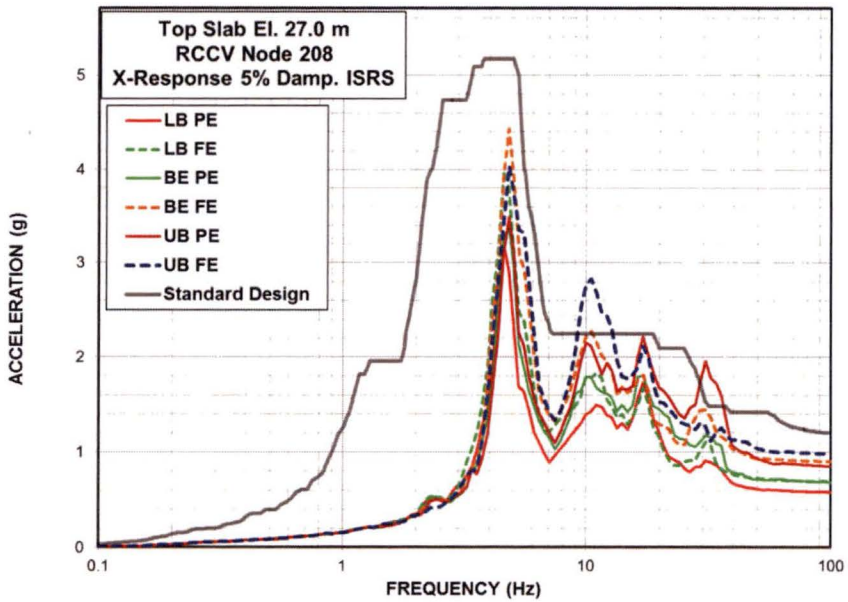

Figure 5.3-1b Comparison of ISRS - RCCV Top Slab in X-Direction

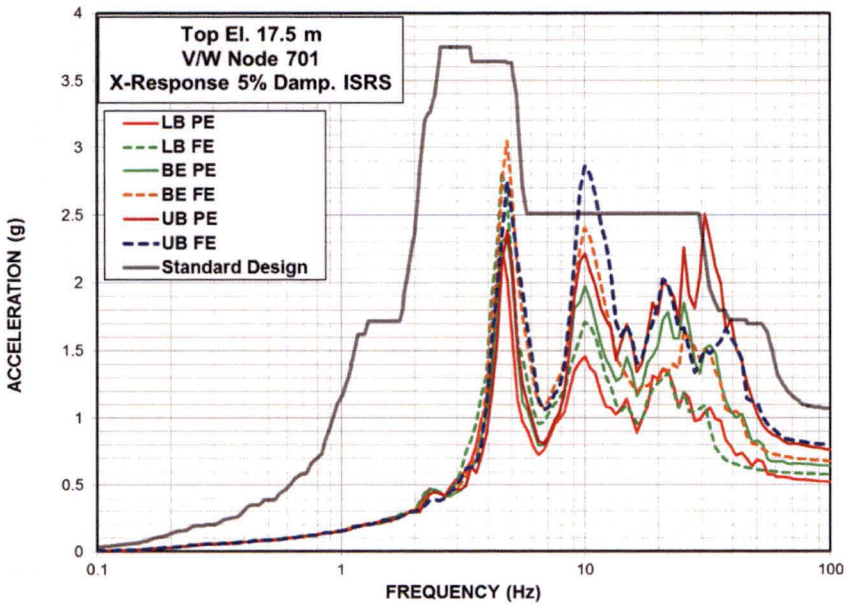

Figure 5.3-1c Comparison of ISRS - Vent Wall Top in X-Direction

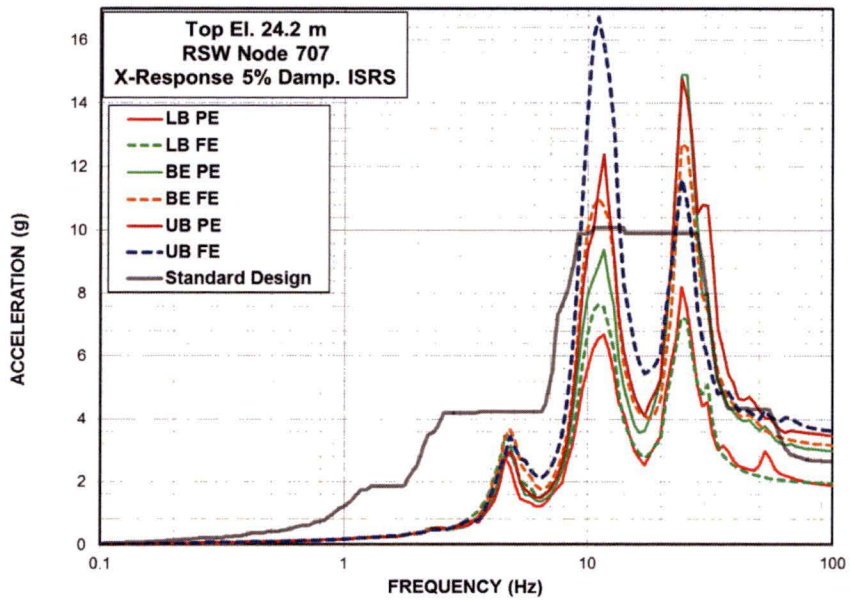

Figure 5.3-1d Comparison of ISRS - RSW Top in X-Direction

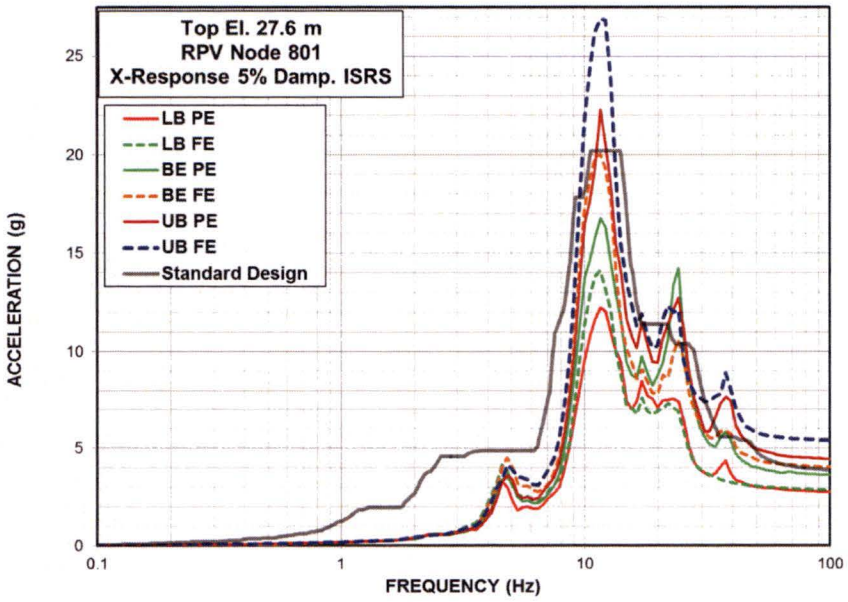

Figure 5.3-1e Comparison of ISRS - RPV Top in X-Direction

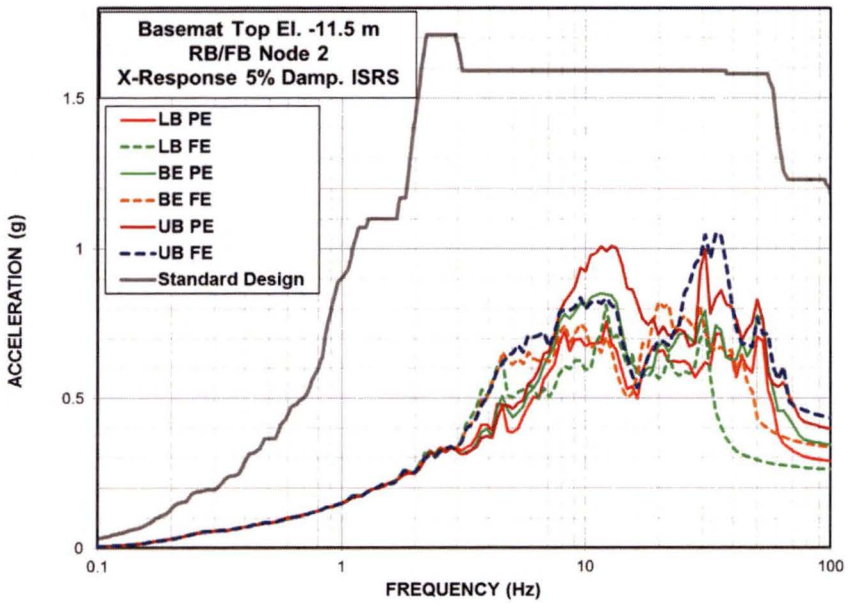

Figure 5.3-1f Comparison of ISRS - RB/FB Basemat in X-Direction

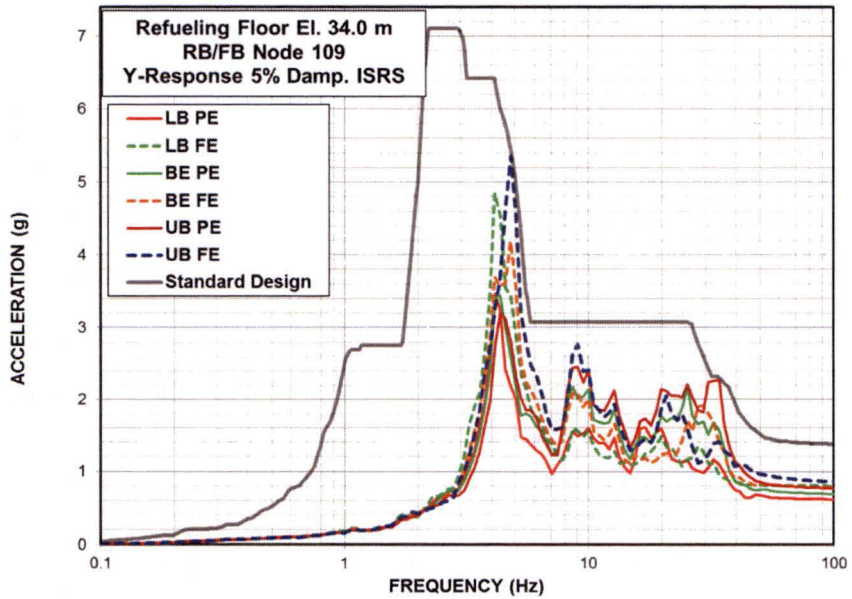

Figure 5.3-2a Comparison of ISRS - RB/FB Refueling Floor in Y-Direction

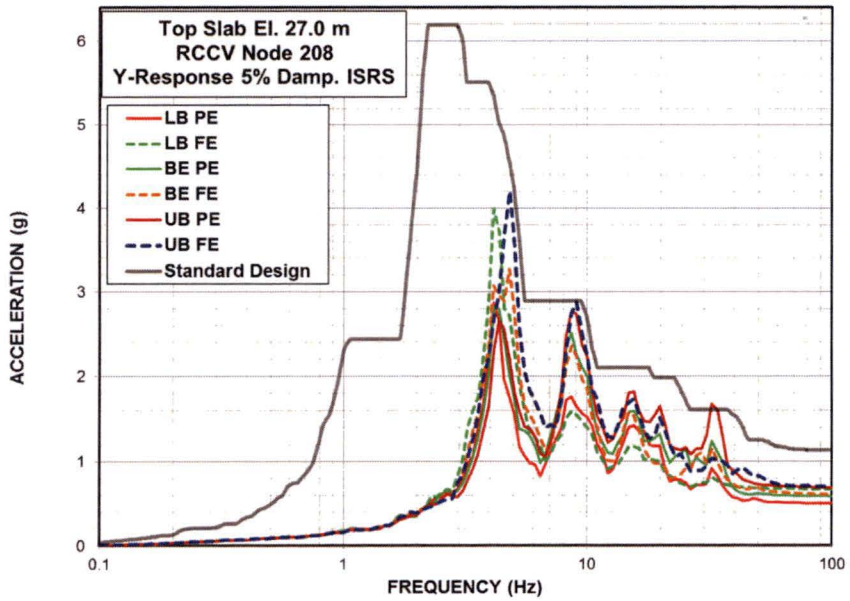

Figure 5.3-2b Comparison of ISRS - RCCV Top Slab in Y-Direction

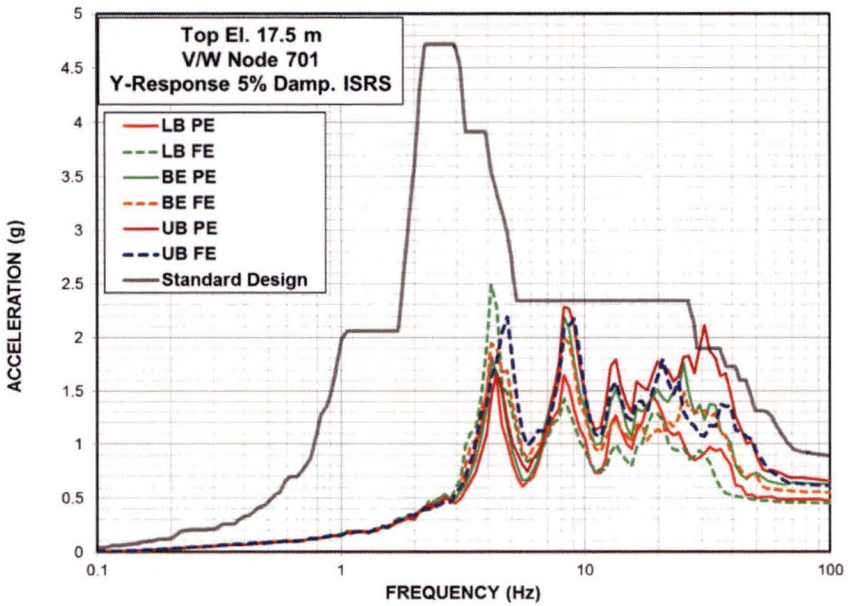

Figure 5.3-2c Comparison of ISRS - Vent Wall Top in Y-Direction

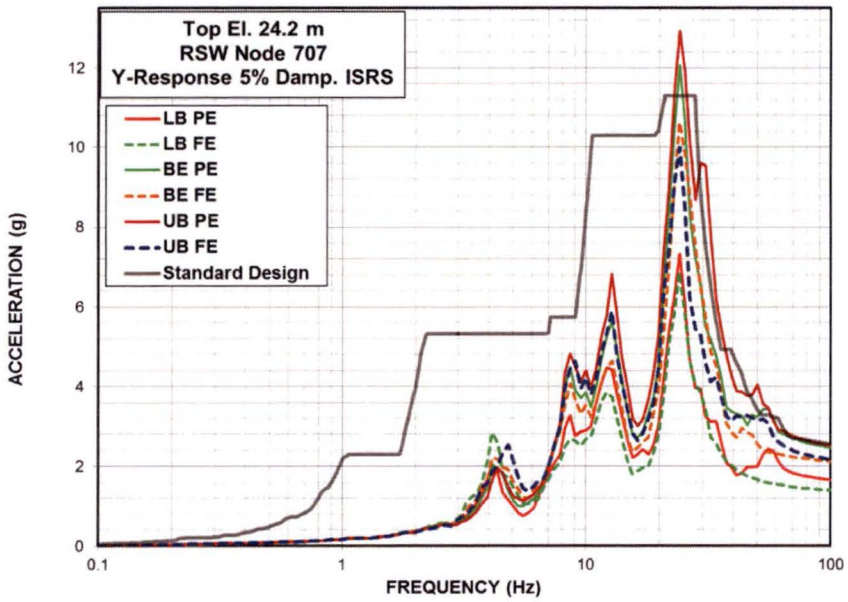

Figure 5.3-2d Comparison of ISRS - RSW Top in Y-Direction

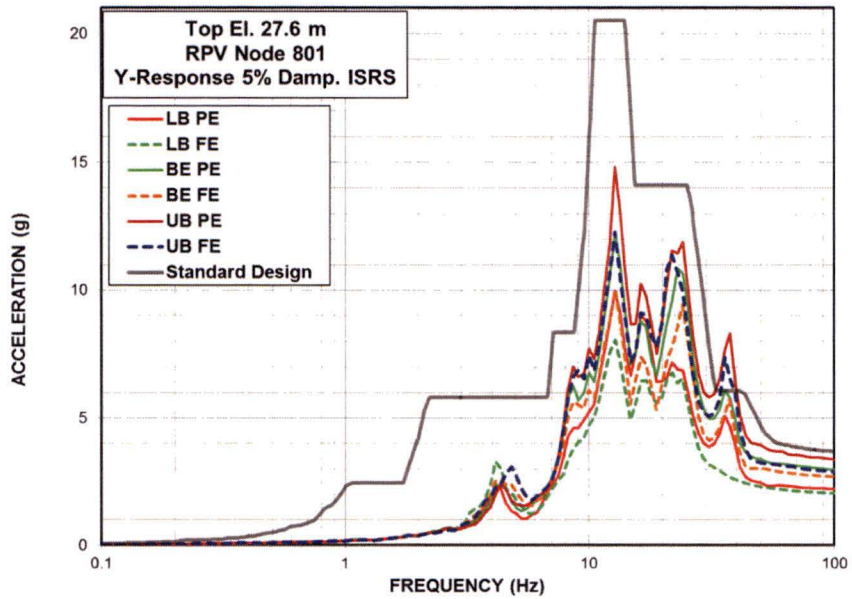

Figure 5.3-2e Comparison of ISRS - RPV Top in Y-Direction

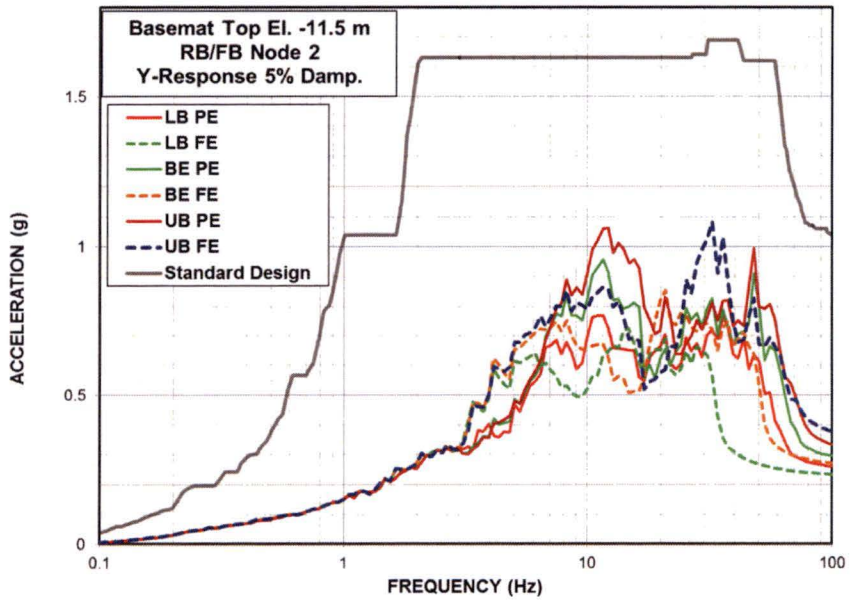

Figure 5.3-2f Comparison of ISRS - RB/FB Basemat in Y-Direction

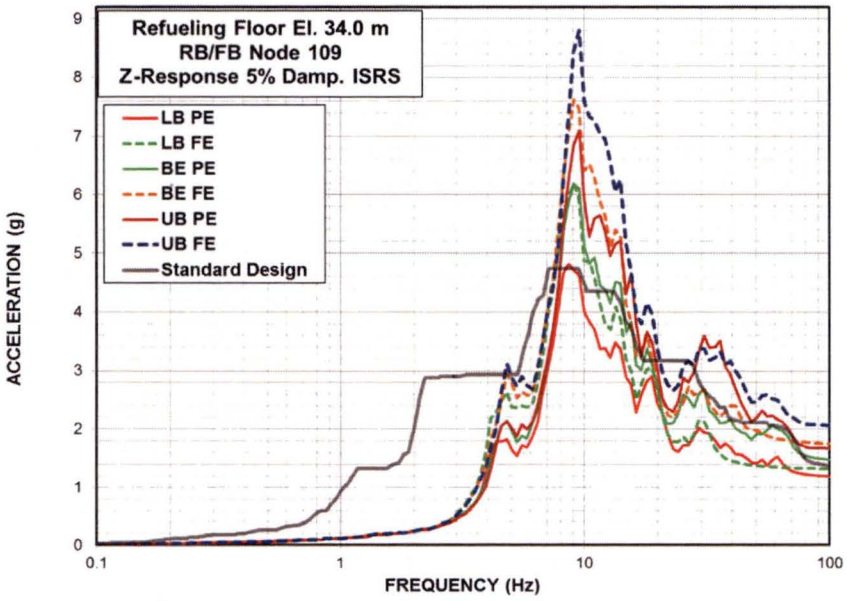

Figure 5.3-3a Comparison of ISRS - RB/FB Refueling Floor in Z-Direction

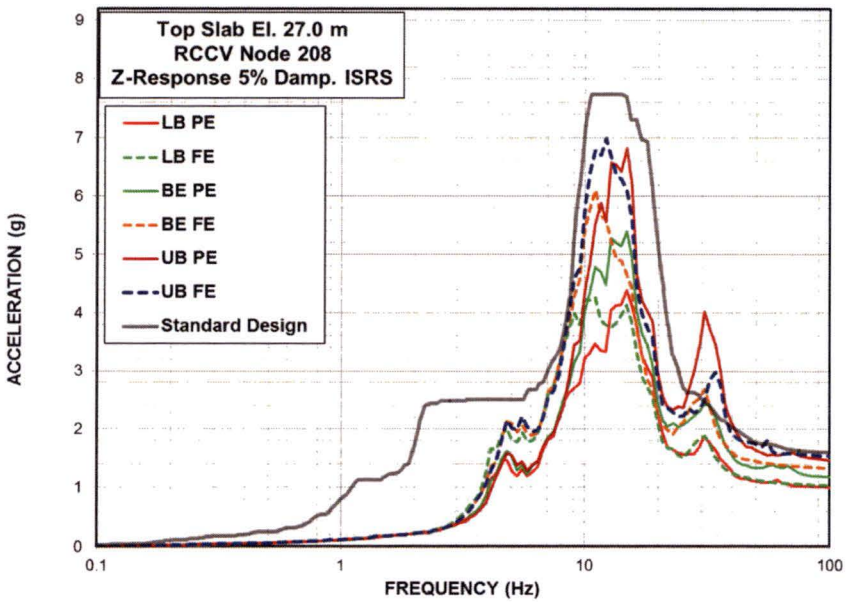

Figure 5.3-3b Comparison of ISRS - RCCV Top Slab in Z-Direction

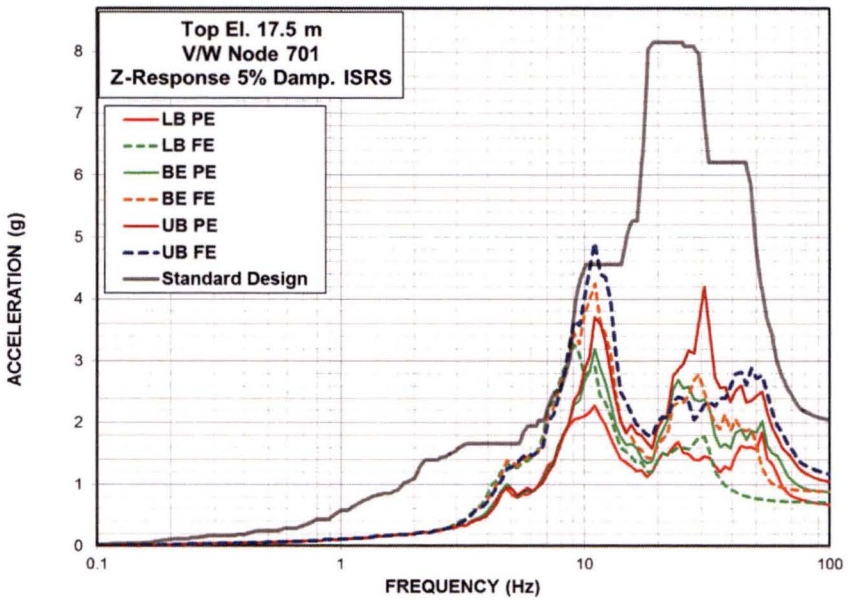

Figure 5.3-3c Comparison of ISRS - Vent Wall Top in Z-Direction

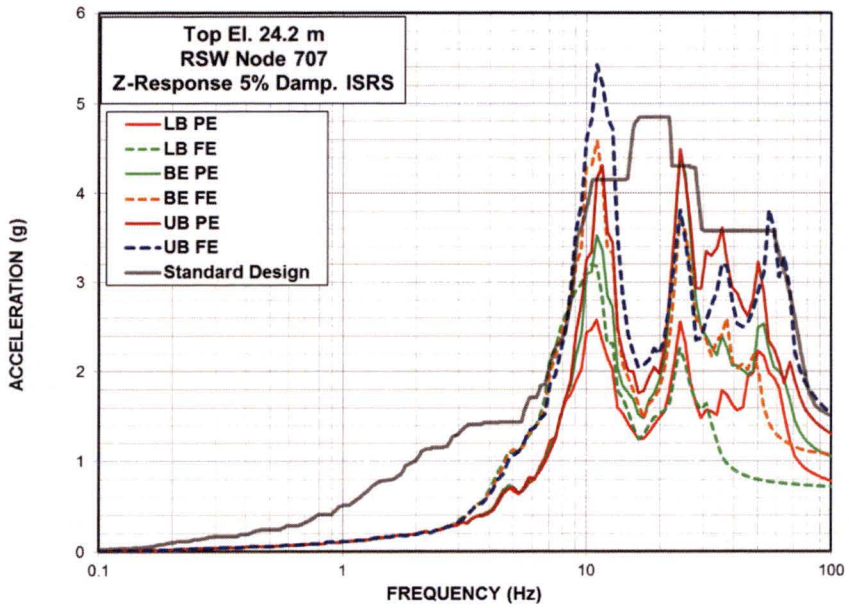

Figure 5.3-3d Comparison of ISRS - RSW Top in Z-Direction

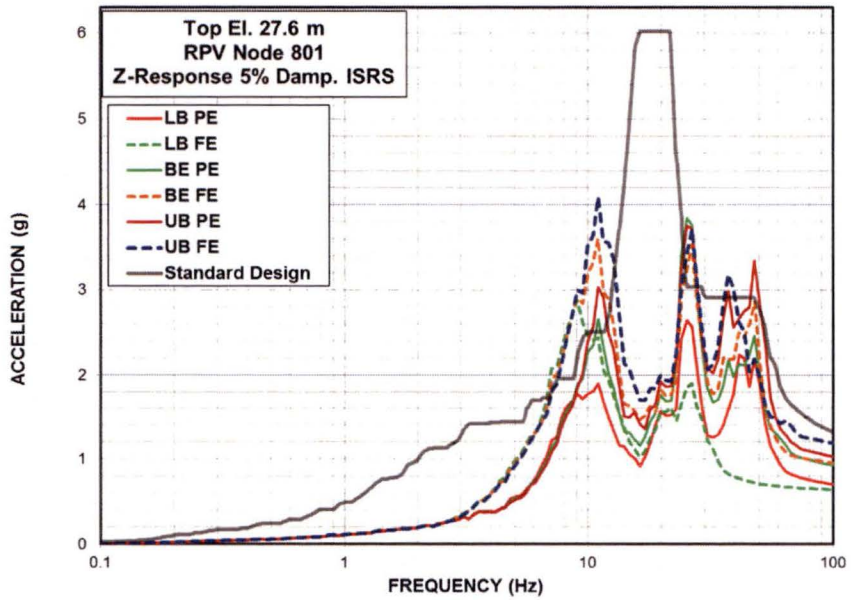

Figure 5.3-3e Comparison of ISRS - RPV Top in Z-Direction

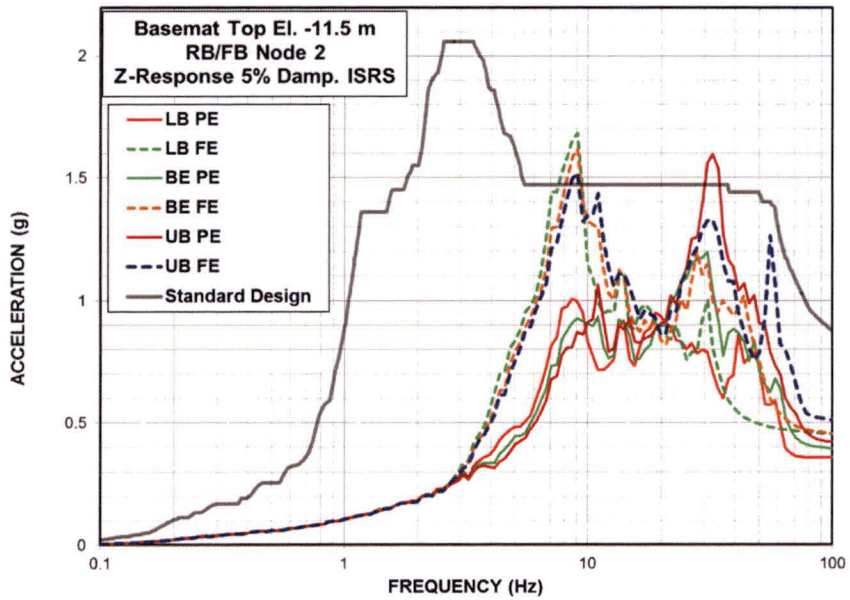

Figure 5.3-3f Comparison of ISRS - RB/FB Basemat in Z-Direction

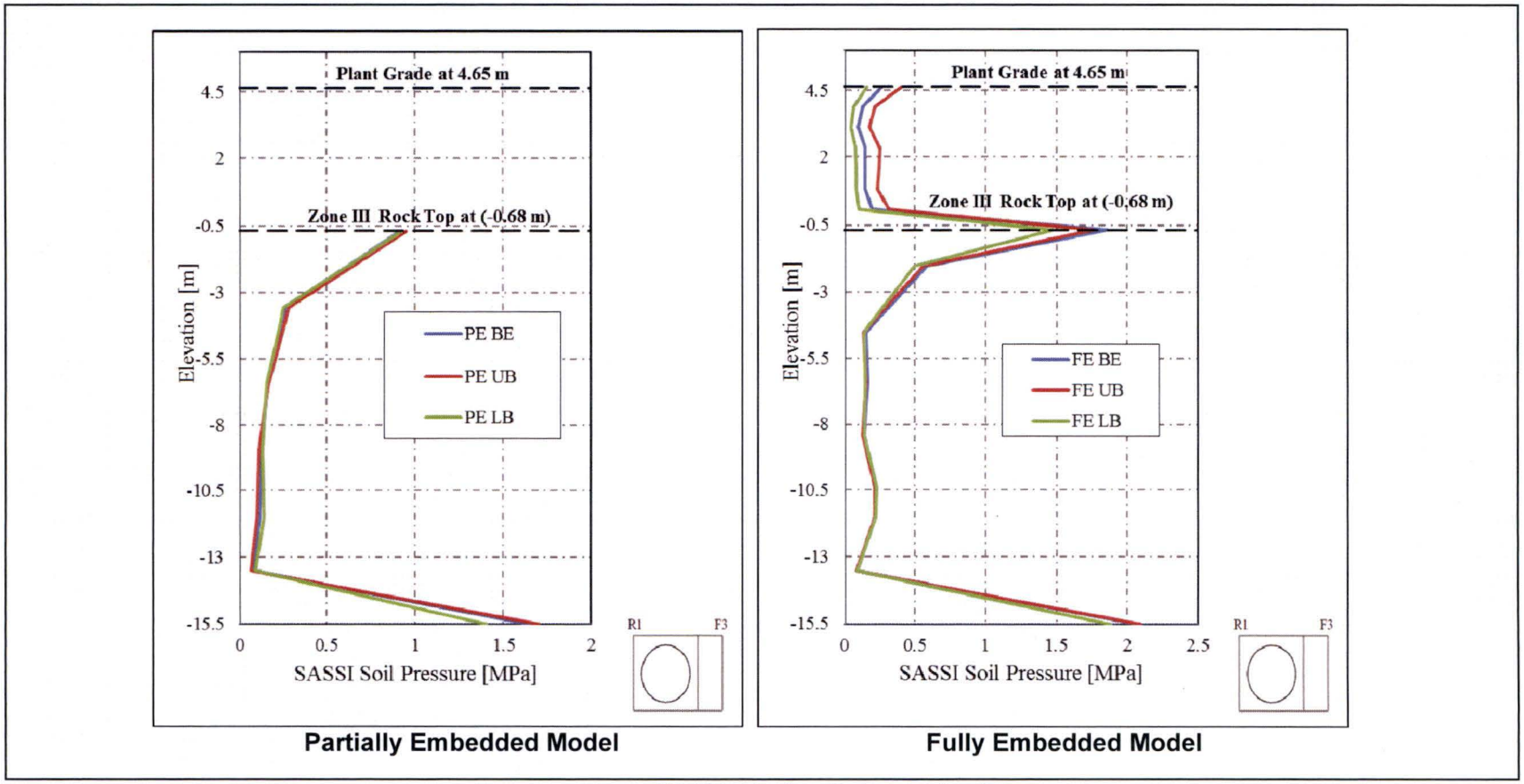

a) RB/FB Wall at Column Line R1

Figure 5.5-1 Dynamic Lateral Pressures on Below-Grade Exterior Walls

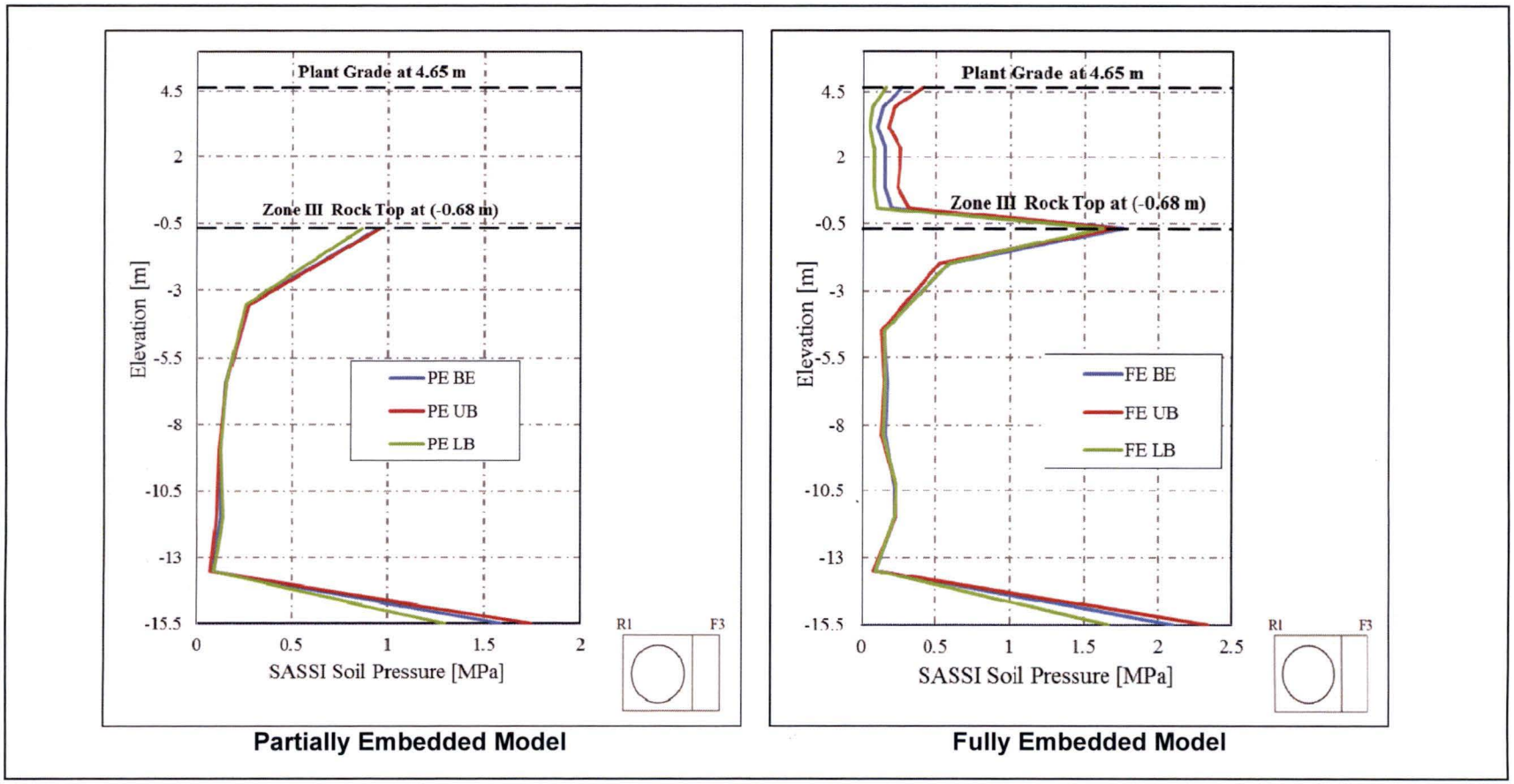

b) RB/FB Wall at Column Line F3

Figure 5.5-1 Dynamic Lateral Pressures on Below-Grade Exterior Walls (Continued)

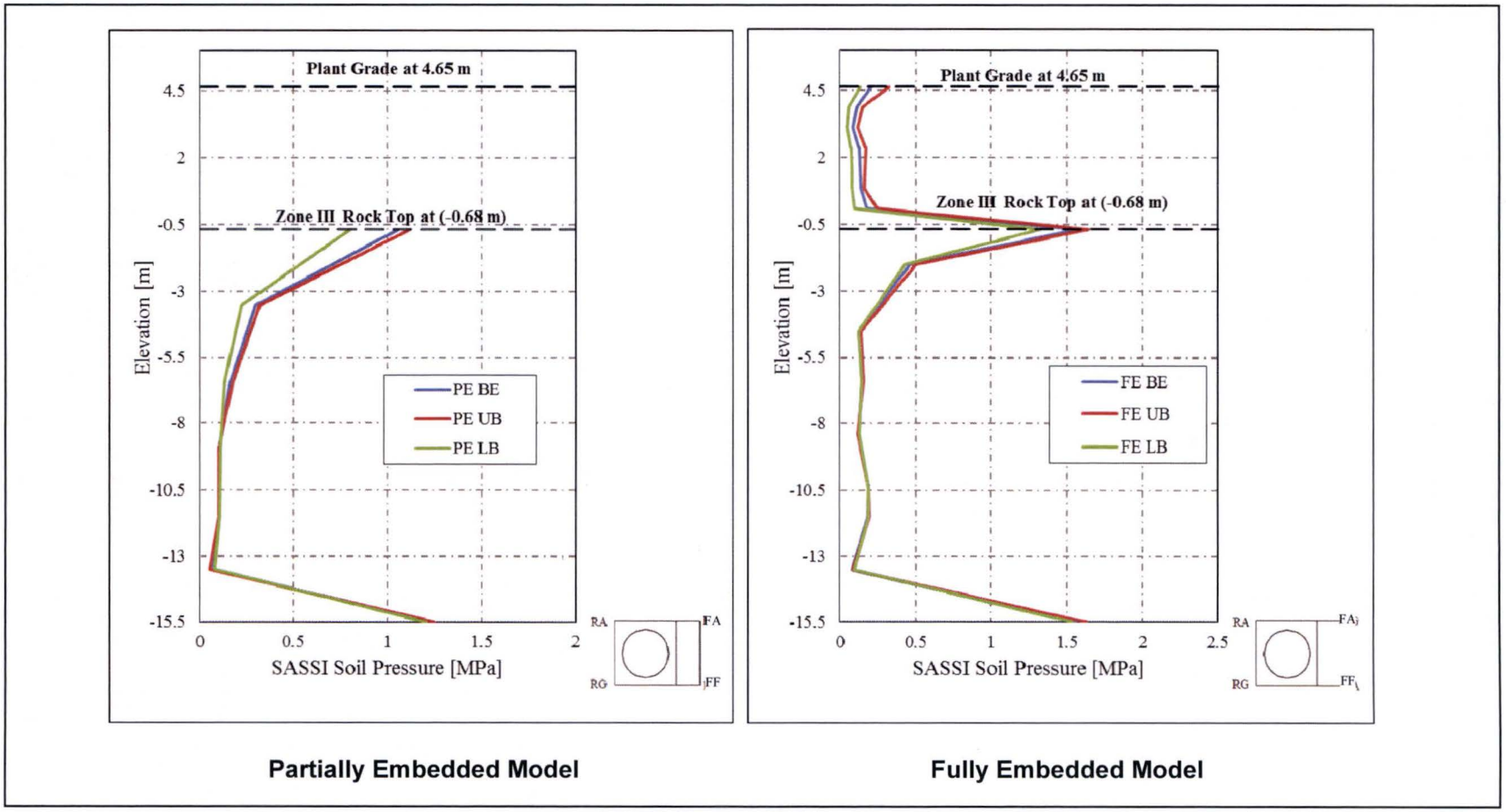

Partially Embedded Model **Fully Embedded Model**

c) RB/FB Wall at Column Lines RA and FA

Figure 5.5-1 Dynamic Lateral Pressures on Below-Grade Exterior Walls (Continued)

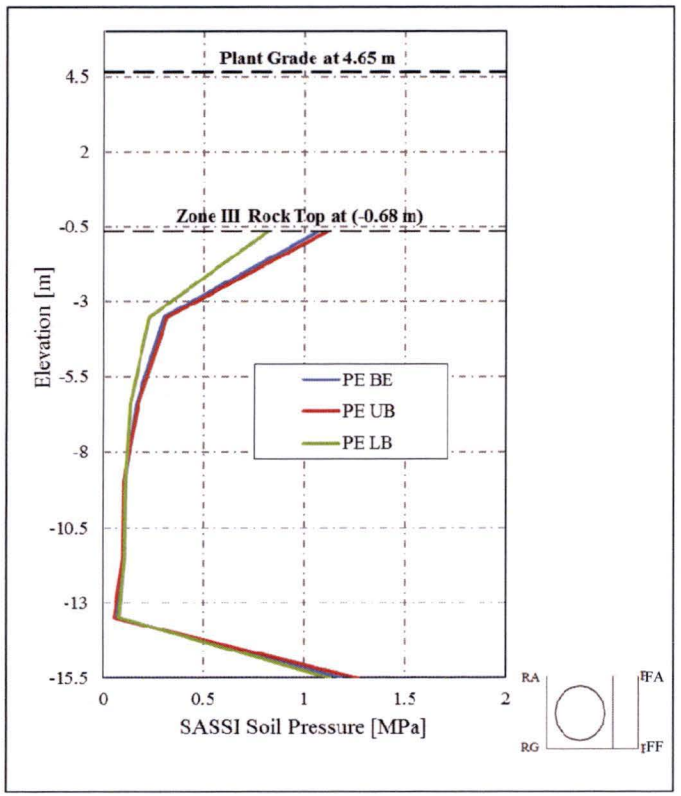

Partially Embedded Model

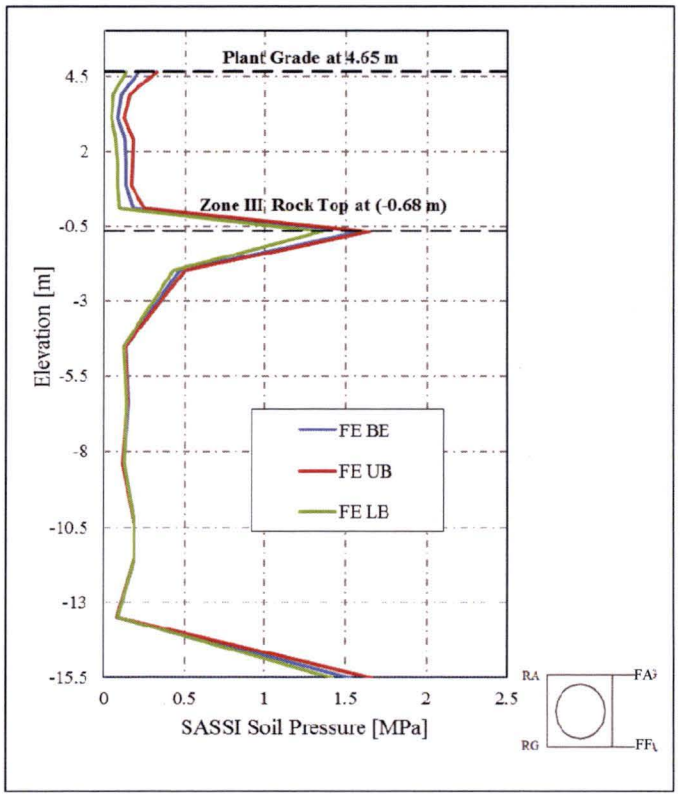

Fully Embedded Model

d) RB/FB Wall at Column Line RG and FF

Figure 5.5-1 Dynamic Lateral Pressures on Below-Grade Exterior Walls (Continued)

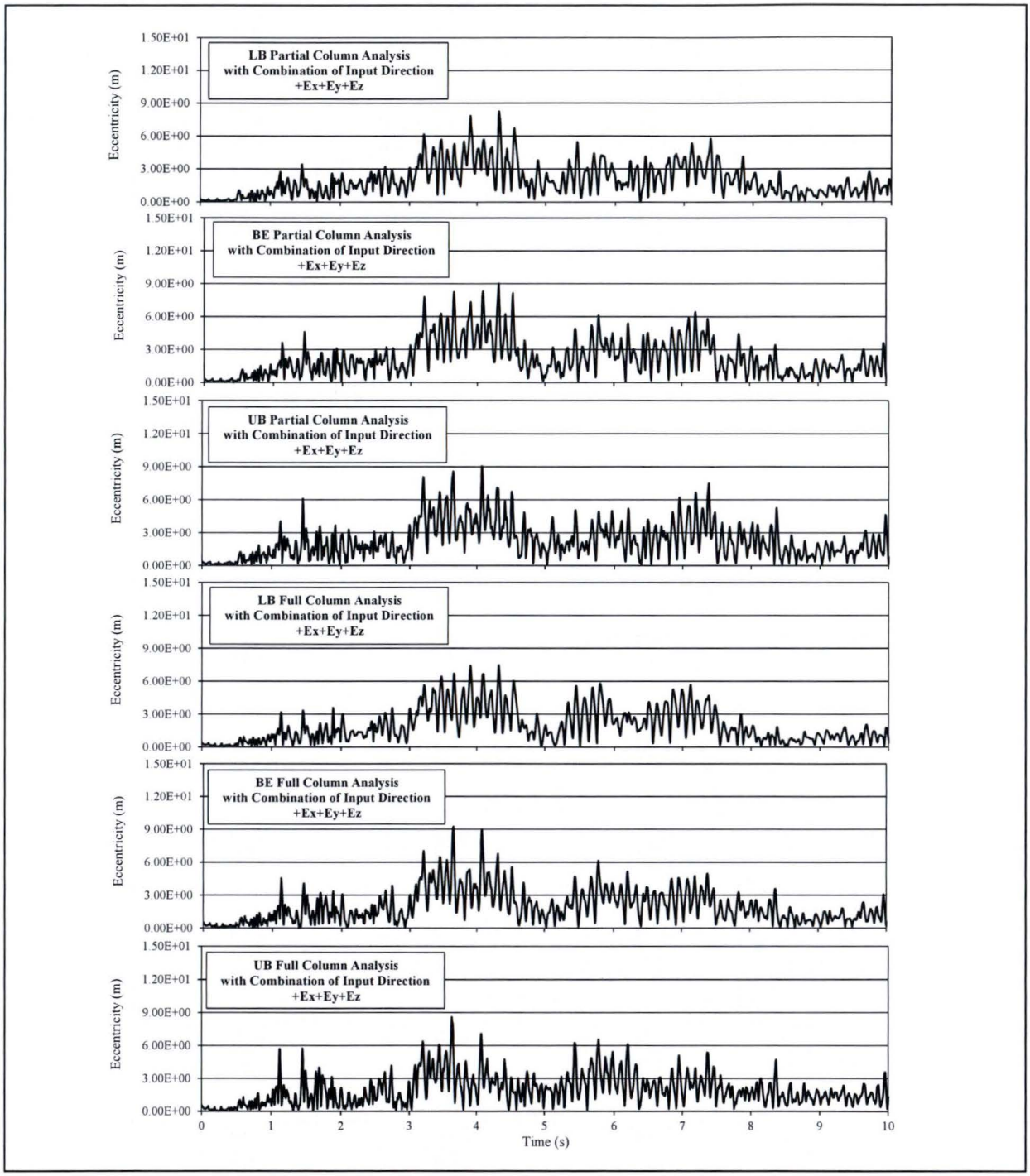

Figure 5.6-1a RB/FB Base Reaction Eccentricity (Combination of Input Direction +Ex+Ey+Ez)

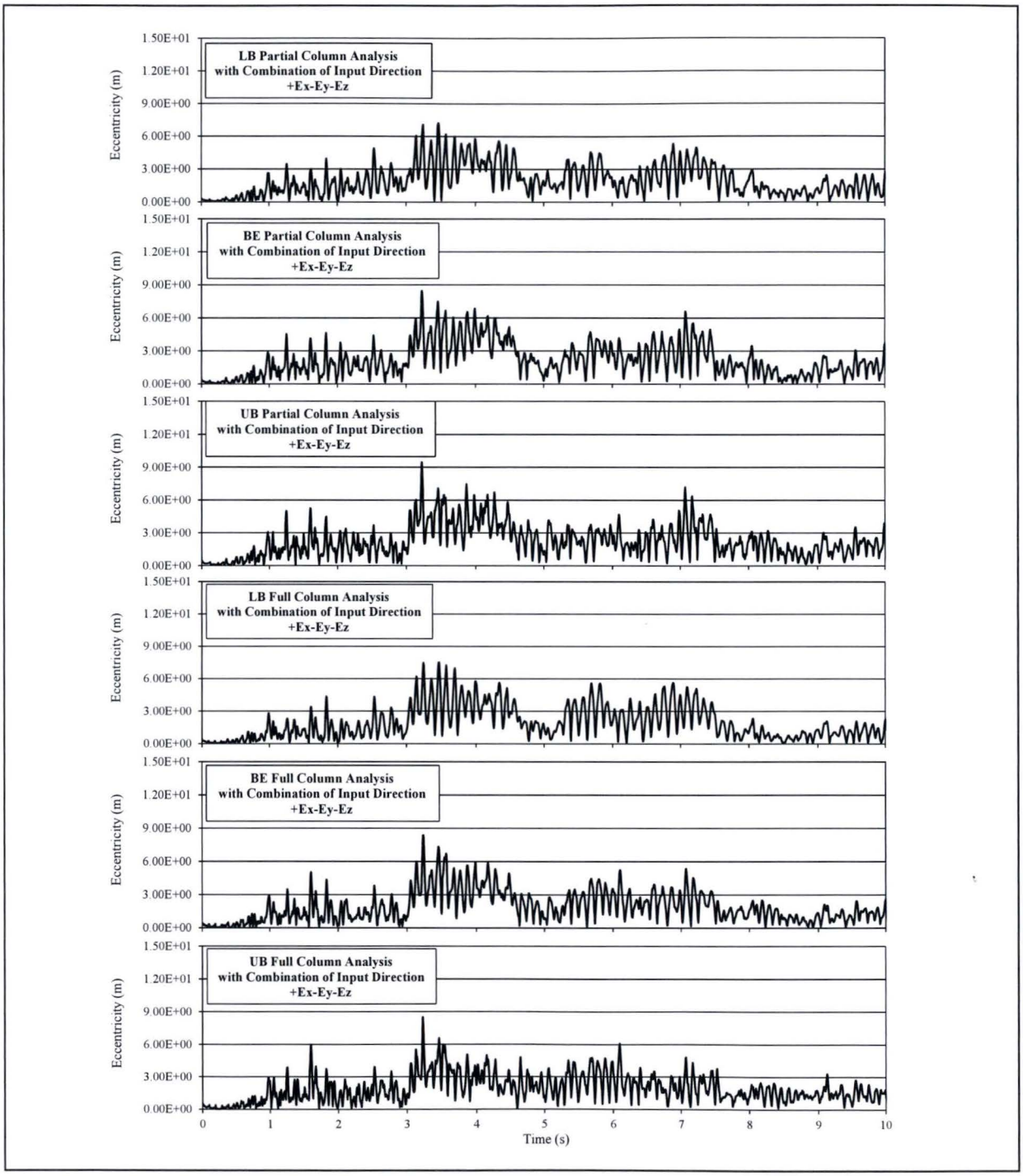

Figure 5.6-1b RB/FB Base Reaction Eccentricity (Combination of Input Direction +Ex-Ey-Ez)

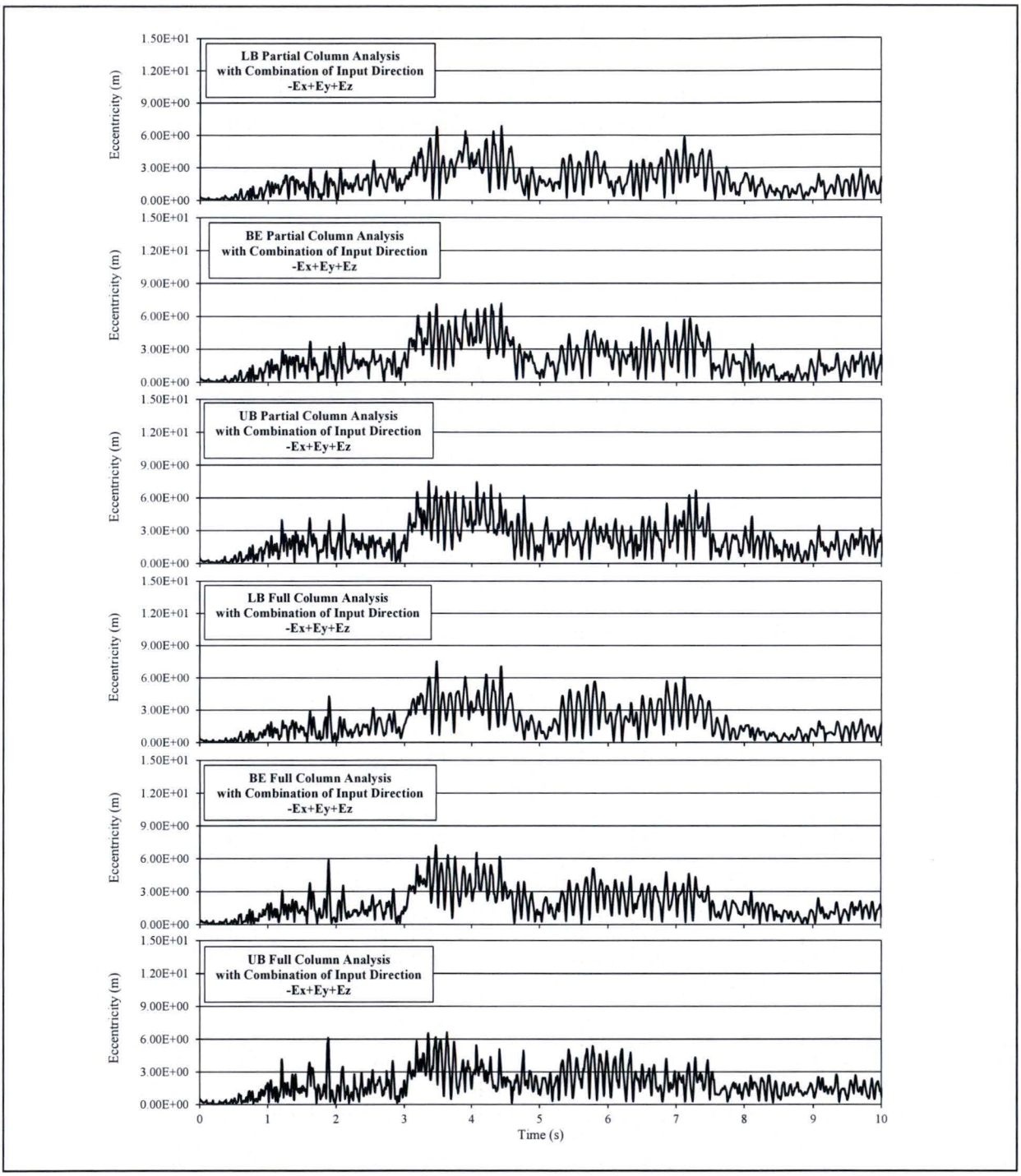

Figure 5.6-1c RB/FB Base Reaction Eccentricity (Combination of Input Direction -Ex+Ey+Ez)

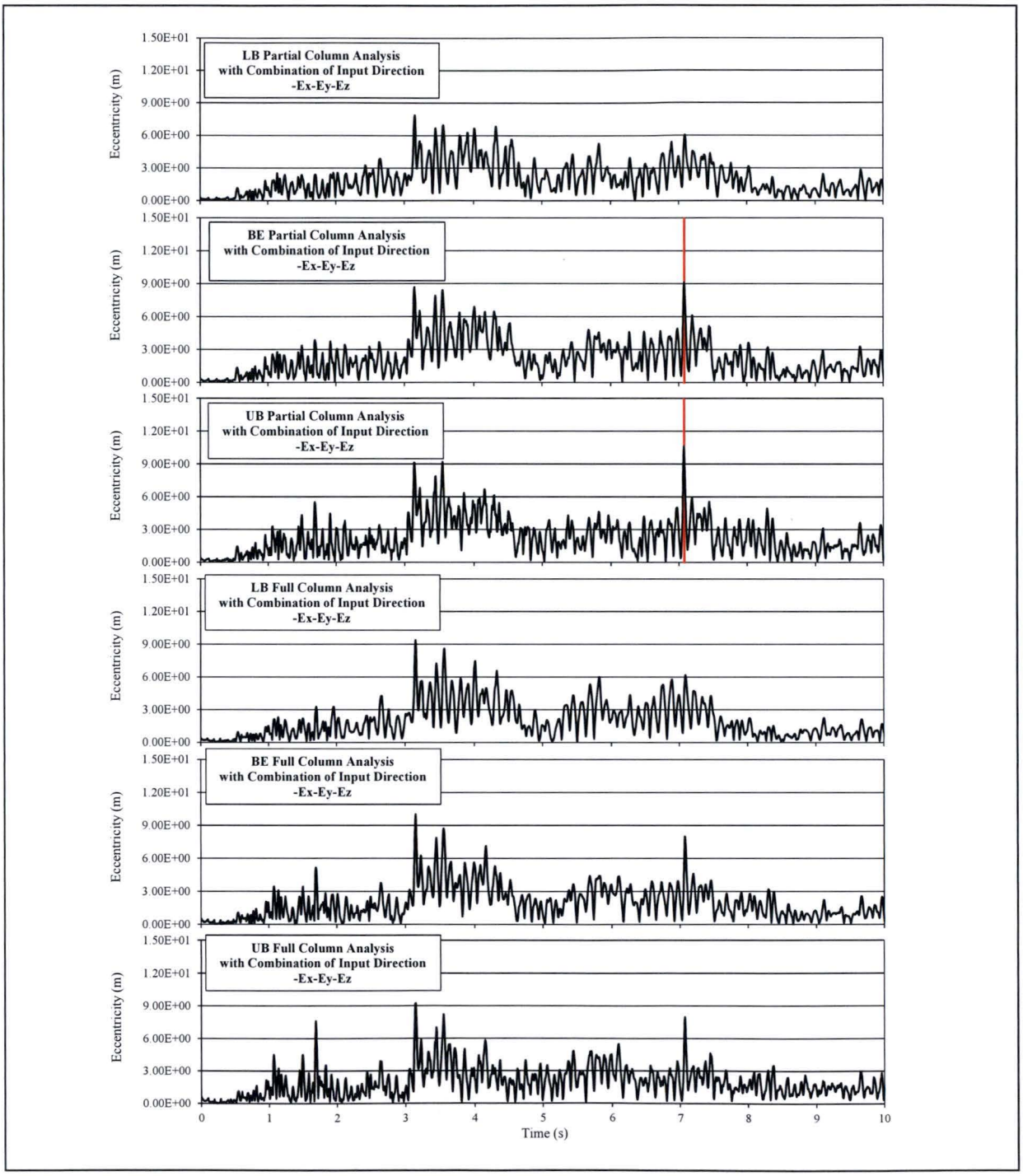

Figure 5.6-1d RB/FB Base Reaction Eccentricity (Combination of Input Direction –Ex-Ey-Ez)

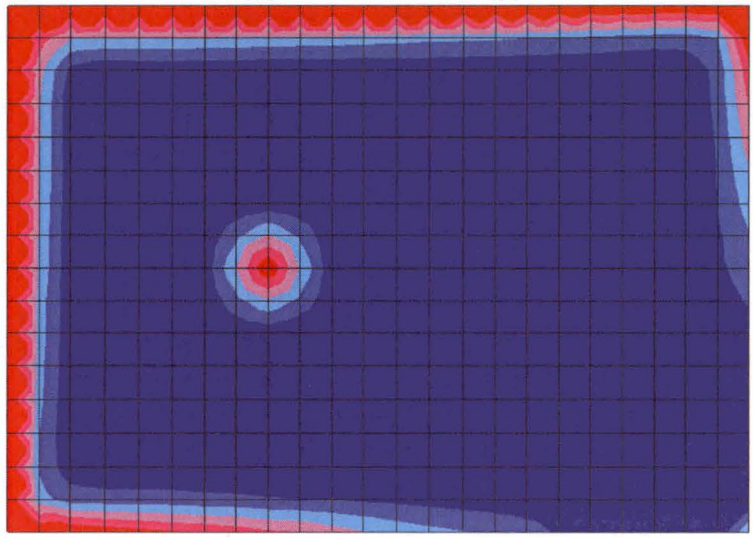

(a) Base Contact Pressures

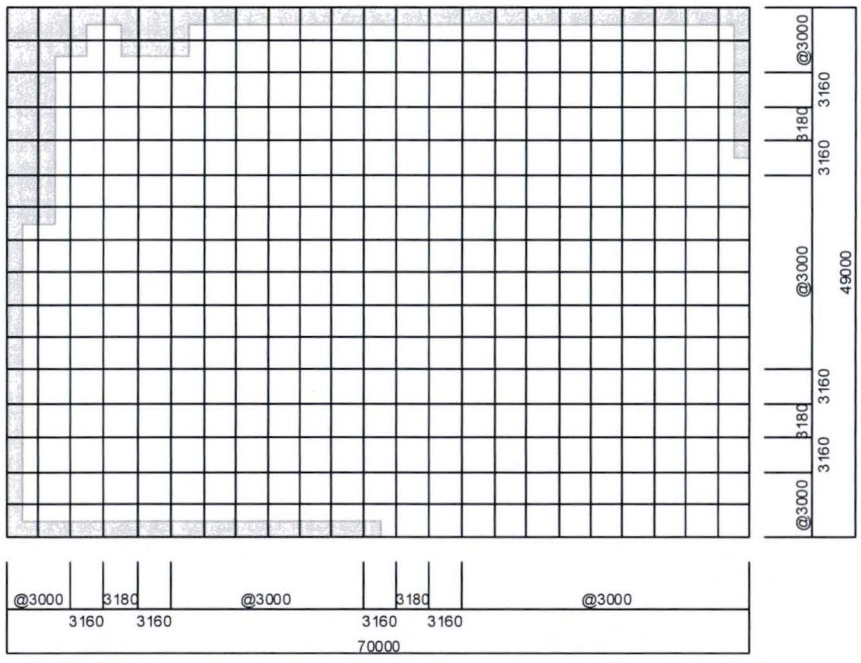

(b) Minimum Contact Area (90% at critical time t = 3.225 sec)

Figure 5.6-2a RB/FB Base Contact Area (UB Partial Column Analysis with Combination of Input Direction +Ex-Ey-Ez)

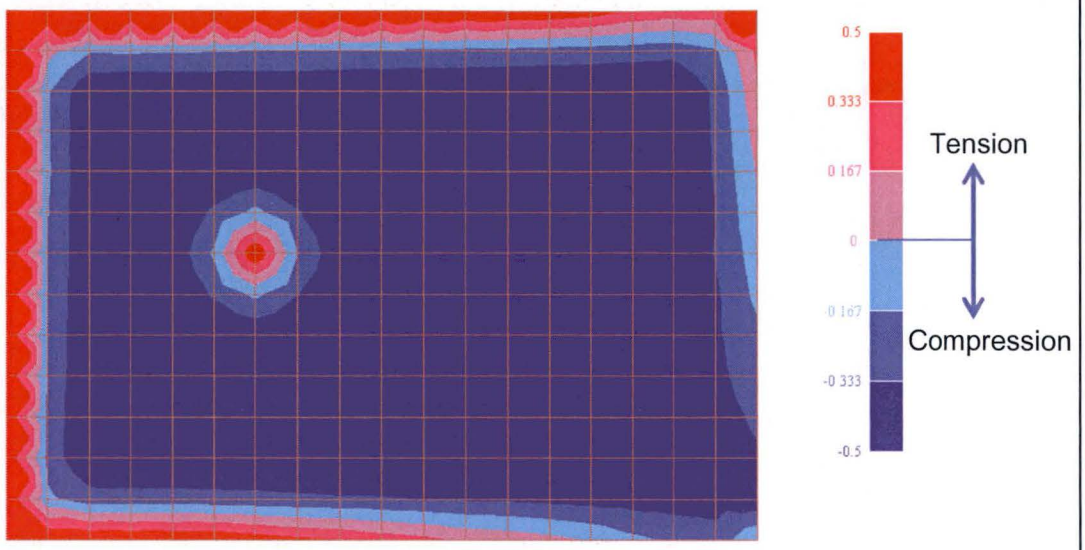

(a) Base Contact Pressures

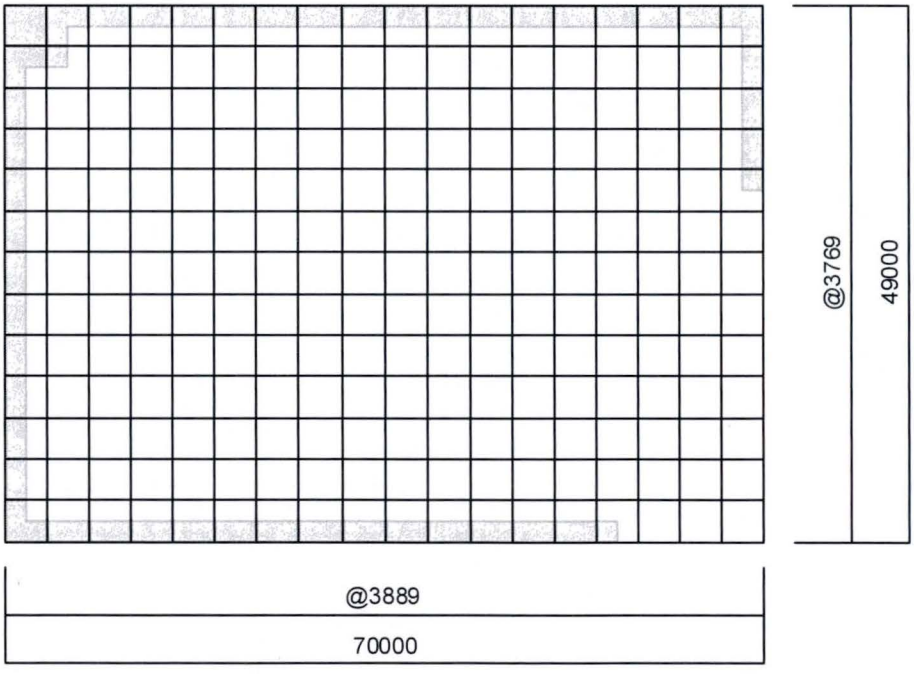

(b) Minimum Contact Area (89% at critical time t = 3.225 sec)

Figure 5.6-2b RB/FB Base Contact Area (UB Full Column Analysis with Combination of Input Direction +Ex-Ey-Ez)

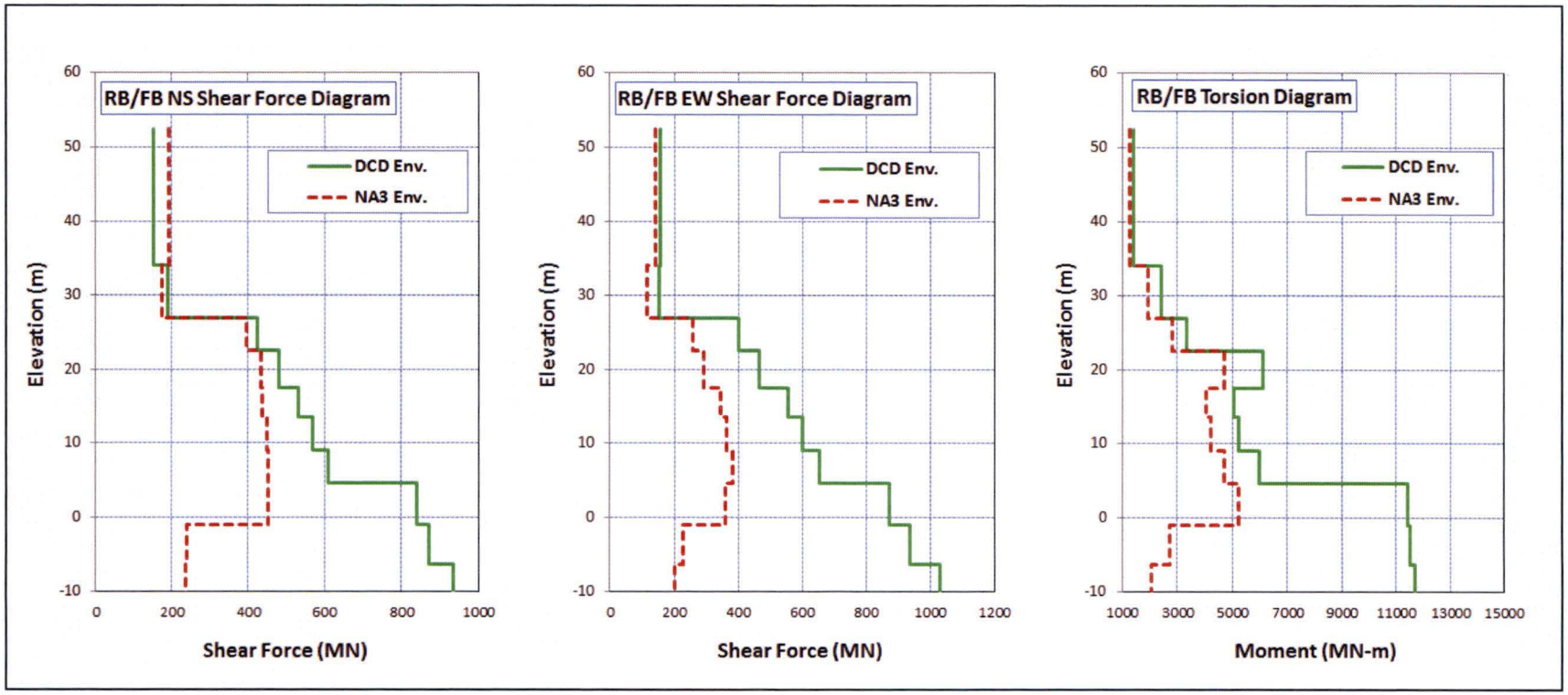

Figure 6.1-1a Site-Specific Horizontal Seismic Load Demands on RB/FB

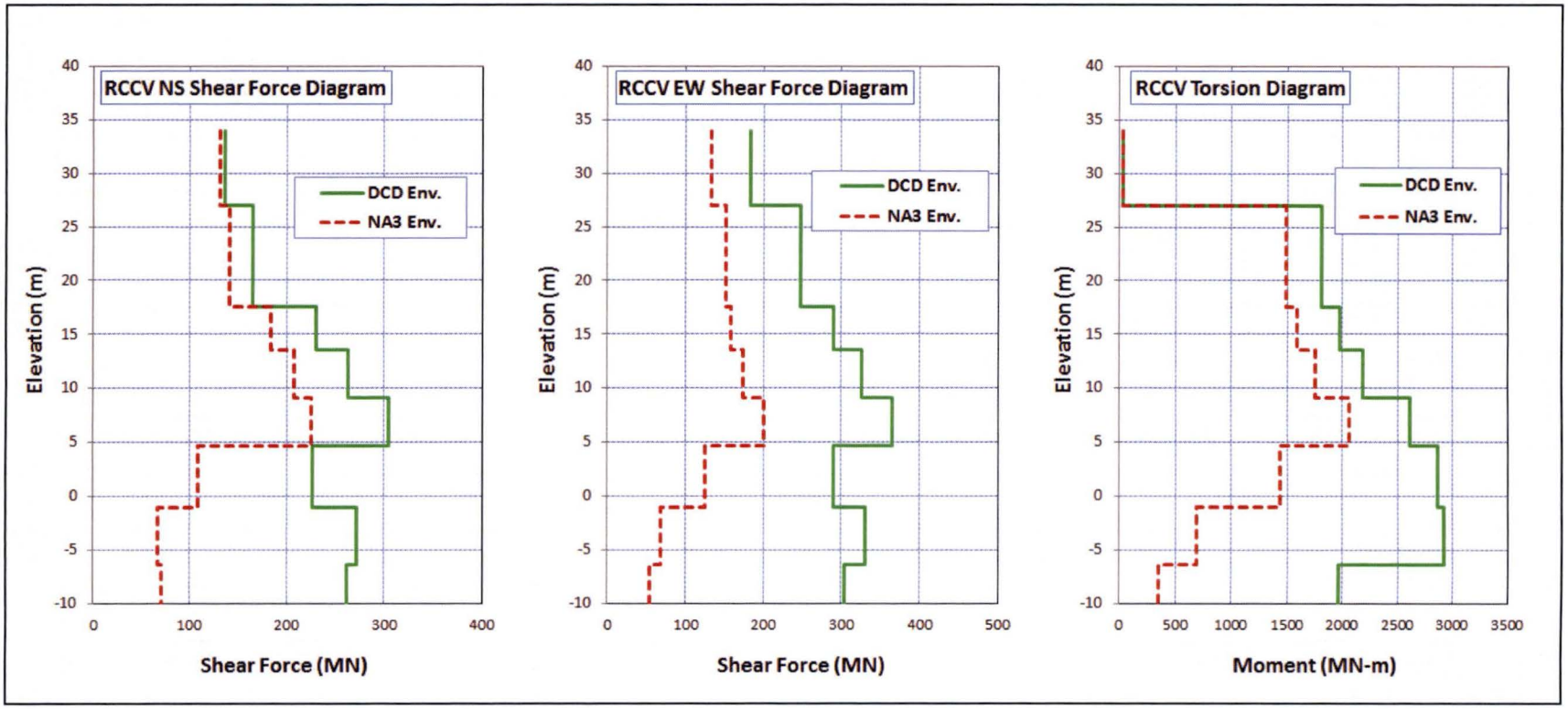

Figure 6.1-1b Site-Specific Horizontal Seismic Load Demands on RCCV

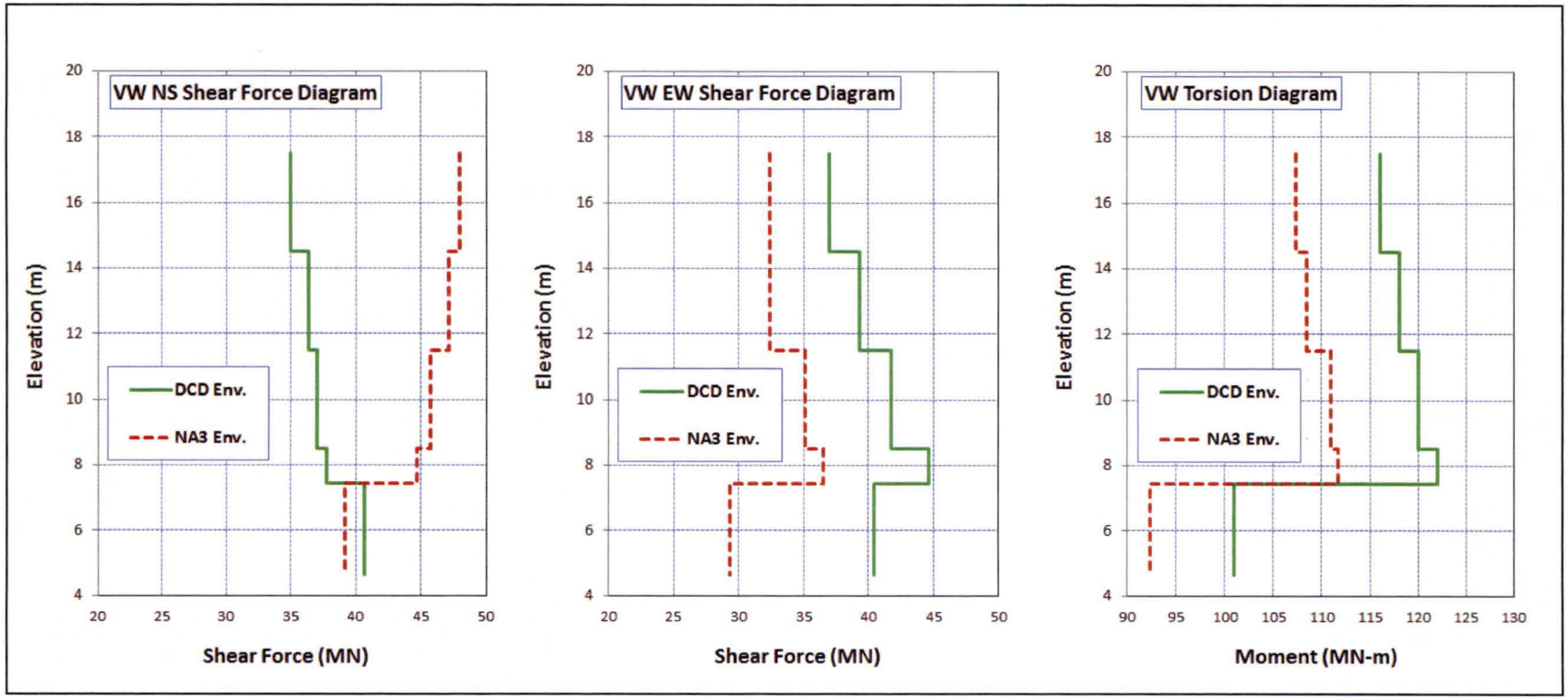

Figure 6.1-1c Site-Specific Horizontal Seismic Load Demands on Vent Wall

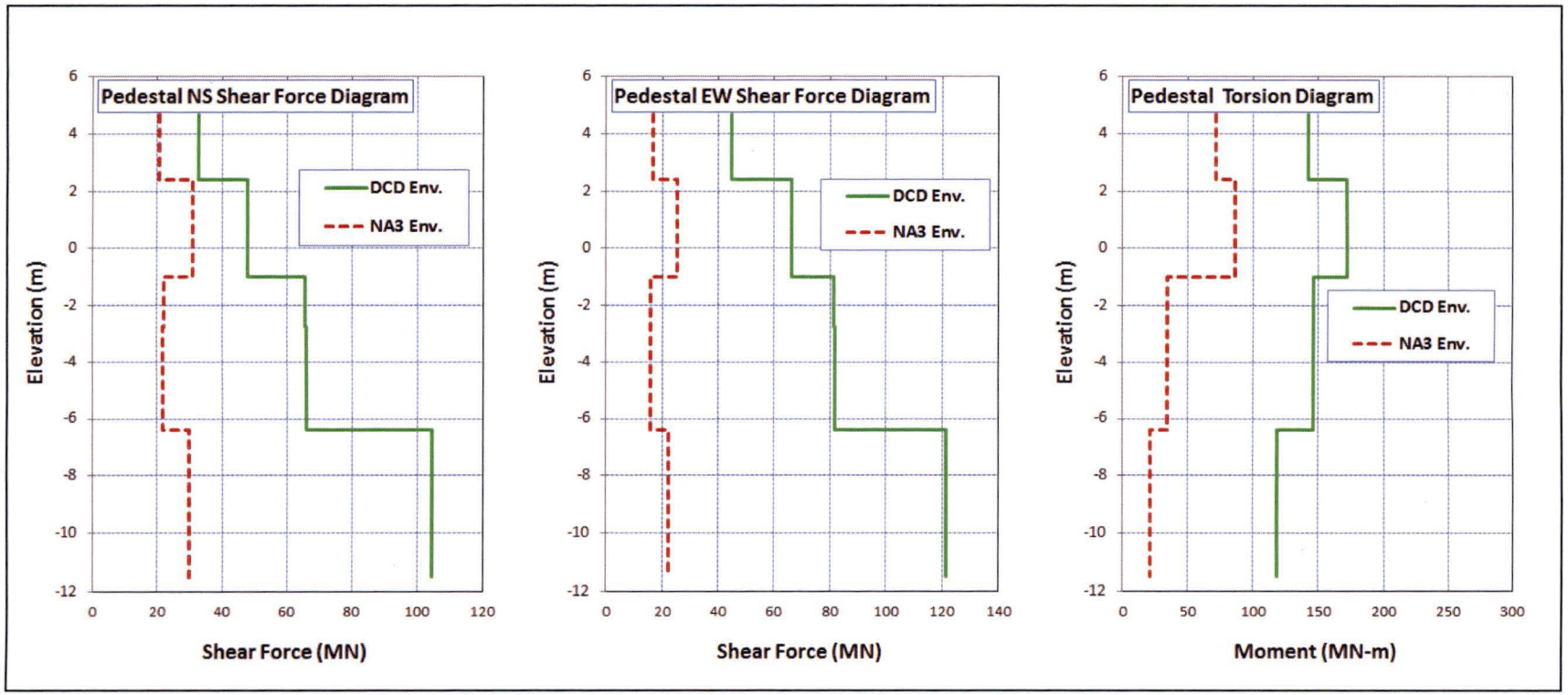

Figure 6.1-1d Site-Specific Horizontal Seismic Load Demands on Pedestal

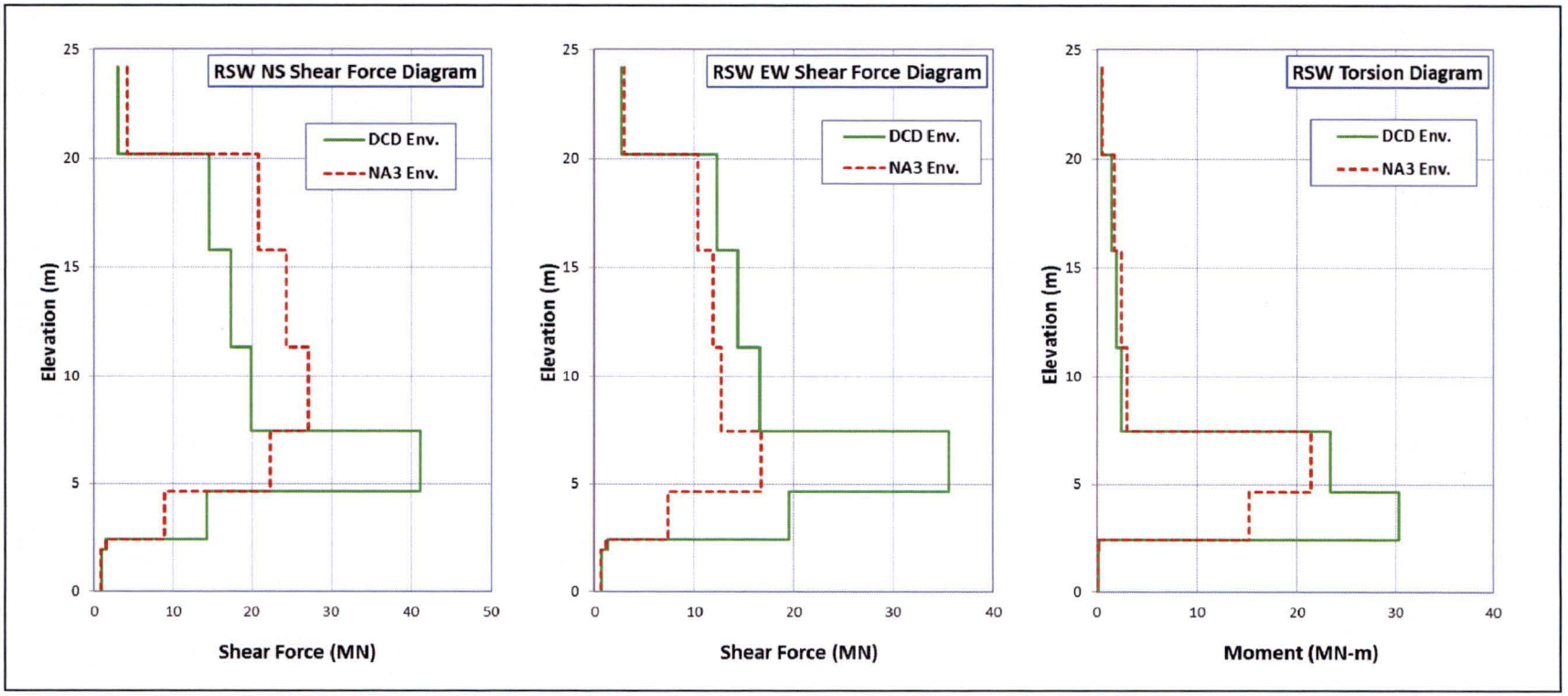

Figure 6.1-1e Site-Specific Horizontal Seismic Load Demands on Reactor Shield Wall

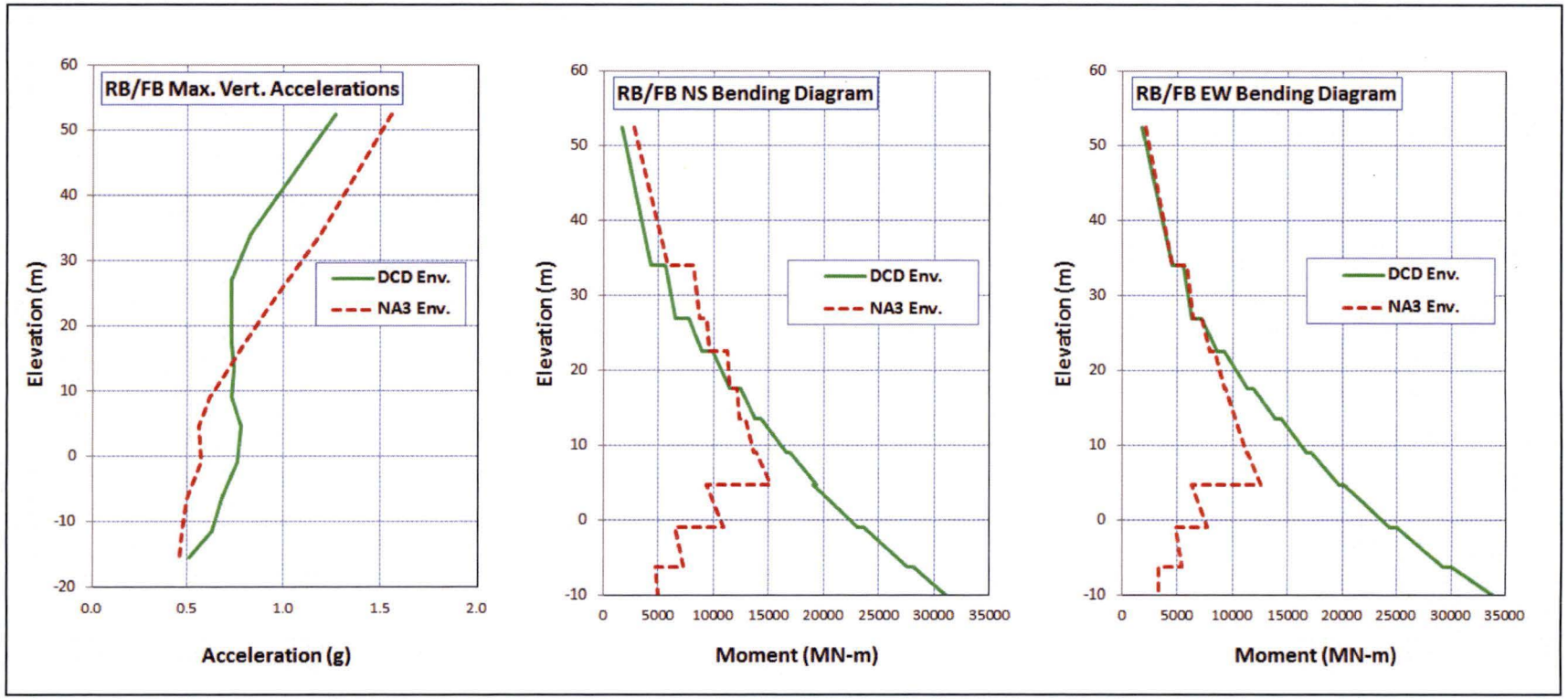

Figure 6.1-2a Site-Specific Vertical Seismic Load Demands on RB/FB

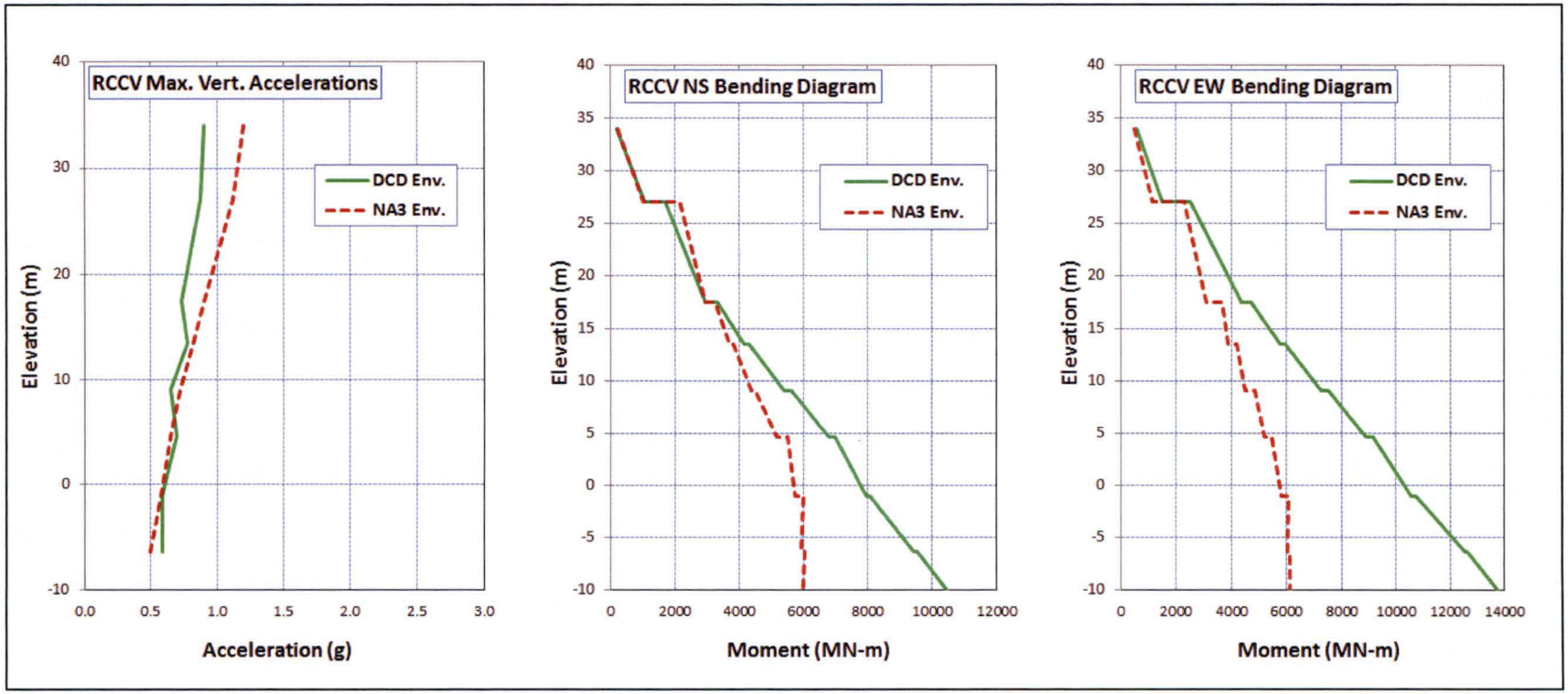

Figure 6.1-2b Site-Specific Vertical Seismic Load Demands on RCCV

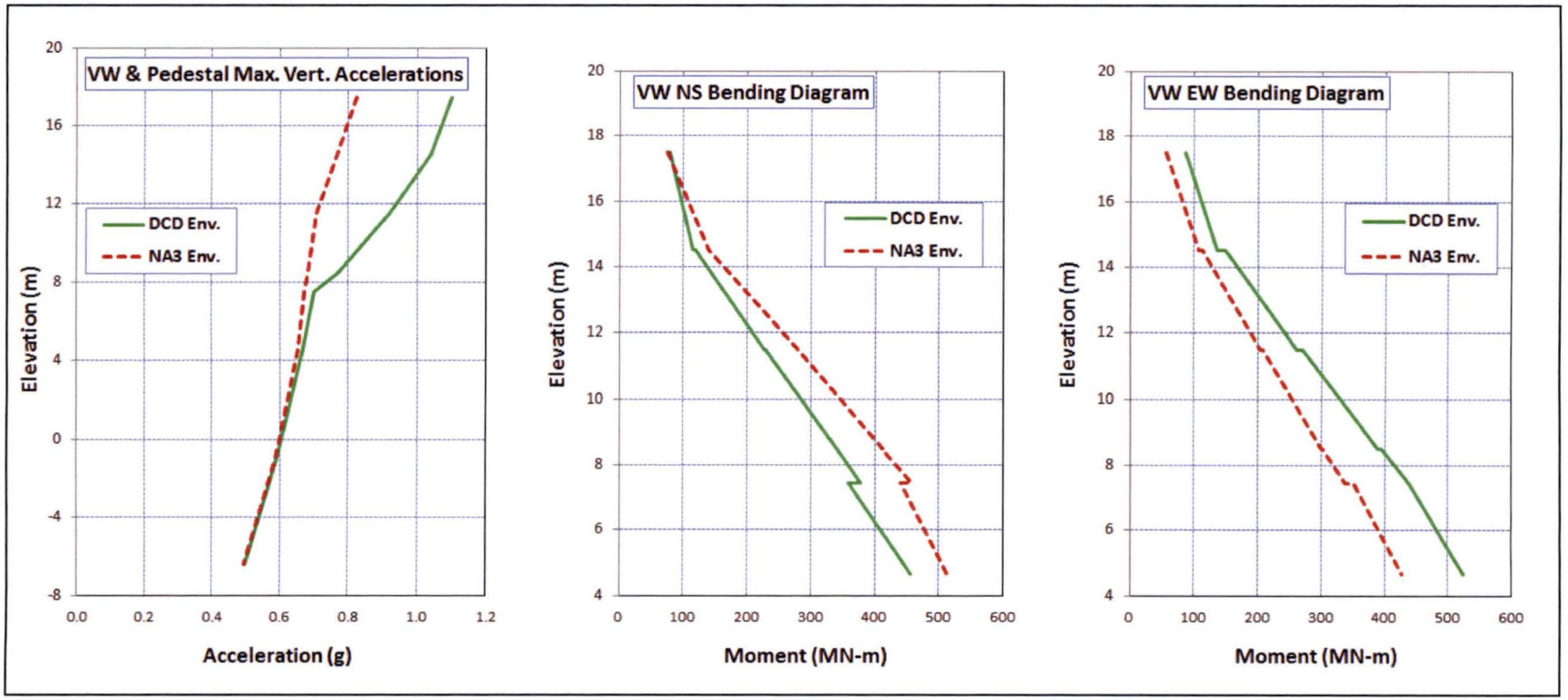

Figure 6.1-2c Site-Specific Vertical Seismic Load Demands on Vent Wall

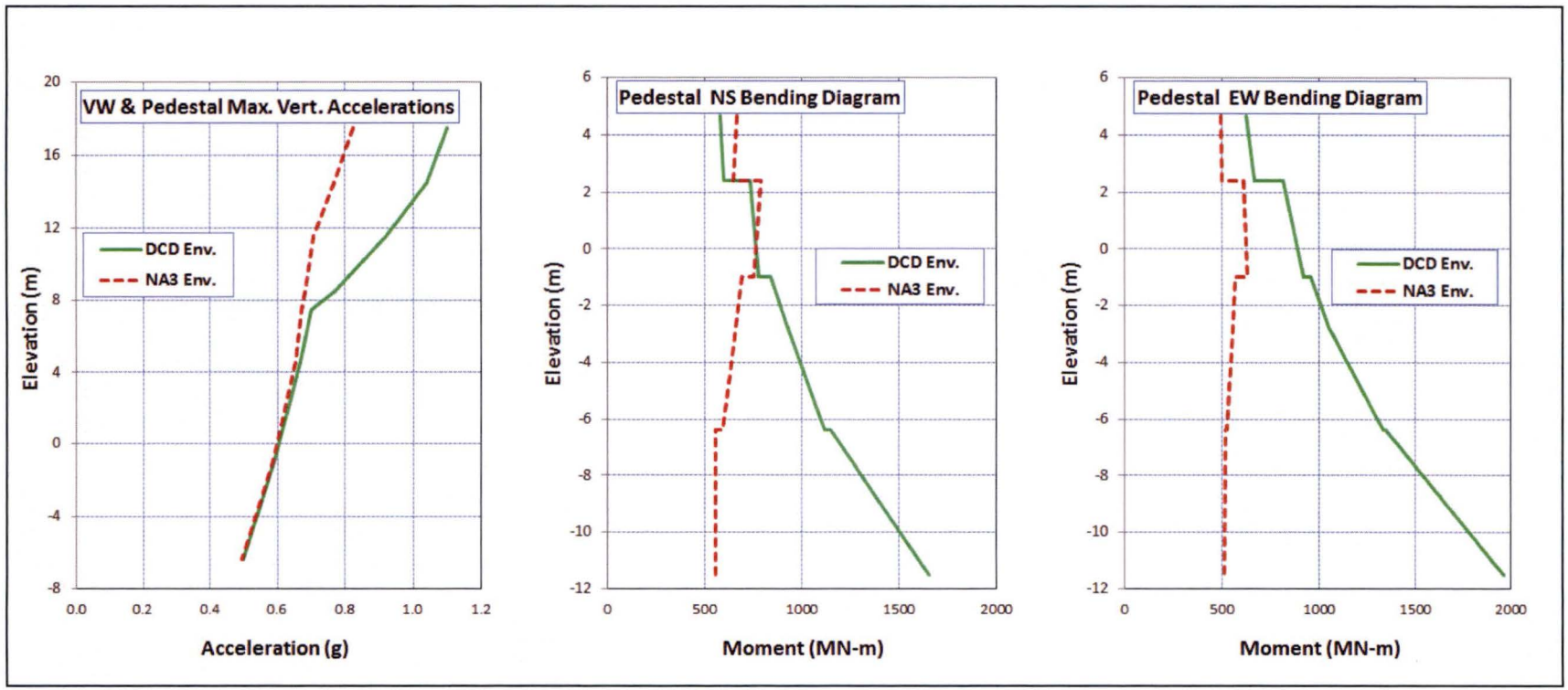

Figure 6.1-2d Site-Specific Vertical Seismic Load Demands on Pedestal

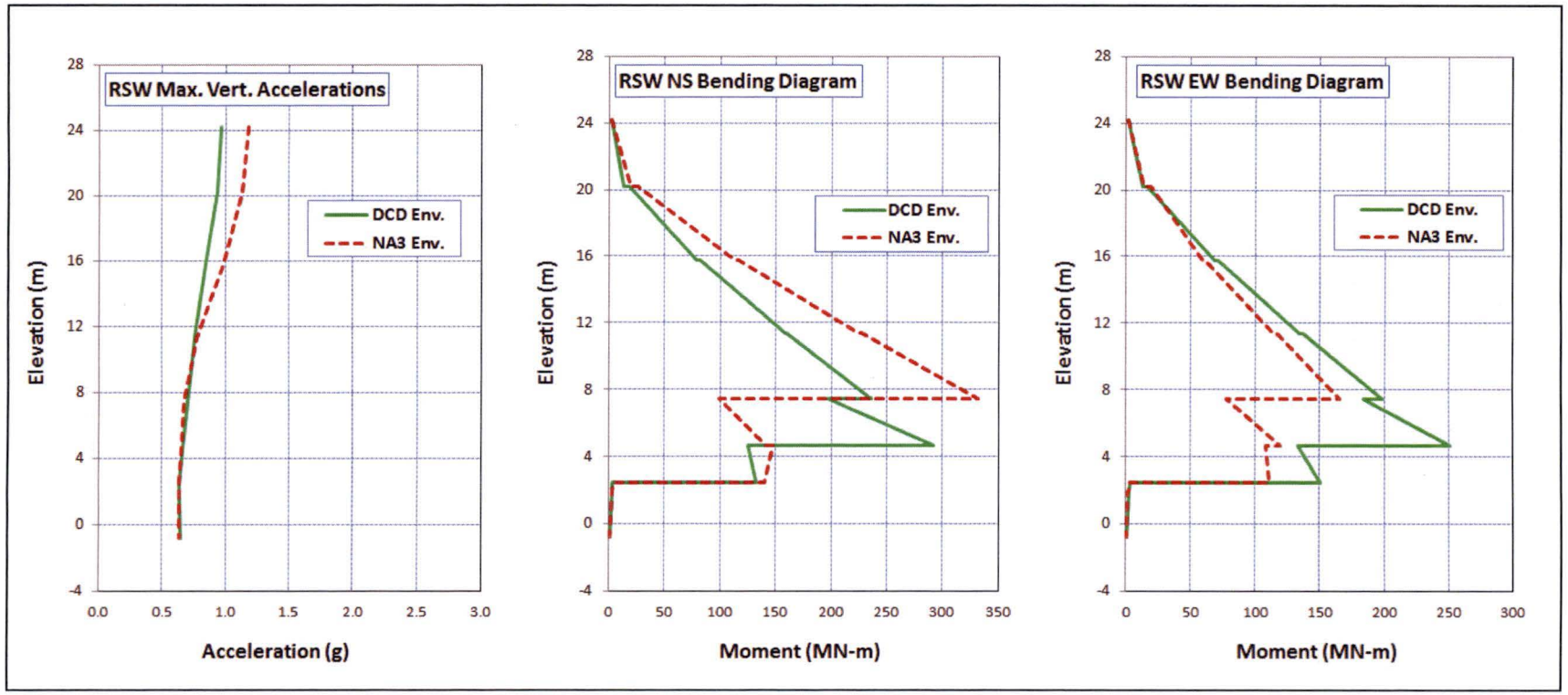

Figure 6.1-2e Site-Specific Vertical Seismic Load Demands on Reactor Shield Wall